Missile Space-based Tracking and Relay

Final Report

DSE Group S12

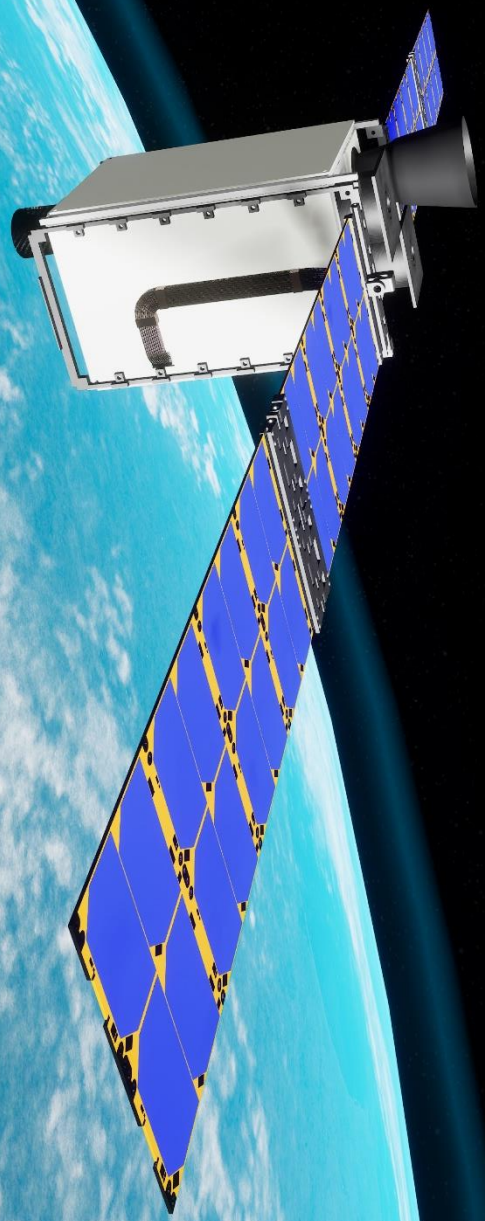

Technische Universiteit Delft

TU Delft

Missile Space-based Tracking and Relay

Final Report

by

DSE Group S12

Authors:

Boby, Sara	4645588
Fortuny Lombraña, Carlos	4651138
Garcia Aparicio, Gabriel	4654579
Harazim, Mateusz	4656377
Hendriksen, Luuk	4654412
Holland, Coen	4681096
Middelhoek, Femke	4552091
Peña Arambarri, Luis	4647041
Presa Magriña, Guillermo	4664884
van Rijthoven, Sharon	4459784
Yoganarasimhan, Mahima	4670019

Version	Purpose/Change	Date	Paragraph(s)
1.0	First Draft	June 22, 2020	all
2.0	Final	June 30, 2020	all

Date: June 30, 2020

Supervisors:	Watts, Trevor	TU Delft, tutor
	Schrama, Ernst	TU Delft, coach
	Maria, Michaël	TU Delft, coach
	Ir. B. Stijnen	Space RNLAF, client
	Capt. D. Wevers	Space RNLAF, client

TU Delft

List of Abbreviations

The list presented below shows the abbreviations used throughout this document.

ACU	Array Conditioning Unit
$ADCS$	Attitude Determination and Control System
BER	Bit error Rate
$CAGR$	Compound Annual Growth Rate
CDH	Commands & Data Handling
CFD	Computational Fluid Dynamics
CGP	Cold Gas Propellant
$COTS$	Commercial Off-The-Shelf
$DATI$	Demonstration, Analysis, Test and Inspection
DC	Direct Current
DOD	Depth of Discharge
DPU	Data Processing Unit
DSE	Design Synthesis Exercise
ECC	Error Correction Coding
$ECSS$	European Cooperation for Space Standardization
EOL	End of Life
EPS	Electrical Power System
EQM	Engineering Qualification Model
ESA	European Space Agency
FBS	Functional Breakdown Structure
FFD	Functional Flow Diagram
Fm	Flight Model
FOV	Field Of View
FPA	Focal Plane Array
FPS	Frame Per Second
GEO	Geosynchronous Equatorial Orbit
$GNSS$	Global Navigation Satellite System
GPS	Global Positioning System
GS	Ground Station
GSD	Ground Sampling Distance
HEO	Highly Elliptical Orbits
$HWCIs$	Hardware Configured Items
$I\&T$	Integration and Test
$ICBM$	Intercontinental Ballistic Missile
IMU	Inertial Measurement Unit
IOD	In-Orbit Demonstration
IR	Infrared
$ISARA$	Integrated Solar Array and Reflect-array Antenna
$ISIS$	Innovative Solutions in Space
ISL	Inter Satellite Link
ISO	International Organization for Standardization
ISR	Intelligence, Surveillance and Reconnaissance
ISS	International Space Station
LEO	Low Earth Orbit
LN	Logical Node
$LWIR$	Long Wavelength Infrared
$M-STAR$	Missile Space-based Tracking and Relay
$MAIP$	Manufacturing, Assembly and Integration Plan
$MarCO$	Mars Cube One
MNS	Mission Need Statement
MoD	Ministry of Defense
$MPPT$	Maximum Power Point Tracking
$MWIR$	Medium Wavelength Infrared
$NASA$	National Aeronautics and Space Administration

$NATO$ North Atlantic Treaty Organization

$NETD$ Noise Equivalent Temperature Difference

OAP Orbital Average Power

OBC On-Board Computer

PAY Payload

PDU Power Distribution Unit

$PIPS$ Power Interface Protection Switches

PM Prototype Model

POS Project Objective Statement

$PROP$ Propulsion

QFD Quality Function Development

$R\&D$ Research and Development

$RAMS$ Reliability, Availability, Maintainability, Safety

$RDT\&E$ Research Development Test and Evaluation

RF Radio Frequency

$RNLAF$ Royal Netherlands Airforce

S/C Spacecraft

SAM Serviceable Available Market

$SBIRS$ Space-Based Infrared System

SCR Signal to Clutter Ratio

$SGP4$ Simplified General Perturbation Version 4

SNR Signal-to-Noise Ratio

SoC Streets of Coverage

$SWCIs$ Software Configured Items

$SWIR$ Short Wavelength Infrared

$SWOT$ Strength, Weakness, Opportunity, and Threat

TAM Total Available Market

$TD-CDMA$ Time Division-Code Division Multiple Access

TFU Theoretical First Unit

TLE TWO-Line Element

TRL Technology Readiness Level

TTC Telemetry, Tracking and Command

UHF Ultra High Frequency

UN United Nations

US United States

$VACNT$ Vertically Aligned Carbon Nanotubes

$VNIR$ Visible and Near-Infrared

List of Symbols

A	Area [m^2].
C_D	Drag coefficient [-].
E	Energy [J].
G	Gain [dB].
I	Moment of inertia [m^2kg].
I_{sp}	Specific impulse [s].
M	Mass [kg].
P	Power [W].
R_e	Earth radius [km].
T	Torque [Nm].
T	Temperature [K].
U	Specific Energy [Wh/kg].
U	CubeSat Volume Unit [10x10x10 cm].
V	Voltage [V].
ΔV	Delta V [m/s].
α	Absorptivity [-].
$\dot{Q}$	Heat transfer rate [W].
$\dot{\theta}$	Angular velocity [$°/s$].
ϵ	Emissivity [-].
λ	Wavelength [μm].
ν	Efficiency [%].
σ	Standard deviation [-].
τ	Thrust [N].
d	Distance [km].
f	Frequency [Hz].
h	Altitude [km].
n	Refraction index [-].
p	Momentum [Nms].
t	Time [s].
v	Velocity [m/s].
z	Refraction angle [°].

Preface

This report is a culmination of 10 weeks of rigorous work by a team of 11 aerospace engineering students, the final project of the TU Delft Aerospace Engineering Bachelors programme. Over the 10 weeks, three building reports were produced that provided the structure and guidance to reach the conclusions portrayed in this report.

Team S12 was given the opportunity to work with the Royal Netherlands Air Force in designing a space based ICBM detection and tracking system. We would like to thank Capt.Dennis Wevers and Ir.Bas Stijnen for giving us this opportunity to demonstrate the team's capabilities. We would especially like to thank our coaches and mentors, Trevor Watts, Ernst Schrama and Michael Maria for all the guidance they have provided to the group. We would expressly like to thank Trevor Watts for his consistent presence in our working days, for always being available to help the group with any internal issues and preparing us for our reviews. Furthermore, we are grateful to Associate Professor Ralph Savelsberg for guiding us through the technical problems posed by the design of this mission and always giving the team detailed answers to our queries. It was an honour to work for and with them all. The team would like to give special regard to its teaching assistant, Samuel van Elsloo, for his rigorous feedback and guidance, simultaneously pushing the group to continue improving its performance and giving the team the support needed to understand the tasks posed by the Design Synthesis Exercise.

The technical design of several subsystems involved in the mission were beyond the scope of material covered within the Bachelor's programme itself, and the team, often with the aid of our coaches, outsourced to experts in the field for advise and knowledge on the specifics of the respective subsystems. To this regard, we would like to acknowledge the immense help provided to the team from Sarah Lammens and Eric Bertels of ISIS; meetings with them helped the group with general specifics about nanosatellite design as well as provided useful advise with regards to systems engineering and project management, by extension improving the efficiency of our team. In addition to this, we would like to thank Roel Arts from Thales Cryogenics for the information provided regarding thermal control for the payload system. Furthermore, we are grateful to Stefano Speretta for the insight provided with respect to the design of the link budget for the intricate communications system involved in the M-STAR mission. Last but not least we would like to thank Bert Monna from Hyperion for his essential advise regarding the attitude control and determination subsystem of the spacecraft.

Lastly we would like to acknowledge the TU Delft Aerospace Faculty for making this possible given the current global situation. All the efforts made to clarify the project's demands and coach the students about Project Management and Systems Engineering, and its vital importance in the industry, have truly augmented our understanding of engineering.

DSE Group S12
Delft, June 30, 2020

Contents

1
Executive Summary

Project Objective

The objective of this project can be retrieved from the existence of Intercontinental Ballistic Missiles (ICBMs) and the threat they pose to society. ICBMs can be detected by means of Early Warning Systems, of which currently two exist worldwide, these are located in the United States and Russia. Since the geopolitical environment is ever-changing, the Netherlands and its allies desire to have more autonomy and obtain a stronger position with regards to Intelligence, Surveillance and Reconnaissance services (ISR). Due to the rapid developments within the space industry over the past decades, the cost of developing space assets has significantly decreased. Hence, a window opened for the Dutch Ministry of Defence (MoD) to investigate the possibilities of developing their own space assets. This resulted in the following project objective as it was commissioned by the Royal Netherlands Airforce (RNLAF): *"Generate a complete design of a technical demonstration mission, maximising effective use of a nanosat constellation to perform Early Warning for the Netherlands and its European Partners against ballistic missile threats"* [1].

Market Analysis

The market analysis allows requirement generation based on the risks and weaknesses in entering the market, as well as the weaknesses and opportunities. Next to this, it provides an overview of the existing missions, as well as the market share and trends. First, the industry is segmented. The Total Available Market (TAM) is the global space market, the Serviceable Available Market (SAM) is space based military operations, and the target market, within these, is 'Early Warning Systems'. Due to large growth in the nanosat market, competitive pricing and COTS (commercially off-the-shelf) modules exist for nanosat buses. Within the target market, two existing missions are publicly known. SBIRS by the United States, and EKS by Russia. SBIRS uses infrared sensors, and currently has four geostationary orbit (GEO) satellites, and two highly-elliptical orbit (HEO) satellites. As the target market is a military based market, defining a monetary market share is not advantageous. Rather, a share of population and land area was defined; if this mission is done for NATO states, security would be provided to 8-12% of the World's population, and 10-16% of the World's land area, depending on whether or not the United States is included. The future market is predicted to have a higher necessity for such a system to be set in place, as political tensions globally are rising.

Finally a SWOT (strength, weakness, opportunity, threat) analysis is performed. The strengths of the mission are identified to be security for The North Atlantic Treaty Organization (NATO) and expert knowledge from the RNLAF. The weaknesses are identified as potential lack of funding in expanding the mission to fully operational, as well as space sustainability. Opportunities were stated as increased necessity for an early warning system to exist for NATO countries, utilizing the competitive nanosat market, using small launchers to decrease environmental impact, and a larger political presence for the Netherlands. Finally, the threats include public fear of space militarisation, increased political tension, the threat of being targeted by a missile due to said tension, and space weather. Requirements were linked in order to maximise strengths and opportunities, and minimise weaknesses and threats.

Functional Breakdown

During the functional analysis of the M-STAR mission, alert levels have been defined in order to consistently refer to milestones that occur during missile detection and tracking. These start at level 1 when an anomaly is discovered with the H_2O filter and escalate to level 2 with a H_2O+CO_2 anomaly. Level 3 is raised when it is detected that the anomaly has a velocity, and levels 4 and 5 are raised on the ground when the tracking data is used for classification.

Concurrently, spacecraft have been classified into SC1, SC2 or SC3 depending on their role during detection and tracking of ICBMs. Any spacecraft in the constellation can take on any role as their hardware is the same. SC1 has the function of raising the alert levels up to 3 and sending the tracking data to SC2, SC2 has the function of tracking the missile and using stereo imaging to triangulate the ICBMs positioning, and SC3 stands by ready to take on SC2's role.

M-STAR Requirements

The requirements that make M-STAR unique and thus drive the design more than average are listed below [1].

REQ-MIS-01-01: The mission shall provide global coverage.
REQ-MIS-01-02: The mission shall alert ground stations of an ICBM detection (alert level 3) within a maximum of 90 seconds after launch of the missile.
REQ-MIS-01-04: The mission shall detect the missiles within a 1 km (3-sigma) accuracy in all 3 dimensions.
REQ-MIS-01-05: The mission shall have 99% availability for communication of detection relays.
REQ-MIS-03: The mission shall be ready for launch by 2024.
REQ-MIS-05: The mission shall cost less than 30M € excluding launch costs.
REQ-MIS-08: The mission orbit shall be LEO.
REQ-MIS-09: The mission's space segment shall be self-sufficient for communication relay.

Preliminary Concept

At the end of the midterm report, four different feasible concepts were selected to be compared in a trade-off. These concepts differ mainly in different payload combinations of Coverage and Focus payload, but also in different communication subsystems being used. The four possible options were:

- Concept 1: Coverage IR + Focus IR with patch antennas.
- Concept 2: Coverage IR + Focus IR and Hyper-Spectrum with patch antennas.
- Concept 3: Coverage Hyperspectral + Focus IR with patch antennas.
- Concept 4: Coverage IR + Focus Visible with high gain or laser antennas.

In order to determine the best performing concept, a trade-off was performed evaluating cost, the use of technical resources, TRL, payload performance and required pointing accuracy. Following this trade-off, concept 1 and 2 were the winners. Therefore, a sensitivity analysis was carried out in order to understand the reasons why the concept 1 was better than the concept 2.

Besides to the trade-off, contingency management was performed and four preliminary budgets were created. When a design, a M-STAR satellite, contains a large number of uncertainties, it is needed to establish different contingencies. The contingencies are being reduced over time as the designs becomes more and more detailed. With the contingency management, the four budgets can be estimated.

The four preliminary budgets are: ΔV (total change in velocity), mass, link and power budgets. The ΔV budget is determined by taking into account three different manoeuvre: orbital station-keeping, de-orbit burn and collision avoidance manoeuvres. The final ΔV is estimated by the sum of the three ΔV manoeuvres and its process is the same for the detailed ΔV budget. However, for the preliminary mass budget, the total mass of the 12U CubeSat is fixed on 24 kg. Then, the masses of subsystems are found using a statistical approach to determine the allocation of dry mass for each subsystem, except for the propellant. The approach has not being changed from the baseline report, only the total mass and size have been doubled. Moreover, the preliminary link budget, taken from the midterm report, was used as a first estimate for the characteristics of the communication subsystem. In comparison to the detailed one, the input parameters such as the frequency band and the maximum distance between in-plane satellites changed. However, the main variation between the preliminary and final budget is the communication accuracy. Finally, considering the power budget performed in

the baseline report was based on the BRIK-II (first satellite of the RNLAF), having doubled the mass and the dimension of the CubeSat, a new power budget has been performed.

Payload

During the midterm phase of the DSE, extensive research has been performed regarding the possibility of using separate instruments for the Coverage and Focus payload. It was concluded that the instruments best suited for the mission are MWIR Cameras that are able to operate in a wavelength range around 3 to 5 µm in order to detect expelled water and carbon dioxide gasses. Following from additional research and insights in limitations regarding the required power, volume mass and cost it was decided to combine the functionalities of both the Coverage and Focus payload into a single instrument.

In the final phase of the DSE, the emphasis was put on a detailed design of the payload subsystem. The research described in the payload chapter is therefore intended to not only aid in making a final choice for the infrared camera, but also to specify additional required components and configurations to achieve a successful mission. With the type of optical instrument decided to be a infrared camera operating in the SWIR and MWIR wavelength range, the first step was to identify the difficulties that both the atmosphere and optical instruments themselves pose to the detection of ICBMs. In the disturbances and noise chapter, the effects of atmospheric absorption and refraction are described as well noise caused by the environment and the instrument itself. Regarding the atmospheric absorption, it was found that the 2.7 and 4.3 µm wavelengths that signify the presence of an ICBM fall in so called radiation absorption bands on sea level. Above an altitude of 14 km, however, the absorption bands disappear and the aforementioned wavelengths can be used for detection and tracking purposes. To further enhance the ICBM signal received, it was decided to make use of filters capable of narrowing the bandwidths of the camera to center around 2.7 and 4.3 µm. The application of the filters was enhances ICBM signals as the background noise is reduced. The payload is able to switch between these filters by means of a filter-switch-mechanism.

The type of camera sensitive to these wavelengths is the chosen InSb camera. As this material shows decreased noise levels and optimal performance at a temperature of 77 K, a cooler is required. To avoid any vibrations induced by Stirling coolers, a pulse tube cooler from Thales Cryogenic is selected. Since the camera, filters and cooler are not optimised for use on this specific mission, additional R&D will be required.

To increase the ground area covered by a single spacecraft and reduce the number of required satellites for global coverage, research has been performed in the benefits of imaging techniques different from a staring camera. Across-track, along-track and circular imaging have been discussed and a trade-off has been performed. Circular imaging was found to be most beneficial and was adopted into the design. The circular imaging technique makes use of a rotating mirror to trace out a ”doughnut like shape” on the Earth’s surface by taking multiple images. The characteristics of the circular imaging are the following, an inner FOV of 15° and an outer FOV of 61°. The only aspect where the circular imaging lacks is in the accuracy of position of the ICBM where only in 95.8 % of the cases the detected ICBM position is accurate within 1km in all directions.

The optical system will consist of a Coverage and Focus part. The Coverage part consists of a lens and a rotating mirror placed under an angle with the camera. The Coverage optics will be able to achieve a largest GSD of 3300 m to achieve a large surface coverage while maintaining the possibility for ICBM detection as was calculated. The Focus payload will consist of a Ritchey-Chrétien telescope able to to fit the 0.7 m focal length in a 1.5U package and allows the Focus payload to achieve a GSD of approximately 22 m for tracking and classification purposes. The payload is able to switch between Coverage and Focus optics by means of a flip mirror.

Table 1.1: Payload characteristics.

FOV Coverage	FOV Focus	Sampl. Freq. Coverage	Sampl. Freq. Focus
15° (inner), 61° (outer)	1.24°	3 Hz	30 Hz

Command and Data Handling

For the Command and Data Handling subsystem, a division can be made between software and hardware.

For software, a preliminary image processing technique was developed, as well as a process to check for a velocity of an anomaly.

The image processing technique is based on the assumption that the payload is able to look into the atmospheric absorption bands. Following this, ICBM exhaust plume intensities are expected to be relatively distinct compared to the background. Hence, the image produced by the IR-Imager is expected to be bimodal. It is proposed an adaptive thresholding technique called Otsu Binarization Thresholding, known to be simple and fast. First for the H_2O filter, anomalies in intensity are detected and given an allowed range to take uncertainties of location on next frame into account. After switching to the CO_2 filter, image evaluation, and detection of pixels containing intensity anomalies that fall within the range as deduced from the H_2O filter data, a pixel is deemed of interest and its coordinates within the frame are communicated to the velocity check algorithm.

Once an anomaly has been identified as a potential missile by the image processing algorithm, the satellite will check that this anomaly has a velocity before initiating the second satellite. This is done by means of the following two-dimensional procedure. For a pixel of interest, two lines can be drawn; from from the spacecraft to beginning and end of the pixel. Over time, these lines will move. The anomaly can be classified as moving when the intersections of these lines are not constant over time, and if the intersection does not occur on the surface of the earth. However, a threshold must be set in order to determine how long it would take in the case that there is no velocity, to say with certainty that there is no missile present. This threshold was approximated to be between 5 and 7 seconds, and was calculated based on boundary conditions imposed by the lines generated, onto one million simplified missile trajectories.

After a velocity is confirmed (which takes 5 s in the worst-case-scenario), a second satellite is initiated, and the triangulation procedure starts through means of a control loop that centers the anomaly into a Coverage image, such that the Focus payload can be used to track.

For the OBC capable of performing the indicated payload data processing procedures specific to the M-STAR mission as well as common activities such as housekeeping it is proposed to develop a 2 processor card, 1 daughter card configuration located on the same daughterboard. The proposed daughtercard is referred to as Data Processing Unit and will perform all image processing functionalities as described above. From the velocity check onwards, the Main OBC will come into play. As high processing frequency is required for real-time image processing, an COTS Processor card is proposed, a 766 MHz dual-core processor [2]. As the OBC is vital to the mission, redundancy is achieved by implementing a Backup OBC that will be in deep sleep mode on continuous standby and the assumption that in case of DPU failure the OBC can take up image processing. As SD and SSD cards are capable of up to 32 GB of storage, storage was found not to be limiting to the M-STAR OBC design process.

Table 1.2: On-board-computer characteristics.

Total # of Cores (+redundancy)	Processing Frequency	Data Storage
3 (+3)	766 MHz	32 GB

Proposed on-ground testing includes error detection, soft-ware robustness, redundancy modes, ability

to recover from single-event-upsets or multi-event upsets. A proposed interface test is concerned with the redundancy of the system, hence addressing the interface between the Main OBC and Backup OBC.

It has been recommended that further research be focused on the required processing power and possible favourable mission-specific architecture of the On Board Computer to achieve sufficient speed and accuracy in calculations. Ideally, a probabilistic model on-board would allow for two satellites to predict where the missile is most likely headed. However, it is unknown as of now if such processing is possible on board. Furthermore, it may be desirable to have two sets of satellites tracking and relaying missile coordinates, specific to a few geographical locations. This may be possible as some overlap exists in the constellation.

Communication

The constellation has a self-sufficient global communication system. Each spacecraft serves both as ICBM detector and as communication relay satellite. The system is capable of rapid information transmission from a satellite at any location to the ground station in seconds.

Quick information transfer is achieved by use of technology which does not require any pointing of the spacecraft for transmission or reception. Moreover, the satellite can relay data while operating the payload. For the inter-satellite communication, UHF quad-monopole near isentropic antennas with UHF transceiver are used. The system is capable of bit rates of 20 kbit s^{-1}. This data rate is sufficient to perform the critical tasks of inter-satellite communication which are:

- Relay of the ICBM detection information to the ground station
- Coordination of ICBM detection between satellites to achieve 3D coordinates of the ICBM
- Coordination of ICBM tracking across FOV of different satellites

For downlink of non-time-critical payload data, the satellite is equipped with a S-Band patch antenna system. It enables downlink transmission speed of 1 Mbit s^{-1}. With this high data-rate, payload raw data is sent regularly to the ground station. It is used for verification, validation and as such improvement of the system.

The system has been designed to be fully redundant. The detection information relay speed is not affected by failure of one satellite per orbital plane, as alternative paths through the constellation can be taken. Moreover, in the case of failure of two satellites in one orbital plane, transmission at a reduced data rate of 10 kbit s^{-1} is possible.

Table 1.3: Communications characteristics.

Interlinking Communication	GS Communication	Peak Power Interlinking	Peak Power GS
UHF, 20 kbit s^{-1}	S-Band, 1 Mbit/s	7 W	9 W

EPS

The Electrical Power System's main function is to provide electrical power to all the relevant spacecraft components. It has been designed as a photo-voltaic system that generates electricity while the satellite is in the sunlit phase of its orbit (lasting 61.1min), and makes use of a secondary battery system to power the components while in eclipse (lasting 35.4min). By taking into account the power required by all the different subsystems and the time they must be operating for, power modes were created. These were then used to perform sizing of the solar arrays and the battery packs.

Due to the high power demand from the scientific instrument and its cooler, the solar arrays have to be mounted on gimbals to reduce the incidence angle with the Sun. For its expertise in this area, MMA Designs has been chosen as the supplier of the solar arrays. For the other EPS components (the array conditioning unit, power delivery unit and battery packs) Gomspace has been chosen as the supplier due to the high modularity of its NanoPower series. This flexibility allows for the a wide

range of output voltages (ranging from 5 V to 24 V) as well as having redundant components to avoid single points of failure.

Table 1.4: Electrical power system characteristics.

Cost	TRL	Solar Array Area	Solar Array Mass	Battery Energy
114 k€	9	0.31 m^2	1.10 kg	226 W h

For future work, further analysis could be carried out on the specific characteristics of the battery packs under operational conditions. Moreover, the gimbal system could be studied in more detail to quantify the effect it could have on the reliability of the system.

Thermal Control

Preliminary calculations were performed in order to calculate the equilibrium temperature of the satellite for a hot and cold case scenario, sunlit and eclipse. It was found that a fully passive thermal control system could be achieved with the reflective white paint Barium Sulphate with Polyvinyl Alcohol. This would lead to an equilibrium temperature for the satellites of 15.7 °C when sunlit and −18.6 °C in eclipse.

Furthermore, a radiator design is presented. Radiators will be present at the backside of the solar array. Their main function is to expel heat which originates from the cooler of the payload. The cooler is connect to the radiator via a copper strap which runs on the exterior part of the satellite.

Propulsion

The propulsion system design focuses on evaluating the most suitable propulsion system for the mission's requirements between ion thrusters and cold gas propellant thrusters (CGPs). Alternative propulsion systems were discarded as options due to stringent thermal and power requirements. Several COTs components are analyzed for both ion thruster and CGPs, and entered in a trade-off to determine the optimal propulsion system based on weighted criteria; the criteria are composed on TRL, cost, operating power, performance, mass and volume. Operating power, mass and performance were considered the highest weighted criteria as they are the hardest requirements to satisfy. The performance criteria involved determining the burn time required for the three main maneuvers to be executed by the propulsion system: orbit maintenance, collision avoidance and deorbitting.

The trade-off concluded that the best suited propulsion system was the IFM-Nano Thruster. Characteristics of this system can be seen in the table below:

Table 1.5: IFM Nano Thruster Characteristics.

Cost	TRL	Volume	Mass (wet)	Operating Power	Thrust	Burn Time Collision Avoidance	Burn Time Orbit Maintenance
38.4 k€	9	<1U	0.9 kg	8-40 W	0.4 mN	10.98 hrs	13.15hrs

The IFM Nano Thruster has a variable specific impulse setting that allows for distinct design points to be chosen tailored to the needs of each maneuver. A sensitivity analysis was conducted that resulted in validating the following design points for the corresponding maneuvers:

- EOL maneuvers are conducted at a thrust level of 0.29 mN, a specific impulse of 6000 s and a total impulse of 14 700 N s.
- Collision avoidance and orbit maintenance: specific impulse of 3200 s is supplied allowing for a thrust of 0.42 mN.

Attitude Determination and Control System

The main function of the ADCS is to provide the spacecraft's attitude and to be capable to slew the spacecraft. Then, to accomplish the mission objectives, the ADCS system needs to be able to adjust

its attitude rapidly to center the Focus payload towards the object detected and accurately track it. The ADCS is essentially divided into three parts: attitude control, attitude determination and orbit determination. The attitude control is composed of six reaction wheels and three magnetorquers, has full-three axis control of the spacecraft and is able to slew the spacecraft rapidly. Besides, the attitude determination is performed with two star trackers and an IMU. The spacecraft embarks a GNSS receiver with an GNSS patch active antenna to precisely its position. Then, a SGP4 propagator is added for redundancy, in case there is no signal or the navigation constellation is out of service.

Most of the components of the ADCS are found inside the integrated ADCS, except three additional reaction wheels, a star tracker and a GNSS receiver with a GNSS patch active antenna. In addition, a tool has been created to determine the time it takes to center the Focus payload onto the bright pixel. Then, it is used to calculate the maximum angular velocity between the three axis to assess if the images become blurry during rotation. Rotating 180° in yaw direction and 23° in the roll direction, the time it takes to slew is about 24.36 s and the maximum angular velocity is 12.95 $^\circ\,s^{-1}$.

Table 1.6: Attitude determination and control system characteristics.

Cost	Max. Time to Slew	Max. Slew Velocity	Attitude Knowledge Accuracy
90.1 k€	24.36 s	12.95 $^\circ\,s^{-1}$	10 $''$

For recommendations, a more detailed analysis can be carried out by quantifying a maximum time needed to slew the spacecraft. Then, more research could be performed into the accuracy of the star tracker while the spacecraft is slewing. Conclusively, a more extensive investigation should be done to investigate the feasibility of just three reaction wheels for full-three axis control in the spacecraft.

Constellation

The constellation design follows from the midterm report were it was decided that a streets of coverage constellation was going to be used. After research was performed into the possible methods in order to decrease the number of satellites it was decided that the best method was to use an imaging technique. Therefore, the constellation was design taking into account the results from the payload section. Once the circular imaging technique was set in stone, calculations for the number of orbital planes and number of satellites per plane followed.

Using an altitude of 600 km, as this is when the payload performs best, the required number of satellites per orbit are 34, and a total of 9 orbital planes are needed. It is important to note that for this final design of the constellation double coverage was taken into account thus increasing the number of satellites needed per orbit. However, this double coverage increased the reliability of the system. Therefore, it was decided that a higher reliability was desirable over a relatively small reduction in the number of satellites.

Table 1.7: Constellation characteristics.

Inclination	# of Orbital Planes	# SC per Plane	Total # of SC
90°	9	34	306

Final System

With the spacecraft fully integrated, see Figure 1.1, detailed budgets on the most relevant technical resources have been created. To do so, the contingency management plan that was set in place for the preliminary system is used. For the mass, the total is 20.27 kg, with the largest contribution being the payload accounting for 43.7 %. For the power, the pulse-tube cooler necessary for the IR camera presents the highest continuously required power and thus drives the design of the EPS. It should be noted that the large contingency on these components, due to further R&D being needed ,accounts partially for their significant contributions. For the time budget, it has proven that the ground station can receive the level 3 alert within 90 s (64.9 s needed), and that the first 3D target location

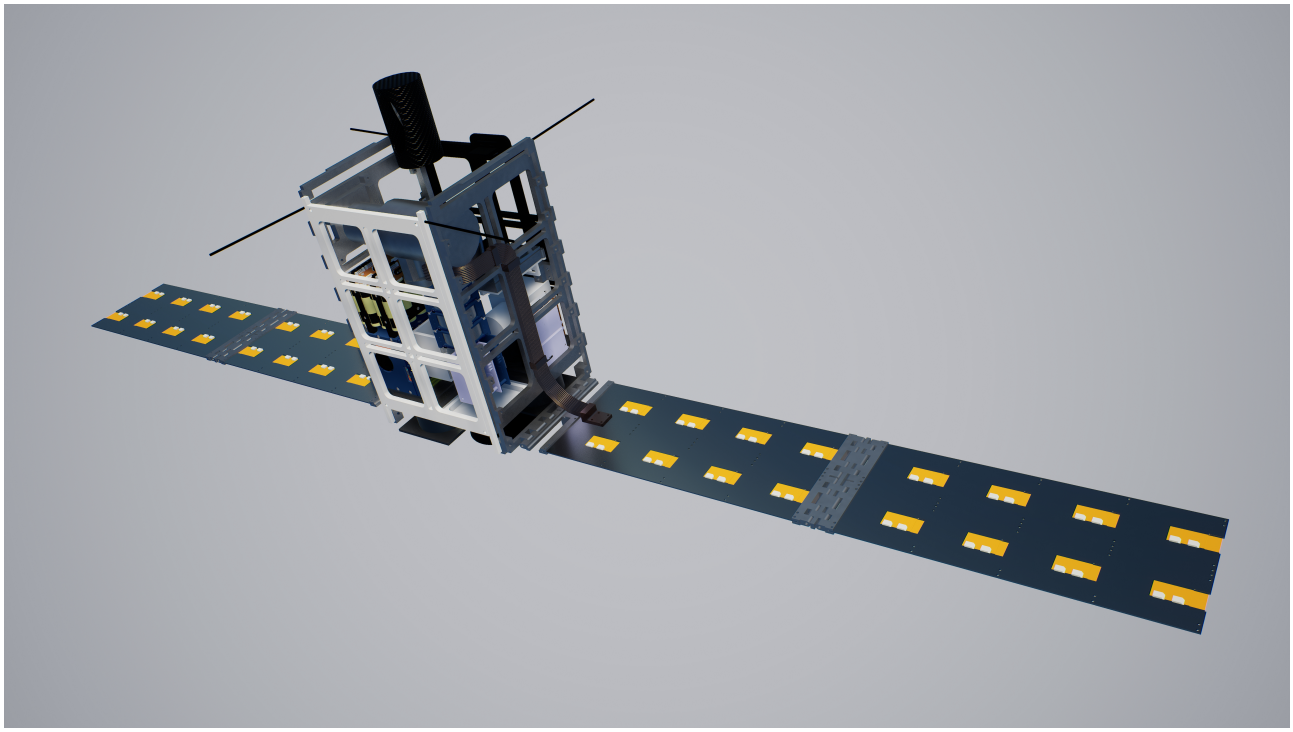

Figure 1.1: Render of the integrated M-STAR spacecraft.

arrives after 92.3 s in the worst-case scenario. Finally, the ΔV budget that accounts for orbital station keeping, collision avoidance maneuvers and an end-of-life burn has been updated with the specific orbital parameters and of the propulsion system chosen, amounting to a total of 187.17 m s^{-1}.

With the final system architecture known, and the sub-system components identified, a detailed cost analysis is performed. It consists of all recurring costs per satellite, such as sub-system components, software, system engineering costs, etc, as well as non recurring cost or R&D. A total Theoretical First Unit (TFU) price of €1,064,050 is estimated, with a total Research, Development, Test & Evaluation (RDT & E) cost of €4,461,922. With a learning curve applied for the manufacturing of the 7 satellites needed for the technical demonstration mission, the total budget needed is estimated at €11,275,943. This is well below the budget requirement set by the RNLAF, and can account for more extensive testing costs if need.

Table 1.8: Final system characteristics.

Total Mass	Total TFU Price	Total ΔV	Time for L3 Alert to GS
20.27 kg	€1,064,050	187.17 m s^{-1}	64.9 s

Following the final configuration and the allocated budgets, a system-wide sensitivity analysis was performed. This was done for the three most critical requirements for the technical demonstration mission; REQ-SYS-01-02, REQ-SYS-01-05 and REQ-SYS-01-06. The power and time budgets were manipulated for the most critical scenarios and it was checked that all the requirements would still be met. It was found that more in depth research has to be done into processing frequency, as well as tracking frequency. Furthermore, the power budget was evaluated against it's most critical case; and it was found that if more power was required for the cooler, all the requirements would still be met.

Since the project reaches a higher level of detail in the final phase of the DSE, new and subsystem specific risks could be identified. Subsequently, a risk management approach according to the ECSS standard has been performed. By means of collaborative brainstorm sessions, around thirty risks have been identified. These risks have been ordered in a risk register and graded on both their likelihood and severity. When possible, mitigation acts have been identified to bring the risks down to

an acceptable level. The ten most mission threatening risks are stated in the risk section together with a more detailed description of their mitigation acts. Out of the identified risks, large errors due to a single satellite being responsible for detection and tracking was found to be most mission threatening. This has been mitigated by an extensive plan of action for the use of multiple satellites for detection, tracking and classification as described in the functional flow diagram.

Development Overview

The development overview is divided into 7 phases. Phases 0, A and B were executed in the previous reports. This is due to the fact that Phase 0 is the project planning phase, which is elaborated on in the Project Plan [3]. Phase A, the feasibility analysis of the mission, is described in the Baseline Review [4]. Finally, Phase B is concerned with the preliminary design phase which is outlined in the Midterm Report [5]. This report focuses on Phases C to F.

Phase C is where the final design is concluded. Phase is divided into 3 parts; Firstly the system compliance matrix is established, enabling to check which system requirements are fulfilled. All but 4 system requirements were found to be fulfilled. Firstly, **REQ-SYS-01-04**, the 1 km ICBM location accuracy is not met. Design choices led to only 95.8 %. For **REQ-SYS-01-05** and **REQ-SYS-01-06** it is out of the scope of the DSE to assess if they will be met. The system has been designed such that communication and tracking can be done while maneuvering but it will not be known for sure until tested. Finally, **REQ-SYS-01-18** is difficult to evaluate as the loads of the mission are not known yet. Once the loads are known, the design can be more detailed and more specific tests can be performed in order to see if the requirement is fulfilled.

The second part of Phase C is the RAMS. The reliability of the system has proven to benefit from the constellation being designed for double coverage and from the use of COTS flight proven components in most bus systems. For the availability, the 99% requirement is met during nominal operation as the spacecraft must only cease imaging operations when performing a propulsive burn. Through these burns, the maintainability of the system is enhanced as orbit degradation can be accounted for. Moreover, the constellation allows for the integration of new satellites in case a spacecraft would go down. In addition, a high level of safety for the mission is attained through the definition of a safe operational mode that the spacecraft can enter when off-nominal readings are provided by its sensors or more than 48 h have passed since the last ground communication.

Thirdly, the manufacturing, assembly, integration and test plan (MAIP) is explained. For the manufacturing most of the components are COTS therefore tests are already performed. For the non COTS components Type Testing will be performed. Since, if a component is certified with Type Testing, all other batches of that component will also be certified as long as the production follows the same steps. For assembly, it was defined that three types of satellites need to be built, a Prototype Model (PM) a Flight Model (FM) and then 6 more satellites for the IODs. For this, the PM and FM will be assembled once all the parts are ready and shipped to the assembling facility. This is due to the fact that in case a component needs to be changed only one needs to change and not all six that need to be produced. As for the assembly site, it will likely be where the provider of the structure is, in this case in Italy. Finally, for the integration and assembly tests need performed.

There are two main sets of tests to be performed. Firstly, environmental tests which test that the spacecraft is able to withstand launch and space conditions. The environmental tests are the following: Acoustics, EMC, flight tests, thermal tests, vibration and shock testing, deployment testing and space simulations.

The second set of tests are integration tests. These tests check the efficiency and co-dependence of the spacecraft. The following integration tests will be performed:group delay measurements, linearity and grain transfer measurements, signal quality measurements, spurious measurements and digital interface testing.

After Phase C comes Phase D. This phase consists on qualification and verification of the mission. In order to show the system works In Orbit Demonstrations (IODs) will be performed, enabling demon-

stration of the feasibility of using the payload for a purpose that it was originally not designed for. There will be three IODs which are the following:

- **IOD1**: IOD1 entails one satellite and is performed to verify all the functions from Chapter 4, Figure 4.1 that can be performed by an individual satellite. The IOD is concerned with verifying payload performance, including Filter Switch, Optics and the Mirror and all data processing performed by the DPU.
- **IOD2**: IOD2 is performed with two satellites and the main focus is verification of the interlinking communication system and triangulation process. As IOD2 will be performed only when IOD1 has been completed successfully, it can be assumed that all functionalities mentioned for IOD1 requried to perform IOD2 have been verified at this stage.
- **IOD3**: IOD3 is performed with 6 to 7 satellites. For this IOD the functionalities that will be tested are less obvious. The main focus will be with regards to the redundancy of the constellation and data relay latency. This entails amongst others out of plane communications and inter-plane and out of plane satellite-skip interlinking.

For mission validation two tests will be done. Firstly, CDH validation will be performed. The CDH is validated using rocket launches, rocket launches are scheduled and can therefore be known. Subsequently cross-referencing of CDH data and known location data assists in CDH validation. The second type of mission validation is data validation. This will be performed by implementing the data collected in M-STAR satellites in validated trajectory prediction programs, and as such enabling validating data completeness and data quality.

Phase E follows, and addresses the operations and logistics involved in both the execution of the technical demonstration mission as well as the transition to a full-scale operational mission. This included the determination of launch procedures: the team hopes to cooperate with Virgin Orbit to facilitate the technical demonstration mission. Furthermore, moving to a full-scale operational mission, design need to be updated starting from Phase C.

Following Phase E comes Phase F where the retiring phase of the mission is elaborated upon. Firstly, the end of life of the demonstration mission is assessed. On the one hand, if the technical demonstration mission is successful (as such IOD3), then the satellites are left in orbit and more satellites are built in order to expand to the full constellation. The satellites will only be de-orbited at the end of the mission lifetime. On the other hand, in scenario where the technical demonstration missions are failing to verify the functions at test, in each IOD, the on-ground team returns to phase B, where feasibility and mechanisms that were not verified need to be analyzed further. Regardless of which path the IODs progress in, the satellites remain in orbit for a minimum of 7 years in order to verify the mission requirement that all subsystem components must have a life time of 7 years.

The second step of Phase E and final step of the development overview is the transition from the demonstration mission to the operational mission. In order to be able to transition to the full constellation the following steps are in order: the MAIP plan needs to be modified as the manufacturing, assembly and integration of 300 satellites required other considerations than 6. Additionally, shipping plans will change too. Furthermore, deeper research needs to be done for the launch capabilities. Launching 300 satellites puts a constraint on which companies you can use and also how many you can fit in one launch. Moreover, the launch site also needs to be taken into account as launching 300 satellites from the same launch site will put a constraint on the Δ needed to reach the correct orbits.

2

Project Objectives

The only constant is change. History shows that this applies seamlessly to the geopolitical environment worldwide. Ballistic missiles have evolved from being national to intercontinental, and the geopolitical environment has been transforming concurrently. With the increasing variety in range for ballistic missiles, establishing an early warning system becomes more important than ever. Momentarily, the only early warning system is located in the United States. The importance to become militarily independent of this single point of failure can not be underestimated.

Deficiencies are present within Europe and NATO with respect to central Intelligence, Surveillance and Reconnaissance. The revolution in the space industry presents opportunities to The Dutch Ministry of Defence to aim to fill this niche. With the decreasing cost in the development of space assets and the ambition of the Royal Netherlands Airforce (RNLAF) to become militarily independent in mind, this project was found. The Design Synthesis Exercise, as it was presented to Project Group S12 of the Faculty of Aerospace Engineering, is the following: *"Generate a complete design of a technical demonstration mission, maximising effective use of a nanosat constellation to perform Early Warning for the Netherlands and its European Partners against ballistic missile threats"* [1]. Accordingly, the project has been named 'Missile Space-based Tracking and Relay' (M-STAR).

Deduced from the goal of the mission as it was presented by the customer, Project Group S12 generated a Mission Need Statement (MNS) and Project Objective Statement (POS) during Phase 0 of the project in the Project Plan [3]. The MNS and POS function as the groundwork for this Final Phase of the project and are defined as follows:

Mission Need Statement. *"Provide a technical demonstration for an early warning system against ballistic missile threats for the Netherlands and its European Partners by 2024."*

Project Objective Statement. *"Design a complete technical demonstration mission concept, by maximising effective use of a constellation of nanosatellites, by 11 students, in 10 weeks."*

In the aim of accomplishing this mission, this is the fourth and final report created by Project Group S12, following the Project Plan and the Baseline and Midterm reports. In this final report, a complete and exhaustive description of the design is presented. Firstly, the target market is analysed in Chapter 3. Secondly, an expanded view on the functional breakdown for the mission is offered in Chapter 4. This is followed by the most relevant top-level requirements in Chapter 5, which, together with a summary of the previous work done in the midterm phase (Chapter 6) set the starting point for the engineering tasks carried out to deliver this report. Consequently, these technical aspects can be found in Chapter 7 through Chapter 14, as they are divided into its relevant spacecraft subsystem. For every one of them, a functional and requirement analysis is performed, together with a description of its design, a sensitivity analysis, its verification and validation, RAMS characteristics and recommendations for future work. In some cases, such as for the payload and propulsion system, a trade-off has been performed. Once all subsystems have been described in detail, the system is integrated in Chapter 16 and the compliance to the stipulated requirements is checked. Subsequently, the detailed plan to complete the technical demonstration mission through the relevant project phases is presented in Chapter 17. Finally, the conclusions from the team and the recommendations for future work are discussed in Chapter 18 to complete this DSE project.

3
Market Analysis

Before the design process, it is essential that an understanding is developed of the market in which the product will be launched. The market analysis is a means of generating relevant requirements based on socio-economic perspectives of the mission. It is important to note that the market in which this mission will operate is one of military importance, and thus accessing information on existing missions and stakeholders is limited. Furthermore, the most important outcome of this market analysis is the SWOT analysis, as this is where important requirements are generated. Understanding market shares, mission costs and market trends is secondary, as a military mission is monetarily non-profitable.

First, it is important to understand the larger industry in which this mission is positioned, and perform an industry segmentation. The total available market (TAM) has been identified as the global space market, the segmented available market (SAM) has been identified to be space based military operations. Finally, the target market, within the TAM and the SAM, has been identified as 'Early Warning Systems'. The SAM, being a military market, has limited publicly available information; consequently, the information on the target market is also limited.

When looking at the SAM, it has been estimated that approximately 320 military satellites are in operation, where the US operates approximately half of them (around 125), followed by Russia (around 75), and China (around 70) [6]. Furthermore, the SAM has a predicted Compound Annual Growth Rate (CAGR) of 6% within the forecast period 2021-2025 [7]. Within the SAM, the largest trend currently is miniaturisation. Thus, it may be beneficial to consider the growth of the nano satellite market. As can be seen from Figure 3.1 [8], the nanosat market started growing rapidly over the last 10 years. Due to this growth, as well as the accessibility and simplicity of satellite development, competitive pricing and COTS modules exists for nanosat buses. Currently, the average cost of an integrated 6U satellite is approximately $1.4 million [8].

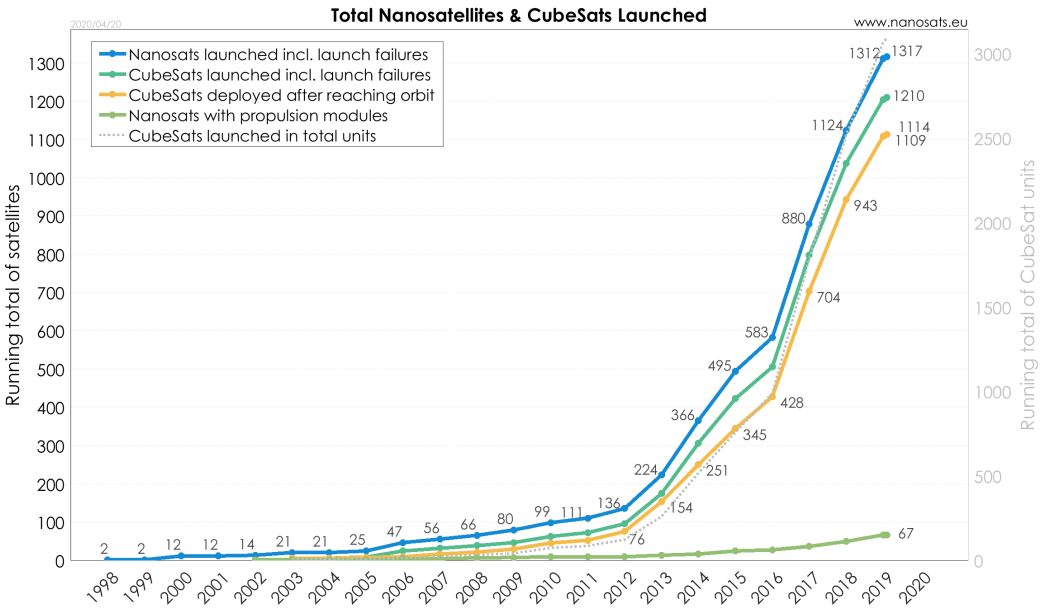

Figure 3.1: Number of CubeSats and Nanosats launched over the last 20 years [8].

When looking at the target market, two known missions exist; operated by the United States, and by Russia. The United States' Space Based Infrared System (SBIRS) has four equal priorities: missile warning, missile defence, enhanced technical intelligence, and battle space characterisation. SBIRS provides global coverage, however the latency of detection has not been publicly disclosed [9, 10]. There are currently four GEO satellites, and two payload sensors in high elliptical orbits (HEO) on host satellites in operation. The HEOs are Molniya orbits, and in the following two years, two more GEO satellites are planned to be launched [9, 10]. The GEO satellite payload consists of approximately 450 kg of infrared scanning and staring sensors for short and mid wave ranges. The cost of the mission has been estimated to be over 20 billion US$ [10]. Russia's EKS is mostly classified, however it is known that the EKS system detects missile launches, and is able to track them to the target[11]. As of now, three out of six satellites are in orbit, and are all in a Molniya orbit. The speculated payload one primary telescope and one side looking scanning sensor [11].

Thus, from this, a market share may be identified. For a military mission, it may be considered meaningless to estimate a monetary market share for two reasons: (i) Existing missions may be classified, meaning that an estimation would be largely speculative, and thus inaccurate. (ii) Missions within this target market are not monetarily profitable missions. Thus, an estimation can be made based on other parameters, such as population and land area. If early warning detection of ICBM's was provided for all NATO countries, security would be provided to 8-12% of the World's population, and 10-16% of the World's land area, depending on whether or not the United States is included.

Furthermore, it is important to identify the key stakeholders in the mission specified by the RNLAF, such that there can be an improvement in space market. That is to say that there is a potential to mitigate the fear of space militarisation, while still being able to fulfill mission requirements. For the mission specified by the RNLAF, the key stakeholders would include: the Dutch Ministry of Defence, TU Delft, the launch provider, the mission operator, NATO, and the tax payers (as this is a publicly funded mission).

Finally, a prediction of the future market may also be made. Today, there are increased political tensions between, for example, the United States, North Korea, Iran and Iraq. Hence, it may be possible for these states launch similar space based military projects. More importantly, with tensions rising, the necessity exists to mitigate the problems of the future market. For this reason, it may be of essence for NATO to implement a Early Warning System supplementary to SBIRS. In terms of technological advancements, an increase in nanosatellites or other small satellites may be observed, as this market is growing rapidly. Such advancements would enable fast paced developments towards launches, and lower costs; implying that spaces-based military operations may accelerate, and that the previously mentioned CAGR may be exceeded.

SWOT Analysis

Following this, a SWOT (Strengths, Weaknesses, Opportunities and Threats) analysis is performed. Outlined below are the central characteristics of entering the target market with a nanosat constellation to detect ICBM's mandated by the RNLAF. The corresponding requirements have been identified as stated in Chapter 5, these requirements either mitigate the weaknesses and threats, and maximise the strengths and opportunities. [4]

S.1: The proposed mission brings security to the partner states. In order to maximise this strength, **REQ-MIS-01**, and all its sub-requirements are defined [4].
S.2: The proposed mission will be mandated by the RNLAF, meaning that the goal of the end product is clear and shall be tailored to the needs of the public, as specified by the RNLAF. In conjunction to S.1; the customer is most aware of the necessity of the missions, and shall be able to maximise S.1 through their global military knowledge [4]. Requirement **REQ-MIS-10** enforces this strength [4].
W.1: Potential lack of funding. Budget is much smaller than similar missions, and fully depended upon by the government. Thus, the necessary funding may not be procured in a timely manner. Such that this weakness may be reduced, **REQ-MIS-03, REQ-SYS-04, REQ-MIS-05, REQ-SYS-06** and all its sub requirements are defined [4].

W.2: Leading from W.1. If funding is not procured in a timely manner, time of development may rise [4]. The requirements to mitigate this are identical to those stated in W.1 [4].
W.3: Space sustainability. Debris creation and collision probability need to be mitigated. The use of a constellation may cause future problems due to space debris creation [4]. To mitigate this, **REQ-SYS-14** and **REQ-SYS-16** are defined.
O.1: In conjunction with S.1, increased necessities for early warning systems due to rising political tensions. See requirements stated in S.1.
O.2: Utilising the growing and competitive nanosat market to decrease cost, mass and potential development times [4]. **REQ-MIS-03, REQ-MIS-05, REQ-MIS-07** and **REQ-SYS-06** are defined to encourage this opportunity.
O.3: The possibility of utilising small launchers to decrease environmental impacts.
REQ-SYS-06 defines launch configurations, this is also in conjunction with cost minimisation [4].
O.4: Currently, there is a lacking system in place for all NATO member states. Thus, a large market gap may be fulfilled. The requirements to profit from this opportunity are identical to those stated in S.1 and S.2.
O.5: There lies an opportunity in using the collected data for civilian use too, if necessary[4]. Examples include bush fires and volcanic eruptions. No requirements have been defined for this opportunity, as this would be a secondary use[4].
O.6: Launching such an early warning system may increase the political and/or military presence of the Netherlands [4].
T.1: Public perception and fear of militarisation of space.This may lead to protests/public outrage [4]. In order to minimise this, **REQ-MIS-10** is defined[4].
T.2: Increased political tensions due to the defensive act of placing an early warning system in space. This is a consideration especially if a false positive is detected. Such that this threat may be weakened, **REQ-SYS-01-01, REQ-SYS-01-05, REQ-SYS-01-06** and **REQ-SYS-01-07** and are defined [4].
T.3: Threat of satellite being targeted by a missile due to T.2. In order to detect, warn the ground segment of such an event, and replace the satellite, **REQ-SYS-07** and **REQ-SYS-12** including all its sub-requirements are specified [4]. Furthermore,
REQ-SYS-01-01, REQ-SYS-01-02, also specified in S.1 and S.2, are beneficial to mitigate this threat.
T.4: The final product needs to be reliable and resilient in order to maximise strengths [4]. Space weather may introduce degradation and communication threats. **REQ-SYS-18** and, **REQ-SYS-08** are defined in order to ensure that the system is designed for such conditions [4]. **T.5**: The trajectory calculation is based on the velocity at burnout. However, if technology is developed in which the ICBM is able to alter its trajectory mid-flight, then this trajectory prediction would no longer be valid. In this case, the missile need to be tracked past burnout.

4
Functional Breakdown

In this chapter, the functionality of the mission is described. With the goals stated in Chapter 2 in mind, the functional flow in Figure 4.1 is created. Due to the complexity of the detection/tracking operation, a second diagram is presented in Figure 4.2 with a more detailed view on the function of the system in those circumstances. These diagrams are then restructured to be presented as a functional breakdown in Figure 4.3, and are referred to in each subsystem functional analysis, as each subsystem function is a flowdown of a block in the diagram. In the following section, alert levels created to clearly define the terms used throughout the report are introduced in Section 4.1. Next, the different roles the spacecraft takes during detection and tracking of ICBMs are detailed in Section 4.2.

4.1. Alert Levels

Alert levels have been defined as being milestones in the process of detection and classification of the ICBMs. They are raised under specific circumstances, and trigger a certain response from the system. The alert levels are defined as shown below.

1. **Alert LEVEL 1 - H_2O anomaly**: the IR instrument reports an anomaly due to a brighter than average pixel, in the wavelengths corresponding to H_2O. This alert is raised after function 4.3.1.2, see Figure 4.2.
2. **Alert LEVEL 2 - H_2O+CO_2 anomaly**: after the previous alert level has been reached, the IR instrument reports the same anomaly to be present in the wavelengths corresponding to CO_2. This alert is raised after function 4.3.1.7, see Figure 4.2.
3. **Alert LEVEL 3 - Confirmation that object is moving**: after the previous alert level has been reached, the OBC determines that the anomaly is not stationary and must thus be tracked and its position triangulated. This alert is raised after function 4.3.2.1, see Figure 4.2.
4. **Alert LEVEL 4 - Missile is classified by burn-time and staging**: the intensity of the pixel dims and then increases again. When this information reaches the ground, classification based on staging and burn time is performed. This alert is raised either during 4.3.3.8 (three stages) or after 4.3.2.11 (single or two stages), see Figure 4.2.
5. **Alert LEVEL 5 - Missile is classified by burnout velocity**: the position of the missile in the last measurements before burnout reach the ground station, where the burnout velocity is computed. This alert is raised after 4.3.2.11 (single or two stages), see Figure 4.2.

4.2. Roles of the Spacecraft During Detection and Tracking of ICBMs

The detection and tracking of an ICBM is an operation that involves multiple M-STAR spacecraft, as can be seen at the bottom of Figure 4.2. Any satellite can take on any of three different roles, categorised below.

- **SC1** is the spacecraft under who's field of view (FOV) the ICBM appears for the first time, and thus it raises an alert level of 3. Its function during the tracking of the target is to provide its positioning data to SC2. Because communication between satellites only occurs after alert level 3 is raised and FOV overlap is possible, multiple spacecraft could take on this role at first. A hierarchy based on the optimal satellite position is thus present.
- **SC2** is the spacecraft who has the function of rapidly locking on to the moving anomaly after level 3 is raised to allow for stereo imaging. As such, SC2 receives the positioning data from SC1 and combines it with its own to triangulate the ICBM.
- **SC3** is the spacecraft that, because of its vicinity to the area towards which the ICBM is moving, stands by to take on the role of SC2 if SC1 becomes too distant to the target.

MISSION FUNCTIONAL FLOW DIAGRAM

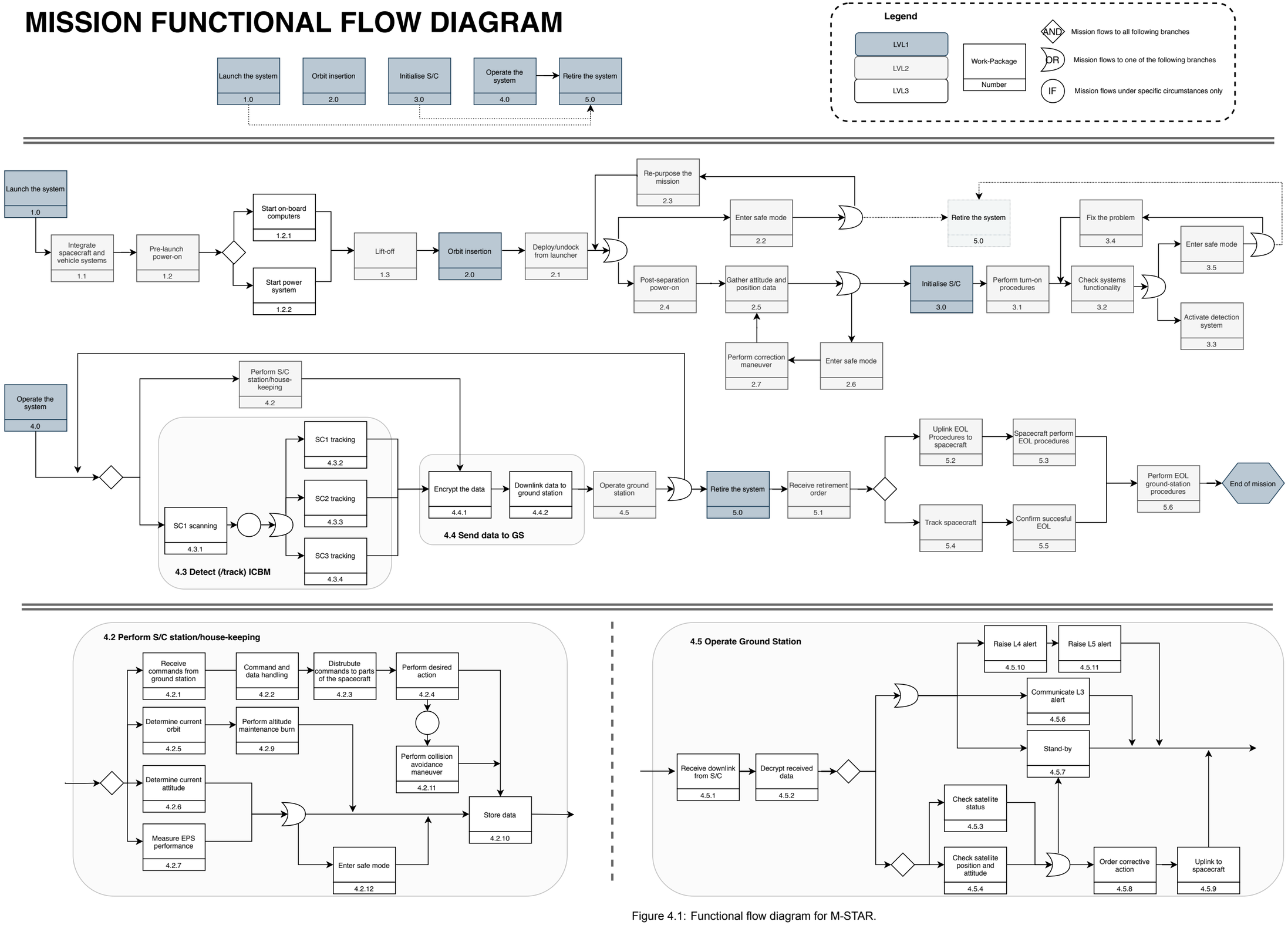

Figure 4.1: Functional flow diagram for M-STAR.

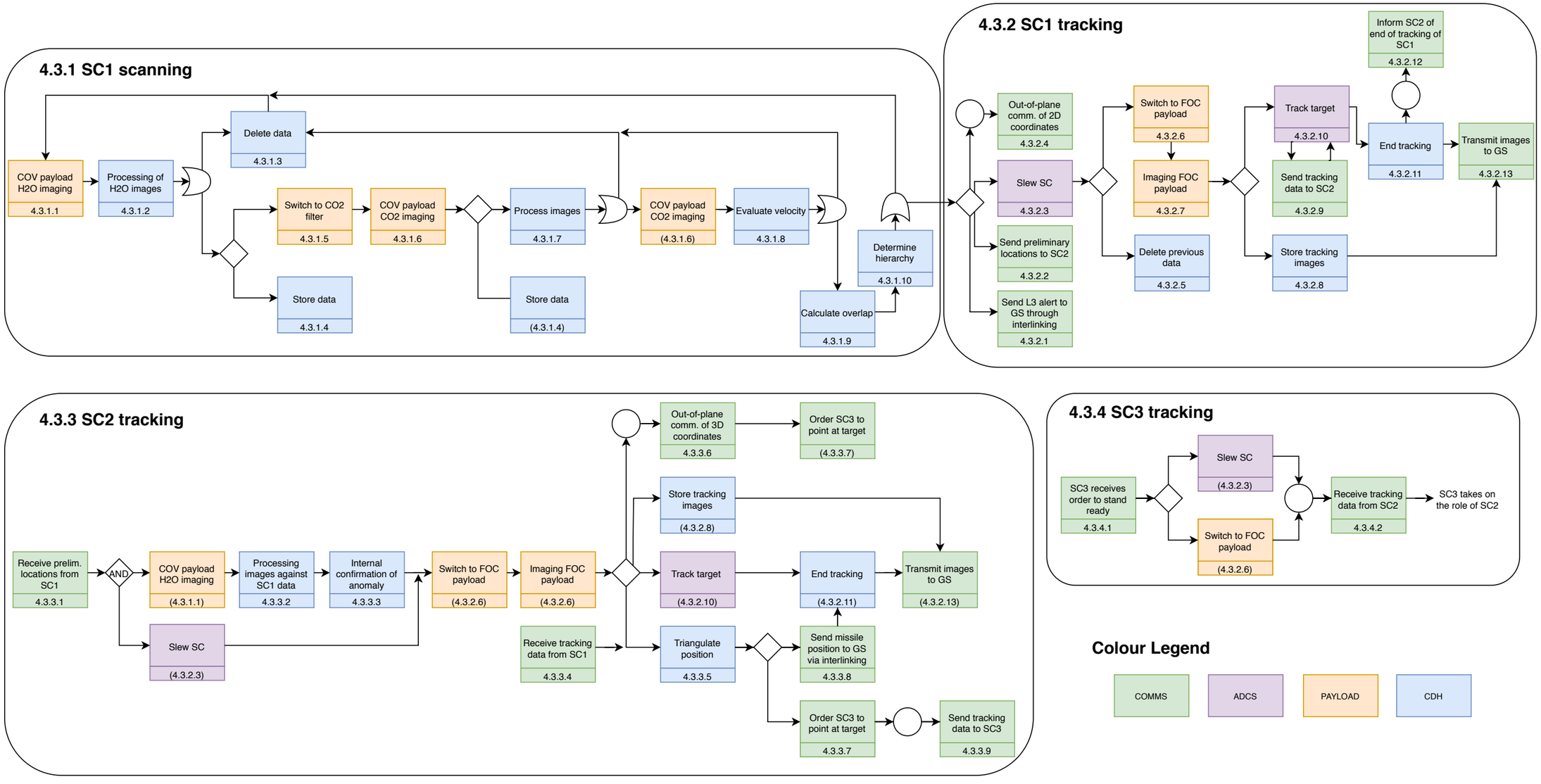

SPACECRAFT INTERACTION FOR EARLY WARNING

ALERT LEVELS
L1: H2O anomaly
L2: H2O+CO2 anomaly
L3: Object is moving
L4: Missile is classified by burn-time and staging
L5: Missile is classified by burnout velocity

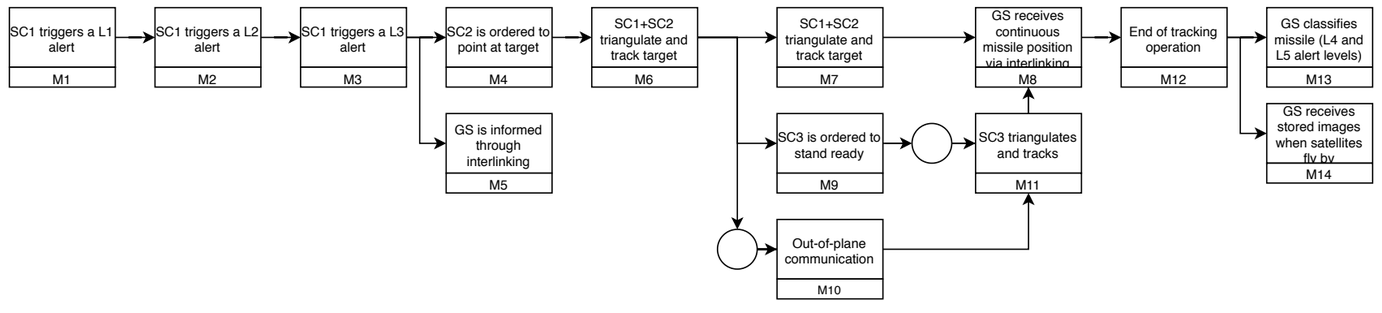

Figure 4.2: Detailed functional flow diagram the detection and tracking of ICBMs.

FUNCTIONAL BREAKDOWN STRUCTURE

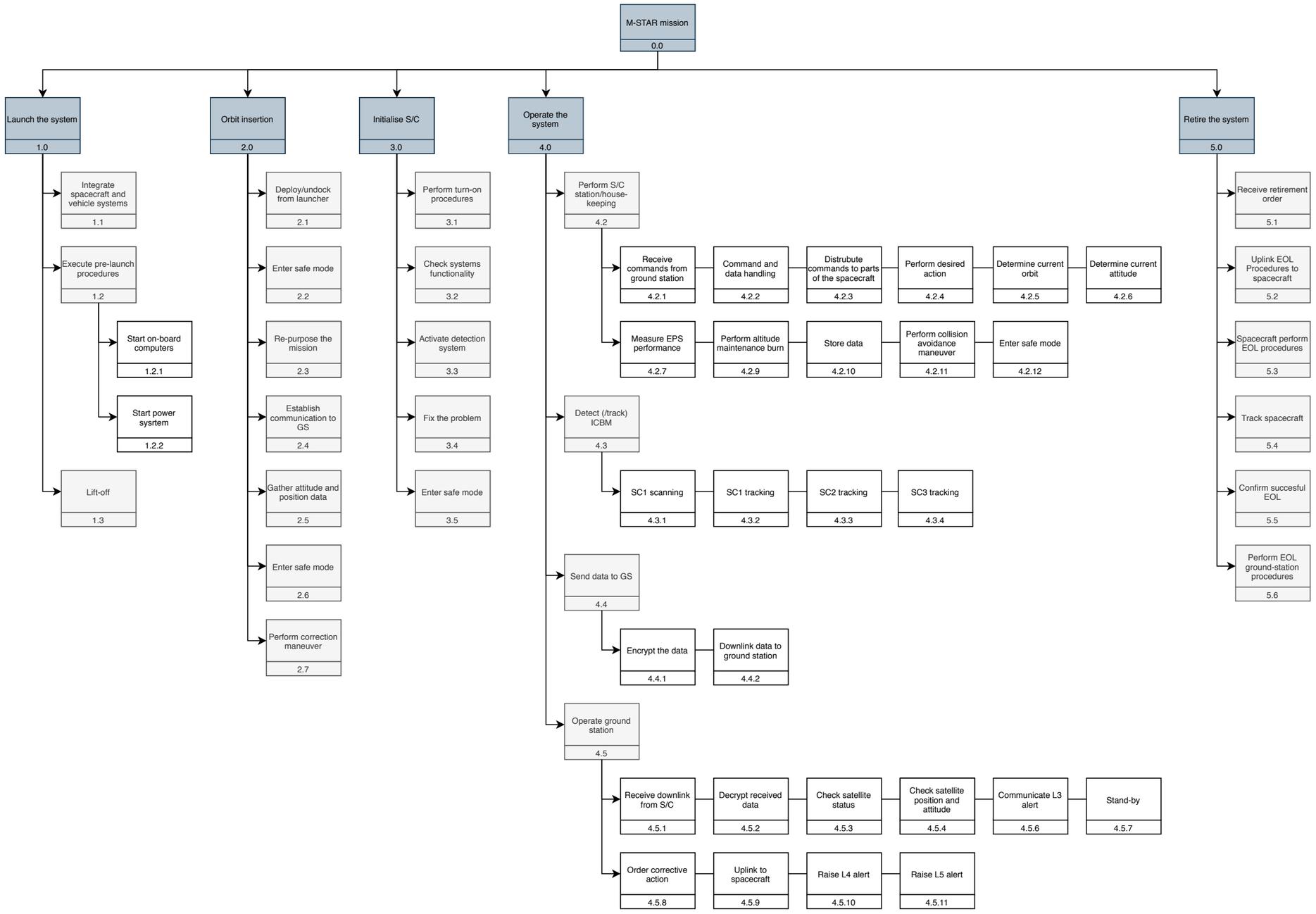

Figure 4.3: Functional breakdown structure for M-STAR.

5
M-STAR Requirements

This chapter outlines the requirements that set the foundation for this DSE project. These are divided in user, coming from the costumer, and system requirements, coming from the design team. User requirements are top-level requirements that express what the RNLAF desires to accomplish through this mission. As such, they represent the starting point for the M-STAR project. System requirements follow from the user requirements and are the ones on which the M-STAR satellites were designed.

5.1. User Requirements

REQ-MIS-01: The mission shall provide Early Warning for the Netherlands and its European partners against ballistic missile threats.
- **REQ-MIS-01-01:** The mission shall provide global coverage.
- **REQ-MIS-01-02:** The mission shall alert ground stations of an ICBM detection within a maximum of 90 seconds after launch of the missile.
- **REQ-MIS-01-03:** The mission shall track ICBMs from detection until the end of the boost phase.
- **REQ-MIS-01-04:** The mission shall detect the missiles within a 1 km (3-sigma) accuracy in all 3 dimensions.
- **REQ-MIS-01-05:** The mission shall have 99% availability for communication of detection relays.
- **REQ-MIS-01-07:** The mission shall be able to differentiate ICBMs from other types of missiles or from space launchers.

REQ-MIS-02: The mission's communication shall be encrypted in AES256 method.
REQ-MIS-03: The mission shall be ready for launch by 2024.
REQ-MIS-04: The mission lifetime shall be at least 7 years.
REQ-MIS-05: The mission shall cost less than 30M€ excluding launch costs.
REQ-MIS-06: The mission shall be compatible with existing nanosat launch options.
REQ-MIS-07: The mission shall accommodate the addition of future nanosats.
REQ-MIS-08: The mission orbit shall be LEO.
REQ-MIS-09: The mission's space segment shall be self-sufficient for communication relay.
REQ-MIS-10: The mission shall be approved by the RNLAF.

5.2. System Requirements

REQ-SYS-01: The system shall provide Early Warning for the Netherlands and its European partners against ICBM threats.
- **REQ-SYS-01-01:** The system shall provide global coverage.
- **REQ-SYS-01-02:** The system shall alert ground stations of an ICBM detection (alert level 3) within a maximum of 90 s after launch of the missile.
  - **REQ-SYS-01-02-01:** The system shall be able detect ICBMs of at least 10 m length and 1.6 m diameter.
  - **REQ-SYS-01-02-02:** *DELETED*
  - **REQ-SYS-01-02-03:** The system shall be able to detect ICBMs flying at altitudes in the range of 13 km to km [12] from Earth's surface.
  - **REQ-SYS-01-02-04:** The system shall inform the ground station of ICBM detection (alert level 3) within 90 s after launch of the missile.
  - **REQ-SYS-01-02-05:** The system shall be able to detect the coordinates of the ICBM with a 1 km (3-sigma) accuracy in all 3 dimensions.
- **REQ-SYS-01-03:** The system shall track ICBMs from detection until the end of the boost phase.
  - **REQ-SYS-01-03-01:** The system shall be able track ICBMs of at least 10 m length and 1.6 m diameter after detection.
  - **REQ-SYS-01-03-03:** The system shall be able track ICBMs flying at altitudes in the range of 13 km to 450 km [12] from Earth's surface.

- **REQ-SYS-01-04:** The system shall locate ICBMs within 1 km (3-sigma) accuracy in all 3 dimensions.
  - **REQ-SYS-01-04-01:** The system shall be able to track the coordinates of the ICBM with a 1 km (3-sigma) accuracy in all 3 dimensions.
- **REQ-SYS-01-05:** The system shall have 99% availability for communication for detection relays.
- **REQ-SYS-01-06**: The system shall have 99% reliability for communication for detection relays.
  - **REQ-SYS-01-06-01:** The system shall be able to detect ICBMs with at most 1% probability of false negatives.
  - **REQ-SYS-01-06-02:** The system shall detect ICBMs with a maximum of one false detection per 100 correct detections.
- **REQ-SYS-01-07:** The system shall be able to differentiate ICBMs from other types of missiles and from space launchers.

REQ-SYS-02: The system's communication shall be encrypted in AES256 method.

REQ-SYS-03: The system shall be ready for launch by 2024.
- **REQ-SYS-03-01:** The system shall use components with at least a TRL of 5.

REQ-SYS-04: The system shall have a lifetime of at least 7 years.

REQ-SYS-05: The system shall cost less than 30 M€ excluding launch costs.

REQ-SYS-06: The system shall be compatible with existing nanosat launch options.
- **REQ-SYS-06-01:** The system shall be compatible with a maximum launcher platform size of 300x200x200 mm.
  - **REQ-SYS-06-01-01:** The system (undeployed) has a maximum size of 300x200x200mm.
- **REQ-SYS-06-02:** The system mass at launch shall be less than 24 kg per spacecraft.
- **REQ-SYS-06-03:** The system shall withstand launch temperatures.

REQ-SYS-07: The system shall accommodate the addition of future nanosats.

REQ-SYS-08: The system orbit shall be LEO.
- **REQ-SYS-08-01:** The system shall be able to cope with the radiation of a LEO orbit.
- **REQ-SYS-08-02:** The system shall be able to cope with the temperatures of a LEO orbit.

REQ-SYS-09: *DELETED*

REQ-SYS-10: The system's space segment shall be self-sufficient for communication relay.
- **REQ-SYS-10-01:** The system shall not make use of any existing satellite constellations for communication relay.

REQ-SYS-11: The system shall be able to store all relevant data locally before transmitting to the ground station.
- **REQ-SYS-11-01:** The system shall transmit the relevant payload data to the ground station(s).
- **REQ-SYS-11-02:** The system shall communicate any failure in payload function to the ground station(s).

REQ-SYS-12: The system shall be able to monitor its own status.
- **REQ-SYS-12-01:** The system shall be able to determine its own orbit.
- **REQ-SYS-12-02:** The system shall be able to determine its own attitude.
- **REQ-SYS-12-03:** The system shall be able to measure its own EPS performance.
- **REQ-SYS-12-04:** The system shall perform ground station(s) check-ins throughout the mission.

REQ-SYS-13: The system shall pass ISO standards.

REQ-SYS-14: The system shall avoid damage due to debris during the mission life time.

REQ-SYS-15: The system shall track the positions of the nano-satellites in the constellation during the mission lifetime.

REQ-SYS-16: The system's presence in the LEO shall be limited to max 25 years after the end of mission. *The reason behind this is to mitigate debris population growth.*

REQ-SYS-17: The system shall be able to perform station keeping space-segment maneuvers.

REQ-SYS-18: The system shall withstand all static and dynamic loading during the mission life time.

REQ-SYS-19: The system shall decrypt down-linked payload data.

REQ-SYS-20: The system shall power itself.

6
Preliminary Concept

In this chapter, the trade-off of the final concept chosen in the midterm report is described. Therefore, the criteria on which the concepts were analysed are presented, as well as the scores of each concept. Next to that, the budget used before the final design is presented. A contingency management and four preliminary budgets are described. The four preliminary budgets are: ΔV, mass, link and power budgets. Most of the preliminary budgets are taken from previous reports as they were still useful for the final budgets.

6.1. Trade-off

In the midterm report [5], four distinct concepts were considered for the final design. In order to understand which is the most suitable concept, a trade-off was performed. The four concepts all use the same constellation pattern, but they vary in payload and communication. For payload, the main differences is that the concepts use different possible combinations between the Coverage and Focus payload. Instead, the variations in communication depend on the payload choose. The four possible concepts are the following:

- Concept 1: Coverage IR + Focus IR with patch antennas.
- Concept 2: Coverage IR + Focus IR and Hyper-Spectrum with patch antennas.
- Concept 3: Coverage Hyperspectral + Focus IR with patch antennas.
- Concept 4: Coverage IR + Focus with high gain antennas or optical communication.

In order to perform a trade-off, a criteria is needed to differentiate which concept is the most feasible. Therefore, a ”quality function development” (QFD) procedure is used and consists of the following steps:

I. The costumer needs are determined and associated to their respective requirements. In this case, these were the need for global coverage (following from **REQ-MIS-01-01**), short alert latency (from **REQ-MIS-01-02**), detection close to burnout (from **REQ-MIS-01-03**), high-position accuracy (from **REQ-MIS-01-04**), a launch in 2024 (from **REQ-MIS-03**), low-cost (from **REQ-MIS-05**), CubeSat dimensions (from **REQ-MIS-06**), and the use of LEO orbit (from **REQ-MIS-08**).
II. The RNLAF grades the different needs in a ”customer importance scale” as follows:
    - 5: the mission’s top priority.
    - 4: crucial for mission success.
    - 3: important for customer satisfaction.
    - 2: desired feature.
    - 1: nice addition but it is not necessary.
III. Each trade-off criteria is then evaluated against each customer’s need according to how strong the relationship between the two is. The possible grades are:
    - 9: need satisfaction follows directly from the criteria.
    - 3: the criteria directly influences the need satisfaction.
    - 1: the criteria indirectly influences the need satisfaction.
    - 0: there is no relation between the two.
IV. The evaluation done in step I. is then weighted by the importance scale reported in step II. to produce the final criteria weight.

The grading scale of all criteria was fixed to be from 1 to 5 (from lowest to highest performing). In addition, a quality function development procedure was established to determine the relative weight

for each criteria. In this way, the weights are set up correspondingly to the requirements given from the costumer, the RNLAF, shown in Table 6.1.

Table 6.1: QFD procedure to determine the criteria weights.

Identifier	Customer Need	Costumer Importance Rating	Cost	Use of Technical Resources	TRL	Payload Performance	Required Pointing Accuracy	Sustainability
REQ-MIS-01-01	Global coverage	*4 [16%]*	0	0	0	3	0	0
REQ-MIS-01-04	Position accuracy	*5 [20%]*	0	0	0	9	1	0
REQ-MIS-01-02	Alert latency	*4 [16%]*	0	0	0	1	9	0
REQ-MIS-01-03	Burnout detection	*4 [16%]*	0	0	0	9	1	0
REQ-MIS-03	2024 launch	*2 [8%]*	3	0	9	0	0	0
REQ-MIS-06	Nanosat	*2 [8%]*	0	9	0	0	0	0
REQ-MIS-05	Cheap	*3 [12%]*	9	3	9	0	0	0
REQ-MIS-08	Use of LEO orbit	*1 [4%]*	1	3	0	3	1	3
			1.36	1.20	1.80	4.00	1.84	0.12
		Criteria Weight	**13%**	**12%**	**17%**	**39%**	**18%**	**1%**

The outcome of the quality function development procedure is shown below with each weight, except for sustainability.

- Cost - 13%: is a measure of the monetary budget for each concept.
- Use of Technical Resources - 12%: is supplementary subdivided into power (0/2), mass (1/2) and volume (1/2). However, power does not have any contribution to it because all the concepts had the same power usage.
- TRL - 17%: is a measure of the necessary development time for each concept.
- Payload Performance - 39%: is supplementary subdivided into classification (1/5), detection (2/5) and tracking (2/5).
- Required Pointing Accuracy - 18%: is supplementary subdivided into required pointing accuracy of the communication system (1/2) and that of the payload (1/2).

Moreover, the scores for each criteria are given in the Table 6.2. From the table, concept 1 is the one with the highest score with a value of 3.7 and leads the cost and TRL criteria. However, concept 2 is just below concept 1 with a difference of 0.1 and has extremely high payload performance. Concept 2 is similar to concept 1, and the main difference is that the concept 2 has an additional instrument (hyperspectral camera) to have an improved classification of the missile detected. Instead, concept 3 does not have the potential to be the best concept for the costumer. While, beforehand concept 4 is the worse option in comparison to the concepts 1 and 2 in all categories.

Table 6.2: Concept trade-off.

	13%	*12%*	*17%*	*39%*	*18%*	
	Cost	Use of Technical Resources	TRL	Payload Performance	Required Pointing Accuracy	**RESULT**
Concept 1	5.0	3.5	4.0	3.8	2.5	**3.7**
Concept 2	4.3	3.0	3.5	4.2	2.5	**3.6**
Concept 3	4.6	4.0	3.0	3.2	2.5	**3.3**
Concept 4	1.0	1.5	3.5	3.0	1.5	**2.3**

After the trade-off was completed, a sensitivity analysis needs to be performed on the trade-off results. Fist of all, the process of the criteria weights and of the trade-off needs to be inspected.

One way to check this is by changing the values of the criteria weights. Through the changes made, the concepts 1 and 2 did not have any significant change and they remain the best performing con-

cepts. Subsequently, the assumption that only one camera works for both Coverage and Focus if an optic system is used is challenged. In case two camera are needed, the outcome still gives concepts 1 and 2 are the best performing concepts, but the concept 3 needs to be considered as well as it gives a better final result. Finally, the assumption that all concepts use the same number of satellites is challenged. As concept 3 has a smaller FOV the number of satellites required for global coverage increases thus the cost increases too.

Overall, concepts 3 and 4 are discarded due to their low performance and only concepts 1 and 2 are considered. The fact that two concepts are considered and not only one is that the difference between concept 1 and concept 2 is not high enough to make a decision on which one is better. However, from the sensitivity analysis it is clear that concept 1 performs consistently better than concept 2 even if the weights and the assumptions are changed. Thus for this reason concept 1 is decided to be the winner of the trade-off. It is important to note that as concept 1 is chosen the satellites will have a dimension of 12U.

6.2. Budgets

In order to define the distinct design options in the final design, a number of key technical resources must be budgeted for. This is because the resources tend to expand as the project advances and goes more in-depth, therefore a maximum value needs to be settled. In this section, first the contingency management is introduced followed by the mass budget. Next to it, the description of the preliminary link, ΔV and power budgets is explained.

6.2.1. Contingency Management

When implementing the distribution of technical resources, the application of contingencies is a key aspect when a design contains a large number of uncertainties. It is needed to establish some margins to obtain a lighter satellite. In order to achieve this aim, the technical resources budgets will be updated as the design advances towards its final iteration. For this reason, the margins are being reduced over time as the designs becomes more and more detailed. The contingencies used for the final design are shown in Table 6.3.

Table 6.3: Contingency management for mass estimations.

		Contingency [%]	
Design maturity		Propellant, Payload	EPS, Thermal, ADCS, Structures, OBC & Data storage, Communications, Propulsion
Conceptual estimate		25%	20%
Detailed design	New system	20%	10%
	COTS with modification	5%	5%
	COTS without modification	2%	2%

For this chapter, the conceptual design contingencies are being used. Instead, for the rest of the report the detailed design contingencies are used. From the Table 6.3, one can see that there is a contingency difference between subsystems only in the conceptual design and in the new system part. This is because for the propellant, the mass follows from the ΔV budget, which depends on orbital parameters. Instead, for the payload, the contingency have some difference to the other subsystems because at the beginning there was not a decision on the sensors that the M-STAR mission will have on the spacecraft.

6.2.2. DeltaV Budget

In order to determine the ΔV budget, three main maneuvers must be taken into account. The three maneuvers are the following:

- **Orbital station-keeping**: the spacecraft needs to perform station keeping space-segment ma-

noeuvres, see **REQ-SYS-17**.

- **De-orbit burn**: The spacecraft is limited to have a maximum of 25 years in LEO and then it should deorbit at the end of its life, see **REQ-SYS-16**.
- **Collision avoidance manoeuvre**: The spacecraft needs to avoid damage due to space debris, see **REQ-SYS-14**.

For orbital station-keeping, the predominant cause for a satellite to maintain in LEO orbit is to compensate for the aerodynamic losses. The amount of ΔV needed for this manoeuvre can be estimated by assuming a close-to-circular orbit. Instead, for the de-orbit burn, the ΔV is estimated by considering that the manoeuvre carries the satellite in an an elliptical orbit with perigee altitude of 50 km. Furthermore, the ΔV for avoiding a collision is calculated using an analytical solution of Kepler orbits. As a first estimate, a comparison with the ISS is made to have an estimation of how many collision avoidance manoeuvres are needed. From 1999 to 2018, the ISS performed 25 collision avoidance manoeuvres [13], therefore it is estimated that each satellite might perform 9 of these type of manoeuvres during its 7 year lifespan.

The preliminary ΔV budget was determined by summing these three orbit manoeuvres. The process of the ΔV has not changed during the final design and it has been taken from the baseline report [4], therefore the preliminary ΔV budget is the same that can be found in Section 16.2.4. However, the ΔV has been changed from the baseline report as the spacecraft size changed from 6U to 12U, the orbital altitude changed from 700 km to 600 km and the chosen thruster has a higher Isp. When the total ΔV is calculated, using the Tsiolkovsky rocket equation the propellant can be estimated by choosing a propulsion system.

6.2.3. Mass Budget

In order to perform a preliminary mass budget, the total mass of the 12U CubeSat is set to 24 kg due to the **REQ-SYS-06**. First of all, the propellant mass needs to be subtracted from the total mass to determine the dry mass of the spacecraft. Having the spacecraft dry mass, the different masses of the subsystems can be found using a statistical approach. The statistical approach is used to determine the allocation of the dry mass for each subsystem. Moreover, this approach has been taken from the baseline report [4] and the primary change is that the total mass has been doubled, and thus the spacecraft size doubled as well. Using the procedure explained, the mass budget is illustrated in Table 6.4 with the contingencies given in the Section 6.2.1.

Table 6.4: Preliminary mass budget for M-STAR.

Subsystem	**Subsystem Mass [kg]**	**Margin [%]**	**Percentage of the Dry Mass [%]**
Payload	6.38 kg	*25%*	*26.8%*
ADCS	2.88 kg	*20%*	*12.1%*
OBC & Data Storage	1.09 kg	*20%*	*4.6%*
Communications	1.42 kg	*20%*	*6%*
Structures	3.99 kg	*20%*	*16.8%*
Thermal	0.46 kg	*20%*	*1.9%*
EPS	4.96 kg	*20%*	*20.9%*
Propulsion	2.56 kg	*20%*	*10.8%*
Total Dry Mass	**23.75 kg**		

6.2.4. Link Budget

In order to determine what are the feasible communications options, a preliminary link budget has been done in the midterm report [5]. The first step to compute the link budget is that the calculations are based on the inter-linking satellite communication in the same orbital plane, known as in-plane. The preliminary link budget depends on the frequency and on the distance between satellites in which are respectively 2.2 GHz (S-Band) and 1000 km. Both input parameters will be changed along the final

design as they depend on several subsystems. The preliminary input parameters are described in Table 6.5a and the results of the link budget are presented in Table 6.5b based on the signal to noise ratio calculations.

Table 6.5: Inter-satellite link budget calculation.

(a) Preliminary input parameters.

Link budget component	Value
System noise temperature	1250 K
Signal to Noise Ratio	9.5 dB
Distance between s/c	1000 km
Transmit frequency	2.2 GHz
System losses L_0	4.2 dB

(b) Transmit power required.

Antenna type	Low bitrate 1 Kbit/s	Medium bitrate 250 Kbit/s	High bitrate 1 Mbit/s
Low gain antenna 1.3 dB gain	2.12 W	530 W	2120 W
Medium gain patch antenna 8.3 dB gain	0.086 W	21.6 W	86.4 W
High gain reflect array antenna 30 dB gain	1e-5 W	0.001 W	0.004 W

The primary variation between the preliminary and the final link budget is accuracy. This is because the coding gain in the preliminary link budget was not included. Due to this decision, the team had the possibility to change the frequency band totally. Then, a more accurate modelling of the system noise temperature has been made. Furthermore, the modulation schemes and bit errors have not been accounted for in this preliminary link budget. In this way, the final link budget will be more realistic in comparison to the preliminary link budget.

6.2.5. Power Budget

For the power budget, the preliminary power budget is based on the power breakdown of BRIK-II [14]. In comparison to the BRIK-II power budget, three changes were made and shown in the Table 6.6.

Table 6.6: Adaptations to BRIK-II Power Breakdown.

Parameter	Value DRM 600/640 km	Change	Reason
TT&C power	15.85 % of total power	+20%	Take into account power for inter-constellation communication
Total power used	5.11 W	-30%	Take into account mission lifetime of 7 years
Peak power generated	18 W	-20%	Possible design difference in amount and type of solar panels

Within the changes made above, the preliminary power budget for the M-STAR mission is illustrated in Table 6.7.

Table 6.7: Power breakdown over subsystems in % for DRM 600/640 km and the CubeSat Constellation.

Parameter	Power	CHDS	TT&C	ADCS	PDHS	Payload	Total Power Used
DRM 600/640 km (BRIK-II)	23.68%	7.63%	15.85%	33.86%	6.46%	12.52%	**100%**
ICBM	15.95%	5.14%	13.31%	22.81%	4.35%	8.44%	**70%**

During determining preliminary power budget, it was assumed that the M-STAR spacecraft would be 6U and its altitude would be around 600 km. However, the M-STAR spacecraft doubled size and mass due to payload circumstances. Therefore, the preliminary power budget done in the baseline report is not appropriate [4]. Having doubled the size and mass, a new power budget has been created and shown in Section 16.4.1.

7
Payload

The chapter begins with function and requirement analysis and then presents detailed discussion. It starts with a description of noise and disturbances that are driving the design. Afterwards, trade-off of payload is presented. Lastly, the winning design is described in detail.

7.1. Functional Analysis

In principle, the payload should be able to allow for three high-level functions to be performed; ICBM detection, ICBM tracking and ICBM classification. Below, these functions are stated as well as sub-functions that contribute to the achieving of the high-level functions. Functions have been identified based on the functional flow diagram Chapter 4, blocks resulting in a payload function have been stated after the brief function description.

- **FUNC-PAY-01** Generate data for ICBM detection. *Flowdown from 4.3*
  - **FUNC-PAY-01-01** Detect IR radiation within the SWIR-MWIR wavelength range. *Flowdown from 4.3.*
  - **FUNC-PAY-01-02** Provide sufficient resolution for detection. *Flowdown from 4.3.1.2, 4.3.1.7.*
  - **FUNC-PAY-01-03** Achieve continuous reliability for ICBM detection.
- **FUNC-PAY-02** Provide data for ICBM tracking. *Flowdown from 4.3.*
  - **FUNC-PAY-02-01** Provide data for acquiring 3D coordinates of detected ICBMs. *Flowdown from 4.3.3.5.*
    - **FUNC-PAY-02-01-01** Provide accuracy in the 3D position of the ICBM. *Flowdown from 4.3.1.8, 4.3.3.5, 4.3.3.8.*
- **FUNC-PAY-03** Generate data for ICBM classification. *Flowdown from4.5.10, 4.5.11.*
  - **FUNC-PAY-03-01** Generate data to determine ICBM velocity.*lowdown from 4.3.1.8, 4.5.10.*

7.2. Requirement Analysis

The payload functions mentioned in the previous section flow down into requirements. These requirements cover all mentioned functions. Meeting the requirements will ensure that all payload functions can be performed.

- **REQ-SYS-PAY-01** The payload shall consist of components with at least a TRL of 5. *Flowdown from FUNC-PAY-01-03.*
- **REQ-SYS-PAY-03** The payload shall be able to locate the coordinates of the ICBM with a 1 km (3-sigma) accuracy in all 3 dimensions. *Flowdwon from FUNC-PAY-02-01, FUNC-PAY-02-01-01.*
  - **REQ-SYS-PAY-03-01** The payload shall be able detect ICBMs of at least 15 m length and 1.5 m diameter. *Flowdown from FUNC-PAY-01-02.*
  - **REQ-SYS-03-02** The payload shall be able to detect ICBMs flying at velocities of at most 7.6km/s. *Flowdown from FUNC-PAY-03-01.*
  - **REQ-SYS-PAY-03-03** The payload shall be able to detect ICBMs up to their burnout altitude. *Flowdown from FUNC-PAY-01.*
- **REQ-SYS-PAY-07** The payload shall inform the ground station of ICBM detection within 90 seconds after launch of the missile. *Flowdown from FUNC-PAY-01-04.*
  - **REQ-SYS-PAY-07-01** The payload shall detect the ICBM at least before the first stage burn down. *Flowdown from FUNC-PAY-01-04.*
- **REQ-SYS-PAY-08** The payload shall track ICBMs from detection until the end of the boost phase. *Flowdown from FUNC-PAY-02.*

- **REQ-SYS-PAY-17** The payload shall be able to classify the detected object. *Flowdown from FUNC-PAY-03, FUNC-PAY-03-01.*
  - **REQ-SYS-PAY-17-01** The payload shall be able to classify the ICBM from all angles of flight. *Flowdown from FUNC-PAY-03, FUNC-PAY-03-01.*
  - **REQ-SYS-PAY-17-02** The payload shall be able to gather information about the velocity, location, and burn time of the stages. *Flowdown from FUNC-PAY-03.*

7.3. Disturbances and Noise

A clear ICBM signal is important for reliable detection and tracking, and therefore for the mission as a whole. There are several factors that influence the signal to noise and clutter ratio. These factors can originate from the environment or from the spacecraft itself. In this section a closer look will be taken at atmospheric disturbances such as absorption and refraction, and more insight will be given into noise inducing factors such as the environment and the spacecraft instruments.

7.3.1. Absorption

Atmospheric absorption is the capability of the atmosphere to absorb light in specific wavelengths. A lot of the electromagnetic spectrum is absorbed by the atmosphere before it reaches outer space. This is primarily caused by gasses like water vapour, carbon dioxide and ozone [16]. In the atmosphere, absorption bands and atmospheric windows can be distinguished. Absorption bands indicate a range of wavelengths in the electromagnetic spectrum where the majority of the light is absorbed by the atmosphere. An atmospheric window, on the other hand, indicates a part of the electromagnetic spectrum in which the light can pass through the atmosphere with minimal absorption. The most prominent signals in ICBM emissions are the hot water and carbon dioxide gasses. Hot water vapour has a center wavelength of 2.7 µm and carbon dioxide a center wavelength of 4.3 µm [17, 18]. These specific wavelengths fall within absorption bands, but the wavelengths in between fall in an atmospheric window. However, absorption bands and atmospheric windows change with altitude. At altitudes higher than 14 km, the 2.7 µm and 4.3 µm wavelengths and all the wavelengths between them are not being absorbed anymore by the atmosphere [15].

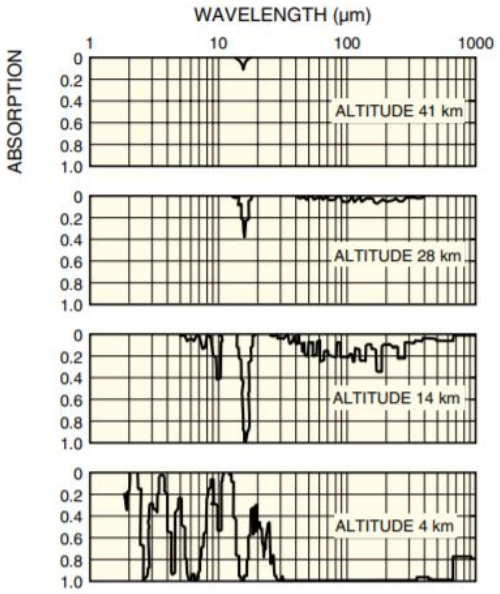

Figure 7.1: Ratio of atmospheric absorption per wavelengths for different altitudes [15].

7.3.2. Refraction

The atmosphere of Earth consists of different layers. Each layer contains distinct molecules and has a specific density. When light passes from one layer to another, the light rays will bend according to Snell's Law. It is important to take this factor into account in order to locate the ICBM accurately. Most refraction will occur in the 10 to 50 km range [19]. It is assumed that above 50 km there is no refraction anymore as the refraction index converges to 1. Furthermore, it is also assumed that the 10 to 50 km layer is a homogeneous area with a single refraction index. This refraction index is estimated to be 1.000079 [19]. With the use of a simplified sketch (see Figure 7.2), the maximum offset caused by refraction can be calculated.

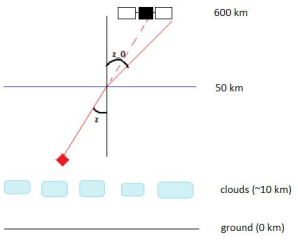

Figure 7.2: Simplified refraction scenario.

The maximum zenith angle will be 61°. With z and n known, the angle of refraction (z_0) can be calculated using:

$$n = \frac{\sin z_0}{\sin z} \tag{7.1}$$

Next, the tangent of the change between the angle of incident and the angle of refraction is taken and multiplied by the remaining distance between the signal and the satellite. The maximum offset the satellite will encounter will be 85.5 m.

7.3.3. Environment Noise

As explained in Section 7.3.1, there are atmospheric bands and windows. Atmospheric windows allow a lot of radiation to pass through the atmosphere, this radiation is caused by different sources from Earth. As it is desired to minimise these signals, it is preferred to look purely into absorption bands. So to look specifically into the 2.7 µm and 4.3 µm wavelengths. This can be achieved with the help of optical filters which only allows passing of a narrow range of wavelengths (±50 nm). The signal from the ICBM will initially also be absorbed by the atmosphere, however, as altitude increases, the level of absorption starts decreasing. When the missile reaches 14 km altitude, the signal will pass the atmosphere without any absorption and there will be minimal background noise from the environment. It can also be shown that this low background noise holds for varies cases. In ”Evaluation of appropriate sensor specifications for space-based ballistic missile detection” Scheitzer performed an analysis of the background noise with the help of MATISSE, which is software that simulates the atmosphere [20]. MATISSE is validated with data from MODIS by NASA [20]. It can be seen that in the spectral radiance for different terrains is at most 0.08 $W/m^2/sr/\mu m$ (Figure 7.3A) and that this holds for day and night (Figure 7.3B). Figure 7.3C shows the spectral radiance caused by scattering of sunlight on clouds. Again, the 2.7 µm and 4.3 µm wavelengths emit extremely low radiance. Finally, Figure 7.3D, displays the spectral radiance of the reflection of sunlight in the case of cumulus, cirrus and no clouds. This graph also has almost no spectral radiance in the wavelengths of interest.

7.3.4. Instrument Noise

Background noise can, beside from the environment, also be caused by the instrument. There are several types of noise created by the instrument [21][22]:

- Read out noise, which is created in the conversion from photon to electric signal.
- Shot noise, which is caused by fluctuation of electrical current due to the fact that the current is not a continuous flow but the sum of discrete pulses in time.
- Dark current, which is caused by random excitation of electrons by thermal activity.
- Fixed pattern noise, which is the noise caused by spatial dislocation of the pixel output.

From these types of noises, the noise which can be most dominant and form a risk for a low signal to noise ratio is dark current. As mentioned above, dark current depends highly on the temperature. The type of IR camera, which is often used to detect the electromagnetic spectrum between 1.5 µm and 5.5 µm is an InSb camera [15]. In Chapter 11 it will be shown that the estimated equilibrium temperature of the satellite will be 256.82 K in eclipse and 312.16 K during day time. Hence, when looking at the corresponding dark current in Figure 7.4, the best case scenario is a dark current of $10 \times 10^{-2.5}$ A and the worst case scenario is located around 10×10^{-1} A. To reduce the dark current, a cooler should be used to cool the focal plane array of the camera. For an InSb camera 77 K is a common operational temperature [23].

7.4. Trade-off

In the previous reports [5], the Coverage payload was assumed to project the number of pixels onto a certain rectangular ground area that does not move across the Earth’s surface, except for the movement due to the satellite velocity itself. This ground area covered by the projected image on the surface can be increased by using different imaging techniques for the Coverage payload. Even though various kinds of imaging geometries have been used [25], only along-track, across-track and

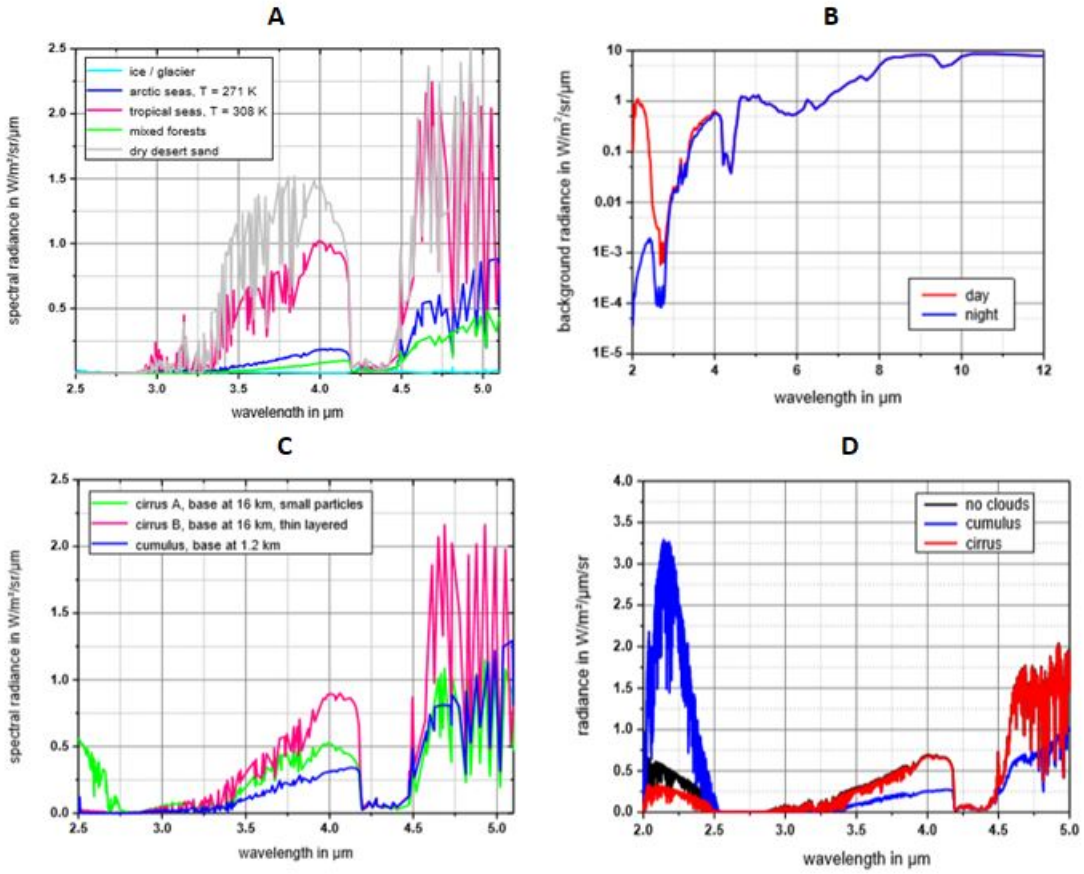

Figure 7.3: Spectral radiance of the background noise from Earth seen from space. A:Spectral radiance for different terrains. B:Spectral radiance in day and night time for a tropical climate. C:Spectral radiance for the scattering of sunlight by various clouds. D:Spectral radiance for reflection of sunlight. [20]

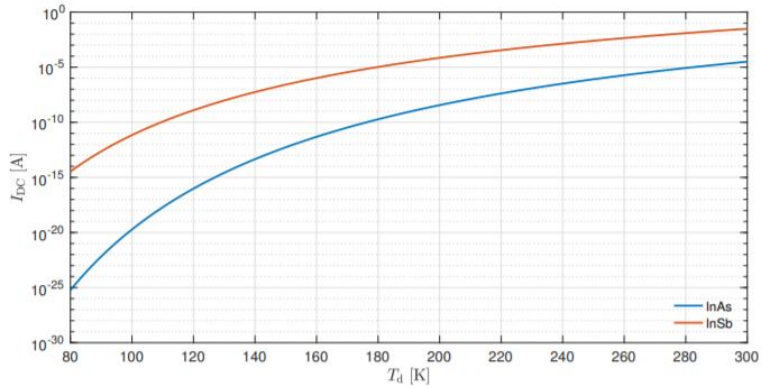

Figure 7.4: Change in dark current over temperature for an InSb and InAs detector [24].

circular imaging will be discussed in this section. After a brief introduction to these imaging methods a trade-off is performed. The trade-off criteria will be introduced after which the scores and the results of the trade-off are shown. The winning imaging technique will be used in the spacecraft design.

7.4.1. Along-track Imaging

Along-track imaging, also known as push broom imaging, consist of a linear array of detectors oriented perpendicular to the flight direction that receive radiation from the Earth's surface. Along-track scanners can achieve high spatial resolutions and relatively high reliability since no moving parts are required. As the camera detector layout has already been fixed to not form a linear array, this method is not taken into further consideration.

7.4.2. Across-track Imaging

Across-track imaging, also known as whisk broom imaging, uses a rotating or oscillating mirror to receive light on a single or 2D array of pixels. The mirror allows for multiple pictures to be taken in a single scan in the across-track direction. Movement of the spacecraft itself results in the scan line advancing over the Earth's surface. Since rotating parts have to be introduced into the design, mechanical reliability might form a problem. Because of the possibility to increase the ground area covered, this technique will be looked at in more detail and will be evaluated in a trade-off.

7.4.3. Circular Imaging

Circular imaging is similar to across-track imaging in the sense that it uses a rotating mirror to receive radiation from different locations on the Earth's surface as well. Instead of a rectangular shape in the across track direction, circular imaging traces out a doughnut-like shape on the surface of the Earth by rotating the mirror 360 degrees at a fixed angle from nadir. Circular imaging is prone to similar reliability concerns because of the need for rotating mechanisms. As this method is also able to increase the surface coverage, it will be researched further and evaluated in a trade-off.

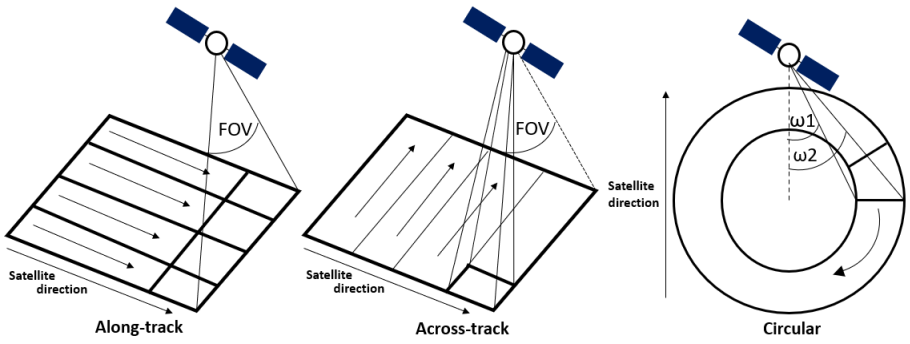

Figure 7.5: Visual representation of the three imaging techniques mentioned. Left: along-track, Middle: across-track and Right: circular imaging.

7.4.4. Trade-off Criteria

The trade-off concepts to be considered are Concept 1: no imaging technique, Concept 2: across-track (linear) imaging and Concept 3: circular imaging. The following six criteria are used: cost, use of technical resources, mission reliability, rotation time, CDH complexity and Location accuracy of ICBM. These criteria will be discussed below. Each criteria is graded on a scale of 1 to 5, here 1 is the worst performing and 5 is best performing. For several criteria a linear scale between 1-5 is used to allow for decimal grades.

Cost In order to take the budget into account, a cost criteria is included. The cost criteria is split into two parts driving the mission cost: the number of planes (separate launch required per plane) and the total number of satellites as more satellites increase mission cost. The orbital planes carry a weight of 30% and the number of satellites of 70% as it contributes more to the total cost. Both the

number of planes and total number of satellites required have been calculated using the calculated ground coverage each imaging technique can achieve. Found values and grading are shown in table Table 7.2 and Table 7.3.

Use of Technical Resources Technical resource criteria are divided into two parts, mass and volume. Both parts carry a weight of 50% as there is no clear preference for on or the other. As for option 2 and 3, additional hardware will be required to for mechanisms and mirrors etc. Therefore an increase in mass and volume is present (mass estimated to be +0.5kg). The required focal length was also taken into account, as this was fixed to fit in a 1U module all options show at least a 1U volume increase. As both option 1 and 2 are not able to alter their attitude while imaging due to their imaging geometry constraints, additional solar panels are required for these concepts. Therefore an addition of 1kg mass is present for these concepts. The found values and grading are shown in Table 7.2 and Table 7.3.

Mission Reliability The mission reliability was defined as the probability that the entire mission would result in a failure. This probability was assumed to be 0.01 for a qualitative comparison to be performed. The allowable failure rate indicates the probability of failure a spacecraft can have for each option to still have a 0.01 probability of complete mission failure over the 7 year mission lifetime. A higher allowed failure rate is thus a less harsh requirement and therefore preferred. As options 1 and 2 allow for single global coverage, a single failing satellite results in a mission failure. The allowed probability of failure was therefore easily calculated by dividing the mission failure probability (0.01) by the number of satellites. As option 3 can achieve double coverage and at some locations triple coverage, the amount of allowed failing satellites is more difficult to compute. Therefore a computer program was generated simulating satellite failure to find a probability failure for option 3. The code starts with a failure probability, runs a mission simulation where each spacecraft has that failure probability and checks the number of missions that fail out of a large sample size to build the mission failure probability. According to the value found, the spacecraft failure probability is tweaked using the bisection method until the computed mission failure probability is within a maximum error of the required one (0.01). The corresponding spacecraft failure rate is then saved, as this would be the failure probability of a single spacecraft that would result in the required mission failure probability. There are multiple failure conditions. Firstly, if one spacecraft fails in one orbital plane, the two satellites in front and the two satellites behind shall not fail to maintain global coverage. Similarly, the satellite to the left and right (next orbital plane) shall not fail either. The most restricting condition is that on the two orbital planes traveling with opposite direction when there is a failure in one of the planes, no failure shall occur on the other. The found values and grading are shown in Table 7.2 and Table 7.3. The inputs of the code are summarised in the following table:

Table 7.1: Inputs used for the spacecraft reliability computation

Parameter	Unit	Value
MissionFailureProb	-	0.01
Loops	-	1000000
N orbital planes	-	9
N satellites per plane	-	34

Rotation Time The rotation time criteria comes from the fact that satellite needs to rotate in order for the Focus payload to be able to focus at a detected ICBM. The rotation time changes for the different concepts as a result of the different imaging geometries and varying FOV angles requiring more or less angular distance to be covered by slewing the spacecraft. The found values and grading are shown in Table 7.2 and Table 7.3.

CDH Complexity There exists a direct relation between the number of overlaps and the complexity of the CDH. Therefore, a trade-off criteria is devoted to it. The amount of overlap is computed using the maximum overlap occurring within orbital planes (Concept 3: 3, Concept 1 and 2: 2 as a small amount of overlap is needed to account for surface irregularities) and multiplying this with the number of orbital planes. This is done since polar orbits will result in all ground tracks overlapping over the

poles. The found values and grading are shown in Table 7.2 and Table 7.3.

Location Accuracy ICBM The final trade-off criteria is the achievable ICBM location determination accuracy (following from the 1km 3D coordinate position accuracy requirement). Depending on the scanning geometry and ground coverage, a certain positioning accuracy can be achieved. This achievable accuracy has been calculated for all concepts using the program described Section 7.5.1. A higher sigma is desired as it indicates a higher accuracy, it should be noted however that the focal length for different concepts can be changed in later stages of the design to tweak the achievable accuracy. The found values and grading are shown in Table 7.2 and Table 7.3.

Table 7.2: Found values for concepts.

	Number of orbital planes	Total number of satellites	Mass (kg)	Volume (U)	Allowable failure rate (%)	Rotation time (s)	Number of overlaps	σ
Concept 1	12	420	+1	+1	0.0024	26	24	3.6
Concept 2	9	666	+1.5	+3	0.0016	22	18	2.5
Concept 3	9	306	+0.5	+3	0.052	44	27	2.03

Table 7.3: Score of concepts.

	Number of orbital planes	Total number of satellites	Mass (kg)	Volume (U)	Allowable failure rate (%)	Rotation time (s)	Number of overlaps	σ
5 Excellent	9 or less	less than 375	+0.5 or less	+1 or less	0.01 or more	<1	1 or less	3 or more
4 High	10	less than 475	+1 or less	+2 or less	0.0075 or more	<11	10.8 or less	2.5 or more
3 Medium	11	less than 575	+1.5 or less	+3 or less	0.005 or more	<22	16.2 or less	2 or more
2 Low	12	less than 675	+2 or less	+4 or less	0.0025 or more	<33	21.6 or less	1.5 or more
1 Poor	13	less than 775	+2.5 or less	+5 or less	less than 0.0025	<44	27 or less	1 or more

7.4.5. Criteria Weights

In order to determine the weights given to the different criteria, a ”quality function development” (QFD) procedure is used. This method consists of the steps explained in Section 6.1. The results of the QFD are shown in Table 7.4.

Table 7.4: QFD procedure to determine the criteria weights.

Identifier	Customer Need	Costumer Importance Rating	Cost	Use of Technical Resources	Mission Reliability	Rotation Time	CDH Complexity	ICBM Location
REQ-MIS-05	Cheap	*3 [15%]*	9	1	1		1	
REQ-SYS-01-06	Reliability	*5 [25%]*			9		3	
REQ-MIS-01-04	Position accuracy ICBM	*3 [15%]*						9
REQ-MIS-08	LEO Orbit	*2 [10%]*	3	3				
REQ-MIS-06	Nanosat	*3 [15%]*	1	9			1	
REQ-MIS-01-02	Latency	*4 [20%]*				9		
			1.8	1.6	2.4	1.8	1.05	1.35
		Criteria Weight	**18%**	**16%**	**24%**	**18%**	**11%**	**14%**

7.4.6. Trade-off Results and Conclusion

The final result of the imaging technique trade-off is shown in Table 7.5. With a score of 3.5, Concept 3 is the winner and outperforms Concept 2 significantly and beats Concept 1 with a margin of roughly 12%. Despite the relatively poor performance of Concept 3 on CDH complexity and ICBM location accuracy, the small weight of these criteria compared to the weight of the mission reliability still resulted in Concept 3 winning. As a 3 sigma 3D position accuracy is a stated requirement Concept 3 is not

able to meet, this was discussed with the customer. It was agreed upon that the decrease in position accuracy does not weigh up against both the decreased number of satellites and higher reliability of Concept 3 due to the possibility of double coverage. The trade-off results will be discussed further in the trade-off sensitivity analysis of Section 7.6.1.

Table 7.5: Final trade-off table payload.

	18%	*16%*	*24%*	*18%*	*11%*	*14%*	
	Cost	Use of Technical Resources	Mission Reliability	Rotation Time	CDH Complexity	ICBM Location	**RESULT**
Concept 1	2.9	4.5	1.0	2.7	1.4	5.0	**3.3**
Concept 2	2.2	3.0	1.0	3.0	2.3	4.0	**2.9**
Concept 3	5.0	4.0	5.0	1.0	1.0	3.0	**3.7**

7.5. Payload Design

In the payload design chapter the final choices for all payload components will be discussed. Firstly, the tools/calculations used to argument the design, and tests for the required components will be explained. After this, the choice of camera, optics, filters, cooler, imaging geometry etc. will be discussed.

7.5.1. Payload Calculations

In this subsection a description of the working principles of the three main tools will be explained. This includes a tool to calculate the effect of the curvature of the Earth on pixel and imaging geometry, an updated version of the pixel size calculation and a tool to find the ICBM position triangulation error using satellites.

Tool 7.1 : Position Error Calculations

The first of the calculations is the position error of the ICBM. In order to do so there are 5 main functions, as seen in Figure 7.9. The first one which transforms 3D coordinates into 2D. The second function calculates the interception points of the pixel lines. The third one calculates the effect of the refraction in the pixel size. The fourth adds the knowledge errors and finally the fifth which gives the difference between two values. The explanation will begin with the first function and follow the order previously stated.

Firstly, it is important to translate the coordinates given from a 3D axis to a 2D axis. Due to the complexity of the three-dimensional error calculation it would be too time intensive therefore it was decided to perform a 2D estimation. In order to do a 2D approach it is important to note that the main factors affecting the error are the pointing knowledge and the distance to the pixel at which the two satellites are looking. Therefore, one finds the 3D distance and translates it into a 2D distance by substituting the height of the satellite. A graphical representation of the process can be seen in Figure 7.6.

Secondly, the line intersection code is created. As both satellites are looking at a pixel there must be an intersection of the pixel. Calculating this interception will give you the error in the y and x directions. This process is done straight forward using linear algebra. A graphical representation can be seen in Figure 7.7.

Thirdly, the refraction is taken into account. The implementation of the refraction on the code creates a new pixel that is refracted. The refracted pixel has a new location depending on the incidence angle of the FOV and the refractive index of the atmosphere, as explained in Section 7.3.2.

Then, the errors of the pointing and position knowledge are added. This is done by adding the value from the error to the calculations and run them again. For instance, if the altitude of satellite 1 is 600 km and the altitude error knowledge is 300 m then the new altitude for all the calculations is 600.3 km. It is

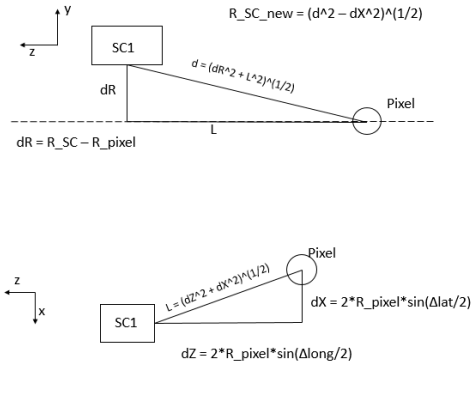

Figure 7.6: Transformation from 3D to 2D.

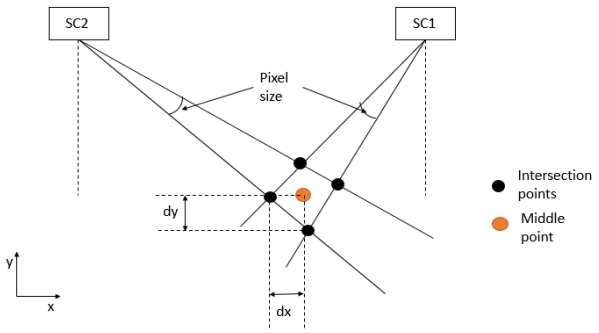

Figure 7.7: Pixel intersection.

important to note that all the knowledge errors are assumed to be normally distributed thus with each iteration of the program the value changes. Error bias and non-random noise in altitude is discussed in Section 7.9.

Finally, the difference between the refracted image and the calculated image with errors and no refraction is calculated. The output of the program is the percentage of the times the error in the x and y coordinate exceeds 1 km. All the inputs used for the program can be seen in Table 7.6. The location of satellites 1 and 2 come from the positioning of them in orbit. The constellation design is explained in Chapter 15. The location of the pixel is for the worst case scenario when the pixel is in the same latitude as one of the satellites and at the maximum longitude of the FOV of the satellite.

Table 7.6: Position Error inputs

Parameter	Unit	Value	Parameter	Unit	Value
σ error in y-direction	m	0.05	σ error in x-direction	m	0.005
σ error pointing knowledge	°	0.005	Altitude	km	600
Latitude of satellite 1	°	10.59	Latitude of satellite 2	°	21.18
Latitude of pixel	°	10.59	Longitude of pixel	°	10
Altitude of pixel	km	600	Pixel size	arcsec	3.5

Tool 7.2 : Earth Curvature Effect

To see the effect of the curvature of the Earth in the deformation of individual pixels for all imaging methods, a similar calculation/tool was made as in the midterm report. The deformation of pixels under an off-nadir angle from an orbital altitude can be visualised using Figure 7.8.

The parameter of interest from figure fig. 7.8 is denoted by d. Using the sine rule/trigonometry it can be shown that d can be found using the following equation:

$$d = \left(\arcsin\left(\frac{R_e + H}{R_e} \sin(\alpha) \right) - \alpha \right) R_e \tag{7.2}$$

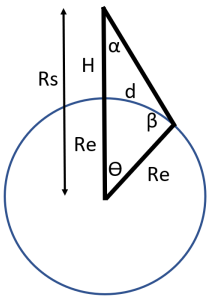

Figure 7.8: Geometrical representation of satellite looking at the surface of Earth under an off-nadir angle.

From this equation, it is evident that the deformation of a pixel is dependent on the orbital altitude H and the field of view (2α), which are inputs for the tool together with the number of pixels in one axis of the pixel array. By dividing the angle α into the number of pixels and calculating d for both the full α and $\alpha - \frac{\alpha}{0.5 \cdot \#\text{Pixels}}$, their difference indicates the largest pixel present within the complete field of view. Using

this method the largest pixel for across-track imaging could be found. For circular imaging the tool was adjusted to account for two angles describing the scanning geometry. When a maximum pixel size is known, the tool can be used to show to what extend the field of view can be increased to still meet the maximum allowed pixel size. Using the pixel pixel dimension obtained from the tool that will be explained below together with the parameters shown in Table 7.7. The Inner FOV, outer FOV and corresponding radii of the circular imaging have been calculated.

Table 7.7: Inputs Curvature tool

Parameter	Unit	Value	Parameter	Unit	Value
Pixel size	m	3300	Orbital height	km	600
Camera resolution	-	1280x1024			

Tool 7.3 : Adjusted Pixel Sizing

Since wavelength filters will be used for the detection of ICBMs, the pixelsize calculation has been adjusted to include the effects of these filters. Even though the general approach to the calculation is the same as described in the midterm [5], the adjusted program's inputs and outputs will be explained together with the general steps followed in the calculation. The programs main input is the desired Signal to Clutter Ratio (SCR), and is defined as the infrared flux emitted by the ICBM only divided by the measured noise flux. The ICBM signal is calculated similar to the midterm report where the exhaust area and temperature has been divided into the three components stated as inputs [26] and where the temperatures were used in Planck's equation. Two sources of background radiation have been implemented as well: Earth's surface and Earth-Sun reflected radiation. Both these sources' flux has been calculated in the exact same way using the different temperatures and emissivities stated. The Sun's emissivity has been chosen such that the Planck curve matched ones representing the Earth-Sun reflection curve from literature [27]. Now that both filters and atmospheric windows will be considered in the calculations these have been implemented into the Planck curves as well. Inside the wavelengths of the filter bandwidth, given as inputs [1], the values of the Planck curves have been multiplied with the transparency of the used filter. Outside of the filter, the values of the Planck curves have been set to zero since they will be blocked. Additionally, the values of the Earth surface radiation has been set to zero inside the atmospheric windows since it will be absorbed by the atmosphere. When running the program, one of the two filters should be chosen. Inside this filter the Planck curve will be integrated resulting in a flux (W/m^2) of the rocket, composed of three parts, a flux of the Earth's surface and a flux of Earth-Sun reflection. Using the arbitrary initial pixel dimensions (arbitrary since they are used purely to start iterations) and rocket plume dimensions, the fluxes are scaled with their areas to obtain power emitted. The powers from all components is added up and divided by the total pixel area to obtain the average flux of a pixel with an ICBM. The flux, purely from the Earth's surface and Earth-Sun reflection together is saved as background radiation. Now, the flux emitted purely by the ICBM is calculated by subtracting the background flux from the total flux of a pixel with an ICBM, this will be the numerator in the SCR calculation. The NETD is given for the operational wavelengths of the camera and for a given well fill. The well fill is a measure for the amount of electrons stored in a pixel as the percentage of its maximum capacity. Every frame, for each pixel, the camera reads out the stored number of electrons into an average representing the pixel value. When assuming the number of electrons stored in a pixel to be sufficiently large, the central limit theorem can be applied [28]. According to the central limit theorem, the sampling distribution of the sample means (pixel readout values) then approximates a normal distribution. The standard deviation of this normal distribution is what is measured to be the NETD of an imaging system [29]. The central limit theorem states that the standard deviation (NETD) is then inversely proportional to the square root of the sample size (well fill): $NETD \propto \frac{1}{\sqrt{\text{well fill}}}$. The well fill is proportional to the amount of flux the camera receives and thus on the area below the Planck curves. Because of the filter, less flux is received by the camera,

[1]Retrieved from `https://www.thorlabs.com/newgrouppage9.cfm?objectgroup_id=9464`

decreasing well fill, increasing the NETD (since a higher frame rate decreases the time after which pixels are read out, it decreases the well fill in turn increasing the NETD as well [30]). The “filter NETD” is calculated by first integrating the Planck curves over the complete wavelength range of the camera without any filters. Then, the exact same is done with the use of filters, this results in a smaller value. Then the “non-filter NETD” is scaled by multiplying it with $\frac{1}{\sqrt{(\text{Area ratio})}}$ to obtain a larger value for the NETD, accounting for the decrease in radiation received due to the filter. A flux is calculated exactly as was done for the background as described before, except that the temperature of the background is increased by the found NETD. After that, the earlier found background flux is subtracted from this newly calculated flux to isolate the noise. This value is used as the denominator of the SCR. Now the SCR can be easily found by dividing the values needed for it $SCR = \frac{\Phi_{ICBM}}{\sigma_{noise}}$. In case the found SCR is larger than the desired SCR, the used pixel area is altered and the program is run again until the desired SCR is obtained. The found pixel dimensions, SCR and “filter” NETD will function as outputs. By running this program with the stated inputs (SCR of 5 is deemed sufficient for ICBM detection [20]) the pixelsize and NETD outputs stated in Table 7.9 were obtained.

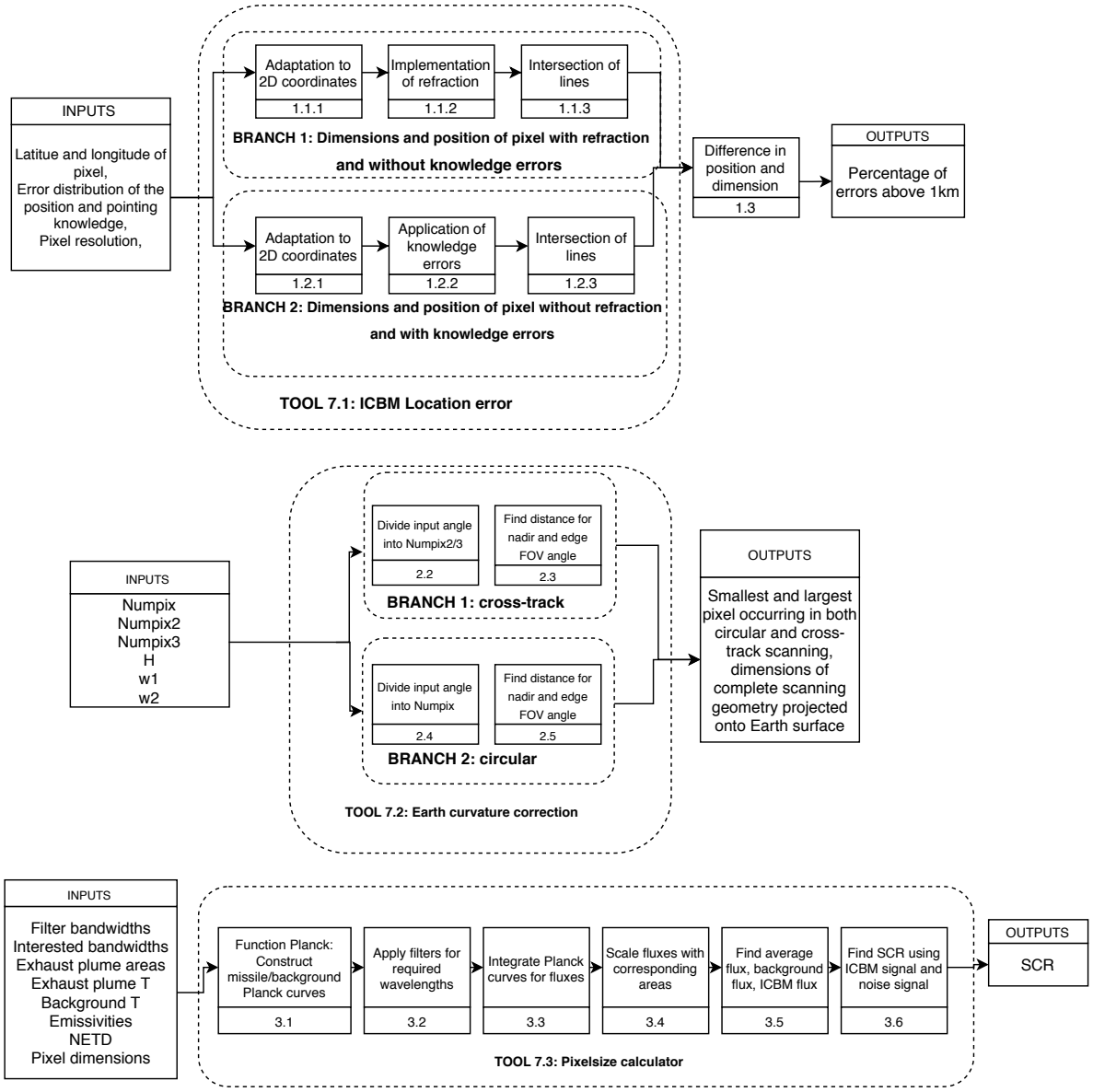

Figure 7.9: Diagrams summarising tool work flow

Table 7.8: Inputs pixel size tool

Parameter	Unit	Value	Parameter	Unit	Value
A_{e1}, A_{e2}, A_{e3}	m^2	11.75,11.75,141	$\lambda_{\text{filter 1}}$ (low, high)	μm	2.625, 2.775
T_{e1},T_{e2}, T_{e3}	K	2500,1700,1200	Transparency 1	-	0.25
T_{sun}	K	5250	$\lambda_{\text{filter 2}}$ (low, high)	μm	4.1,4.45
ϵ_{sun}	-	0.000028	Transparency 2	-	0.8
T_{earth}	K	303.15	Integration lines	-	1000
λ_{camera} (low, high)	μm	2.6,5	Normal angle	rad	0
$\epsilon_{\text{exhaust}}$	-	0.1	Atmospheric window 1	μm	2.7,2.9
$\epsilon_{\text{background}}$	-	0.8	Atmospheric window 2	μm	4.22,4.45
NETD (no filter)	mK	25	Input SCR	-	5

7.5.2. Results from chosen payload design

Table 7.9 shows the results of the calculations above. Together with the design choices made below, which are also stated in the table, this table summarises the payload design.

Table 7.9: Results chosen payload design

Parameter	Unit	Value	Parameter	Unit	Value
Inside FOV (ω_1)	°	15	Outside FOV (ω_2)	°	61
Inner radius of coverage	km	161	Outer radius of coverage	km	1348
Pixel size Coverage payload	m	3300	Pixel size Focus Payload	m	22
Focal length Coverage	m	0.0177	Coverage lens diameter	cm	2.5
Aperture of lens	-	f/1.4	Mirror dimensions	cm	4x2.5
Mirror rotational speed	rad s^{-1}	6.28	Pixel size on payload	µm	12
ICBM location error in y-direction	%	4.3	ICBM location error in x-direction	%	0
NETD (using filter 2)	mK	92.6			

7.5.3. Payload Components

Below, the different payload components to be used are discussed. The to be used imaging technique parameters will be discussed as well together with the required components to realise the required mechanisms.

Camera

The camera should be able to see the 2.7 µm and the 4.3 µm wavelength as explained in Section 7.3.1. The type of camera which is able to detect both wavelengths and has the highest specific detectivity (~10^{11} cmHz$^{1/2}$/W) is the cooled InSb camera (see Figure 7.10). The camera which lies closest to the desired characteristics and which was used for calculation is the QuazIR$^{TM}_{HD}$ from IRCameras [31]. However, an explanation now follows on some cameras and why COTS cannot be used.

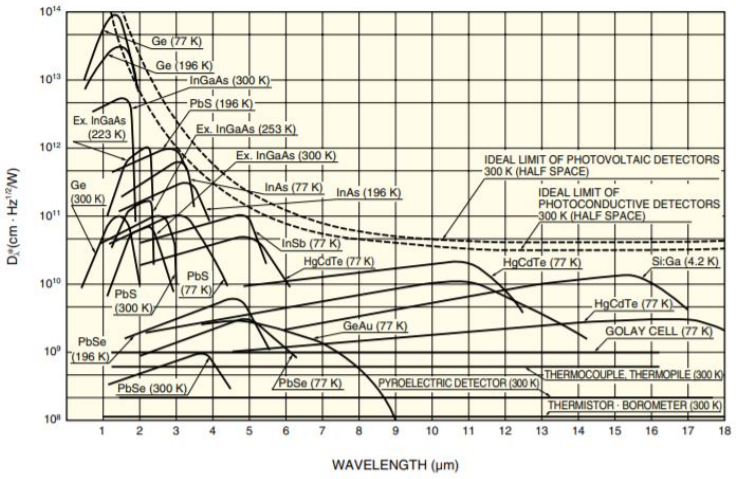

Figure 7.10: The spectral response for various infrared detectors [15].

There are several InSb COTS cameras. The ones which are specifically designed to operate in space, like the

AXIR MW from Lynred, are often too large, require too much power and have undesirable characteristics[2]. Furthermore, most of these cameras are designed to observe the atmospheric window between 3 µm and the 5 µm, carry a built in filter which is not desired in the payload design. Finally, many of the smaller InSb cameras, like the payload from the Arkyd-6, use a Stirling cooler.Stirling coolers are notorious for the vibrations they impose on the spacecraft and their general short lifetime (around 3 years) due to their moving parts [3].

Hence, because of all of the reasons stated above it is not possible to select a COTS camera. It is common in the space industry to take the requirements of the desired camera to a camera manufacturer, who will help you design the camera. Some components of the camera could be off the shelf, like for example the electronics of the camera, other need to be specifically designed for M-STAR, but this is to be determined by the manufacturer. So for the camera there has to be performed quite some Research and Design (R&D). To be more specific, the spectral response of the wavelengths have to be tweaked as most remote sensing cameras are designed of the atmospheric window between 3 and 5 µm [16]. Furthermore, it has to be investigated if the camera can survive the space environment and what implementations have to be performed in order to be able to operate in these conditions. Moreover, a selection has to be made for the filters and the cooler, which are explained in more detailed in the following paragraphs. Finally, it could be possible that some parameters or combinations of parameters assumed for the payload in Section 7.5.1 are not available for COTS camera components, in that case R&D has to be performed in order to achieve these parameters, but again that is to be determined by the manufacturer of the camera. It should be noted that IRC is an American company. If R&D is performed here, it could take up more time because of regulations. So an European company, like Lynred, would be preferred instead.

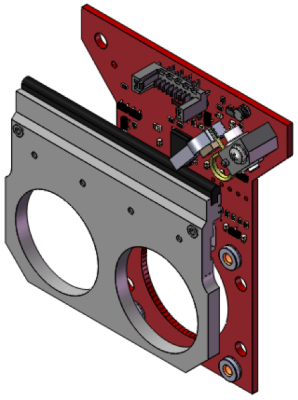

Figure 7.11: Proposed filter switch mechanism configuration for M-STAR[4].

Cooler

In order to function properly, the InSb camera needs to be cooled. A cooled camera will have less dark current and thus a lower instrument noise (see Section 7.3.4). The cooler which is proposed in the payload design, is the 6510 Pulse Tube cooler from Thales Cryogenics [32]. This Pulse tube cooler has a long life time (10 years) and imposes almost no vibration at all on the satellite. R&D is required for the interface between the camera and the cooler in order to create an efficient and successful system as this interface is not simply a plug-and-play system according to Roel Arts from Thales Cryogenics.

Filters

The InSb camera will have a spectral response between 2 µm and 5.5 µm. However, it was desired to only observe the absorption bands for 2.7 µm and 4.3 µm in order to reduce the background noise (see Section 7.3.3). This can be achieved with two optical filters. The filters will be placed on a filter mount after the optic system and before the camera. In spite of the knowledge that moving parts within a satellite are undesirable, no alternative could be found as it remains necessary to physically switch the filters. Research done for this mechanism was focused on limiting the induced force due to the movement as much as possible to limit the impact on spacecraft attitude. As the switch is time critical, implementing a filter wheel was discarded due to the relatively slow switch time [33]. Other variations on a rotating mechanism were eliminated due to the torque they create. The final

[2]Retrieved from `https://satsearch.co/products/sofradir-axir-mw-in-sb-vga-idca-mwir`
[3]Retrieved from `https://www.ricor.com/products/k508n/`
[1]Retrieved from `https://www.thorlabs.com/newgrouppage9.cfm?objectgroup_id=9464`

filter switch mechanism design that was deemed feasible to propose for the M-STAR can be seen in Figure 7.11.

,The filters and filter mount can be bought from Thorlabs. However, R&D is required for the filter mount and slider combination in order to make it suitable for space applications and to make it compatible with the payload system. As the slider will be accelerated in one direction, and subsequently in the other direction with a force of the same magnitude the induced torque will be negligible. However, it is expected that implementing a mechanism like this will induce vibrations. Throughout the R&D process the magnitude of the vibrations need to be assessed and a coping mechanism needs to be presented.

Imaging Technique
The payload will be imagining in a circular manner. This was decided from the trade-off done in Section 7.4. From the earlier explained adjusted pixel size calculation, a maximum ground pixel size of 3300 m was obtained in order to maintain a SCR of 5. Together with the Earth curvature program and the orbital altitude of 600 km, the complete imaging geometry as shown in Figure 7.5 was found. The circles traced out by the imaging method will have an inner radius of 161.3 km and an outer radius of 1348.8 km. This is achieved using an off-nadir angle of 15° towards the inner circle and an off-nadir angle of 61° to the outer radius. The thickness of the ”imaging ring” will be 1187.5 km and will be formed by the 1280 pixel dimension of the camera. In order to image in a circular manner a rotating mirror needs to be implemented. After doing the calculations explained in the previous sections the focal length of the Coverage payload would be of 0.0177 m. With this, the altitude and the width of the image it is possible to calculate the diameter of the lens. This comes out to be 0.0123 m [34]. It was decided that a 2.5 cm lens would be use as it is more common in manufacturing.The aperture of the lens does not depend on the size of the lens therefore the aperture will still be f/1.4 . With this aperture it is possible to get images with sufficient ground resolution.

With this calculations it is now possible to calculate the size of the mirror and the angle at which it needs to be placed. The mirror will be placed at 19° from the normal of the payload. This way the reflected image is at the middle of the scanning line. The size of the mirror will be an ellipse with a long side of 4 cm and the short side of 2.5 cm. For the rotation of the mirror the calculations followed from reference [35]. It was decided to take three pictures in 1 s in order to complete the circular scan. Using the calculations from reference [35] it comes out that a rotational velocity of 6.28 rad s^{-1} is required. In case more images want to be taken, a maximum of 59 images per second can be taken as there is a constraint on the maximum rotational speed and the frequency of the camera itself.

Focus Optics
The Focus payload optics must provide a focal length of roughly 0.7m inside the smallest volume possible. Reflective optic systems are capable of providing larger focal lengths in constrained volumes when compared to refractive optics, specially when considering the focal length required is larger than the vehicle itself. Different telescope options were looked into including the possibility of having the Focus payload move its FOV instead on slewing the whole spacecraft. The use of a moving primary mirror was discarded due to low reliability and the use of a spherical primary mirror and a moving secondary mirror was discarded due to the volume required for a wide FOV steering and the optical aberrations induced. The chosen optic system for the Focus images consists on a Ritchey-Chrétien telescope that can provide a 0.7m focal length in roughly 15 cm depth. This CubeSat telescope is based on the design presented in [36]. This telescope presents a simple compact design with the required focal length and low optical aberrations due to the use of hyperbolic mirrors that help minimise off-axis optical error. The preliminary sizing of the focus payload mirror system was taken from this mission. Again, R&D has to be performed for the interface between the optics, the filters and the camera as is cannot be assumed that these components will fit together seamlessly. Furthermore, the set-up of the optic system and the calibration also will require R&D.

Coverage Optics
The coverage optics consist on a set of lenses to achieve the 0.017 m focal length required and the

rotating mirror. The lenses were sized by based on [34]. Following the same process it came out that a lens of diameter 1.25 cm is required. However, due to manufacturing abilities a diameter of 2.5 cm was chosen. For the rotating mirror the dimensions were computed using trigonometry. If the mirror is at an angle of 19° from the vertical axis of the lens then the mirror needs to be of 4 by 2.5 cm. The velocity at which the mirror needs to rotate is calculated following the steps of reference [35]. Using the same process NASA uses then the velocity of rotation for taking 3 images in one second came out to 6.28 rad s^{-1}. Using this velocity the image will not be blurry. If a higher rotational velocity is used then the frequency of the images needs to increase in order to prevent blurriness.

Payload Switch Mechanism
With the current payload design one camera must be able to use two separate sets of optics to image with different ground sampling distances, this is done by means of a flip mirror. A flip mirror is a device that allows switching of an optical path, its commonly used in telescopes, reflex cameras and imaging spacecraft. Despite being widely flow in spacecraft they aren't commonly used to switch the optics used but rather to image a calibration black body. The flip mirror employed is inspired in mainly in an infrared imaging 6U cube sat called CIRiS [37]. This mission uses a flip mirror allowing for imaging of four different areas. One nadir scan, one zenith scan and two Carbon Nanotubes black bodies for calibration. The preliminary sizing of the flip mirror was taken from this mission. Again, as there are no COTS flip mirrors available for M-STAR, R&D has to be performed to design a flip mirror specifically for M-STAR.

7.6. Sensitivity Analysis

In this section a sensitivity analysis will be performed for the trade-off and for the tools used for the calculations.

7.6.1. Trade-off Sensitivity Analysis

As the trade-off is not an exact method it is important to perform a sensitivity analysis. This is done in order to be able to have a critical evaluation of the decisions made during the trade-off. As no major assumptions have been made the sensitivity analysis will consist of only changing the weights in use of technical resources and ICBM location. These three variations were chosen as they are the most critical ones for the design.

For the QFD, relationships were quantified between customer requirements and technical criteria. For the trade-off a exponential scale of 9-3-1 was used. If there is a change in the scale to other possible ones, such as the 4-2-1 scale, no changes in the ranking appear. Thus, it can be concluded that the relationship scale used is objective and the use of a different scale would not affect the output of the trade-off.

For the weight of the "ICBM Location" the important test is to see how much the weight needs to change in order for Concept 1 to win. The change would need to be of 10 %, so from 14 % to 24 %, in order for Concept 1 to win. This is almost doubling the current weight in order for Concept 1 to win.

Finally, for the technical resources one could argue the weight of the mass and volume is not the same. If one assumes the mass is not relevant then Concept 2 wins. However, that is not a realistic assumption as there is a cost that needs to be paid in order to send mass to orbit and that there is a constraint in mass from the volume itself. By changing the volume to 65 % and the mass to 35 %, concept 1 receives the same final score as Concept 2. However, this change is hard to justify as the mass comes from the different solar array architectures for each concept as mentioned in the technical resources criteria explanation.

7.6.2. Error Calculations Sensitivity Analysis

A sensitivity analysis was performed on the tools used. Different values were changed and the results were recorded. The effect can be seen in Table 7.10. It is important to note that the output present in the sensitivity analysis is only the error in the y direction. This is due to the fact that the error in the x

direction never exceeded the 1km value thus there is no point in analysing it.

Table 7.10: Sensitivity analysis results error calculations.

Input	Output	% Change	Conclusions
Pixel size = 2 arcsec	0.23 %	94.5	Decrease of pixel size to 2 arcsecond gives an accuracy of 3 σ
y error = 0.2 km	9.3 %	121	Increase in error by more than 100%. The accuracy is below 2 σ now
x error = 0.01 km	3.9 %	7	There has been a decrease of the error by 7 %. The decrease is unexpected but the little percentage change is expect as the x-direction is not the critical one.
Pointing error = 0.01°	18.8 %	337.2	As expected a small change in the pointing error causes a big change in the total error

The reason that such values are chosen is the following. The y and x errors are the errors in case the GPS receiver of the satellite fails, and Two Line Error Orbit Determination (TLEOD) needs to be used. The average error in y is of around 200 m and in x of around 10 m [38]. As for the pointing knowledge error of 0.01° is used. This is as the average pointing knowledge error for the ACDS system. Finally, for the pixel size it was decided that the pixel size such that the error is below 3 σ will be calculated.

From the sensitivity analysis it became clear that the variable that had the biggest impact is the pointing error. A change in this variable causes the result to increase by more than 300 %. This is due to the fact that as the satellite is at very high altitudes a small change in the angle results in a very high change on the distance at ground. It is therefore recommended to try and achieve the best pointing knowledge possible. If possible, it is recommended to use a device that has a pointing knowledge error of 0.0025° or less as this is the highest error such that **REQ-SYS-PAY-03** is complied with.

One more important result that comes out of the sensitivity analysis is that by decreasing the pixel size from 3.5 to 2 arcsec the position accuracy increases to more than 3 σ which means **REQ-SYS-PAY-03** is now completely fulfilled. It should be further explored if the increment in the focal length cause by such decrease in pixel size would out weight the fact that accuracy with 3.5 pixel size is of 4.3 %.

7.6.3. Adjusted Pixel Size Sensitivity Analysis

To use the Planck curve approach as described for the pixel size tool, both the missile and the background had to be modeled in a simplified way. For the rocket modeling, the hot exhaust plumes are of interest which have been divided into three areas with their own size and temperature. One plume area was assumed to be 11.75 m^2 with a temperature of 2500 K, one to be 11.75 m^2 at 1700 K and one area to be 141 m^2 at a temperature of 1200 K. These assumptions are based upon ICBM CFD calculations from literature and scaled to the expected ICBM size [26]. Since the signal intensity calculated by the program relies heavily on both the area and temperature of the plumes, a sensitivity analysis was performed on the effect of changing these values. For this, a paper that models the exhaust plume as a single area with a uniform temperature was used as a baseline. Firstly, only the area was changed to a total of 80 m^2[ref] to asses the effect. Secondly, only the temperature was changed to be uniform 2400 K[ref] to assess its effect as well. The changes in the resulting SCR are shown in Table 7.11.

A second assumption that has a large impact on the calculated SCR is the assumed background temperature. The background temperature serves as a source of background noise and was assumed to be an average of 30°C worldwide in an attempt to have conservative SCR estimates. In reality the the background temperature might fluctuate and temporarily achieve higher values. The effect of a slight temperature increase is tested in Table 7.11 as this would be a worse scenario.

Table 7.11: Sensitivity analysis results pixel-size calculation.

Inputs							Output
A_{e1} [m^2]	A_{e2} [m^2]	A_{e3} [m^2]	T_{e1} [K]	T_{e2} [K]	T_{e3} [K]	T_b [K]	SCR
11.75	11.75	141	2500	1700	1200	303.15	5
11.75 · 0.49	11.75 · 0.49	141 · 0.49	2500	1700	1200	303.15	2.5
11.75	11.75	141	2400	2400	2400	303.15	17.68
11.75	11.75	141	2500	1700	1200	308.15	4.33

From this table, it can be concluded that the SCR appears to scale linearly with the plume area. A multiplication of the areas with ≈ 0.5 results in half the original SCR value. The only source of a signal in the SCR calculations is the exhaust plume. In the SCR calculation, the flux of the exhaust $[\frac{W}{m^2}]$ gets scaled directly with the area. Therefore linear behaviour is expected in the SCR as a result of changes in the exhaust plume area. It should be noted that this only holds if all three separate areas are scaled with the same number. The scaling with the changed temperatures is more difficult to identify because of the temperature appearing in Planck's law and being divided into separate parts as well. The SCR does appear to scale more for a temperature change than for a same increase in area, relatively speaking. The small background temperature increase (roughly 1.5%) already resulted in a significant SCR decrease. For this program to be used for accurate results it is therefore required that both the temperatures and areas of the rocket and background are modelled accurately. For the purpose of detecting multiple ICBM types, calculations should be performed using the missile generating the smallest exhaust plume with the lowest temperatures.

7.7. Verification & Validation

In this section the verification of all calculations done in Section 7.5.1 will be performed as well as subsystem and requirement verification.

7.7.1. Tool 7.1 Verification

The verification for the position error calculations was done by parts. All boxes in Figure 7.9 are verified with unit tests followed by verification of the branches and finally verification of the whole program. The unit tests are the following:

- **Unit test block 1.1.1 and block 1.2.1**: set dX to zero and the new radius should be equal to d, see Figure 7.6. This was true
- **Unit test block 1.1.1 and block 1.2.1**: the new radius should be the same for both satellites. This was indeed true.
- **Unit test block 1.1.2**: set the refraction index to zero and the position of the pixel should not change. This was indeed true.
- **Unit test block 1.1.3 and block 1.2.3**: set the lines parallel should return no intersection. This was indeed true.
- **Unit test block 1.2.2**: set errors to zero, the results should be the same as with no errors. This was true.
- **Unit test block 1.3**: set refraction index to 1 and errors to zero, difference between pixels should be zero. This was true.

Once all the unit tests are done, branch tests can be performed. The main test done for the branches was to place the pixel in between the two satellites and set refraction and error to zero. The pixel dimensions should be symmetrical and both calculates pixels, from branch 1 and 2, should be in the same place. This was indeed true.

7.7.2. Tool 7.2 Verification

The principle of the Earth curvature effect on the pixel size program was explained in Section 7.5.1. The architecture of the program is shown in figure Figure 7.9. Since the program consists of a single

function that finds the parameter d using the equation shown in section Section 7.5.1, the function can be tested against an analytical solution. This will be done for two simple cases, once for an extremely low altitude and FOV (h =5 km, $\alpha = 15°$) where the Earth curvature has a small effect and d should approaches the orbital altitude multiplied with the tangent of α. The second test will be done using a α of 35° and at an orbital altitude of 1000 km, here the the calculated d should be larger the the simple calculation using the tangent and should obviously give the same results as the analytical solution. The results of these two tests are shown in the first two rows of the table below:

Table 7.12: Sensitivity analysis result.

Input	Output Program	Calculated Output	% Change
$H = 5$ km $\alpha = 15°$	$d = 1.339$ km	Flat Earth: $d = 1.339$ km Analytical: $d = 1.339$ km	0 0
$H = 1000$ km $\alpha = 35°$	$d = 731.117$ km	Flat Earth: $d = 700.207$ km Analytical: $d = 731.117$ km	4.41 0
$H = 1000$ km $\alpha = 35°$ Numpix $= 1280$	Largest pixel $= 810.907$ m	Analytical: Largest pixel $= 810.907$ m	0

The result of the function tests is as expected, since the program is based on an analytical equation, the only source of error between the program and the equation should be the result of floating point errors resulting in a negliglible error. Compared to a calculation using a flat earth assumption, the program results in a larger value for d. This is also as expected since a flat Earth would under estimate the length d. As the purpose of the program is to find the largest pixel size occurring within a FOV for a given altitude and number of pixels, a complete system test can be performed by additionally inputting a number of pixels for the FOV (1280 is used as 1280x1024 is a common camera resolution) to be divided in. Since, this calculation would still be completely based on the d function (pixel sizes are found by dividing the FOV into smaller angles for which d is executed individually), no error should be present. The result of the complete program test is shown in the third row of Table 7.12.

7.7.3. Tool 7.3 Verification

The Pixel size calculation code consists of a single function called ”Planck”. It can be used to generate Planck curves following Planck’s law. These curves can be used to calculate the signal to clutter ratio for an ICBM in front of a background of a certain area. The exact approach to this calculation has been explained in the midterm report. As mentioned before, the choice to look at specific small bandwidths of wavelengths (using a filter) resulted in the need for adjustments as explained above. To verify parts of the code, several unit- and system tests have been performed. Since no analytical solutions to the full pixel sizing problem exist only the expected behaviour of the program could be tested. The unit and system tests performed are described below:

- **Unit test for Planck curve:** Since the function producing Planck curves is used for all computations it was tested for correctness against the analytical Planck’s law. For a given temperature, several wavelengths were which resulted in values with no difference with respect to the analytical solutions besides floating point errors after 10-14 decimals. The curves also showed the expected behaviour of having peaks at lower wavelengths for higher temperatures.
- **Unit test Stefan-Boltzman:** By integrating Planck’s law over all wavelengths, the Stefan-Boltzman law is obtained. By integrating a constructed Planck curve from a wavelength of 0.01 to 100 micrometers (using 1000 steps) at a temperature of 300K an error in the order of 1% was measured. By increasing the upper integration limit and increasing the number of integration steps, the error converged to 0.
- **System test SCR and input behaviour** Even though no analytical solution can be used for system testing purposes, the signal to clutter ratio of a missile on a background is described to be inversely proportional to the square of the pixel dimension [20]. This behaviour was tested by running the program with exactly the same inputs except for a change in pixel size from 500m to

1000m. The SCR decreased from 210 to 52 with a ratio of 4 as expected. As a sanity check, the effect of increasing several inputs has been tested as well. The plume temperature, plume area ad the NETD have all been increased separately which resulted in an increase, increase and decrease of the SCR respectively. This is as expected as both the flame area and temperature increase the ICBM signal while the NETD increases noise.

7.7.4. Reliability Calculations Verification

The code used to determine the allowable spacecraft failure rate consisted of the following verification strategies:

- **Convergence test** The sample size to compute mission reliability is increased from a small number and convergence is verified
- **Multiple random seeds** Simulation is run multiple times with different random seeds and differences between runs are analysed
- **Single failure mode** A mode where only one spacecraft is allowed to fail is simulated and compared to hand made calculations. This mode is easily toggled by changing one Boolean in the code

7.7.5. Subsystem Verification

The tests for the subsystem of the payload are similar to those explained in Table 17.2. Even though the tests are explained as system tests they can also be applied to subsystems and their components. The main tests that would need to be applied to the payload are Thermal tests, special Focus should be placed on the cameras and the cooler. This is due to the fact that these components are the most affected ones by the Thermal tests. Space simulation tests would also need to be performed on the filters as they have never been in space. It would be important to test the behaviour in space conditions and how their lifetime is affected by such conditions. Furthermore, vibration tests

Special tests to be performed on the payload also include the following:

Test for Camera and Filters Thermal Measurement
Description: Place the payload at a certain distance of the launcher and measure the temperature changes.
Goals: Analyse how big the thermal signature of the launcher is. Analyse what the dissipated power of the FPA is. Analyse conduction loses of the FPA. Analyse behaviour of instrument noise. How does it change with respect to temperature and frame rate.

Test for Filters
Description: Set space like conditions and run the filters mechanism and check the output.
Goals: Measure the number of cycles before the filters start failing in space like conditions. Additionally, measure the effect of the degradation of the filters in the quality of the images. Furthermore, check the effect of the speed at which the filter is moving on the ACDS of the spacecraft.

Test for Cooler
Description: Simulate space like conditions and run the cooler.
Goals: Determine heat load (flows down from FPA dissipated power and conduction losses). Measure power usage for different temperatures and heat rejection. Analyse if the copper strap can transfer heat fast enough to the radiators.

7.7.6. Requirement Compliance Matrix

In this subsection the compliance matrix is shown. Any of the requirements that are not completely fulfilled will be discussed afterwards. In the requirement matrix, Table 7.13, a green colour means that the requirement is met while an orange colour means partial or unknown compliance.

As it can be seen from Table 7.13, all the requirements that are green also have R&D on them. This means that as of now it is not known if they will be met. However, these are different from the

Table 7.13: Payload Requirement Compliance Matrix.

REQ	Compliance	(Sub)Section
REQ-SYS-PAY-01	R&D	Section 7.8
REQ-SYS-PAY-03		Section 7.5.1
REQ-SYS-PAY-07	R&D	Section 16.2.3
REQ-SYS-PAY-08	R&D	Section 7.3
REQ-SYS-PAY-17	R&D	

orange requirements as the system is design to be able to meet them and the requirements can be achievable with the current technology. As for the partially satisfied requirement, **REQ-SYS-PAY-03**, this is due to the fact that it was decided to compromise accuracy in the position of the location of the detected ICBM and increase the reliability of the system. This was done it was presumed that a better reliability is more important than an accuracy of 3 σ on the location of the ICBM. As seen in Section 7.7 by decreasing the pixel size to 2.5 arcsec it would be possible to achieve it. As of right now the accuracy is of 95%, just above 2 σ.

7.8. RAMS Characteristics

A RAMS analysis will now be done for the payload subsystem.

Reliability The factor that affects the reliability the most is the extensive amount of R&D that still needs to be performed. All components on their own have a TRL of 5 or higher. However, the payload as a system still needs to be integrated and tested. Hence, the exact reliability of the system is unknown.

Availability For the availability of the system a few factors are taken into account. Firstly, the cooler is working 24/7 therefore the camera should have optimal temperature to work all the time. Secondly, as there is a considerable amount of overlapping in the satellite FOV from the satellites the availability is increased as even if one satellite fails there should still be other satellites working and covering the area. Some constraints imposed on the payload system are the switching of the filters and the switching between Focus and Coverage payload.

Maintainability For maintainability there are a few aspects that need to be taken into account. The cooler requires active monitoring by a thermometer in order to keep the FPA at 77 K so that instrument noise is kept at a minimum. [23]. Furthermore, the velocity of the rotating mirror needs to be measured over time since the velocity will slowly decrease due to friction

Furthermore, the misalignment between the lenses and the mirror have to be considered. to check for miss alignment, it is possible to take unfiltered pictures of the same place on Earth and compare them. If a misalignment is detected the images will need to be corrected.

Finally, as time passes the instrument noise increases. To measure this change in instrument noise the filter is switched to a blackbody filter. These images are compared with images at the start of the mission with the blackbody filter to find the increase in instrument noise.

Safety Finally for the RAMS the safety is taken into account. For payload, the most critical safety concern is the detection of the ICBM. If the payload does not function properly, and the interfaces between payload and the other subsystems are not well defined, the mission would fail. Thus, the detection of an ICBM is a safety-critical function.

7.9. Recommendations

For the future it would be important to improve on different aspects, some of which will be briefly discussed in this section.

In future research it is advised to determine the exact instrument noise. It was not possible to calculate

that number in this report, as many parameters which have to be used in the calculations are unknown. These parameters are company secrets and only if there is genuine interest in the camera, these parameters are provided to the customer. Furthermore, research has to be performed in how strong the signal of an ICBM is. If these two parameters are known the precise signal-to-noise ratio can be determined. If the SNR is found to be excessively high, another type of camera could be selected, which does not require cooling. Currently, High Operating Temperature (HOT) detectors are the latest technology for IR detection. The HOT-IR^{TM} from Leonardo DRS, for example, is able to operate in conditions well above 110 K [39]. Combined with a high SNR this could potentially mean that no cooler is required.

In this design a filter was selected for its low mass, low cost and simplicity. In further research a hyper spectral spectrometer could be selected which makes use of diffraction grating instead of filters. This will increase the payload performance, but it will also bring increased cost, more power consumption, a higher mass and a lower TRL [5].

In follow up research the possible damage by direct sunlight on the filters and camera should be investigated. If significant damage does occur, the probability of accidentally observing the sun should be calculated and the risk should be mitigated. In the case that a manoeuvre has to be performed and there is a possibility that the camera detects the sun, the filter should switch to the black body filter in order to protect the filters and the camera.

In general the specific parameters from the camera need to be known in order to achieve a more detailed design. For example, it is not known for the selected pulse tube cooler what the exact input power and heat rejection are to be able to keep the camera at 77 K. This could drastically change the design of the entire spacecraft. If a pulse tube cooler is found to be too big and power consuming after all, a Stirling cooler could potentially be selected. In general, they are more efficient and smaller. However, it should be investigated whether the vibrations have no significant effect on the images.

For the position error calculations it is necessary to create a 3D model. This is due to the fact that the other direction that is not being calculated this time could behave differently than what it is expected. Having a 3D model will give the actual error values and therefore the team would be able to modify the payload characteristics if necessary.

Additionally, looking into error bias, non-random noise and altitude jitter would be necessary. As of now this is out of the scope of the DSE but these errors could be critical in the accuracy of the location of the ICBM thus they should be investigated and implemented in the 3D program. A better understanding and modeling of the errors will lead to a better calculation on the location of the ICBM.

There is also room for future improvements in the Pixel size calculations. The Planck curve approach makes use of the black body assumption. Even though this assumption describes the radiation of the Earth quite accurately, larger errors are present in the modeling of the rocket exhaust. More research should be performed in accurately modelling the composition of the exhaust gasses. This will result in a more accurate result as the spectral radiance peaks of both water and carbon dioxide can be accounted for. Since it was shown that the program is sensitive to accurate estimations of the temperatures and areas of the exhaust, CFD modelling or testing of these properties can greatly increase the Pixel size accuracy as well with respect to the made assumptions.

Finally, the last recommendation is to calculate how long a missile is inside the doughnut for different possible trajectories. This is important in order to understand better how the detection works and how much time there is to detect the ICBM.

8

Command and Data Handling

The design of the command and data handling (CDH) subsystem is considered. Section 8.1 and Section 8.2 perform the functional and requirement analysis, Section 8.3 considers some software options, Section 8.4 considers hardware design.

8.1. Functional Analysis

The functional analysis of the command and data handling subsystem outlines the main functions performed and are a flow down of the Functional Flow Diagram (see Figure 4.1).

- **FUNC-CDH-01-03:** Process the H2O and CO2 filtered images. *Flow down from functions 4.3.1.2 and 4.3.1.7.*
  - **FUNC-CDH-01-01:** Provide threshold for which an anomaly is considered a potential missile.
- **FUNC-CDH-02:** Provide storage for on ground verification data and housekeeping data. *Flow down from function 4.3.1.4.*
  - **FUNC-CDH-02-01:** Collect housekeeping data from all other subsystems
- **FUNC-CDH-03:**Evaluate velocity of anomaly found from image processing. *Flow down from 4.3.1.8.*
- **FUNC-CDH-04:** Provide coordinates of missile to extrapolate the trajectory of the detected missile on ground. *Flow down from 4.3.3.5.*
  - **FUNC-CDH-04-01:** Calculate number of overlapping images between satellites. *Flow down from 4.3.1.9.*
  - **FUNC-CDH-04-02:** Decide which satellites should track missile. *Flow down from 4.3.1.10.*
  - **FUNC-CDH-04-03:** Triangulate with second satellite.
  - **FUNC-CDH-04-04:** Process data into coordinates of missile.
  - **FUNC-CDH-04-05:** Give command to payload to switch from Coverage to Focus payload. *Flow down from 4.3.2.6.*
  - **FUNC-CDH-04-06:** Give ADCS slewing command to track missile. *Flow down from 4.3.2.3.*
- **FUNC-CDH-05:** Provide data to classify missile.
- **FUNC-CDH-06:** Receive commands from ground station to perform tasks. *Flow down from 4.2.1 and 4.5.8.*
- **FUNC-CDH-07:** Receive commands from subsystems to perform nominal operations.

8.2. Requirement Analysis

- **REQ-SYS-CDH-01:** The CDH shall be able to extract coordinates of the pixel containing the anomaly from the coverage infrared image. *Flow down from FUNC-CDH-01-03.*
  - **REQ-SYS-CDH-01-01:** The CDH shall compute the intensity threshold based on the image taken.
  - **REQ-SYS-CDH-01-02:**The CDH shall be able to extract the pixels with an intensity of – above the established threshold of the CO2 filtered image.
  - **REQ-SYS-CDH-01-03:**The CDH shall be able to extract the pixels with an intensity of – above the established threshold of the H2O filtered image.
- **REQ-SYS-CDH-02:** The CDH shall provide at least 1.5GB of data storage. *Flow down from FUNC-CDH-02.*
  - **REQ-SYS-CDH-02-01:** The CDH shall have sufficient storage to log data for TBD [time unit] before overwriting

  - **REQ-SYS-CDH-02-02:** The CDH shall have sufficient storage to log 1.6 MB of housekeeping data every day
  - **REQ-SYS-CDH-02-02:** The CDH shall have sufficient storage to log 16 MB of payload data every 2 weeks
- **REQ-SYS-CDH-03:** The CDH shall classify an anomaly to be moving within 20 seconds. *Flow down from FUNC-CDH-03 and time budget*
- **REQ-SYS-CDH-04:** The CDH shall detect ICBM 14km after launch. *Flow down from FUNC-CDH-04.*
  - **REQ-SYS-CDH-04-01:** The CDH shall provide the coordinates of the ICBM with a 1km (3-sigma) accuracy in all dimensions.
  - **REQ-SYS-CDH-04-02:** The CDH shall be able to detect ICBMs up to their burnout altitude.
  - **REQ-SYS-CDH-04-03:** The CDH shall be able to detect the ICBM from all angles of flight.
- **REQ-SYS-CDH-05:** The CDH shall initiate the stereo-imaging process after the anomaly has been confirmed to be moving. *Flow down from FUNC-CDH-04.*
- **REQ-SYS-CDH-6:** The CDH shall track ICBMs within 1km (3-sigma) accuracy in all dimensions. *Flow down from FUNC-CDH-04.*
- **REQ-SYS-CDH-7:** The CDH shall provide inputs for the other subsystems for tracking of missile. *Flow down from FUNC-CDH-04.*
  - **REQ-SYS-CDH-07-01:** The CDH shall provide a data link of at least – to the ADCS.
  - **REQ-SYS-CDH-07-02:** The CDH shall provide a data link of at least – to the payload.
  - **REQ-SYS-CDH-07-03:** The CDH shall provide a data link of at least – to Communications.
- **REQ-SYS-CDH-08:** The CDH shall process data for on ground classification. *Flow down from FUNC-CDH-05.*
  - **REQ-SYS-CDH-08-01:** The CDH shall be able to provide classification data from all angles of flight.
- **REQ-SYS-CDH-09:** The CDH shall provide data interfaces to all other systems. *Flow down from FUNC-CDH-07.*
- **REQ-SYS-CDH-10:** The CDH shall perform housekeeping tasks. *Flow down from FUNC-CDH-02-01.*
  - **REQ-SYS-CDH-10-01:** The CDH shall monitor the temperature of critical locations of the satellite.
  - **REQ-SYS-CDH-10-02:** The CDH shall record all data from temperature sensors, ADCS sensors, and Power sensors.

8.3. Data Processing

A preliminary overview is given of the on-board data processing algorithms that must be considered.

8.3.1. Data Handling

Table 8.1 outlines the different packages of data the system will be handling throughout the detection, tracking and relay process. Each data package has an associated 'sender', 'receiver', and a data quantity specified in bits. Furthermore, each data package flows down from a function specified by the functional flow diagram [FFD] in Chapter 4.

These packages are most constraining to the communication subsystem, as discussed in Chapter 9. However, they are specified in the Data handling section as they are also used to design the OBC and the data handling system. As can be seen, spacecraft 2 has must receive data from spacecraft 1 (DP-1D) and simultaneously send data to the ground station during the tracking period (DP-2A). Thus, this is the design point for which the communication subsystem was designed. In order to ensure that this communication may operate without disturbances, the OBC is designed to allow for multiple tasks to be carried out at once. This is considered further in Section 8.4.

Table 8.1: Data Packages.

Name	Description	FFD	Sender	Data	bits	Receiver
DP-1A	Initiating second satellite after level 3 alert	4.3.2.2	SC-1	Timestamp, SC-1 position, Vector to bright pixel, SC-1 identifier	232	SC-2
DP-1B	Out of plane level 3 alert	4.3.2.4	SC-1		0	SC-3 [out of plane]
DP-1C	Level 3 alert to ground station	4.3.2.1	SC-1 + Interlink	Timestamp, SC-1 position, Vector to bright pixel, SC-1 identifier, Alert	264	Interlink, GS
DP-1D	2D Tracking data	4.3.2.9	SC-1	Timestamp, SC-1 position, Vector to bright pixel, SC-1 identifier	232	SC-2
DP-1E	Attitude threshold alert	4.3.2.12	SC-1	Timestamp, SC-1 identifier, Alert	72	SC-3 + Interlink
DP-2A	3D Tracking data	4.3.3.9	SC-2 + Interlink	Timestamp, Missile position, Intensity of pixel, Identifier	144	SC-3
DP-2B	Order third satellite to point at target	4.3.3.7	SC-2	Timestamp, Missile position, Identifier, Alert	168	SC-3
DP-2C	Out of plane 3D alert	4.3.3.6	SC-2		0	SC-3 [out of plane]
DP-0A	3D missile position to ground station	4.3.3.8	Interlink	Timestamp, Missile position, Intensity of pixel, Identifier	144	Interlink, GS
DP-0B	Full images to ground station	4.3.2.13	All SC	Timestamp, Full images, Identifier	1×10^7	GS

8.3.2. Image Processing

The first step in the IR-imager data processing aiming to verify the presence of an ICBM is the analysis of images generated by the IR-imager. The preliminary image processing procedure was set up based on the following assumptions:

- The IR-Imager is able to look into the atmospheric absorption bands, hence the presence of atmospheric background noise is expected to be minimal.
- The H2O and CO2 filters are able to look at the set wavelengths of 2.7 and 4.3 nm ±0.05 nm.
- The IR-imager will produce grayscale images of 1024 by 1280 pixels with a pixel depth of 8 bits[40].
- Deduced from these assumptions above it is found feasible that the peaks in registered intensity originated from an ICBM will appear as very apparent intensities on the produced image.

As no values could be found with regards to the H_2O or CO_2 intensity produced by an exhaust plume, it was decided that the threshold to deem a pixel to be of interest should be set based on the image taken and thus to implement an adaptive thresholding algorithm. Following on the assumptions as stated above, the generated image is expected to be bimodal, hence to have two distinct image values present; respectively background noise and ICBM induced intensity peaks. For a bimodal image it is feasible to adopt Otsu's Binarization algorithm [1]. Otsu thresholding techniques are known to be simple, robust and adaptable [41]. The following roadmap aims to show the proposed set of steps to be taken for the image processing:

1. Evaluate H_2O grayscale image and set threshold (Figure 8.1).
2. Establish pixels of interest, generate square allowable pixel range around pixels for which an anomaly is established (Figure 8.2).
3. Evaluate CO_2 image and set threshold (Figure 8.3).

[1]Retrieved from `https://opencv-python-tutroals.readthedocs.io/en/latest/py_tutorials/py_imgproc/py_thresholding/py_thresholding.html`

4. Establish pixels of interest, check if they fall within pixel range set based on H_2O image (Figure 8.4).
5. If match is found, store: Timestamp, Pixel Coordinates and intensity of pixel deduced from CO2 image (Figure 8.4).

Presuming the road map to be largely self-explanatory, step 3 as indicated requires an explanation. The ”generate pixel range” functionality is presumed necessary for two reasons; Firstly, if a H2O pixel of interest is found, the filter switch to the CO2 filter takes time allowing the suspected ICBM to move. Second, a certain approximation is performed in locating the exhaust plume, giving room for an uncertainty in pixels of the exact location of the H_2O plume as well as for the CO_2 plume as to where to appear after the time a filter switch takes is passed by. The location of the pixel with a CO_2 anomaly will be used as the input to the Velocity Check.

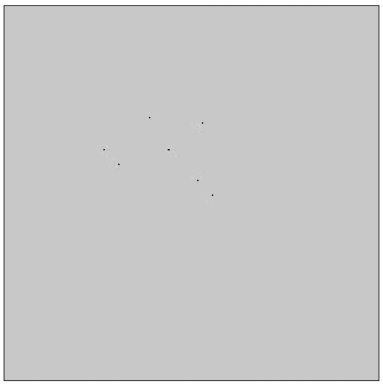

Figure 8.1: Original H_2O Filter Image.

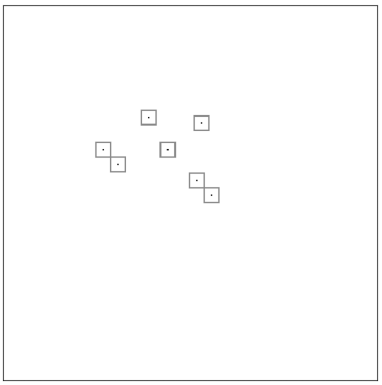

Figure 8.2: H_2O Filter Image after Otsu Thresholding, pixels of interest and allowed pixel ranges indicated.

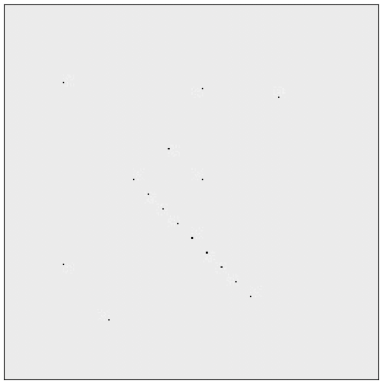

Figure 8.3: Original CO_2 Filter Image.

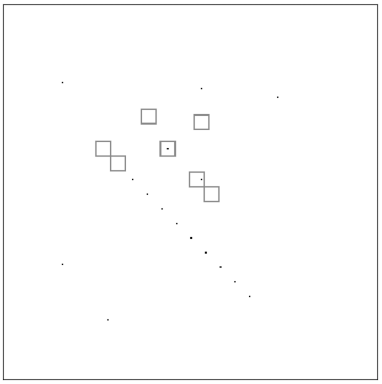

Figure 8.4: CO_2 Filter Image after Otsu Thresholding, pixels of interest that fall within H_2O Image deduced allowable ranges indicated.

8.3.3. Velocity Check

Once an anomaly has been identified as a potential missile by the image processing algorithm, the satellite will check that this anomaly has a velocity before initiating the second satellite. This is done by means of the following two-dimensional procedure.

For a coordinate system placed at the centre of the Earth, with the positive y-axis pointing to the north pole, and the x-axis pointing to the right, the position of a satellite may be expressed by an angle θ_i at a time t_i. Where θ is measured counterclockwise positive from the positive x-axis, to the nadir pointing axis of the spacecraft.

Given this angular coordinate (θ_0) and the coordinates of the bright pixel, two lines in space exist. One line from the spacecraft to the beginning of the pixel, and one line from the spacecraft to the end

of the pixel. At time t_1 a new angular position θ_1 is reached, for which two new lines exist. This is illustrated in Figure 8.5. As the angular resolution of a single pixel is very small, these two lines are represented by one line in order to provide a simplified illustration. The intersections between two lines in Figure 8.5 are thus small areas. Thus, from this, two conditions can be established in order to conclude that an anomaly has a velocity:

- L(t_2,θ_2) does not intersect at the intersection of L(t_0,θ_0) and L(t_1,θ_1).
- Intersection of L(t_i,θ_i) and L(t_{i+1},θ_{i+1}) is not at y = Re.

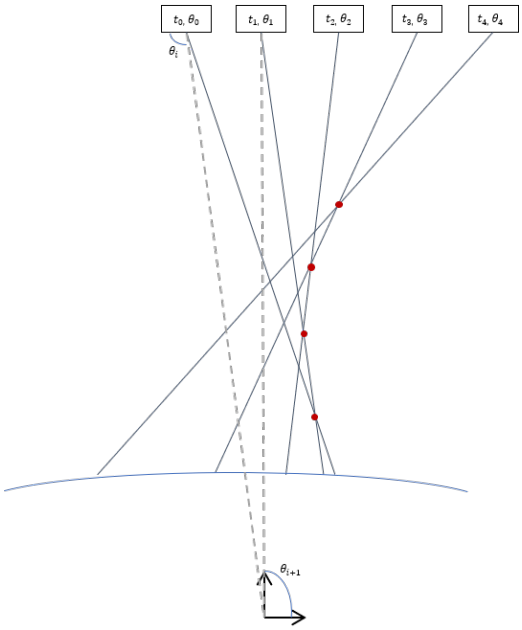

Figure 8.5: Simplified Schematic Representation of Velocity Check.

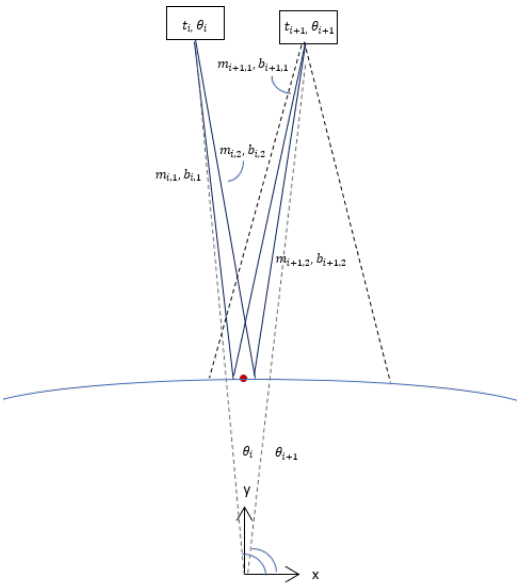

Figure 8.6: Schematic Representation of Boundary Conditions for two Time Steps.

In the worst case scenario, the anomaly is stationary. Thus a threshold must be established for which one can say with certainty that the anomaly can not be a missile, such that the spacecraft does not remain fastened on an anomaly. In order to determine this threshold, a program was written in which the two lines to the beginning and end of the bright pixel impose a boundary condition that should be satisfied in order to confirm that the object is non-moving.

This boundary condition is checked for one million simplified missile trajectories modelled after the SS18 and the Minutemann-III in order to determine the time at which all trajectories satisfy these conditions. The time at which this happens is the time threshold at which it can be said with certainty that the anomaly is stationary. The program works more specifically as follows:

A simulation was created to estimate the possible trajectories. This involved simplifying the problem to 2D and numerically integrating equations of motion based on the following assumptions about the SS-18 and Minutemann-III:

- Thrust vector of the missile is co-linear with its velocity vector. Gravity is the only force that turns the missile trajectory.
- Propellant burns at a constant rate.
- All propellant is burned during each respective stage's burntime.
- Drag above 80 km is negligible and so the drag coefficient c_d of the missile is 0 above this altitude.

Given these assumption it is possible to use the following equations of motion [42]:

$$\frac{dv_x}{dt} = \left[\frac{T - \frac{1}{2}\rho A C_d v^2}{M}\right]\frac{v_x}{v} - \frac{GM_e x}{(x^2 + y^2)^{3/2}} \tag{8.1}$$

$$\frac{dv_y}{dt} = \left[\frac{T - \frac{1}{2}\rho A C_d v^2}{M}\right]\frac{v_y}{v} - \frac{GM_e y}{(x^2 + y^2)^{3/2}} \tag{8.2}$$

where v_x and v_y represent the x and y components of the missile's velocity vector in the respective directions in the Earth centered coordinate system. T represents thrust as function of burnstage, A is the cross sectional area of the missile, ρ the atmospheric density as function of missile altitude, M the mass of the missile as function of time, M_e the mass of the Earth (5.97×1024 kg), G represents the gravitational constant ($6.67 \times 10^{-20}\ km^3 s^{-2} kg^{-1}$) and C_d is the drag coefficient as a function of velocity. Given the earth centered coordinate system, the missile's altitude was estimated using eq. (8.3).

$$h = \sqrt{x^2 + y^2} - R_e \tag{8.3}$$

Density, drag and temperature as a function of altitude and velocity of the missile in analysis were created by interpolating recorded valuces [42]. Mass was modelled as a function of time through eq. (8.4), where t_{bn} represents the burn time for the nth stage, M_t is the total missile mass, M_{bn} represents the burn out mass jettisoned at the end of the nth stage and t indicates the instance in time the mass is being evaluated at.

$$\begin{aligned}
M(t) &= M_t - M_{p1} \cdot (t/t_{b1}) && [t < t_{b1}] \\
M(t) &= M_t - M_{p2} \cdot \left(\frac{t - t_{b1}}{t_{b2} - t_{b1}}\right) - M_{p1} - M_{b1} && [t_{b1} \le t \le t_{b2}] \\
M(t) &= M_t - M_{p3} \cdot \left(\frac{t - t_{b2}}{t_{b3} - t_{b2}}\right) - M_{p1} - M_{p2} - M_{b1} - M_{b2} && [t_{b2} \le t \le t_{b3}]
\end{aligned} \tag{8.4}$$

With all parameters in eq. (8.2) and eq. (8.2) defined, the second order differential equations are integrated using Euler's forward integration; once integrated the missile's velocity as a function of time can be deduced and twice integrated the missile's 2D position in the Earth centered coordinate system over time is obtained. Euler's integration is essentially: $\mathbf{v}^{i+1} = \mathbf{v}^i + (d\mathbf{v}/dt)^i \cdot \Delta t$ and $\mathbf{x}^{i+1} = \mathbf{x}^i + \mathbf{v}^{i+1} \cdot \Delta t$ [2].

Euler's forward integration depends on the initial conditions of the equations known. To simulate the trajectory of the SS-18 and Minuteman-III missiles, the equations of motion are numerically integrated from $(x = 0, y - R_e)$ till $z = R_e$, where R_e is the radius of the Earth. Essentially integrating the missiles motion from launch till impact. Furthermore, in this simplified model, a control input is created which essentially deviates the direction of flight of the missile from the vertical by a given angle at a given altitude. This essentially controls where the missile is headed, or targeting.

In order to make it possible to simulate a million distinct trajectories, these functions were altered to take the 2D launch position of the missile, the altitude at which the missile turns to create its trajectory takes place as well as the angle by which it turns as inputs when doing the aforementioned integration. It was also made possible to simulate trajectories that would be detected if the missile was only spotted by the payload a certain alterable amount into its flight.

These trajectories can be checked against boundary conditions. As can be seen in Figure 8.6, at a given time two lines exist, each with a gradient m, and an intercept b, resulting in two linear equations. Where $x_{i,missile}$ is the x position of a hypothetical missile trajectory at time t_i.

[2]Retrieved from `https://www.sciencedirect.com/topics/engineering/forward-euler#:~:`

- $y_{i,1} = m_{i,1} \cdot x_{i,missile} + b_{i,1}$
- $y_{i,2} = m_{i,2} \cdot x_{i,missile} + b_{i,2}$

Thus, two sets of two boundary conditions exist for a stationary anomaly. For an anomaly located in the right FOV (scenario t_i in Figure 8.6):

- $y_{i,missile} < y_{i,1}$ **or** $y_{i,missile} > y_{i,2}$

For an anomaly located in the left FOV (scenario t_{i+1} in Figure 8.6):

- $y_{i+1,missile} > y_{i+1,1}$ **or** $y_{i+1,missile} < y_{i+1,2}$

If one of the two boundary conditions is met, it may be concluded that that particular missile trajectory can not satisfy these boundary conditions. This program is run for an assumed stationary anomaly located at (0,Re+14) km, as long as this anomaly remains in the FOV of the satellite. This can be checked for many trajectories, and a time threshold can be determined at which no trajectories are valid under the given boundary conditions, meaning that it is considered 'statistically impossible' for a missile trajectory to exist that satisfies the imposed boundary conditions.

Following this velocity check, given that the anomaly has a velocity, a level 3 alert is sent to the ground station as specified by Section 4.1. However, as circular scanning will be used, some complexity arises due to overlapping with regards to satellites taking images of the same point on earth at the same time. This implies that when a velocity is found, more than one satellite may be looking at the same point, and they might all send this alert, and also initiate a second satellite. This risk is something that needs to be mitigated in order to allow for clear communication to the ground station. The following preliminary process was defined:

1. Once a velocity is detected, an algorithm should be run that checks which satellites would be looking at the same point given satellite position and attitude inputs, time stamp, camera angle, and the pixel number of the anomaly.

2. Given that multiple satellites are found to be looking at the same point, a method needs to be determined such that all these satellites are able to run an algorithm which can assess which satellite is most suitable to initiate tracking. Three possible methods were identified for this:

- The satellite for which the pixel containing the anomaly is most centered in the image.
- Each satellite has a database of known missile trajectories. The database would include the position of the missile above 14km, at the same frequency as the scanning method, for approximately 20 seconds. By running through the database, the most likely trajectory can be determined given the pixels in which the anomaly was visible. From this, the most suitable satellite may be determined. This method takes into account the probable direction of the missile too, such that the second satellite can be chosen more effectively.
- The final proposed method is one resembling the Metropolis-Hastings Markov Chain Monte Carlo (MH-MCMC) in which normal distributions are approximated for the sequence of pixels that the anomaly has been detected in. This method is probabilistic rather than deterministic, and can therefore provide a more accurate most likely estimate for which satellites are most suited to track the missile.

3. Each satellite will either output a 'yes' or a 'no' value. If it is a yes value, it means that that satellite needs to track the satellite, and initiate the second satellite. If a no value, the satellite resumes with coverage payload imaging, and does not track the missile. The second satellite should be decided upon through a similar probabilistic model as described in the second two methods above. Doing so ensures that the missile remains within these two satellites' fields of view for the longest possible time.

4. An alert has to be sent to the ground such that confirmation is received that a satellite is tracking the missile.

Choosing a method is dependant on the available computing power on board, and the time delay that would be incurred through running such algorithms. Ideally, the probabilistic model should be employed, but more analysis must take place in order to determine if it is feasible to run such an algorithm on board.

Once the second satellite has been initiated, the stereo imaging process begins. This method, as described in Chapter 7, uses control loops to centre the missile into a Coverage image before the Focus payload is triggered. Once the Focus optic is on, the two satellites will triangulate to find the 3D coordinates of the missile, and this data will be processed on board the second spacecraft, and sent down continuously through interlinking as specified in Table 8.1. The velocity of the missile may be calculated on board from these 3D position coordinates, such that a prediction can be made on the local trajectory of the missile, allowing for more accurate tracking. However, it is currently deemed unnecessary to send this velocity data to the ground. The differentiation of the 3D position coordinates with respect to the time stamps can be done on ground to determine the velocity characteristics. Together with the intensity sequence of the pixel of interest, a classification of the missile can be made (see alert levels 4 and 5).

8.4. Command and Data Handling Design

The following section is concerned with the hardware design of the On Board Computer (OBC) and Data Processing Unit (DPU). First, research was performed into the hardware components of a Command and Data Handling system of interest to the M-STAR satellites. After this, a distinction is made between the DPU and OBC supported by reasoning. Both subsystems are examined in detail, a proposed hardware setup is given together with the connections between the two, and subsequently an executed COTS component research is elaborated upon. Finally, a COTS component is presented together with proposed adaptations to make it more fitting to the M-STAR mission.

Research showed that the OBC hardware design is most frequently customized to the specific mission [43] [44] [45][3]. The same applies to payload data processing, it became apparent that different payloads posses different data processing characteristics and thus can give a variaty of outputs. Thus, data processing can or cannot be a task assigned to the main OBC. For M-STAR, a distinction was made between the DPU and OBC, for which reasoning can be found in Section 8.4.1.

8.4.1. Data Processing Unit

It was determined to set up a Data Processing Unit (DPU) separately from the OBC. The reason for this decision can be found in the current setup for the payload. The proposed design takes performance data from COTS available products and proposes to pursue an R&D process aiming to combine those characteristics in the most optimal configuration for the M-STAR satellites. Hence, future research will show the feasibility of implementing actions currently suggested for the DPU in the IR-imager to be designed.

In the DPU primary data processing is executed. Primary data processing entails image processing, respectively the detection of anomalies in water exhaust intensity and subsequently anomalies in carbon-dioxide intensity. Next to this, the DPU is able to impose a filter switch after H_2O anomaly detection. And, after detection of the second anomaly, the DPU starts to transfer its data to the OBC continuously to enable velocity detection. When a velocity is detected for the pixel with the anomaly in intensity, the DPU should execute the received command from the OBC to adapt the optics to switch respectively from Coverage to Focus. The tasks for both the OBC and DPU are set up according to a priority queue. The method is based on time-slices; after each time interval an interrupt is raised, the queue is evaluated and it is decided which task should be executed [46]. The following three situations can occur when a new task is appended:

1. If the running tasks have the highest priority out of all ready tasks, they will continue running

[3]Retrieved from `https://directory.eoportal.org/web/eoportal/satellite-missions/p/proba-v`

and the queue will arrange in order of priority with the newly appended task included.
2. If the newly task has the same priority as another ready task, it will switch with that task.
3. If the one of the running tasks has a lower priority than a ready task, the running task is swapped out, and the highest priority task is swapped in.

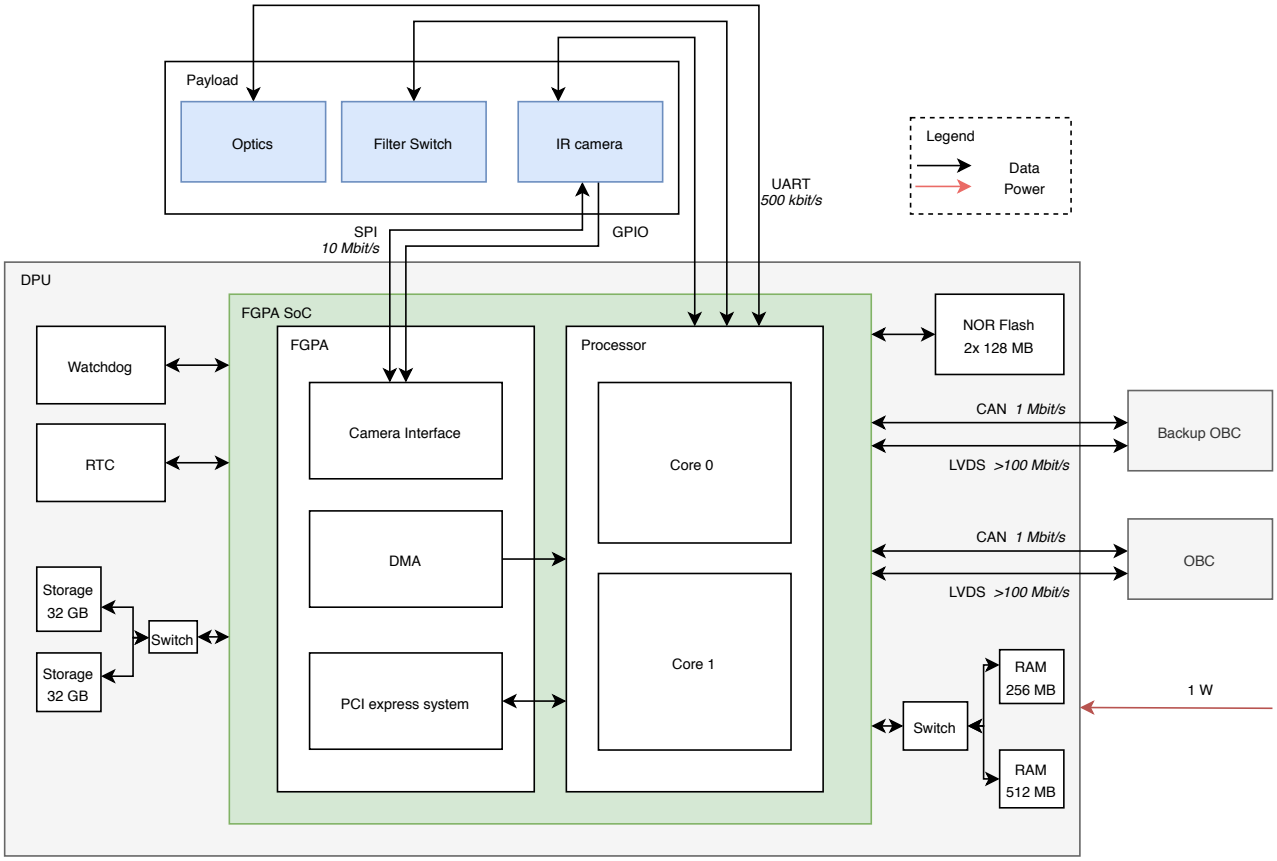

Figure 8.7: Block Diagram of proposed Data Processing Unit

The tasks as they were defined for the DPU can be found in Table 8.2 together with their priorities. For the design of the DPU, the processing speed was found to be limiting. As the DPU should be able to perform real-time image processing, the framerate, image size and pixel depth should be used as inputs. However, to examine the relation between image processing and processor frequency was found to be out of the scope of the DSE and is left for further research.

Table 8.2: DPU tasks and priority level.

TASK	PRIORITY	DATA	RESPONSIBILITY
Command Handling	VERY HIGH	Commands	Perform commands issued by OBC (i.e. filter switch, Coverage to Focus)
Data Transmission	VERY HIGH	Bright pixel location vector	Continuous data transmission to OBC
Anomaly H_2O	HIGH	Raw payload data	Process raw payload data, check for brightness anomaly with H_{20} filter
Anomaly CO_2	HIGH	Raw payload data	Check for brightness anomaly with CO_2 filter within range deduced from H_2O anomaly
Error Detection	MEDIUM	All Data	Check that no data has been corrupted
Housekeeping	LOW	payload house-keeping Data	Gather and store telemetry data

The proposed hardware design for the DPU can be found in Figure 8.7, based on [45] and [46]. A dual core processor was found to be required. Considering, for example, when continuous data

transmission of position vectors to the OBC is required, the DPU needs to be able to perform both the processing payload data task and transmitting data task simultaneously, hence requiring the two cores. It can be seen that an SoC FPGA is implemented, enabling in-field updates and upgrades. Next to this, an FPGA SoC has integrated both the processor and FPGA on the same device improving efficiency [47].

8.4.2. On Board Computer

To enable more robust computing, a main On Board Computer is implemented next to the DPU. Again, a dual core setup is proposed enabling to execute two of the tasks as listed in Table 8.3 simultaneously. For example, a limiting case would occur during missile tracking where data needs to be interlinked continuously and triangulated at the same time. The tasks will be presented to the processor following the same priority queue method as elaborated upon in Section 8.4.1. As is presented in the Velocity Procedure task, Coverage data will be continuously processed during a certain timestamp to establish that the detected anomaly is not stationary. When the Velocity Procedure has a positive outcome, the command is sent from the OBC to the DPU to switch the payload from Coverage to Focus. The Focus data will subsequently be processed separately from the Coverage data, they will not be combined on board. A data package can be created combining both data sets to enable verification on ground, this will be elaborated upon in Chapter 17.

Table 8.3: OBC tasks and priority level.

Task	Priority	Data	Responsibility
Command Handling - GS	VERY HIGH	Commands	Execute commands from GS
Communication - GS	VERY HIGH	Data Packages	Transceive data, build downlink data package
Communication - Interlinking	VERY HIGH	Data Packages	Transceive data, build interlink data package
Triangulation Procedure	HIGH	Data Packages from 2 distinct S/C	Perform triangulation for missile coordinates
Velocity Procedure	HIGH	Continuous bright pixel vector data	Perform velocity check for bright pixel
ADCS	MEDIUM	ADCS Data	Read data, give attitude adaptation commands
Error Detection	MEDIUM	All Data	Check that no data has been corrupted
Housekeeping	LOW	Housekeeping Data	Gather and store telemetry data

Next to the processor frequency, it is of importance to create an OBC that is reliable and forms a redundant system throughout the M-STAR mission lifetime. Erik Bertels, Systems Engineer at ISIS, stated that a single OBC should be able to perform the tasks as indicated in Table 8.3. However, depending on the required accuracy of the on-board calculations, one would need to consider adapting the design. As the accuracy of the software will not be examined into more detail during the DSE, it is assumed that one OBC is sufficient to execute all tasks as stated and thus the recommendation for a redundant system is to implement two OBCs. Some characteristics are crucial for an on-board computer and are thus implemented in the proposed OBC design as displayed in Figure 8.8. The black arrows indicate data interfaces, the red arrows indicate power distribution.

For data interfaces within a satellite, a large variety of options can be implemented, for example those as found in [46]. A trade off can be done depending on, amongst others, user needs and requirements, voltage requirements and required data transfer rate. An apparent distinction for the required transfer rate in data interfaces present in the M-STAR satellites is the following: On the one hand, the data rate between the payload, DPU and Main OBC or Backup OBC needs to be relatively high magnitude and high speed as payload data needs to be transferred and data processing is aimed to be executed in real time. For this interface, one could consider LVDS or SPI [48] [46]. On the other hand, when considering the Thermal Control System, the two types of data transfer to be considered are housekeeping data and OBC commands. The magnitude of this data is much smaller, and when

considering housekeeping data, the data transfer speed can be much lower. To establish this data interface, USART[4], CAN[5], UART or I^2C [46] could be considered. Next to this, it is found that data interfaces fastly evolve. For example, it is claimed that LVDS transfer speeds can be bumped up to 155 or even 400 megabytes per second [6]. Furthermore, UART has transitioned into USART enabling a synchronous universal receiver transmitter to be adopted for satellite on-board data handling. For the reasons as stated, only an indication of possible suitable data interfaces is presented in the OBC but the final decisions are left to future research.

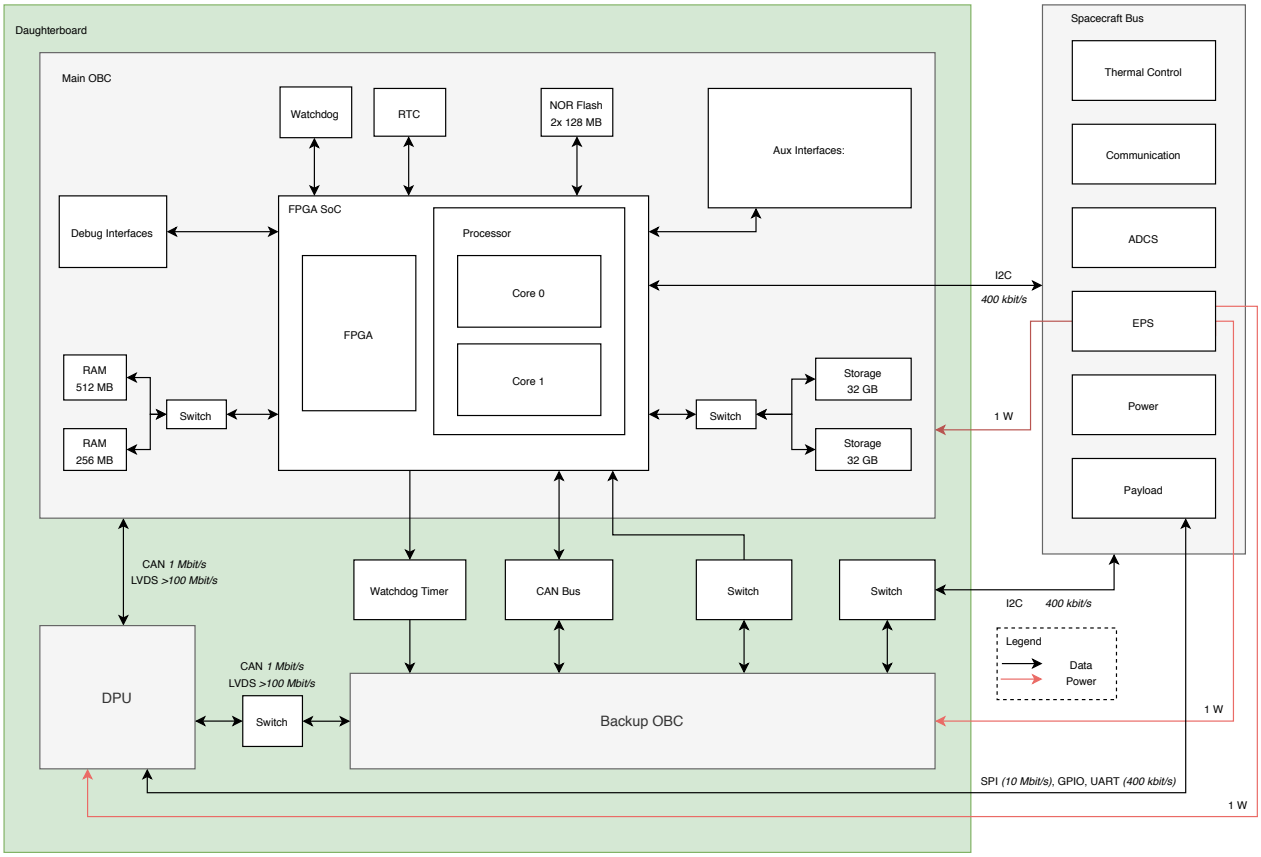

Figure 8.8: Block Diagram of proposed OBC.

In Figure 8.8 it can be seen that a backup OBC is presented in order to establish redundancy for the OBC system. The redundant configuration is based on the study presented in [49]. During the mission, the Main OBC will be in run mode and the Backup OBC will be in deep sleep mode [2]. The external watchdog timer as indicated will continuously monitor processor activity of the Main OBC and generates an interrupt signal if it operates incorrectly. As this signal is fed into the Backup OBC, it will send a message via the CAN Bus to the Main OBC checking for activity. If this message is not received, a reset signal is send to the Main OBC several times to prevent failure. When failure is confirmed, the Main OBC will be disabled via the CAN Bus and power supply is turned of to prevent erroneous operations from occurring. The backup OBC will possess the autonomous reconfigurability feature.

Next to the redundancy for the OBC, the DPU should also have a backup system. For now, it is assumed that DPU failure can be covered by the presence of the OBC. While the function specific components within the FPGA as proposed in Figure 8.7 might not be present, the algorithm for data processing should be included in the NOR Flash Memory of both the Main and Backup OBC. As a

[4]Retrieved from `https://www.edn.com/usart-vs-uart-know-the-difference/`
[5]Retrieved from `https://www.can-cia.org/can-knowledge/can/high-speed-transmission/`
[6]Retrieved from `https://www.militaryaerospace.com/power/article/16705901/lvds-data-transmission-catches-on-in-defense-and-satellite-applications`

data interface is present between the payload and the OBC at all times, the OBC can take up DPU functionalities when the DPU Watchdog indicates the necessity to do so.

Data Storage
For data storage it is deemed that the available storage requirement should be based on the amount of data that can be downlinked to a GS in 3 days as to avoid continuous data accumulation within the S/C. For the S-Band Antenna an average downlink rate of 1 Mbps is defined. Next to this, a conservative assumption of 5 minutes of downlink time per GS passing is established. Analysis showed that an average of 36 GS passages occur per satellite per day. For this it was assumed that 5 ground stations from the ESA could be used. These are, Kiruna, Kourou, Malargue, New Norcia and Redu. Once the locations were known a Longitudinal Ascending Node was set. For the M-STAR constellation there are 9 LAN equally spaced between 0° and 180°. It was then found that on average each satellite passes over a ground station 36 times every 24 h. This is based on a positive assumption in which the satellite will almost always be in the FOV of the station and there are no objects blocking the GS preventing a successful passing. Hence, assuming 36 GS passages, each M-STAR satellite has a total downlink capability of 1.35 GB per day. Therefore, a storage requirement of 4.05 GB for three days can be deduced. As research showed that SD cards can easily allow for as much as 32 GB storage [2], the data storage required is established not to be limiting for the OBC or DPU design of the M-STAR Mission.

While several types of data are present within a satellite, the payload data and housekeeping data were deemed to make up the most important part. The limiting payload data package required to enable on-ground verification for the complete M-STAR mission is seen in Table 8.4 , this would equal a total data size of approximately 2.616 GB, requiring 70 successful GS passages to downlink. Detailed research in to what raw data is required on-ground to enable verification of all processes done on board such that the total payload data package can be send within one day of passing is left for future studies.

Table 8.4: Maximum Data Package Generated per S/C.

Data	Packet Size
H_2O Images	0.002 62 GB
CO_2 Images	0.002 62 GB
Bright Pixel Vector	232 bit
S/C Position	96 bit
Identifier	8 bit
Timestamp	32 bit
Velocity Check Images (5s, 2Hz)	0.0131 GB
Triangulation Data	0.000 324 GB
Triangulation images (10% of 600 s, 30 Hz)	2.359 296 GB
Total Data	2.378 GB
Margin (10%)	2.615 77 GB

With regards to the housekeeping data required to assess the health of M-STAR satellites, a preliminary budget was established as can be found in Table 8.5. It was deemed for all components that time, power and temperature are required at specified time intervals. Other aspects that were implemented are the characteristics mentioned in the maintainability section of the RAMS analysis for each subsystem. The housekeeping data budget for OBC and DPU is deduced from BRIKII [14], characteristics such as sampling frequencies for other subsystems are similar. After comparison with the housekeeping budget as mentioned in [14], the budget for M-STAR was found to be around a factor of 3 lower. Hence, the housekeeping data budget to assess storage requirements is deemed to be 6.80 Mbit d^{-1} equal to BRIKII [14] with 25% additional contingency management, thus 0.001 062 5 GB d^{-1}. Within this housekeeping data assessment, the components as mentioned in Table 8.5 should be present.

When assuming detection of a missile every three days, the total amount of data generated equals 2.619 GB, including 3 days of housekeeping data and 1 missile detection data package as elaborated

upon in Table 8.4. Out of the optimum of 108 GS passages this would require 70 to be successful, a success rate of 64.8%. Hence, storing and downlinking raw data for verification of ICBM detection is considered feasible. As the amount of ICBM launches occurring is expected to be limited, future studies should show whether there is room for a secondary application of the M-STAR satellite constellation and thus additional downlink and storage required.

Table 8.5: Preliminary Assessment Housekeeping Data Budget.

Component	Subcomponent	Data (bit)	Sampling Frequency (Hz)	Duty Cycle	MB/day	Margin	MB/day
ADCS	GPS	104	1	50%	0.5616	25%	0.702
	Attitude	288	1	100%	3.1104	25%	3.88
	ADCS OBC	224	1	100%	2.4192	25%	3.024
Prop	Thrusters	352	0.01	25%	0.0095	25%	0.0118
	Propellant	32	0.01	25%	0.00086	25%	0.0011
EPS	PDU	1024	0.05	100%	0.553	25%	0.6912
	ACU	192	0.05	63%	0.06532	25%	0.0816
	Batteries	384	0.05	100%	0.207	25%	0.26
payload	Cooler	96	1	100%	1.037	25%	1.3
	Camera	128	1	100%	1.38	25%	1.728
	Mirror	96	1	100%	1.037	25%	1.269
	Filter Switch	96	1	50%	0.518	25%	0.648
TTC	Transceiver and Encrypter	992	0.01	100%	0.107	25%	0.134
	Software	128	0.01	100%	0.0138	25%	0.0173
DPU		256	1	100%	2.765	25%	3.456
OBC		384	1	100%	4.143	25%	5.184

Software Diagram

In Figure 8.9 the software diagram for the M-STAR mission can be found. The mission-specific software blocks are indicated, together with the aimed for outcome. The other types of software expected to be required are for example housekeeping data processing, this is assumed to be included in standard OBC design and therefore not indicated. It can be seen that most processing is done on board, while classification happens in the GS.

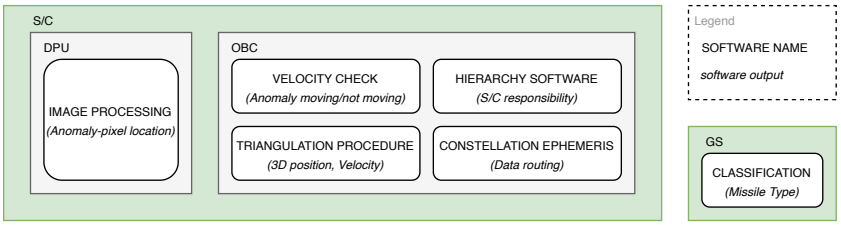

Figure 8.9: Software Diagram for M-STAR Mission.

8.4.3. OBC COTS Research and Feasibility Study

The launch date for the Technical Demonstration Mission as requested by the Royal Netherlands Airforce is proposed for 2024, based on this time constraint a research was executed for Commercial-Of-The-Shelf OBCs both compatible with the mission requirements as well as in possession of a flight heritage. Furthermore, implementing a COTS component is also in line with the sustainability plan, as specified in Section 16.6. Important factors that come into play when looking at the trade off for an COTS OBC are deduced from the research by satsearch: An overview of on-board computer systems available on the global space marketplace (March 2020)[7]. The characteristics are as follows:

[7]Retrieved from `https://blog.satsearch.co/2020-03-11-overview-of-on-board-computers-available-on-the-global-space-marketplace`

Processing capability including clock speed, Bus Size and MIPS, Flight Heritage, Memory, Lifetime, Power Requirements, Reliability, Size, Weight and Redundancy.

When considering the M-STAR satellites it was found that real-time processing is of vital importance to the mission. However, the ability of a processor to achieve the indicated is heavily dependent on the specific algorithms implemented. Since the data processing was found to be out of the scope of the DSE, the processor card with the highest clock speed was chosen as a baseline. This resulted in opting the Q7S, with two ARM dual-core Cortex-A9 MPCore processors each with a processing frequency up to 766 MHz, a bus size of 32 bits and the capability to perform 2.5 Million Instructions Per Second per MHz [2] [50]. Next to this, it has been stated by NASA to be a fraction of the cost when compared to other similar COTS products [8]. Hence, it is deemed that the processor card as shown in Figure 8.10 is able to meet all requirements. A redundant system can be created when two processor cards will be implemented, feasible to do on the same daughterboard. In addition to this, a mission-specific daughtercard can be added which would fulfil the functionalities as they were proposed for the DPU (Section 8.4.1)[9] .

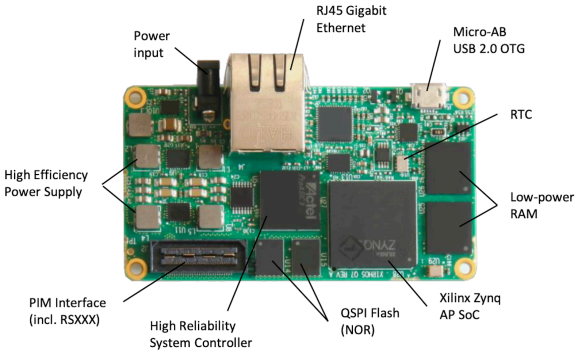

Figure 8.10: Q7S Processor Card by Xiphos Technologies Front [2].

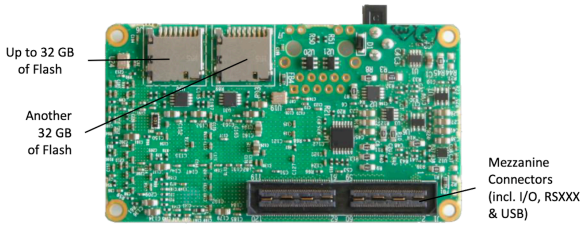

Figure 8.11: Q7S Processor Card by Xiphos Technologies Back [2].

While the current OBC design is expected to be able to fulfil all mission requirements, the design could be more specific. At the end of this chapter, recommendations will be given with regards to future developments and research for the project. These will be focused on the development of a custom OBC, when time and budget permit, optimized for the M-STAR mission.

8.5. Sensitivity Analysis

8.5.1. Tool 8.1: Image Processing

For the image processing, time was lacking to implement a background noise filter such as Gaussian Filtering. Hence now, when a non-uniform background noise is present, certain noise pixels will pass the Otsu Threshold. Creating pseudo-images with non-uniform background noise was found to be out of the scope of the DSE. For future studies, it is recommended to implement both background noise filters as well as Otsu Threshold optimization algorithms.

A sensitivity check was done considering the ability to manually implement the threshold in the Python Opencv functions. Since the pseudo-images as presented in Section 8.3.2 are evidently bimodal, adapting the threshold resulted in the same pixels being returned. This analysis should be repeated after implementation of the functionalities as stated above, and performed with non-uniform background noise containing pseudo-images.

[8]Retrieved from `https://www.nasa.gov/mission_pages/station/research/news/b4h-3rd/it-small-computers-tackle-big-space`
[9]Retrieved from `http://www.xiphos.com/products/q7-processor/`

8.5.2. Tool 8.2: Velocity Check

This sensitivity analysis is performed on tool 8.2 as a whole. Two important technical assumptions were made in the construction of this program.

- The scanning frequency was assumed to be 1Hz, such that the camera passes over the same point on earth after every second.
- The program was written for a stationary anomaly located at (0, Re+14) km, as it was assumed that a missile would not be visible to the infrared camera till it had reached an altitude of 14km.

The worst case scenario for the location of the spot is the surface of the Earth, as the velocity here would be the lowest, and hence the time threshold would be higher. Table 8.6, shows the time threshold calculated for an anomaly located at the surface of the Earth. Although the percentage change is high, the time at which the level three alert reaches the ground increases from around 65 seconds after launch, to 67 seconds after launch; a 3.4% increase. The time latency requirement is still met, as well as the time requirement for confirming a velocity.

Table 8.6: Sensitivity Analysis for Velocity Check Tool.

Input	Output	Percentage Change	Conclusion
Sx,Sy = (0, Re) km	7 s	40%	**REQ-SYS-CDH-03** and **REQ-SYS-01-02-04** met

Table 8.7: Influence of time step on trajectory simulator accuracy.

dt (s)	Final Values for Simulation Running till t = 180s			Average Difference	Percentage Deviation (%)		
	x (m)	y (m)	h (m)		x	y	h
0.001	250483.6842	6987828.423	622316.365				
0.01	250404.3688	6987769.258	622254.3964	25.5041	0.0317	0.0008	0.0100
0.1	250359.07	6989118.889	623601.5404	39.7746	0.0497	0.0185	0.2065
1	241902.211	6983469.97	617658.3707	2760.6439	3.4260	0.0624	0.7485
10	207427.4777	6977730.461	610812.8854	13883.5631	17.1892	0.1445	1.8485

Table 8.7 explores the influence of the magnitude of the time step used in the accuracy of the trajectory simulation. As mentioned before, the trajectories are generated by numerically integrating differential equations of motion over time, thus the time steps involved in the integration have a large impact on the accuracy of the outcomes. In order to assess this, the same trajectory was generated using different time steps, with the smallest time step possible being regarded as a bar for accuracy. These values are indicated in the greys cells of Table 8.7. It is evident, that once the time step is in the order of magnitude of one second, the absolute deviation in values becomes much more significant. This analysis justifies setting the time step for the trajectory simulator 0.1 s. Furthermore, it should be noted that as it is a simplified 2D model of trajectories, the purpose of this part of the simulation is to allow for a first order estimation of the time required to determine whether an anomaly could be a missile. The method for which this accuracy could be improved and ensure is elaborated on in **??**.

The integrated simulation that overlays the satellites' FOV with possible simulated trajectories was run with a time step of 1 s. This was done to minimize run time and doesn't have a large consequence on the validity of the results as if a 1 s time step is used the outputed value for minimum time to conduct a velocity check will remain conservative, as the model round up to the nearest whole second.

8.6. Verification & Validation

In the following section, the performed verification and validation process with regards to the CDH subsystem will be elaborated upon. Firstly, the image processing tool created is examined, followed by an assessment of the velocity check program created. Finally in subsystem verification the hardware

testing deemed required is assessed, concluding the section with an elaboration upon requirement verification.

8.6.1. Tool 8.1: Image Processing

The image processing based on Otsu Thresholding is performed with the opencv tool for Python Programming. The function takes an image as an input and provides the thresholded image and threshold implemented as an output. The combination of THRESH_BINARY and THRESH_OTSU enables the program to establish a threshold based on the image itself following Otsu's method, and subsequently to output the image with binary values clearly indicating which parts were below and which ones fell above the threshold. Both the functions enable you to manually establish the threshold, which was implemented in evaluating the sensitivity of the program.

Verification of the method is done by means of manual unit tests. As the pseudo images were created by hand, it was known beforehand which pixels were expected to be returned after all the steps as elaborated upon in Section 8.3.2 are performed. This process was performed with a sequence of pseudo-images and executed according to expectations.

8.6.2. Tool 8.2: Velocity Check

Reference verification diagram illustrates the functions and branches of Tool 8.2. Unit, branch and system tests were performed to verify this tool.

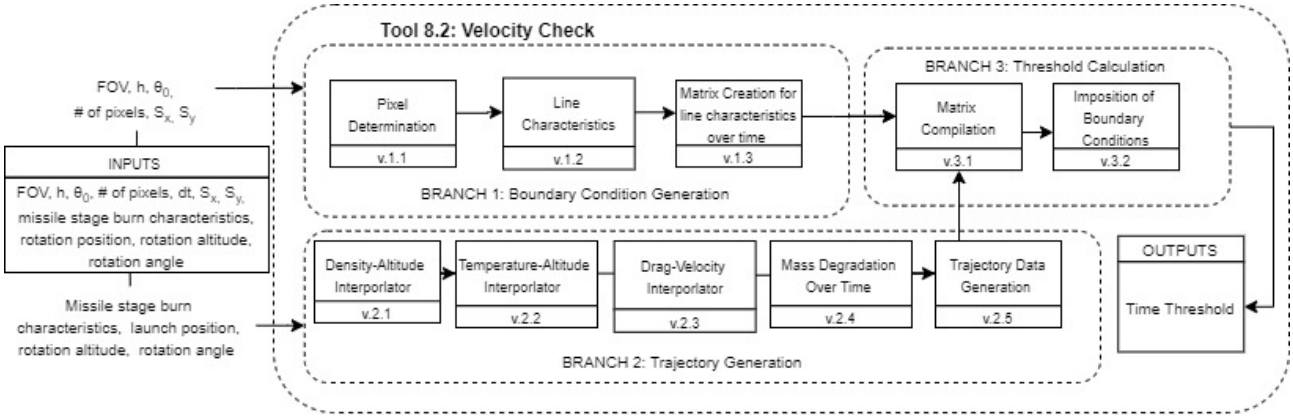

Figure 8.12: Tool 8.2.

Unit tests for function v.1.1 included changing the number of pixels to zero, for which there should be the output should be None; changing S_x and S_y for the same θ_0 such that the spot is not in the FOV of the satellite, for which there should be no output should be None; changing the number of pixels to a small number such as 3 to ensure that the angular resolution of each pixel was calculated properly, and the correct pixel was determined, as this can be calculated by hand. Unit tests for v.2.1 included changing the input of θ_0 to 91 degrees and 89 degrees for an anomaly located at S = (0,Re) in order to check that the gradients for the two lines at 91 degrees were both negative, and at 89 were both positive. Unit tests for v.1.3 included checking that θ updates properly. For dt = 0 (related to scanning frequency), the same line should print, and the satellite should never move out of view of the anomaly. For a high dt, for example dt = 100, only one line should be created, and then the satellite's FOV should no longer cover the anomaly. Branch tests for Branch 1 included changing θ_0 such that the anomaly would be outside of the FOV of the satellite. This outputted an empty matrix as expected. Next, the program was run for 3 pixels, for time steps of 10 seconds, and with a θ_0 of 95 degrees. It was checked that the sequence of highlighted pixels was first pixel, second pixel, third pixel, and that the the gradients changed even though the anomaly was in the same pixel for a long period of time.

Units v.2.1-v.2.3 are functions that are built on interpolating measurement data. These functions serve

to interpolate this discrete data into a continuous data set to allow for the input to be any float value, and the function should output a value from the continuous data set. For example, density at different altitudes in 10 km intervals were interpolated allowing for any altitude to be received as an input and a corresponding density would be produced. These programs allow for accuracy in the parameters involved when performing forward integration over time using Equations (8.1) and (8.2). Verification of these blocks can be done by checking the accuracy of this interpolation with known measurements. Unit v.2.3 was built under the assumption that all propellant mass was burned during flight, as each stage jettisoned the burn out mass at the each of the stage burn time. Thus the mass value over time can be verified simply by checking whether the mass generated by the model at the end of each stage is the same as the burnout mass of a given stage, and ultimately the end mass should be the dry mass of the last stage, which is also a known value [12]. Unit v.2.5 represents the culmination of the outputs of the aforementioned units and so unit tests on this function will by extension verify the units composing it as well, serving to be branch verification tests. This is verified by conducting several sanity checks on the trajectory produced for a given launch location, rotation altitude and angle. It can be easily verified by inspection whether the launch site is logical, i.e the missile begins its trajectory at the surface of the Earth and impact is at another location also at the surface of the Earth. Furthermore, the programme takes into account that the system payload can only detect missiles once they've reached altitudes above 14 km, this can also be verified by inspection to see that trajectories begin 14 km above the surface of the Earth, $y = R_e + 14$. Furthermore, maximum altitude reached when standard trajectories are generated for the SS-18 and Minutemann-III have measurements available to which the model's prediction can be compare [12].

Unit tests for function v.3.1 included checking the dimensions of the missile trajectory matrix for different step inputs. Unit tests for function v.3.2 included checking that none of the trajectories were eliminated after t_0. Furthermore, specific boundary conditions were chosen, as well as a specific $y_{missile}$, in order to check that the boundary conditions were evaluated properly and that the final matrix was appended correctly. Branch tests for Branch 3 included checking the dimensions of the final matrix for given a small number of rotation angle and rotation height steps, and specified boundary conditions such that the trajectories that satisfied the boundary condition at t_i could be verified manually.

As a final system test for Tool 8.2, three tests were performed. Case one checks that for only one fully vertical trajectory that passes through the anomaly, the outputted trajectory matrix has a length of 1. As the missile passes straight through the point, the time threshold should not be zero. The second case evaluates that for four straight trajectories, none of which go through the anomaly, the time threshold is 0 seconds (as none of the trajectories should satisfy the boundary conditions). The last case checks that at an anomaly located at an altitude of 14km, and for missiles that have a rotation such that they travel through the anomaly, the matrix has a length of 9 at time 0. This is done to ensure that no trajectories are eliminated when they shouldn't be.

Table 8.8: Full system tests: Tool 8.2.

Case	S_x, S_y [km]	$x_{0,missile}, y_{0,missile}$ [km]	y_{step}	Rotation	Expected Output	Verified
1	0,Re	0,Re	1	No	length of trajectory matrix = 1, should not go to zero immediately	
2	0,Re	Re·sin(γ), Re·cos(γ)	4	No	time threshold = 0 seconds	
3	0,Re+14	Re·sin(γ), Re·cos(γ)	9	Yes	At time=0, length of trajectory matrix = 9	

8.6.3. Subsystem Verification

A large portion of the command and data handling subsystem is software related, and in order to verify the OBC fully, the on board algorithms must first be extensively verified, and if possible, also validated against existing missile data. The OBC proposed is a COTS component with an extensive

flight heritage, it is has been in orbit since 2016, is certified for manned spaceflight, has been used on ISS and is implemented in the PICASSO [2], [10].

The hardware verification tests that can be performed would be concerned with error detection, software robustness, redundancy modes, ability to recover from single-event-upsets or multi-event upsets and more. While some of these are mentioned in [2], it is assumed that the Q7S processor has been verified according to space standards. Record shows that other missions have implemented the 2 processor cards and 1 daughter card configuration as was proposed, hence interface tests are expected to be executed already. A proposed interface test is concerned with the redundancy of the system, hence addressing the interface between the Main OBC and Backup OBC. The proposed mechanism should be verified accordingly, taking into account all switch mechanism as indicated in Figure 8.8 for the data interfaces present. Next to this, the interface between DPU and payload should be examined carefully. As it was stated, the layout of the DPU might change according to the IR-imager design following from R&D, however, considering the Optics and Filter Switch, interface tests are of vital importance here. Next to this, all subsystems have an interface with the OBC, and in Chapter 17, Section 17.2, the required testing for this has been defined in more detail.

8.6.4. Requirement Verification

Table 8.9 shows the compliance matrix for the Command and Data Handling subsystem requirements as were specified in Section 8.2. As can be seen, one requirement has been partially met, and the remaining have been met. The right column indicates in which sub-section calculations/diagrams/tables are given that show that the requirement has been met. **REQ-SYS-CDH-06** has been partially met, as was discussed in Section 7.5.1, more in depth error calculations are needed in order to verify that this requirement has been complied with.

Table 8.9: Command and Data Handling Requirement Compliance Matrix.

REQ	Compliance	(Sub)-Section
REQ-SYS-CDH-01		Section 8.3.2
REQ-SYS-CDH-02		Section 8.4.2
REQ-SYS-CDH-03		Section 8.3.3
REQ-SYS-CDH-04		Section 8.3.2
REQ-SYS-CDH-05		Section 8.3.3
REQ-SYS-CDH-06		Section 7.5.1
REQ-SYS-CDH-07		Section 8.4.2
REQ-SYS-CDH-08		Section 8.3.1
REQ-SYS-CDH-10		Section 8.4.2

8.7. RAMS Characteristics

In the following section an analysis is performed with regards to the reliability, availability, maintainability and safety of the CDH system mostly focused on the OBC and DPU hardware.

Reliability The reliability of the OBC and DPU is composed of multiple aspects. One should consider amongst others flight heritage, redundant memory, accuracy of on board computer, processor frequency. As the available COTS component for the OBC is proposed but not finalized yet, a detailed qualitative study is left for future research. However, the interface between the payload and OBC can be assessed. As the payload is connected to the DPU, Main OBC and Backup OBC, it is expected to function throughout the mission lifetime even in case of failure.

Availability A requirement is put for the communication to be available 99% of the time (Chapter 9). In the aim of meeting this, the OBC plays a vital role as it creates the data packages for transmitting to other S/C or the GS and processes the data that is received through the communications subsystem. Hence, it is required for the OBC to have a duty cycle of 100% to enable processing latency. This automatically flows into a continuous power availability requirement. Next to this, redundancy should

[10]Retrieved from `https://directory.eoportal.org/web/eoportal/satellite-missions/p/picasso`

be present in the data interface between OBC and Communications to enable a robust and continuous data transmission possibility.

Maintainability In satellites, the OBC is responsible for processing telemetry data and as such, assessing the health of all other subsystems and creating an alert in case of anomalies. The process is different for evaluating itself, maintainability of the OBCs and DPU is established by implementing watchdogs. Watchdogs or supervisors oversee the health of the processors, and gather the housekeeping data required to enable on-ground health assessment. The OBC was determined comparable to the one employed on BRIK-II and thus requires 32 bytes of housekeeping data [14]. The full set should be gathered for the Main OBC and DPU, and 16 bytes are estimated to be required to make sure that functionality is present in the Backup OBC.

Safety The OBC is always a mission critical system, it must work. It is vital for communication, payload data processing and all other subsystems. It is thus essential to create a redundant system, enabling various control loops before failure occurs. The redundancy of the proposed OBC design is elaborated upon in Section 8.4.2, elaborating upon the control loop for DPU failure and Main OBC failure. Stating that in case of DPU failure the functionalities can be adopted by the Main OBC, whereas in subsequent main OBC failure all functionalities would be transferred to the Backup OBC, as the data interfaces as specified in Figure 8.8 allow.

8.8. Recommendations

For Image Processing, the recommendations for future studies have been quickly elaborated upon in the sensitivity analysis. When no details are found about missile exhaust plume intensity related to time, it remains to be recommended to pursue Otsu Thresholding. When doing so, background noise filters should be implemented and optimization can be achieved by implementing advanced Otsu methods.

As was mentioned in Section 8.3.3, a shift towards a continuous, probabilistic approach is more desirable compared to the discrete, deterministic approach outlined. If a probabilistic method resembling the Metropolis Hastings Markov Chain Monte Carlo (MH-MCMC) was used for the velocity check algorithm, it would be possible to determine, while checking the anomaly for velocity, the most probable trajectory. By doing so, the spacecraft is able to know (i) whether the anomaly is moving, and if it is moving (ii) the most probably trajectory of the potential missile. From this, in the event that multiple satellites are looking at the same anomaly, the trajectory may be used in order to determine the most suited first satellite, and the most suited secondary satellite. Moreover, as the discrete method above runs existing trajectories and eliminates them, a continuous method as recommended above would generate trajectories that could fit through the given sequence of highlighted pixels, and assign probabilities to them. If the on-board computed power would allow for such a method, the 99% reliability requirement would be positively benefited. Furthermore, with regards to the overlapping algorithm; it may be desirable to have two sets of satellites tracking and relaying the missile coordinates, especially specific to certain geographical locations that have a higher probability of launch. This would allow for some redundancy, as well as verification of coordinates between two pairs of satellites.

For the hardware design, more research must be done into processing frequency required for the mission. Next to this, a detailed assessment should be made with regards to the required amount of memory and storage to be present. As the proposed design for redundancy is custom, the interfaces located on the daughterboard should be tested accordingly. Next to this, interfaces between subsystems and the OBC have to be examined in detail. As well as this, a detailed reliability study of these interfaces and the hardware must be performed, to ensure that the 99% reliability and availability requirements are met. Finally, lifetime of the OBC subsystem should be assessed, ensuring reliability until End-Of-Life of the M-STAR Mission.

9 Communication

This chapter will cover the design of the communication subsystem. It consist of the functional and requirement analysis, an explanation of the design features of the system, link budget tool analysis (including sensitivity, verification and validation), and a RAMS analysis. Finally, the chapter is completed with some recommendations for further research.

9.1. Functional Analysis

- **FUNC-COMM-01:** Communicate with the Ground Station
  - **FUNC-COMM-01-1:** Transmit housekeeping information to the GS
  - **FUNC-COMM-01-2:** Transmit Payload raw data to the GS
  - **FUNC-COMM-01-3:** Receive commands from the GS
  - **FUNC-COMM-01-4:** Transmit the Detection information to the GS
    - **FUNC-COMM-01-4-1:** Transmit the L3 alert to the GS
    - **FUNC-COMM-01-4-2:** Transmit the stereographic measurement information to the GS
    - **FUNC-COMM-01-4-2:** Transmit 'ICBM leaves FOV of the satelltie' information to the GS
- **FUNC-COMM-02:** Coordinate detection with adjacent satellites
  - **FUNC-COMM-02-1:** Enable link between adjacent satellites for stereo graphic measurement 4.3.2.9
  - **FUNC-COMM-02-2:** Transmit information between satellites to allow for continuous tracking of the ICBM
    - **FUNC-COMM-02-2-1:** Transmit information between satellites in the same orbital plane when ICBM leaves FOV System Function: 4.3.2.2
    - **FUNC-COMM-02-2-2:** Transmit information between satellites in different orbital planes when ICBM leaves FOV System Function: 4.3.2.4 and 4.3.3.6
- **FUNC-COMM-03:** Relay information between adjacent satellites
  - **FUNC-COMM-03-1:** Relay the L3 detection alert in the direction of the Ground Station System Function: 4.3.2.1
  - **FUNC-COMM-03-2:** Relay the ICBM coordinate data in the direction of Ground Station System Function: 4.3.3.8
  - **FUNC-COMM-03-3:** Relay the ICBM information in the direction of desired satellite for out-of orbital plane ICBM tracking
  - **FUNC-COMM-03-4:** Relay component failure emergency information in the direction of GS
  - **FUNC-COMM-03-5:** Relay the GS commands in the direction of a desired satellite
- **FUNC-COMM-03:** Provide sufficient link security for the information transmission
  - **FUNC-COMM-03-1:** Provide sufficient redundancy to eliminate single points of failure in communication of ICBM detection
  - **FUNC-COMM-03-2:** Provide sufficient link security to minimise the probability of information capture by third parties
  - **FUNC-COMM-03-3:** Transmit sufficient data to the ground station to provide redundancy in the ICBM classification

9.2. Requirement Analysis

- **REQ-SYS-COM-01** All information transferred by the telecommunication system shall be encrypted using AES256 standard

- **REQ-SYS-COM-02** The telecommunication system shall have 99% availability for the relay.
  - **REQ-SYS-COM-02-1**The telecommunication system shall enable a link between two adjacent satellites on the same orbital plane with 99% availability.
  - **REQ-SYS-COM-02-2** The telecommunication system shall enable a link between satellites in two adjacent orbital planes with 99% availability.
- **REQ-SYS-COM-03** The telecommunication system shall have 99% reliability. *Flowdown from FUNC-COM-06.*
  - **REQ-SYS-COM-03-1** The telecommunication system shall remain functional at 20 kbit s^{-1}data rate capacity with failure of one relay satellite *Flowdown from FUNC-COM-11.*
  - **REQ-SYS-COM-03-2** The telecommunication system shall remain functional at 10 kbit s^{-1} data rate capacity with failure of two satellites in the same orbital plane.
  - **REQ-SYS-COM-03-3** The telecommunication system shall remain functional at 20 kbit s^{-1} data rate capacity with failure of two satellites in different orbital planes.
- **REQ-SYS-COM-04**The telecommunications system shall transmit the payload data to the GS. *Flowdown from FUNC-COM-01.*
  - **REQ-SYS-COM-04-01** The telecommunications system shall transmit the coordinates of the detected ICBM to a Ground Station within 90 sec after the launch of the ICBM. *Flowdown from FUNC-COM-01.*
  - **REQ-SYS-COM-04-02** The satellite shall transmit payload detection data to the GS from any orbital postition. *Flowdown from FUNC-COM-01.*
  - **REQ-SYS-COM-04-3**The telecommunications system shall communicate failure in payload functionality to the ground station(s). *Flowdown from FUNC-COM-12.*
- **REQ-SYS-COM-05**The telecommunication system shall alert ground station of failure of elements in the inter-satellite communication constellation. *Flowdown from FUNC-COM-12.*
- **REQ-SYS-COM-06** The telecommunication system shall have a downlink rate of 1 Mbit s^{-1} to the ground station directly below the satellite.
- **REQ-SYS-COM-07** The telecommunication system shall have an uplink rate of 20 kbit s^{-1} from the ground station directly below the satellite.
- **REQ-SYS-COM-08** The telecommunication system shall have inter-satellite data transfer rate of 20 kbit s^{-1} at a distance of 1300 km between satellites with a clear line of sight.
- **REQ-SYS-COM-09**The telecommunication system shall consume 9 W peak power.

9.3. Communication Design

It was decided that only one type of spacecraft it to be used, due to resource and time constraints of the test mission. The multi-constellation system is explored in recommendations in section 9.7. With that in mind, the design cases were explored for the system where each spacecraft has multiple roles: It works both as a detection platform, but also as a data relay node.
Each spacecraft is capable of inter-satellite communication with adjacent satellites on the same orbital plane at all times. The information can be transferred to different orbital planes at a latitude between 65 and 89 degrees. This is explained further in Section 9.3.6. The inter-satellite connection is established with Ultra High Frequency (UHF) near-isotropic antennas.
The S-band patch antenna set-up is a primary downlink system. The UHF antenna is a secondary downlink tool, used when the spacecraft attitude is not suitable for S-band transfer. Uplink from the ground-station is performed in the UHF band.

9.3.1. Data Relay Design

To properly quantify the time it takes between a detected ICBM and data relay of this information to a ground station, the data routing across the constellation is analysed. Several studies have been performed on this subject. All of them are based on topology optimisation methods. It was determined that the method of static topology layout is preferred for the constellation [51]. Each orbital plane in the constellation will have a number of evenly spaced nodes corresponding with the number of satellites in the orbital plane called logical nodes (LN). These LN's will have a stationary mapping

onto a geographical location on the Earth's surface. As the satellites travel around in their orbits, a particular satellite will not be connected to a certain LN permanently. A satellite following it in the same orbital plane will take over the LN as it approaches the location. An one to one mapping of the satellites actual position and the LN's will refresh with period T_c, where $T_c = \frac{T_0}{N}$ with T_0 being the orbital period and N being the number of satellites in one orbital plane [51]. As the entire topology is basically propagating from east to west from an Earths observers perspective (due to the rotation of the Earth, J2 gyroscopic procession, etc.), the geological location on Earths surface will change periodically as well. In order to have each satellite know what it needs to do with a data package it received, the following solution is proposed.

The topology of the logical nodes is evaluated at a static moment in time, and data paths between different nodes can be generated by using the K-shortest path algorithm described in [52]. This algorithm will optimise the data paths in a way to minimise data congestion in the constellation, and reduce the time for data to go around in the constellation [52] [53]. According to [51], this means each satellite will need to have $3N$ routing tables that contain data paths, to maintain at all times. Again, here N is equal to the number of satellites in a single orbital plane.

As the location of ground stations compared to logical nodes will change with the precession of the orbital planes around the poles, a per-packet decision on the destination LN is made. This way the effect of the complete logical topology consisting of LN's "rotating" around the Earth is accounted for.

9.3.2. Design Cases

The constellation has requirements that are very difficult to meet without the use of inter-satellite communication. It is unfeasible to assume that the satellite will be within the reach of the Ground station within 90 sec from any location of Earth, to meet the Global coverage requirement, as described in chapter 5. This creates a need for an inter-satellite link. The communication relay has to be self-sufficient, according to **REQ-MIS-09**, therefore the data relay needs to occur within the constellation. The communication could be realised in two different manners. The spacecraft used for detection could have the capability of information relay, or an additional constellation layer could be created with dedicated communication spacecraft for this purpose. The latter option brings more complexity to the project, because it would be necessary to design an additional constellation layer, as well as a second spacecraft type. This would greatly increase the cost of the mission. Moreover, the cost of initial testing would be much higher. For those reasons, it was decided that the mission will use information relay with the same satellites that perform detection. The concept of multiple constellation layers is proposed for further research in Section 9.7. Analysed cases that are considered for the design correspond to data packages given by Table 8.1

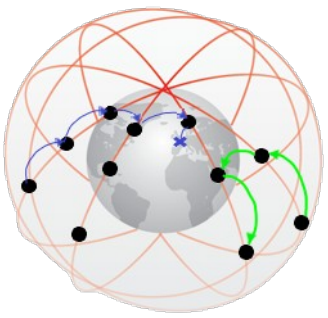

Figure 9.1: Representation of Communication links. Blue (left side) link: Detection of ICBM signal relay to GS in the Netherlands. Green (right side) link: Relay of information for tracking for out of plane ICBM trajectory.

9.3.3. Link Budget Inputs

As with the design of all spacecraft communication subsystems, a link budget analysis [54] has been performed to see the parameters needed to close the communication link between transmitter and

receiver. In the case of radio frequency (RF) inter-satellite link (ISL), the link budget equation is the following:

$$\frac{E_b}{N_0} = 10log_{10}(P_t) - L_t + G_t - 20log_{10}(\frac{4\pi d}{\lambda}) - L_{polar} - L_r + \frac{G}{T} - 10log_{10}(k) - 10log_{10}(R) \quad (9.1)$$

$$\text{Final Margin} = \frac{E_b}{N_0} - (\frac{E_b}{N_0})_{threshold} - L_{imp} - \text{Link Margin} \quad (9.2)$$

The different parameters involved in Equation (9.1) and Equation (9.2) are listed in Table 9.1 below.

Table 9.1: Link budget equation parameters

Parameter	Symbol	Unit	Parameter	Symbol	Unit
Energy per bit to Noise power density	E_b/N_0	dB	Noise Figure	$\frac{G}{T}$	dB
Transmitting Power	P_t	W	Boltzmann Constant	k	$\frac{m^2 kg}{s^2 K^1}$
Transmitter loss	L_t	dB	Data rate	R	bit s^{-1}
Tx Antenna Gain	G_t	dB	Distance	d	m
Polarization Loss	L_{polar}	dB	Wavelength	λ	m
Receiver Loss	L_r	dB	Implementation Loss	L_{imp}	dB

In order to check a communication subsystem design, certain parameters need to be inputted into the link budget that is unique to the different types of communication subsystem. A total of 273 different test cases are generated and tested with the link budget tool developed based on Equation (9.1). Each case is built out of three iterable components, namely a certain frequency band, a modulation scheme and an error correction coding scheme. An overview of the different properties to be linked with these components is given below:

Frequency RF communication is possible at many different frequencies, ranging from very low frequencies like UHF band (around 0.4 GHz) all the way up to Ka-band (around 30 GHz). These bands all have different channel sizes called bandwidth that can be licensed. An allocated bandwidth can limit the maximum data rate to be supported through a certain RF link. The third property in the frequency component is antenna gain. Antenna gain roughly follows the trend of higher frequency equals higher antenna gain. For example, an UHF antenna will have a gain that can range from 0 dB (isotropic antenna) up to 8 dB (Helical antenna). X-band antennas (core frequency around 9 GHz) can have highs gain antennas of for example 30 dB, but struggle to have low gain antennas under 5 dB [54].

Modulation A modulation scheme is used to put the signal to be transmitted on the carrier wave. Examples of these schemes are BPSK, QPSK of GMSK. Each scheme has a property called spectral efficiency which is expressed in bit/s/Hz. As the available bandwidth is known with the core frequency chosen (as explained above), each modulation technique is checked to see if the spectral efficiency is high enough to send the required data over the allocated bandwidth. The modulation technique then has a given threshold value for E_b/N_0. This is the minimal E_b/N_0 that the signal must reach in order to close the link budget. It is dependent on the desired bit error rate (BER) of the received signal. This will be elaborated upon later in this section.

Error Correction Coding In order to lower the required E_b/N_0 of a signal, a error correct coding scheme (ECC) can be applied. These schemes provide a so-called coding gain at the cost of using more bandwidth. These coding gains are subtracted from the threshold E_b/N_0 value coupled with a certain modulation scheme and BER. Examples of ECC's are convolutional codes, Reed-Solomon codes (a particular set of convolutional codes), Turbo codes and LDPC [54]. The codes use more bandwidth then uncoded signals, and this is called the coding rate. It relates the amount of bandwidth used by a coding scheme compared to an uncoded signal, given as a fraction. For example, convolutional can have a coding rate of 1/2 [54], which implies that it uses twice the amount of bandwidth compared to a signal that doesn't have any ECC applied.

The link budget also has multiple inputs that are kept constant during iterations. Those are estimated based on current available CubeSat COTS components, taken from literature, or estimated with simplified models. An overview of these constant parameters is given in Table 9.2 below:

Table 9.2: Constant input parameters link budget.

Parameter	Value	Unit	Parameter	Value	Unit
Distance	1300	km	Implementation Losses	1	dB
Polarisation Losses	0	dB	Receiver Losses	2	dB
Transmitter Losses	1.2	dB	Bit Rate	20	$\mathrm{kbit\,s^{-1}}$
Output Power	3.5	W	Link Margin	3	dB
System Noise Temperature	1260	K	Bit Error Rate	10^{-6}	-

Distance The distance between two neighbouring satellites in the same orbital plane. It was chosen based on payload capability to achieve global continuous coverage. The communication distance is set to allow for redundancy in the system, as described in Section 9.6.

Losses Losses in the system were based on the typical values for CubeSat literature [55] [56] and available models.

System Noise Temperature Every component in the communication subsystem introduces a little bit of noise into the system that is added to the noise received in the signal. In order to model this noise, a total system noise temperature is calculated, which tries to model the total noise generated in the system. In Equation (9.1), the noise is introduced by the term $\frac{G}{T}$, which is the receiver antenna gain divided by the system noise temperature T_{sys}. Equation (9.3) below gives the definition of the system noise temperature [57]:

$$T_{sys} = T_a + T_0 \frac{L}{1-L} + T_0(10^{F/10} - 1) \tag{9.3}$$

Here T_a, T_0, L and F are antenna noise temperature in Kelvin, reference temperature of 290 K, cable length in meters and transceiver noise figure in dB respectively.

Output Power The power setting was determined by available power in the EPS, as well as the capability of the COTS components [56]. The EPS can accommodate continuous transmission of information while tracking an ICBM for the whole duration from launch till the burnout.

Bit Rate The data packages that need to be transmitted are explained in more detail in table 8.1. The communication is designed such that it can transmit those packages while receiving information. With the use of TD-CDMA (Time Division Code Division Multiple Access) and maximum uplink speed of $20\,\mathrm{kbit\,s^{-1}}$ the satellite is capable of transmitting and receiving with the time division. Therefore, at 50% time spent transmitting the average upload speed is $10\,\mathrm{kbit\,s^{-1}}$ s. It is possible to send all

necessary data as the maximum data rate necessary is less than 7 kbit s^{-1}. The remaining data rate can be spent on housekeeping data and additional information.

Link Margin It is industry standard for communication to take a contingency link margin of 3dB [57].

Bit Error Rate The necessary bit error rate was estimated to have a high probability of error-free transmission during one detection. The data bit error rate has to be such that during 300 s of transmission, the chance of a faulty bit is minimized. The value was compared with other space missions as well [57], and set at 10^{-6}.

9.3.4. Link Budget Methodology

In order to find the final combination of frequency, modulation type and coding scheme to be used for this mission, all different combinations of these three components are tested in the link budget tool. They are checked to close with a final margin larger than 0, as defined in Equation (9.2), and that the bandwidth used (including the coding rate) is lower than the bandwidth tied to the frequency band used. For example, in the case of a UHF link, the total bandwidth used may not exceed 50 kHz. Using the input values listed in Table 9.2, out of the 273 cases tested, 52 cases pass this filter. After this, the results are narrowed down manually by looking at which cases meet the requirements set on this subsystem. The results of this method are presented in the following subsection.

9.3.5. Link Budget Results

After numerous iterations, the communication subsystem has been finalised to following parameters, given in Table 9.3.

Table 9.3: Results chosen link budget.

Parameter	Unit	Value	Parameter	Unit	Value
Data rate required	kbit s^{-1}	20	Bit Error Rate	-	10^{-6}
Frequency band used	-	UHF	Modulation type	-	QSPK
Frequency used	MHz	400	Spectral efficiency	bit s^{-1} Hz^{-1}	1.4
Bandwidth Allocated	kHz	50	Error correction Coding	-	Convolutional
Assumed transmitting power	W	3.5	Coding Gain	dB	6
Worst case distance	km	1300	Encryption	-	AES256
System noise Temperature	K	1260	Transceiver efficency	-	0.45
Antenna gain	dB	0	Access method	-	TD-CDMA
Coding rate	-	0.5			

The most important choice in the communication subsystem was the antenna type/frequency band. The winner of the detailed link budget is different than the solution proposed in the mid-term review [5]. The final design solution has been changed for two main reasons:

- Required pointing for Focus payload
- Error Correction Coding

After an in-depth analysis of pointing devices for Focus payload, it was decided that the reliability and capability of such a system would not be sufficient to meet the mission requirements. As described in Chapter 7, such systems are very complex and prone to failure, while providing very limited FOV deflection. Therefore the spacecraft would need to rotate as a whole to aim at the ICBM. The inter-satellite connection has to be ensured irrespective of the spacecraft's attitude.

9.3.6. Architecture

In this subsection, components of the spacecraft for communication system are described. The subsystem in the spacecraft consists of two main branches. Firstly, the UHF system described, which consist of radio and an antenna. Secondly, S-band transmitter and patch antenna are discussed. Lastly, required bandwidth allocation and its significance is described in detail.

UHF Radio For the modulation, a transceiver is determined to be the best option. This is because the single UHF antenna is used for both transmission and reception of data. The transceiver can combine both capabilities into one device, reducing the mass and volume footprint of communication subsystem in the spacecraft.
For this analysis COTS components were used as a benchmark [58] [59]. However, the transceiver needs to be purpose-made for the mission. This is because of different military standards, operating frequency and security. The most important design parameters for the transceiver are summarised table 9.4 and are further explained afterwards.

Table 9.4: Transceiver Parameters.

Parameter	**Chosen option**	**Parameter**	**Chosen option**
Modulation type	QPSK	Duplex type	Time Division Full Duplex
Operational Data Rate	>25 kbit s^{-1}	Chanel access method	TD-CDMA
Operating frequency	400 MHz	Encryption specification	AES256
RF Output Power	3.5 W	Error correction code	Convolutional

The modulation method was chosen because it provides a good balance between spectral efficiency and simplicity. Spectral efficiency is especially important because the communication system operates in a bandwidth limited domain. Therefore simpler BPSK was not used, as it severely reduced the data rate due to low spectral efficiency of 0.7 when compared to 1.4 of QPSK. More complicated schemes such as 8-PSK were not used, as they increase required bit energy which would require dramatically increased power consumption for the same BER.

Emitted signal power was designed in such a way that the EPS is able to provide necessary input power when assuming the efficiency of 45% found on COTS components. For detailed information about the power consumption, frequency and the necessary data rate, please refer to Chapter 10 and Chapter 8 respectively.

The emitted power would not be sufficient to close the link budget without error correction coding. As explained in Section 9.3.3, encoding has a big influence on the capability of the system. [54]. The convolutional coding was used because it is suitable for time-critical applications. It is continuous code as opposed to block coding techniques, which enables the data to be retrieved faster. Moreover, this type of coding is not computationally intensive which makes it suitable for satellites which have limited processing capabilities.

The system uses TD-CDMA access method which allows for communication across the constellation at the same frequency. Even though the system uses a near-isotropic antenna, TD-CDMA gives the capability to target specific satellites to ensure the correct information path, thus reducing data congestion. Encryption is one of the reasons why custom transceiver is necessary. AES256 is a standard used for military purposes, therefore it is used in the system. In this phase of the design influence of the encryption on the performance of the system can be ignored [60]

UHF Antenna It is proposed that the Quad-Monopole UHF Antenna from Nanoavionics [61] would be used. It is configurable to fit on the variety of CubeSat sizes, from 2U all the way to 12U sizes. It offers, near isotropic coverage to reduce fading in tumbling conditions. Additionally, it can accommodate up to 10W of RF transmitted power at a very low mass of 30 grams. The UHF antenna is located near the side that faces Earth. Thanks to this configuration, solar panels are not obstructing the view of ground stations or neighbouring satellites on the same altitude when facing nadir. It is especially important, as the satellite has to be able to receive commands from other spacecraft and GS without prior notice. In case of excessive rotation of the spacecraft out of standard position, the spacecraft is adjusted in order to minimize the impact of solar panels on the signal transfer.

The S-band Antenna and Transmitter For the ground station communication, an Nanoavionics patch

antenna [1] and transmitter [2] are used as templates. The compact size of the patch antenna enables it to be mounted at the nadir pointing side, while not interfering with the optic system. The limited gain of the antenna allows it to be used without changing attitude of the spacecraft. Therefore detection and GS communication are performed simultaneously. S-Band frequency offers much higher data rate when compared with the UHF system, at the cost of transmitting power. The transmitter would need to be modified or purpose made to match the military specification.

Bandwidth Allocation The UHF system uses two standard allocation windows of 25kHz. It is common practice to use such extended bandwidth for missions that require it. For the current system, the transmission speed is bandwidth limited. With current parameters, the system uses 32kHz out of 50kHz for data. Around this centre frequency, an additional margin of 8kHz is taken from both sides, to account for the Doppler shift, which leaves a safety margin of 1kHz from each side. This Doppler shift safety margin allows for communication of satellites with the relative velocity difference of up to 6 km/s. The relative velocity of two neighbouring orbital planes is the highest at the pole and is equal to $4.9\,\mathrm{km\,s^{-1}}$. Therefore the system can communicate between two neighbouring co-rotating orbital planes as long as the distance of the satellites is below 1300 km. The correction for Doppler effect is not achievable when there is a rapid change of the relative velocity, such as when the trajectories of the satellites are crossing at the pole. Therefore, 1-degree latitude safety margin around the pole is taken to overcome this problem. S-Band transmission is power limited. A standard allocated bandwidth window is much higher than required.

9.3.7. Communication Flow Diagram

In order to illustrate the flow of communication data inside the system, Figure 9.2 is constructed. It shows an overview of two complete satellites, a ground station and a third data link via ISL. All data packages outlined in Table 8.1 are shown with their respective identifiers.

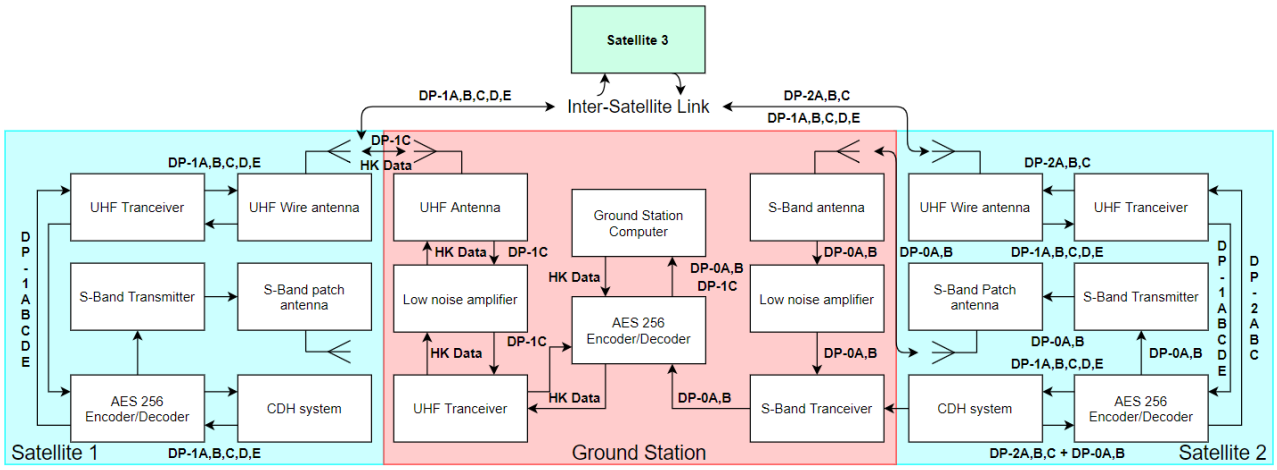

Figure 9.2: Data flow diagram.

9.3.8. Cost Breakdown

As the final subsystem layout is known, a cost breakdown of the system has been made, with the estimation of the cost of the several components. Table 9.5 below gives an overview of the estimated cost of different components.

[1] Retrieved from `https://nanoavionics.com/cubesat-components/cubesat-s-band-patch-antenna/`
[2] Retrieved from `https://nanoavionics.com/cubesat-components/cubesat-s-band-transmitter/`

Table 9.5: Cost breakdown of the communication subsystem.

Component	Unit price	Amount	Component	Unit Price	Amount
Custom made UHF Tranceiver with AES256 encryption build-in	€ 15.500,-	1	UHF Isotropic Antenna	€ 3.500,-	1
S-Band Tranceiver with AES256 encryption build-in	€ 15.500,-	1	S-Band patch Antenna	€ 2.500,-	1
			Ground station	€ 86.500,-	n.a.

The ground station is taken from ISISpace, but this is already in use by the RNLAF, thus it might not be needed to acquire a new one for the technology demonstration mission. All transceivers need to be custom built in order to incorporate the AES256 encrypter and decoder. Several companies provide these services, like ISISpace, Endurosat, Nanoavionics, etc. The cost estimate is based on the regular price of a UHF transceiver [62] with an additional 50 % increase to account for the custom order.

9.4. Link Budget Sensitivity Analysis

In order to check the robustness of the link budget and to check the final communication subsystem design, a sensitivity analysis is performed. Its aim is to make sure the assumptions made in the setting up of the link budget are valid, and the result is not very prone to changes with little tweaks of certain parameters. Firstly, the following assumptions are made in the setup of the link budget equation tool:

- Transmitter losses, polarisation losses, implementation losses and receiver losses are assumed to be constant for all different types of cases checked. This is done as it is quite complicated to properly model these losses when the final system architecture is not yet defined. These values can increase or decrease depending on the exact components used, and thus need to be checked in the sensitivity analysis.
- System noise temperature is a second component of the link budget that is simplified by the use of Equation (9.3). This equation is used quite often in literature, such as [54] and [57]. However, it is still an approximation of the noise temperature, as actually antenna noise temperatures and exact cable lengths are unknown.
- Bit Error Rate is taken at 10^{-6}, but this is also dependent on the robustness of the communication software. Several types of software can handle the higher bit error rates, but this is not yet determined for the technology demonstration mission software.

Table 9.6 below gives an overview of the different sensitivity tests performed on the link budget, together with a short comment on each result.

Table 9.6: Sensitivity analysis link budget.

Changed Parameter	Final Margin [dB]	% Change	Conclusion
Baseline	1.534	0%	-
Increase combination of assumed system losses with 1.5 dB	0.034	-100%	As the link equation simply subtracts the system losses from the final margin, there is a 1.5 dB margin to rise and still be able to close the link budget.
Increase T_{sys} to 1800 K	0.02	-100%	The system noise temperature can rise with almost 50% and still have a link budget that closes. Thus the assumption on the noise temperature is quite robust.
Decrease the required BER to 10^{-7}, and consequently increasing Eb/N0 required to 11.5	0.534	-65%	Decreasing the with a factor of 10 decreases the link margin by 1 dB. This is due to the fact that for lower and lower BER's, the required Eb/N0 per modulation scheme doesn't decrease much more.

9.5. Verification & Validation

9.5.1. Link Budget Verification and Validation

This section will present the method and results from the verification and validations processes taken to check the results of the link budget tool created to aid in the design of the communication subsystem. As a base, Speretta [54], Cervone [63] and Anderson [57] are used as literature for verification. Figure 9.3 below gives a schematic overview of the link budget tool. Blocks 4.1.1 to 4.1.3 are all implementations of the ”normal” link budget equation (Equation (9.1) and Equation (9.2)). Block 4.2 is where based on the data rate specified (from the constant inputs Table 9.2), modulation type spectral efficiency and coding rate the total bandwidth needed for the signal is calculated. The complete system then checks whether the final margin is greater then 0 and the total bandwidth needed is smaller than the bandwidth specified with the core frequency.

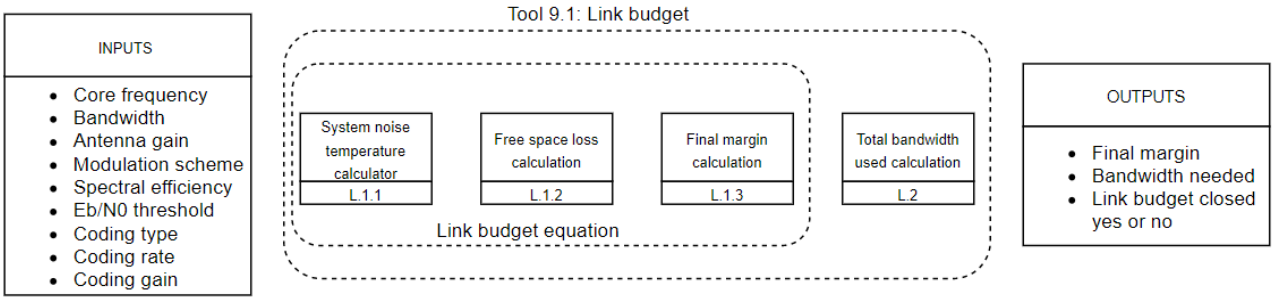

Figure 9.3: Block diagram of the link budget tool

Some unit tests have been performed on the tool, namely on the system noise temperature estimation and the free space loss calculation. A complete system test is also performed, to compute final margin and bandwidth required. The results are recorded in Table 9.7.

Table 9.7: Verification of link budget tool.

Unit test	**Output tool**	**Output verification source**	**Error**
Unit L.1.1 with inputs from example Cervone	225.722 K	225.7 from Cervone[63]	0 %
Unit L.1.2 at d = 500 km and f = 1 GHz	146.42 dB	146.42 from Speretta[54]	0 %
System test Tool 9.1	**Output tool**	**Output verification source**	**Error**
Inputs: d = 400.000.000 km f = 8.4 GHz G_t = 51 dB T_sys = 20 K P_t = 200 W Bitrate = 10 Mbit s^{-1} Modulation scheme = QPSK	Free space loss = 282.97 dB Uncoded margin = 4.625 dB Encoded margin = 10.625 dB Bandwidth used = 17.8 MHz	Free space loss = 283 dB Uncoded margin = 4.6 dB Encoded margin = 10.6 dB Bandwidth used = 18 MHz Source: Anderson [57]	0 % 0% 0% 1.11%

The only error in the verification of the link budget tool comes from the bandwidth used in the final system test. As it is based on example 5.2-5 from [57], one can see that the values computed in this example are rounded off, thus the error most likely originates from the rounding done in [57]. Also, the error 1.11% is not large, and will thus have almost no impact on the outcome of the link budget tool.

9.5.2. Compliance Matrix

Below, Table 9.8 shows the compliance matrix for the communication subsystem. Each requirement is met, and the reference to the different sections are included.

Table 9.8: Communication Requirement Compliance Matrix.

REQ	Compliance	(Sub)-Section
REQ-SYS-COM-01		Section 9.3
REQ-SYS-COM-02		Section 9.6
REQ-SYS-COM-03		Section 9.6
REQ-SYS-COM-04		Section 9.3.5
REQ-SYS-COM-05		Section 9.6
REQ-SYS-COM-06		Section 9.3
REQ-SYS-COM-07		Section 9.3.5
REQ-SYS-COM-08		Section 9.3.5
REQ-SYS-COM-09		Section 9.3.6

9.6. RAMS Characteristics

Reliability Reliability of the communication system is crucial for multiple reasons. This subsystem is the only link between the Ground Station and the spacecraft. Therefore the loss of communication system means complete loss of the spacecraft. Moreover, as the system transmits the payload data to the ground station, it is of utmost importance that the received information is trustworthy. Therefore multiple measures are taken to ensure the very high reliability of the whole constellation, as well as each individual spacecraft.

Starting with a big picture, the communication philosophy is to decentralise and spread information across the system. This prevents single points of failure in the communication link, as well as making it more difficult to stop the information from reaching the Ground Station. The information from any satellite has always multiple ways to reach any ground station. In the worst-case scenario, where there is detection at the equator, the satellite is can transmit data both to the north as well as to the south. Moreover, once the information reaches latitude that allows for inter-planar communication, the information channels increase dramatically. In case of failure of any satellite in the chain where intra-planar communication is not possible the alternative path is taken. For example, in case a satellite to the north is faulty, the southern path is taken. The system is able to cope with the failure of both northern and southern satellites failing. It can jump over one satellite with reduced data-rate in case of such unlikely event occurs in a region that no inter-planar communication is possible. Another reliability measure is a two-way communication method. TD-CDMA enables satellites to receive information and send the confirmation of reception within the same timeframe. This enables the system to rapidly find faulty satellites and act accordingly.

Now, going the reliability measures in a spacecraft are both in hardware as well as the communication method. The communication system uses well-tested antennas with TRL of 9 and presentable flight heritage [61]. It uses one of the simplest and the most reliable deployment mechanisms used for CubeSats. After deployment, there are no moving parts in the subsystem. Moreover, the antenna uses 4 wire monopole units that deploy independently. Therefore the system would be able to work at reduced performance even with multiple deployment failures.

The isotropic transmission creates very robust communication. There is no need for mechanical movement of antenna both for transmission and reception of information. This not only eliminates the possibility of mechanical failure of actuators but also enables communication in the event of loss of control of attitude of the spacecraft. The ability to communicate is not impeded by the failure of the attitude determination nor the attitude control of the spacecraft.

Availability The requirement for the availability of 99 % applies also to the communication system. To match it, it was important that no need of pointing of the spacecraft would be necessary to receive information. As the direction of transmission is not known beforehand, the system would not be able to relay information in some scenarios.

The isotropic transmission has the benefit that irrelevant of the position of ICBM, the satellite can track it with Focus payload and still transmit information to its neighbours.

Thanks to the isotropic antenna, the spacecraft is capable of relaying information even in an event of major component failure.

Maintainability The communication subsystem is responsible for transmitting the information about the failure of components of the spacecraft to the ground station. This subsystem also enables the ground station to send orders and software fixes to maintain the spacecraft. Therefore the communication subsystem is a crucial tool for maintenance of the spacecraft.

Safety One of the high-level objectives of the mission is to ensure the safety of its users. Global communication network between detecting satellites is crucial for the success of the mission, therefore contributing to national safety.

A total failure of communication subsystem means loss of spacecraft, as this is the only link between the satellite and the Ground Station. One of the safety features that shall be implemented to ensure the safe operation is to autonomously perform emergency procedures if the communication link is broken for a certain amount of time. Those procedures would include a possible change of attitude of the spacecraft, restarting the communication system and restarting the OBC. If the communication link retrieval procedure would not succeed, the spacecraft will perform a deorbit manoeuvre. This debris mitigation measure would reduce the risk of polluting LEO with nonoperational spacecraft.

9.7. Recommendations

Additional Relay Constellation: Currently, the mission uses one type of spacecraft. This spacecraft has two roles: an ICBM detector and information relay satellite. However, those roles could be split into two different constellation layers. Detector satellites would be smaller and would only communicate with Relay satellites. This option requires the use of bigger relay satellites to fully use its benefits. It is due to a high gain antenna or laser receiver necessary for effective operation, as well as required power for long-range transmission.

Optical Communication Link: The optical inter-satellite communication is currently very challenging for CubeSats. Small size, power and low pointing knowledge pose serious challenges for laser link. Currently, CubeSat lasers require the pointing of the whole satellite to transmit information. This comes in conflict with the Focus payload requirements. This could be mitigated if the laser would be placed on a independent gimbal mechanism, which is currently only feasible for satellites of mass above 100kg. Laser communication is especially attractive when combined with additional constellation layer as proposed above.

Reed Solomon Error Correction Code: Currently, convolutional error correction coding is used in the system. It is a very quick method suitable for time-sensitive applications. However, if more gain is required to reduce transmission power, block coding techniques could be used. Reed Solomon is block coding with small blocks, which creates lesser delay than compared to other block methods. Moreover, reed Solomon coding does not require excessive computing power to be produced or received. It is recommended for the customer to make detailed trade-off regarding the significance of time with relation to used transmission power.

Encryption Analysis: Encryption process has impact on the required data package size and processing speed. During analysis its impact was assumed to be negligible. Further investigation on that topic is recommended in more detailed phase of the project. It is especially important for transmission over multiple nodes in the costellation.

10
Electrical Power System

In this chapter, the electrical power system (EPS) will be looked into in more detail. As per other chapters, first a functional analysis is carried out for this subsystem, followed by its requirement analysis. Following, the design of the EPS is carried out, and the tools used to do so are introduced. For these tools, a sensitivity analysis and a verification is described, together with the verification procedure for the subsystem as a whole. Similarly, the RAMS characteristics are discussed in their own section. Finally, the recommendations for further work are presented.

10.1. Functional Analysis

The EPS is the subsystem responsible for the harnessing and distribution of electrical energy to all the components of the spacecraft. These components must have sufficient power to operate both during sunlight and during eclipse, and different power modes must be supported. From Chapter 4, the following four power operational modes have been identified for the nominal spacecraft operation and will be used throughout the chapter.

- ***PM1, Imaging power mode***: the Coverage payload is performing circular imaging and no interlinking or significant slewing is present.
- ***PM2, COV detection power mode***: a level 3 alert has been triggered and the spacecraft is interlinking and slewing while it continues imaging.
- ***PM3, FOC tracking power mode***: the spacecraft has target lock and operates the payload while inter-linking occurs. This power mode is also used by the network of satellites even if they are not tracking.
- ***PM4, GS communication power mode***: the spacecraft continues imaging while in a communication link with the ground stations.

With this premise in mind, the functions of the EPS system follow. Note that they not refer to the blocks of the FFD as they are specific for this system.

- **FUNC-EPS-01**Provide electrical power to the spacecraft's payload. *This is the main function of the EPS, which allows the payload to operate nominally and continuously, see REQ-SYS-20.*
  - **FUNC-EPS-01-01** Provide continuous electrical power to the IR camera during operation. *This includes both sunlight and eclipse time.*
  - **FUNC-EPS-01-02**Provide continuous electrical power to the camera cooler during camera operation. *This includes both sunlight and eclipse time.*
  - **FUNC-EPS-01-03**Provide continuous electrical power to the mirror motor during COVERAGE payload operation. *This includes both sunlight and eclipse time, for as long as circular imaging is operational.*
- **FUNC-EPS-02** Provide electrical power to the spacecraft's bus. *This function allows the bus to support the payload continuously, see REQ-SYS-20.*
  - **FUNC-EPS-02-01** Provide continuous electrical power to the ADCS during operation.*This includes both sunlight and eclipse time, and powers all components of the subsystem.*
  - **FUNC-EPS-02-02** Provide electrical power to the propulsion system during orbital maneuvers. *This is only needed when the system must perform such a burn.*
  - **FUNC-EPS-02-03** Provide continuous electrical power to the OBC and other data processing units. *This includes both sunlight and eclipse time, for the computers as well as the DPU.*
  - **FUNC-EPS-02-04** Provide electrical power to the communications subsystem. *This includes both sunlight and eclipse time, with peak performance when interlinking is neces-*

sary.

- **FUNC-EPS-03** Provide housekeeping data. *Flowdown from REQ-SYS-12-03.*
- **FUNC-EPS-04** The EPS shall consider instruments that have already undergone sufficient validation in relevant environments.
- **FUNC-EPS-05** Provide the safety measures necessary to protect the spacecraft components from electrical failure. *For example, failure due to a too high current intensity.*
- **FUNC-EPS-06** Provide sufficient redundancy to minimise single points of failure in the EPS subsystem.

10.2. Requirement Analysis

From the functional analysis presented above, the requirements shown below follow.

- **REQ-SYS-EPS-01** The EPS shall provide up to 42.3 W of electrical peak power to the payload. *Flowdown from FUNC-EPS-01*.
  - **REQ-SYS-EPS-01-01** The EPS shall provide a continuous supply of 10 W[1] of electrical power at 12 V to the payload. *Flowdown from FUNC-EPS-01-01.*
  - **REQ-SYS-EPS-01-02** The EPS shall provide a continuous supply of 31.25 W of electrical power at 24 V[2] to the cooler system. *Flowdown from FUNC-EPS-01-02, power value from Section 16.2.2.*
  - **REQ-SYS-EPS-01-03** The EPS shall provide a continuous supply of 1.05 W[3] of electrical power at 12 V to the mirror motor during PM1, PM2 and PM4. *Flowdown from FUNC-EPS-01-03.*
- **REQ-SYS-EPS-02** The EPS shall provide up to 40 W of electrical peak power to the spacecraft bus. *Flowdown from FUNC-EPS-02, maximum figure corresponds to propulsive manoeuvre.*
  - **REQ-SYS-EPS-02-01**The EPS shall provide a continuous supply of 2 W (PM1, PM3, PM4) or 6 W[4] (PM2) of electrical power at 5 V to the ADCS. *Flowdown from FUNC-EPS-02-01.*
  - **REQ-SYS-EPS-02-02** The EPS shall provide a continuous supply of 40 W of electrical power at 12 V to the propulsion system during orbital maneuvers. *Flowdown from FUNC-EPS-02-02.*
  - **REQ-SYS-EPS-02-03** The EPS shall provide a continuous supply of 2.22 W[5] of electrical power at 5 V to the data processing units. *Flowdown from FUNC-EPS-02-03, includes OBC and DPU.*
  - **REQ-SYS-EPS-02-04** The EPS shall provide a continuous supply of 0.6 W[6] (PM1) or 7.78 W (PM2, PM3) or 1.05 W [7] (PM4) of electrical power at 5 V to the communication system. *Flowdown from FUNC-EPS-02-04, power values from Section 9.3.*
- **REQ-SYS-EPS-03** The EPS shall provide the OBC with temperature, current and voltage measurements of its components. *Flowdown from FUNC-EPS-03.*
- **REQ-SYS-EPS-04** The EPS shall consist of components with at least a TRL of 5. *Flowdown from FUNC-EPS-04, REQ-SYS-03-01.*
- **REQ-SYS-EPS-05** The EPS shall contain the safety measures necessary to protect the spacecraft components from electrical failure. *Flowdown from FUNC-EPS-05.*
- **REQ-SYS-EPS-06** The EPS shall have redundant components for its power management and energy storage. *Flowdown from FUNC-EPS-06.*
- **REQ-SYS-EPS-07** The EPS shall be functional at all temperatures within the range −16 °C to

[1]Retrieved from `http://52ebad10ee97eea25d5e-d7d40819259e7d3022d9ad53e3694148.r84.cf3.rackcdn.com/UK_ICA_QuazIR-MWIR-InSb-Camera-Cores_DS.pdf`
[2]Retrieved from `https://www.thales-cryogenics.com/product-category/cde/`
[3]Retrieved from `https://www.servocity.com/130-rpm-micro-gear-motor`
[4]Retrieved from `https://hyperiontechnologies.nl/wp-content/uploads/2015/07/HT_iADCS400_v2.1-flyer.pdf`
[5]Retrieved from `https://satsearch.co/products/xiphos-technologies-q7s`
[6]Retrieved from `https://www.isispace.nl/product/isis-uhf-uplink-uhf-downlink-transceiver/`
[7]Retrieved from `https://satsearch.co/products/space-inventor-ttc-p3-dual-hot-redundant-vhf-uhf-satellite-tt-c-radio`

40 °C. *From Chapter 11.*
- **REQ-SYS-EPS-08** The mass of the EPS shall not exceed 3.97 kg. *From Table 6.4.*

10.3. EPS Design

The electrical power system has been designed as a photo-voltaic system that generates electricity while in the sunlit phase of its orbit (lasting 61.1), and makes use of a secondary battery system to power the components while in its eclipse phase (lasting 35.4 min). The electrical diagram of the complete system can be seen in Section 10.3.2, and is followed by a more detailed explanation of the different components in Section 10.3.3. Before doing so, however, the method used to create a power budget is described in Section 10.3.1.

10.3.1. Power Calculations

To create a power budget (see Section 16.2.2), the first step is to determine the electrical power usage of all the spacecraft subsystems/components. From the component data sheets, the power usage reported in Section 10.2 is found. These values contain the relevant contingencies, as specified in Chapter 6. This information can then be combined together with the functionality of the mission described in Figure 4.2 to determine the different power modes, which were introduced in Section 10.1. It is thus possible to know for how long a certain amount of power is required. The goal of this section is to combine this information to size the solar arrays and battery packs. To do so, two cases were studied, as listed below.

- **Case A, Missile launch during eclipse**: the spacecraft must operate in PM1 as nominal, but has peak power demand when PM2, PM3 and PM4 are activated during its eclipse phase. Case A represents the worst case scenario for the power required from the solar array and thus constrains the solar array sizing.
- **Case B, Nominal scanning during full orbit**: the spacecraft must operate in PM1 as nominal, with PM4 activated when flying by a ground station. Case B represents the nominal usage of the system and will thus run for the most cycles throughout the spacecraft's lifetime, constraining the depth of discharge (DOD) and with it the battery sizing.

Table 10.1: Input parameters for the power calculations.

Input	Value
η_{SA}	29.5 %
Incidence (i)	5°
Degradation	1.5 %/year
$P_{sp_{SA}}$	120 W kg^{-1}

Input	Value
η_{ACU}	85 %
η_{PDU}	85 %
η_{BAT}	90 %
DOD (peak)	17% (23%)
U_{BAT}	154 W h kg^{-1}

Input	Value
PM1	48.33 W
PM2	59.78 W
PM3	54.52 W
PM4	57.27 W

For both cases, the efficiency of the components is the same. In the calculations, four efficiencies are taken into account: the efficiency of the solar arrays to convert solar intensity into electrical power, the efficiency of the ACU, the battery efficiency and the efficiency of the PDU. The battery efficiency being less than 1 is the reason why the system has higher power losses during the eclipse phase. Additional parameters are the DOD, the incidence angle and the degradation factor of the solar cells, all of which will be discussed in more detail in its respective sections in Section 10.3.3. Finally, battery and solar array performance characteristics (power/energy densities) are used to perform the sizing. The inputs are summarized in Table 10.1, while the outputs are presented in Table 10.2.

Table 10.2: Outputs of the power calculations.

Output	Value	Limiting Case
A_{SA}	0.31 m^2	Case A
M_{SA}	1.05 kg	Case A
E_{BAT}	226 W h	Case B
M_{BAT}	1.47 kg	Case B

10.3.2. EPS System Architecture

The two solar arrays, placed at opposite sides of the spacecraft and mounted on gimbals, transport the electricity generated through 4 channels. These connect to the EPS through an electrical switch, which can let the electricity flow through to the redundant side of the motherboard in case of a faulty component. Then, 4 MPPT converters optimize the current for the spacecraft needs and the charging of the batteries. The Power Interface Protection Switches (PIPS) are circuit breakers that protect the motherboard from non-operational electrical conditions. Before the power can be sent to the different subsystems, the 3 DC-DC converters condition the voltage for the different channels, and the HW configuration matrix links each converter to up to 3 output channels. These channels then flow out of the EPS through the stack connector towards the other spacecraft systems. A schematic of this process with the relevant circuit currents and voltages is shown in Figure 10.1.

10.3.3. EPS Components

In this subsection, the components of the EPS are linked to COTS options that fulfill the requirements set in Section 10.2. The total mass of the subsytem, when including contingencies, is 3.91 kg. All components are chosen such that they can operate within the limits specified by **REQ-SYS-EPS-07**.

Solar array For the solar array, state-of-the art triple-junction GaAs solar cells provided by MMADesign[8] are used. The voltage provided by these arrays can be set to 16 V. The high power demand (PM1 sums up to 48 W) forces the system to mount these on gimbals, in order to ensure a minimum incidence angle. This system has already been flown in NASA's MarCO mission, with the gimbal containing a solar array drive supporting up to 120 W[9]. Moreover, the spacecraft must yaw as it orbits around the Earth to have an unobstructed view of the energy source. This is however not an issue for the system, as the circular imaging allows to continue imaging at any yaw attitude. The calculations in Section 10.3.1 result in a solar array area of 0.309 m^2 which corresponds to 1.04 kg. The gimbals mass is 0.243 kg. Based on similar solar array by ISIS, the price has been estimated to be 50.000 €. In addition, 800.000 € have been budgeted for the R&D costs deriving from the use of gimbals.

Motherboard, ACU and PDU The EPS power conditioning and management components have been chosen from the provider Gomspace. Its NanoPower P60 series[10] offers a modular motherboard with the safety components (such as the PIPS circuit breakers) necessary for the mission at hand. Moreover, it allows for the presence of redundant ACUs and PDUs, eliminating the risk of a single point failure. The P60 ACU receives the four power channels from the solar arrays, measures its current and voltage, and adjusts the voltage in the circuit (which can be increased up to 34 V). Conversely, the P60 PDU uses three DC-DC converters to reduce the voltage to the three values necessary for the other spacecraft components (see right-hand-side in Figure 10.1). Both these components are commanded by its respective integrated controllers, and send housekeeping data about its temperature to the rest of the system. The total mass of the NanoPower P60, including the redundant components, is 0.302 kg, and its cost is estimated at 34 000 €.

Batteries Four 77 W h lithium-ion NanoPower BPX batteries from Gomspace[11] are carried on board, with three of them providing enough energy for the nominal operation of M-STAR and one being for redundancy. Each battery pack is connected to its own PCB, which controls its status, and they are charged by a variant voltage (which must always be higher than the battery voltage) and current (up to 1.25 A per stack). Following, battery voltage must be above the maximum circuit voltage because the DC-DC converters in the PDU can only reduced it. For this reason, each battery places seven battery cells in series, increasing the voltage up to 34 V. The battery packs themselves are placed in parallel for three reasons: to reduce the voltage level needed to charge them, to increase the current

[8]Retrieved from `https://mmadesignllc.com/product/hawk-17ab36/`
[9]Retrieved from `https://mmadesignllc.com/products/gimbals/`
[10]Retrieved from `https://gomspace.com/shop/subsystems/power/default.aspx`
[11]Retrieved from `https://gomspace.com/shop/subsystems/power/nanopower-bpx.aspx`

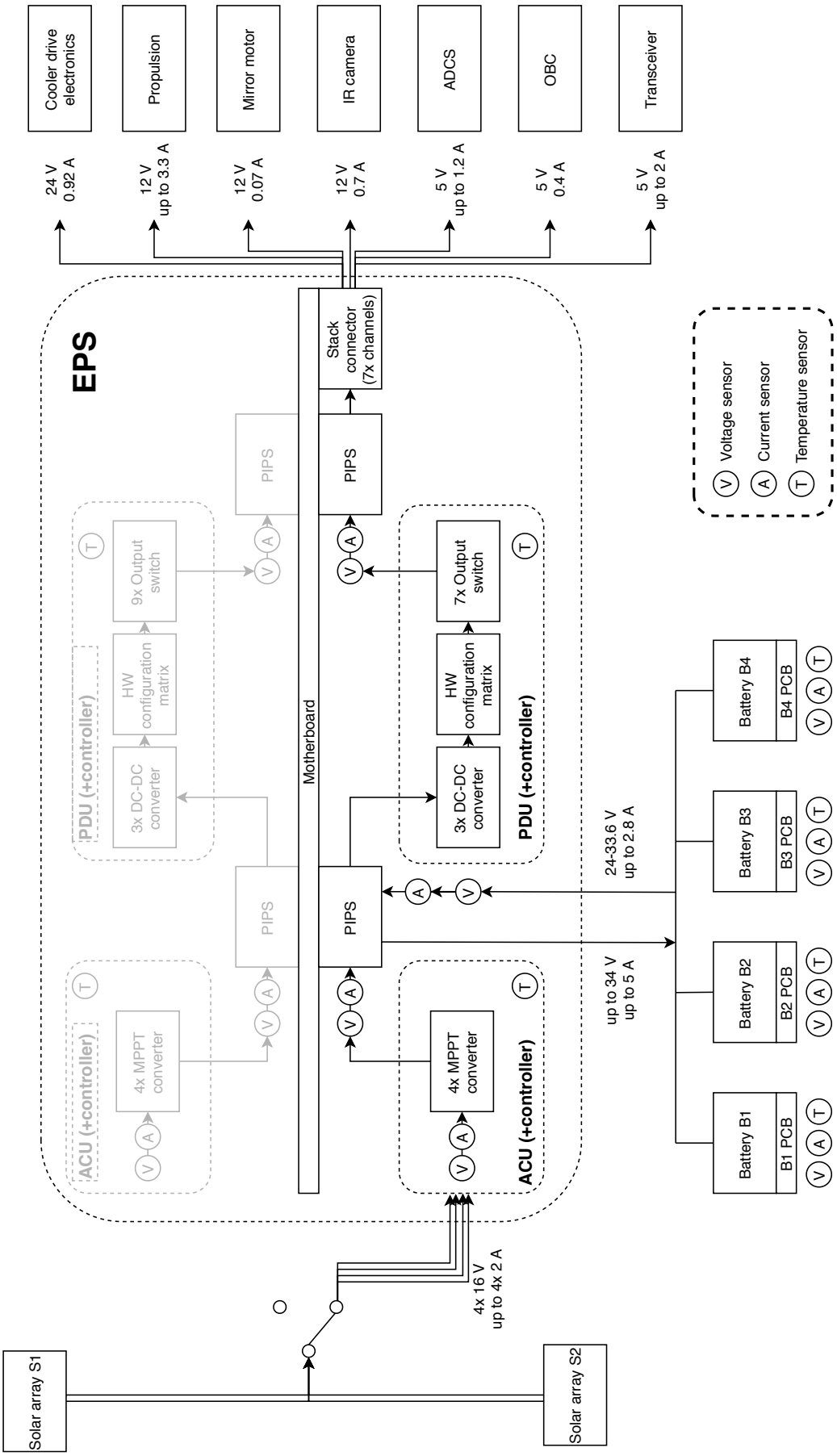

Figure 10.1: Electrical power diagram.

output and for safety reasons (if one pack fails the others can still perform). In addition, given that case B might repeat for up to 38000 cycles, the DOD must be limited to 17%[12] during this case. The same does not hold for case A, which can draw more energy from the battery system (up to 23%) due to the exceptional situation. The choice of this specific component is optimal for two reasons: the high degree of modularity that allow for a tailored solution to M-STAR needs, and the easy integration with the other EPS components. The calculations in Section 10.3.1 result in a required energy battery 3BPX packs, which corresponds to 1.5 kg, plus the 0.5 kg of the redundant BPX. The price of this component if estimated at 7.500 €.

10.4. Sensitivity Analysis

In this section, a sensitivity analysis is carried out on the power calculation tool. Two main questions are answered: how much the DOD can change before the three BPX packs are insufficient and what would be the effect of having a large incidence angle on the solar arrays. This second questions tests against the assumption that the gimbals can be moved as the orbit advances and do not have to be fixed in one specific position. The results of the sensitivity analysis can be seen in Table 10.3.

Table 10.3: EPS Sensitivity Analysis.

Input	Output	Change	Conclusion
DOD = 15.85%	Battery energy needed > 231 W h	7.4%	A deeper investigation on the specific behaviour of the battery at the design conditions must be carried out in the future, as a change in DOD could make the amount of battery packs insufficient.
Incidence angle = 60°	Solar array area = 0.605 m^2	95.79%	If the gimbals are fixed in one position, the solar array area might need to be increased drastically. This could be done either by double-sided arrays or by increasing the number of arrays, which would result in **REQ-SYS-EPS-07** not being met. More research would be necessary to study the incidence angle.

10.5. Verification & Validation

In this section, the V&V procedures regarding the EPS will be carried out: the calculations are verified, the compliance matrix is presented as well as the V&V plan for the subsystem.

10.5.1. Tool 10.1: Power Calculation Verification

In order to verify the tool introduced in Section 10.3.1, a number of tests have been performed. Firstly, if all power modes are given the same value of required power, case A and B should result in the same solar array power required. Secondly, the results for a specific case should be compared against the same procedure performed analytically. Finally, the total energy consumed in one orbit should be equal to the total energy produced during one orbit, taking all efficiencies into consideration. All tests were successful.

10.5.2. Requirement Verification

The requirements introduced in Section 10.2 have been met and justified through this chapter. The compliance matrix for the subsystem is shown in Table 10.4.

10.5.3. Subsystem Verification and Validation

All the components of the EPS have flight heritage and have thus undergone extensive testing. Some aspects, however, must be tested again as they are specific for M-STAR. For example, the solar panels will be sized specifically for the mission. Testing of these will be taken care of by the supplier,

[12]Retrieved from `https://gomspace.com/UserFiles/Subsystems/datasheet/gs-ds-nanopower-battery_2600mAh.pdf`

Table 10.4: Electrical power system requirement compliance matrix.

REQ	Compliance	Section
REQ-SYS-EPS-01		Section 10.3.1
REQ-SYS-EPS-02		Section 10.3.1
REQ-SYS-EPS-03		Section 10.3.2
REQ-SYS-EPS-04		Section 10.3.3
REQ-SYS-EPS-05		Section 10.3.2
REQ-SYS-EPS-06		Section 10.3.2
REQ-SYS-EPS-07		Section 10.3.3
REQ-SYS-EPS-08		Section 10.3.3

MMA Design, at their Louisville facility [13]. Similarly, the EPS components from Gomspace are COTS and go through a testing phase with the supplier. Once all components reach the customer, testing of the integrated EPS will be performed and the models for the battery charge/discharge behaviour can be validated. Special attention must be paid to the solar array drivers in the MMA gimbals (for which extra R&D cost has been budgeted) interfacing with the Gomspace PDU.

10.6. RAMS Characteristics

Reliability The NanoPower P60 system has gone through extensive ground testing and has been flown before, in the GOMX-4 A and B spacecraft[14] launched in 2018, which places the system in a TRL of 9. Moreover, the system is designed to be redundant (see Section 10.3.2) and contains circuit breakers to minimize the probability of electrical power system failure. Gomspace's solution appears as a state-of-the-art in the 2018 NASA report for CubeSats [15].

Availability The EPS services all the spacecraft main components. If there is no electricity supply, the payload, communications, OBC, propulsion and ADCS cannot function, thus making the system unavailable. To mitigate this risk, conservative design philosophy on the battery pack design is used (see Section 10.3.3), as well as redundant battery energy.

Maintainability The system cannot be maintained after launch, but the modularity of the solution allows for individual components to be changed in case a fault is discovered during ground testing. Moreover, the health of the system is monitored through the sensors shown in Figure 10.1: the temperature of the main components and the circuit characteristics are made available to the OBC.

Safety The safety of this subsystem can be assessed in two ways. Firstly, the EPS does not exceed the 50 V that classifies a circuit as "high-voltage", and thus is safer for the personnel in charge of production/integration/testing. Secondly, if a satellite would run out of power, it could pose a safety threat as it becomes uncontrollable: the redundant battery is present to eliminate this scenario.

10.7. Recommendations

The notably high power requirement on the spacecraft's EPS pushes the design of this subsystem to technological solutions outside what is common for most spacecraft of this size. Such is true for the mounting of the solar panels, and the complexity of the gimbal mechanism should be investigated further in following design phases. Depending on the conclusions of this study, a different solar array configuration could be considered (not using gimbals but potentially doubling the number of solar panels). Next to this, the design life of M-STAR exceeds the more common 5 year mission lifetime of most LEO satellites. This increases the number of cycles the system is designed to go through. Thus, as mentioned in Section 10.3.3, in future steps the specific behaviour of the battery cells in operational conditions could be modeled, to more accurately predict the necessary DOD.

[13]Retrieved from `https://mmadesignllc.com/about/our-facility/`
[14]Retrieved from `https://directory.eoportal.org/web/eoportal/satellite-missions/g/gomx-4`
[15]Retrieved from `https://www.nasa.gov/smallsat-institute/sst-soa`

11
Thermal Control

This chapter elaborates on the thermal control of the satellite. A short functional and requirement analysis is presented, after which the equilibrium temperature of the satellite is determined in a hot and cold case scenario. Furthermore, a radiator design will be proposed, followed up by a sensitivity analysis, Verification & Validation, RAMS characteristics and future recommendations.

11.1. Functional Analysis

There is one function for thermal control that encapsulates the entire thermal subsystem.

- **FUNC-TH-01** Be capable of keeping all subsystems within their operational temperature range. During the complete mission all subsystem should be operated only within the operational temperature range in order to prevent failure of the subsystem. *Flown down from block 3.1 and 3.2*

11.2. Requirement Analysis

The requirement analysis flows down from the functional analysis.

- **REQ-SYS-TH-01** The thermal system shall keep every system and their parts inside their operational temperature range. *Flown down from FUNC-TH-01.*
  - **REQ-SYS-TH-01-01** The thermal system shall keep the batteries in their operational temperature range between 253.15 K and 333.15 K.
  - **REQ-SYS-TH-01-02** The thermal system shall keep the solar arrays in their operational temperature range between 168.15 K and 383.15 K.
  - **REQ-SYS-TH-01-03** The thermal system shall keep the sensors in their operational temperature range between 243.15 K and 323.15 K.
  - **REQ-SYS-TH-01-04** The thermal system shall keep the thrusters in their operational temperature range between 253.15 K and 313.15 K.
  - **REQ-SYS-TH-01-05** The thermal system shall keep moving mechanisms in their operational temperature range between 273.15 K and 323.15 K.
  - **REQ-SYS-TH-01-06** The thermal system shall keep the on-board computers in their operational temperature range between 233.15 K and 333.15 K.
  - **REQ-SYS-TH-01-07** The thermal system shall keep the telemetry and telecommand in their operational temperature range between 253.15 K and 333.15 K.
  - **REQ-SYS-TH-01-08** The thermal system shall keep the camera in its operational temperature range between 233.15 K and 338.15 K.
  - **REQ-SYS-TH-01-09** The thermal system shall keep the cooler in its operational temperature range between 243.15 K and 323.15 K.
- **REQ-SYS-TH-02** The thermal system shall be able to withstand launch temperatures

11.3. Equilibrium Temperature

In this section, the thermal equilibrium temperature will be calculated for a hot and cold case. These temperatures will mark the extreme cases. When the satellite is designed for these worst-case scenarios any milder conditions can be managed by the thermal control as well. As the calculation for the thermal control are only preliminary, a high number of assumptions were made. Such assumptions are the following:

- The spacecraft is a homogeneous black box of 3x2x2 units.

- The distance between Sun and satellite will be constant.
- The albedo factor of Earth is taken average and is constant.
- All components of the satellite are uniformly heated.
- The temperature of Earth is constant.
- Dissipated heat within the satellite is constant in the hot or cold case.
- The solar panels are not taken into account as surface area for the spacecraft equilibrium temperature, as it is assumed that they will instantly emit all incoming heat with the radiators at the other side of the solar array.
- Absorptivity for IR wavelengths is equal to the emissivity for IR wavelengths.
- Constant eclipse time.

For the hot case, the satellite being sunlit, it is assumed that the satellite receives heat from sunlight, albedo radiation and IR radiation from Earth. In the cold case, during eclipse, only IR radiation will be received. In the worst case scenario for the sunlit phase, all radiation is able to reach the three sides of the satellite under a 45° angle. The worst case scenario during eclipse would be that the IR radiation of Earth would only hit one small side of the spacecraft at 90°.

In order to find the equilibrium temperature, the incoming heat transfer rate and heat accumulations within the satellite should equal the output heat transfer rate (see Equation (11.1)).

$$\dot{Q}_{absorbed} + \Sigma P_{dissipated} = \dot{Q}_{emitted} \tag{11.1}$$

In the hot case scenario, $\dot{Q}_{absorbed}$ consist of the heat transfer rate from sunlight, albedo radiation and IR radiation from Earth, and $\dot{Q}_{emitted}$ will consist of the radiation the spacecraft emits into space. With this information Equation (11.1) it can be rewritten to [64]:

$$\alpha_s \cdot J_{sun} \cdot A_i + \alpha_s \cdot J_{albedo} \cdot A_i + \alpha_{IR} \cdot J_{IR} \cdot A_i + \Sigma P_{dissipated} = \epsilon_{IR} \cdot \sigma \cdot A_e \cdot T^4 \tag{11.2}$$

Where α_s= solar absorptivity, J_{sun} = solar intensity, A_i = area of incidence, J_{albedo} = albedo intensity, α_{IR}= IR absorptivity (is equal to ϵ_{IR}), J_{IR} = IR intensity from Earth, ϵ_{IR} = infrared emissivity, A_e = area of emittance and T is the equilibrium temperature.

J_{sun} can be calculated with [64]:

$$J_{sun} = \frac{P}{4 \cdot \pi \cdot d^2} \tag{11.3}$$

Where P is the power emitted by the sun, which is 3.856×10^{26} W and d is the distance between the Sun and Earth, which is 149 597 870 700 m [64][65].

Furthermore, J_{albedo} can be obtained using[64]:

$$J_{albedo} = a \cdot J_{sun} \cdot F \tag{11.4}$$

Where a is the albedo factor which is taken to be 0.3 and F is the visibility factor which lies between 0 (cold case) and $(\frac{R_{planet}}{R_{orbit}})^2 = 0.747$ (hot case) [66] [64]. Moreover, J_{IR} can be found with [64], where T_{Earth} is the effective radiation temperature of Earth, which is estimated to be 255 K [64].

$$J_{IR} = \sigma \cdot T_{Earth}^4 \tag{11.5}$$

The dissipated power ($\Sigma P_{dissipated}$) is the heat all the components in the satellite produce during operation. It is assumed that the nominal budgeted power usage of each system in Table 16.2 is completely converted to heat. The only system that deviates from this table is the EPS system. During daytime, the heat generated by the EPS system depends on the incoming power induced by sunlight, the efficiency of the ECU, the power that runs through the system, the efficiency of the PDU

Table 11.1: Operational temperature ranges per component. Green = satisfies the operational range of the spacecraft. Red = does not satisfy he operational range of the spacecraft.

	Hot case temperature	**Cold case temperature**
	15.7 °C	−18.6 °C
Component	**Maximum operational temperature (°C)**	**Minimum operational temperature (°C)**
Batteries	60	-20
Sensors	50	-30
Thrusters	40	-20
Mechanisms	50	0
OBC	60	-40
TTC	60	-20
Camera (excluding FPA)	65	-40
Cooler	-30	50

and the efficiency of charging the battery. In total, this leads to a dissipated heat during the day of 28.83 W. In eclipse, this decreases to 11.60 W as there is no incoming power from sunlight.

All input values are now identified, what is left to decide is the coating that will determine the the solar absorptivity and IR emissivity. After several rounds of testing different coatings, the reflective white paint Barium Sulphate with Polyvinyl Alcohol was chosen [67]. This coating gives a equilibrium temperature of 15.7 °C during day time and −18.6 °C during eclipse.

It can be seen in Table 11.1 that all components of the spacecraft fit in this range except for the the minimum temperature for the mechanisms. However, the temperature range that was found for the mechanism was an estimated average value from reference [64]. Hence, this problem can be easily mitigated by selecting a cold-resistant product or performing a R&D in order for it to fit the temperature range. Since the equilibrium temperatures fall within the operational temperature ranges for all components, a passive thermal control can be achieved. A passive thermal control system is preferred over an active thermal control system from a sustainability perspective. It is economically justified as it is a simple and cheap solution. Furthermore, no radioisotope thermoelectric generator has to be used, which is environmentally justified.

The equilibrium temperature was calculated for the satellite, but the solar panels were not taken into account as they were assumed to be a separate system. If radiators were placed on the opposite side of the solar arrays, the hot case scenario equilibrium temperature would be 90.1 °C and for the cold case this would be −60.9 °C. However, the difference is quite small compared to no radiators but solar cells on the other side of the solar array; 93.8 °C in the hot case and −58.7 °C in the cold case. Hence, whether the solar array has radiators or not, does not affect its equilibrium temperature severe enough to go outside the range of its operational temperature. However, a radiator is required for the cooler. As explained in Section 7.3.4, the payload requires a cooler in order to keep the temperature of the FPA low enough to prevent high levels of instrument noise. The function of the cooler is to transfer heat from the FPA to another area. Heat in space can only be lost through radiation. Therefore, the cooler should be connected to a radiator. The best location to place this radiator is at the backside of the solar array, as this will not affect the equilibrium temperature as explained earlier. To connect the lower disk of the expander of the cooler to the radiator a copper flexible strap is used. This will run across the exterior part of the spacecraft (see Section 16.1.4. The Cabled Copper Thermal Straps (CuTS®) from Technology Application. Inc. are selected for the design as they can be easily customized and have extensive flight heritage [68].

11.4. Sensitivity Analysis

The calculation for the equilibrium temperature contained several numbers which were estimated or averaged. This section will investigate if these assumptions affect the end result. The parameters which are changed for the sensitivity analysis are: the albedo factor, the visibility factor and the distance between the Sun and the satellite.

Albedo Factor The albedo factor is assumed to be 0.3 on average. However, it can change depending on the terrain below the satellite. The maximum albedo factor for Earth is 0.6 for icecaps and high clouds and the minimum albedo factor is 0.05 for open oceans [64].

Distance The distance between the satellite and the surface of the Earth was assumed to be 1 au. This number is taken from the center of the Sun to the center of Earth. The exact distance would be:

$$\text{Distance} = 1AU - R_{sun} - R_{earth} - 600km = 1.495971682 * 10^{11}m \tag{11.6}$$

This number is called $d1$ in the input column in Table 11.2.

The distance between Earth and the Sun also changes over time as Earth's orbit is not a perfect circle, but rather slightly elliptical. This distance between Earth and the Sun is 1.475×10^{11} meter in perihelion and 1.526×10^{11} meter in aphelion. The distance in perihelion is called $d2$ in Table 11.2 and the distance in aphelion is called $d3$ [69]

Visibility Factor The visibility factor was estimated to be at most 0.747. In theory, however, the visibility factors could lie between 0 and 1 [64]. Hence, a visibility factor of 1 is tested.

Table 11.2: Sensitivity analysis for equilibrium temperature calculation.

Input	Spacecraft temperature hot case (K)	Change (%)	Solar array temperature hot case (K)	Change (%)
a= 0.05	287.7	-0.394	350.4	-3.56
a= 0.6	290.1	0.466	377.2	3.82
d1	288.8	1×10^{-5}	363.3	1×10^{-4}
d2	289.0	0.0734	365.6	0.627
d3	288.5	-0.100	360.1	-0.871
F=1	289.3	0.158	368.2	1.34

Conclusion In Table 11.2, the changes in temperature are shown for different parameters. It should be noted that all parameters only affect the hot case scenario, so the cold case scenario is not taken into account. Table 11.2 shows that the changes are insignificant and that they will not change the outcome for the equilibrium temperature in such a way that a different coating should be used.

11.5. Verification & Validation

11.5.1. Tool Verification

In this section the tool used to calculate the equilibrium temperatures is verified. First, unit tests are performed for Equation (11.3) and Equation (11.4). When the Sun would not emit any power, J_{sun} and J_{albedo} should become 0 W m^{-2}. This was verified. Furthermore, J_{sun} was calculated for various planets and verified using Figure 53 from reference [64]. Another unit test for Equation (11.4), was to set the albedo factor and visibility factor equal to one, which would mean that sunlight is perfectly reflected. This was also verified. Equation (11.5) was verified by setting the effective radiation temperature of Earth equal to zero for which there should be no IR intensity present. Again, this was confirmed. Further verification of this equation was achieved by checking the number for various

planets using Table 33. from reference [64]. The system as a whole was tested for a scenario in which all units were zero, resulting in an equilibrium temperature of 0K.[1]

11.5.2. Subsystem Verification and Validation

All components from the thermal control have high TRL. The white paint Barium Sulphate with Polyvinyl Alcohol, which will be used as coating for the entire satellite and the radiator, has been used before on satellites [67]. The same holds for the copper straps from Technology Application Inc. which have extensive flight heritage. However, mission specific tests should be executed in order to test if it functions properly as a complete system. Therefore, the following tests should be performed at the ESA ESTEC: thermal balance test, thermal vacuum test, infrared radiation test and Photogrammetry measurements. [70].

11.5.3. Compliance Matrix

In table 11.3 the compliance matrix of the thermal control is given. Requirement **REQ-SYS-TH-01** and almost all its sub-requirements are met. Only **REQ-SYS-TH-01-05** is not completely met, but this was easily mitigated as explained in Section 11.3. The requirement **REQ-SYS-TH-02**, could not be tested as the launch vehicle is unknown and outside the scope of the DSE.

Table 11.3: Thermal Requirement Compliance Matrix.

REQ	Compliance	(Sub)Section
REQ-SYS-TH-01		Section 11.3
REQ-SYS-TH-02		

11.6. RAMS

In this section a RAMS analysis is performed.

Reliability The white paint, radiator and copper straps all have flight heritage and therefore have a TRL 9. Furthermore, a significant margin is present for the operational temperature for most of the components of the satellite (see Table 11.1).

Availability The thermal control ensures that all the components can function within their operational temperature. If no coating is applied, the spacecraft will endure extreme temperatures which will lead to ultimate failure of the satellite. It is essential that a long-lasting coating is applied to mitigate this.

Maintainability The thermal control of the satellite is completely passive and can therefore not be maintained after launch. The degradation of the coating and radiator can be monitored over time my measuring the surface temperature. However, no action can be performed when degradation is found to be too severe.

Safety In case the thermal control fails and the spacecraft will be exposed to extreme temperatures, dangerous situation could potentially occur. There exists an exceptional case in which extreme temperatures could in the worst-case scenario lead to explosions of components which store energy.

11.7. Recommendations

In this report, only preliminary calculations were performed for the thermal subsystem. A more elaborate thermal analysis should be performed, taking into account the temperature over time for each component. Furthermore, conductive heat transfer between components should be taken into account. Finally, no calculations were performed for the copper straps yet, as it was not clear how much heat the cooler has to reject. These calculations can be performed as soon as detailed information of the FPA from the camera is acquired.

[1] More system testing should be performed but due to the oversimplification of the equilibrium temperature, no data could be found to validate the system.

12
Propulsion

This chapter elaborates on the propulsion design of the spacecraft. The propulsion design was finalized by narrowing down types of propulsion based on requirements and functions and doing a detailed trade-off of the remaining options. Furthermore, sensitivity analysis is conducted on the technical design details to ensure that the chosen propulsion design was optimal.

12.1. Functional Analysis

- **FUNC-PROP-01** Perform collision avoidance maneuver. *Flow down from 4.2.11.*
  - **FUNC-PROP-01-01** Provide consistent thrust performance for entire mission life time.
- **FUNC-PROP-02**Perform altitude maintenance burn. *Flow down from 4.2.9.*
- **FUNC-PROP-03**Perform EOL procedures. *Flow down from 5.3.*
- **FUNC-PROP-04** Initiate thrust when maneuvers initiate. *Flow down from 4.2.11, 4.2.9, 5.3.*
  - **FUNC-PROP-04-01** Provide continuous constant thrust performance during mission lifetime.
- **FUNC-PROP-05** Terminate thrust at the end of maneuvers. *Flow down block 4.2.11, block 4.2.9, block 5.3.*

12.2. Requirement Analysis

- **REQ-SYS-PROP-01**The propulsion system shall have a total ΔV capability of 183.5 m/s.
  - **REQ-SYS-PROP-01-01** The propulsion system shall have a ΔV capability of 19.52 m/s for orbit maintenance during its lifetime. *Flow down from FUNC-PROP-02*
  - **REQ-SYS-PROP-01-02** The propulsion system shall have a ΔV capability of 7.31 m/s for collision avoidance. *Flow down from FUNC-PROP-01.*
  - **REQ-SYS-PROP-01-03** The propulsion system shall have a ΔV capability of 156.7 m/s for EOL deorbitting maneuvers. *Flow down from FUNC-PROP-03.*
- **REQ-SYS-PROP-02**The propulsion system shall have a lifetime of 7 years. *Flow down from FUNC-PROP-04-01.*
  - **REQ-SYS-PROP-02-01**The propulsion system shall have consistent thrust performance for the mission life time.
- **REQ-SYS-PROP-03** The propulsion system shall be have operating temperatures compatible with the spacecraft's thermal configuration. *Flow down from FUNC-PROP-04-01.*
  - **REQ-SYS-PROP-03-01** The propulsion system shall be functional at all temperatures within the range −16 °C to 40 °C.
- **REQ-SYS-PROP-04** The propulsion system shall be compatible with nanosatellites.
  - **REQ-SYS-PROP-04-01**The propulsion system shall occupy at most 1U per unit.
  - **REQ-SYS-PROP-04-02**The propulsion system shall have a mass of at most 2 kg.
- **REQ-SYS-PROP-05** The propulsion system shall operate while spacecraft is operational.
  - **REQ-SYS-PROP-05-01**The propulsion system shall need a maximum operating power of 48 W.

12.3. Trade-off Criteria

The power, mass and volume constraints of the mission narrowed down the propulsion systems feasible for this application to two main categories: Ion thruster and Cold Gas Propellant(CGP) thrusters. Furthermore, as was concluded in the previous Chapter 11, the spacecraft thermal system is designed such that the spacecraft will experience temperature between −16 °C and 40 °C. This further

narrowed the available COTs option for ion and CGP thrusters significantly, leaving only four possible COTs propulsion system options. In order to sufficiently characterize each concept to allow for a valid trade-off between the concepts, the following trade-off criteria were established: cost, TRL, volume, mass, system performance and operating power. In this section, these criteria are elaborated on and the characterization of all possible concepts using these criteria is performed.

12.3.1. Cost

The cost of the complete propulsion systems were graded using a linear scale, with the most affordable concept receiving a 5 and the least affordable concept receiving a 1.

12.3.2. TRL

The system requirement that states the every component of the mission shall have a TRL larger than 5, **REQ-SYS-03-01**, guided the grading composition for this criteria. The scale is shown in Table 12.3.

12.3.3. Volume and Mass

The criteria addressing the mass and volume of each propulsion system concept can be seen in Table 12.1 and Table 12.2 [1].

Table 12.1: Scale description: Mass criteria.

	System Mass (kg)
5 excellent	<1.0
4 high	1.0-1.5
3 medium	1.5-2.0
2 low	2.0-2.5
1 poor	2.5<

Table 12.2: Scale description: Volume criteria.

	System Volume (U)
5 excellent	<1.0
4 high	1.0-1.5
3 medium	1.5-2.0
2 low	2.0-2.5
1 poor	2.5<

Table 12.3: Scale description: TRL assessment.

	TRL
5 excellent	9
4 high	8
3 medium	7
2 low	6
1 insufficient	5

12.3.4. System Performance

Analysing the system performance of each concept was done by considering the ΔV required for the three main maneuvers that drive the propulsion system design: orbit maintenance, collision avoidance and EOL deorbitting maneuvers. The values for the ΔV required for orbit maintenance and collision avoidance were as followed from the technical resource budget [4].

The total ΔV allocated to orbit maintenance is $19.52\,\mathrm{m\,s^{-1}}$. Assuming that an orbit maintenance maneuver is required to be performed once every month, and given a mission life time of 7 years (**REQ-MIS-04**), this implies a required ΔV capability of $0.23\,\mathrm{m\,s^{-1}}$ for each time this maneuver is executes. In addition to this, the total ΔV budgeted for collision avoidance was $7.31\,\mathrm{m\,s^{-1}}$. Assuming this maneuver will need to be executed at least 9 times in the mission life time [4], this implies a ΔV of $0.812\,\mathrm{m\,s^{-1}}$ per execution of the collision avoidance maneuver. It is to be noted that this budget was determined assuming a short-term collision avoidance plan is sufficient for the mission. Long term collision avoidance maneuvers are possible that don't significantly impact the required amount of propellant on-board; one that allows anticipation of a collision 8h or 24h before impact[71]. However, the necessity for these advanced maneuvers will depend on the selected propulsion system and it's

[1] The criteria addressing the system mass does not follow as linear scale as, when the available COTs where characterized, the large difference in mass between ion thruster and CGP systems would cause a linearized scale to become skewed: all concepts except for the CGP would receive a grade 5. In order to deal with this, a scale was made based on the maximum difference in mass between concepts, constrained by the lightest concept receiving a grade 5 and the heaviest a 1, and the resulting ranges can be see in Table 12.1. Regarding volume, all concepts were a maximum of 1U away from each other so a partially linearized scale was possible.

capability to perform timely maneuvers. Therefore, this performance parameter plays a driving role in the grading of this criteria, as can be seen in Table 12.4.

Table 12.4: Scale description: System performance.

	System Performance
5 excellent	Maneuvers require less than a minute to execute, collision avoidance can be estimated once debris is closer to the satellite, increased accuracy and decreased risk in collision avoidance. Less than 30 minutes for collision avoidance.
4 high	Maneuvers require less than 6 hours to execute, requires 8h collision maneuver (long term collision avoidance maneuvers).
3 medium	Maneuvers require less than 12 hours to execute, requires 24h collision maneuver (long term collision avoidance maneuvers).
2 low	Maneuvers require more than 12 hours to execute, no existent long term collision maneuvers feasible, requires separate design.
1 poor	Maneuvers require a large amount of time, collision avoidance not possible.

For each concept, the time required to perform each of these maneuvers was calculated with

$$\Delta V = \frac{\tau_b \cdot \Delta t}{m_{sc}} \tag{12.1}$$

Where ΔV is that ΔV which is required for a single execution of a given maneuver, τ_b is the thrust of a single propulsion unit, m_{SC} is the estimated mass of the spacecraft and Δt is the time required to execute the maneuver in question. All parameters besides the time required is known either by the COTs' characterization or the technical resource budget[4].

The most constraining maneuver is the collision avoidance maneuver, as here the time required is critical. Thus this became, as mentioned before, a driving factor in the grading of system performance.

12.3.5. Operating Power

Table 12.5: Scale description: System operating power.

	Operating Power
5 excellent	Minimal power required and only during initiation of manuvers.
4 high	Significant amount of power required to initiate manuvers.
3 medium	Requires feasible continous power supply for operation for entire duration of manuvers.
2 low	Requires large amounts of power only when initiating manuvers, requiring the spacecraft to be shut down. .
1 poor	Requires continous operational power, only feasible when the entire spacecraft is shut down the entire duration.

The primary divider when assessing the performance of a propulsion system with regards to demanded operating power is whether or not it requires continuous power during the entire duration of a given maneuver. CGP thrusters have the advantage that they only require power for maneuver initiation whereas ion thrusters vary from requiring large amounts of power only during activation

to requiring a continuous power during the entire maneuver. Therefore, the grading of the power performance of propulsion systems are driven by these factors, as can be seen in Table 12.5.

12.3.6. Criteria Weights

Criteria weights are established following the same methodology outlined in Section 6.1. The only difference is in the first step which involved identifying and grading customer needs based on mission requirements. In this case, the relevant mission or system requirements and corresponding customer needs are as follows:

Table 12.6: QFD procedure to determine the criteria weights.

Identifier	Customer Need	Costumer Importance Rating	Cost	TRL	Volume	Mass	Performance	Operating Power
REQ-MIS-05	Cheap	*3 [15.79%]*	9		3	1		3
REQ-MIS-04	Life Time	*4 [21.05%]*					1	
REQ-MIS-06	Nanosat	*4 [21.05%]*		9	9	9		9
REQ-SYS-16	EOL manuvers	*3 [15.79%]*	1				3	
REQ-SYS-14	Collision avoidance	*5 [26.32%]*					9	
			1.58	1.89	2.37	2.05	3.05	2.37
		Criteria Weight	**12%**	**14%**	**18%**	**15%**	**23%**	**18%**

12.4. Propulsion System Design

12.4.1. COTs Characterization

Using the criteria outline in Section Section 12.3, the COTs propulsion units that remained valid given the strict operating temperature constraints were characterized in order to go through a trade-off[2][3][4][5].

Table 12.7: Characterization of COTs Concepts for Trade-off Based on Criteria Section 12.3.

	Cost (Euros)	TRL	Volume (U)	Mass (kg)	Operating Power (W)	Performance		
						Thrust (mN)	Δt (hour) orbit maintnance	Δt (hour) collision avoidance
Concept 1: NPT30	-	7	1.5	1.3	30-60	1.1	1.18	4.07
Concept 2: IFM Nano Thruster	38,400	9	<1	0.9	8-40	0.4	3.18	10.98
Concept 3: MEMs MicroSpace	129,000	9	1	7.24	2	10	0.17	0.54
Concept 4: RIX 10 ENVO	-	8	<2	1.8	145	5	0.27	0.92

12.4.2. Trade-off Results

As is evident from Table 12.8 concept 2, the IFM Nano Thruster, wins the trade-off. Furthermore, it is to be noted that for two of the options a cost quote was unavailable and thus their final scores are a weighted average of the remaining criteria. Between concept 2 and 3, as can be seen in Table 12.7, concept 2 is significantly more cost efficient.

[2]https://satsearch.co/products/thrustme-npt30
[3]https://satsearch.co/products/enpulsion-ifm-nano-thruster
[4]https://www.cubesatshop.com/product/nanosatellite-micropropulsion-system/
[5]https://space-propulsion.com/spacecraft-propulsion/propulsion-systems/electric-propulsion/index.html

Table 12.8: Final trade-off table propulsion.

	12%	*14%*	*18%*	*15%*	*23%*	*18%*	
	Cost	TRL	Volume	Mass	Performance	Operating Power	**RESULT**
Concept 1	-	3.0	3.0	4.0	4.0	3.0	**3.0**
Concept 2	4.0	5.0	5.0	5.0	3.0	4.0	**4.2**
Concept 3	3.0	5.0	4.0	1.0	5.0	5.0	**4.0**
Concept 4	-	4.0	2.0	3.0	4.0	1.0	**2.5**

In order to ensure that, given the information for cost, concept 2 would still win the trade-off, the trade was also conducted given a scenario where concept 1 and 4 were given the highest grade in the cost criteria. Furthermore, as concept 1 and 4 are also ion thrusters with similar thrust ranges and composition to concept 2 the cost would not deviate largely from that of concept 2. Assuming a worst case scenario, where concept 2 performs a grade less than concepts 1 and 4 in the cost criteria, the concepts receive the grades as shown in the table below:

Table 12.9: Considering best cost case for unknown values.

	Cost	**Final Grade**
Concept 1	5.0	3.6
Concept 2	4.0	4.2
Concept 3	3.0	4.0
Concept 4	5.0	3.1

As is evident from Table 12.9 even when concept 1 and 4 are given the highest relative scores in the cost criteria, concept 2 still wins the overall trade-off. Therefore, it can be concluded that concept 2, the IFM Nano Thruster, is the best option for a propulsion system for this mission.

12.4.3. Propulsion System Characterization: IFM Nano Thruster

The IFM Nano Thruster is a complete propulsion unit that has a volume of approximately 0.8U. One of the major advantages of the IFM Nano Thruster is its capability to have variable specific impulse setting; this means that in one mission, there are several thrust and power settings possible, allowing you to design specifically to each maneuver involved in the mission.

As is visible from Figure Figure 12.1, the IFM Nano Thruster has a large range for specific impulse in its operating envelope. As mentioned before, the propulsion unit needs to handle three maneuvers: orbit maintenance, collision avoidance and the EOL deorbitting. For this stage of design the ΔVs approximated in the preliminary technical resource budget is used[4].

Due to power constraints imposed by a demanding payload system, Chapter 7, it is not possible to sustain the IFM Nano Thrusters even at their lowest performance setting while having the payload remain functional. It is to be noted that of the concepts that went into the trade-off the IFM Nano Thrusters were the cheapest ion thrusters with regard to operational power. Thus, the only way to successfully perform orbit maintenance and collision avoidance maneuvers is to cease payload operation for the duration of the maneuvers. This does not pose a large a risk as the constellation was designed for double coverage; as long as successive spacecraft are not performing maneuvers simultaneously, continuous global coverage is still possible. Nonetheless, it remains a design driver to minimize the time required for the aforementioned maneuvers so as to minimize the time payloads are inactive. As the communications system is still active the entire time, the mission requirement dictating a 99 % availability is still met (**REQ-MIS-01-05**).

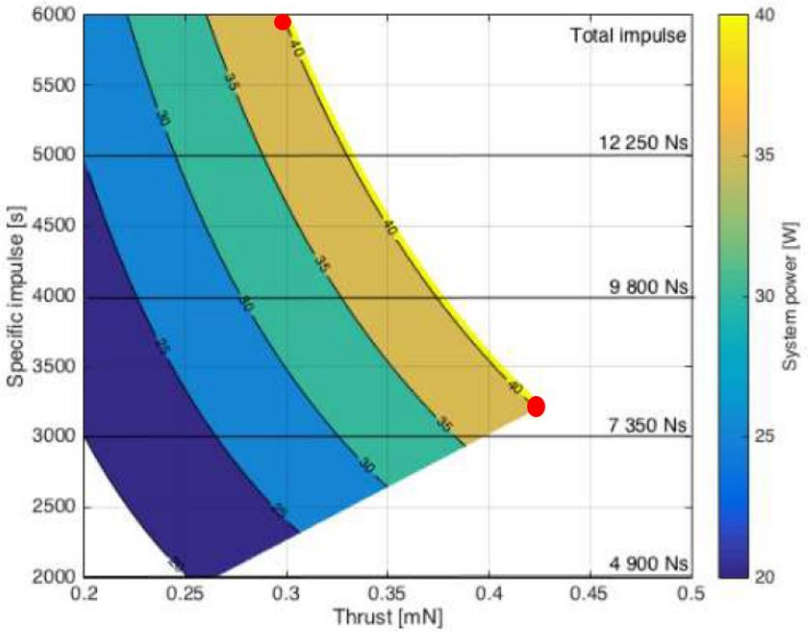

Figure 12.1: Propulsion system characteristic design points.

Table 12.7 shows the time required for collision avoidance and orbit maintenance assuming the maximum thrust performance of the IFM Nano Thruster. For performing collision avoidance avoidance maneuvers time is a critical factor and thus it must be designed at a point of maximum thrust. This is indicated in Figure Figure 12.1, the lower red point; at this point, a specific impulse of 3.200 s is supplied allowing for a thrust of 0.42 mN. However, this comes at the expensive of demanding 40 W of operating power for the entire duration of the maneuver. Due to the disconnection of the payload system from the power line, however, the available power during nominal operation (labeled as PM1 in Chapter 10) is enough to provide energy to the thruster. Orbit maintenance maneuvers are performed at the same design point in order to minimize the duration of the mission where the payload would have to be inactive.

For purposed of design, the ΔV required for EOL was estimated to be 156.66 m s^{-1} based on a preliminary maneuver determined for deorbitting. This value was used in the design as it would allow for a conservative design. This is because this ΔV is for an extreme deorbitting maneuver that consists of bringing the spacecraft into an elliptical orbit with perigee altitude of 50 km in one motion, terminating the spacecraft in a single motion. EOL maneuvers are conducted at at the maximum specific impulse, because as it occurs at the end of the mission life time, time and power constraints are relaxed. It can be afforded to shut down the entire spacecraft during the maneuver. Furthermore, all remaining propellant can be burned thus the high total impulse implied does not pose as a problem. The design point for the deorbitting maneuver is also indicated in Figure 12.1, the upper marked point. EOL manuvers are conducted at a thrust level of 0.29 mN, a specific impulse of 6.000 s and a total impulse of 14.700 N s.

12.5. RAMS Analysis

Reliability The IFM Nano Thruster has been through extensive on ground testing which includes thruster burning intervals and in-orbit demonstrations([72]) of its performance in LEO CubeSat mission. This factor of flight heritage helps achieve the strict system reliability requirement. The high TRL score of 9 follows from this. The IOD involved independent orbit maneuvers and confirmation demonstrating the propulsion unit's capabilities and reliability. Further testing, specific to the application of this propulsion unit to this mission will be necessary and will be elaborated on in the succeeding chapter.

Availability As mentioned before, all maneuvers performed require a continuous operational power of 40 W. This means that for the entire duration of each maneuver at least the payload system is inactive. This design choice has an impact on the compliance of two requirements, one dictating a 99 % availability of communication relays for detection and a 99 % reliability in detection, **REQ-SYS-01-05** abd **REQ-SYS-01-06** respectively.

In particular, collision avoidance is a critical function of the propulsion system for these requirements as if it is not sufficiently accounted for, it results in the loss of a spacecraft. This immediately puts the compliance of both these requirements at risk because it puts the inter-satellite communication system and its functionality at risk; this was elaborated on in Chapter 9.

Maintainability As the system is in space there is no manual maintainability that can take place, however implementing a fuel flow detector would allow to keep track of the fuel flow during maneuvers and while the system is doormant. This would allow for the detection of leakage. This would allow for the groundstation to be aware that another satellite needs to take its place. Furthermore, the IFM Nano Thruster has a burn time of 17,000 hours per unit[6]. It needs to be ensured that the propulsion system remains inactive unless a maneuver is triggered by the spacecraft as otherwise it drains the power available to other subsystems, specifically the payload. Furthermore, the thrust setting at the initiation of the afore mentioned maneuvers need to be assessed, as if it is too long, maneuvers will take longer than anticipated resulting in a faster depletion of the available propellant. In relation to this, the specific impulse and total specific impulse need to be monitored for the same reason.

Safety The most important safety measure that needs to be delved into for the functionality of the propulsion system is the sufficient and successful capability to perform collision avoidance, **FUNC-PROP-01**. As mentioned before, the time required to perform collision avoidance dictates the procedure used to anticipate said collision. The IFM Nano Thruster needs approximately 11 hours to perform a collision avoidance maneuver, this means that collision must be anticipated at least 20 hours prior to its occurrence. Existent maneuvers that can predict collisions upto 24 hours prior to its occurrence can be explored to be ensure this [71]. The issue with using long term collision avoidance maneuvers is that the estimate of impact contains more errors that if the debris was analyzed once closer to the missile.

12.6. Technical Design Sensitivity Analysis

As the trade-off occurred between already characterized COTs propulsion systems, extensive calculations were not involved on which sensitivity analysis could be performed on. However, in order to proceed to a more detailed design of the propulsion subsystem, it is important to consider the opportunity to optimize the propulsion. Within the trade-off criteria assessed, it is clear that mass and operating power were heavily weighted in the trade-off. This is because of the constraints that arise from nanosatellite dimensional constraints and the on-board power system. The payload demands the majority of available power and thus the power available to the propulsion system to perform maneuvers is limited.

In order to assess the possibility and implications of exploring higher performance thrusters, two different design points for each maneuver considered were evaluated. This was possible because, as elaborated on in the previous section, the IFM Nano Thruster has the capability of allowing for variable specific impulse settings during a mission. This means that a tailored design point was chosen for each maneuver. In this sensitivity analysis 2 alternate design points are explored for each maneuver, evaluating the implications of a higher and lower specific impulse setting.

For each design point, the impact of its characteristics on maneuver burn time, the total impulse required and thus propellant mass required are evaluated. The burn time for each maneuver is cal-

[6] https://satsearch.co/products/enpulsion-ifm-nano-thruster

culated using Equation (12.1). The required total impulse for each maneuver is given by the following formula:

$$I_{tot_r} = \Delta V \cdot m_{sc} \tag{12.2}$$

where I_{tot_r} represents the total impulse required to perform the maneuver during the mission lifetime. Based on this value, Equation (12.3) calculates the total mass of propellant the maneuver in consideration demands. This is represented by m_{prop_r}. I_{tot} refers to the total impulse capability for a given design point. Considering the ratio $\frac{I_{tot_r}}{I_{tot}}$ determines the fraction of the total propellant required by the maneuver.

$$m_{prop_r} = m_{prop} \cdot \frac{I_{tot_r}}{I_{tot}} \tag{12.3}$$

Table 12.10 does the explained evaluation for the orbit maintenance maneuver. As mentioned in the previous section, at any possible power setting, the payload must be inactive in order for this maneuver to take place. From the it is clear that when considering design points with higher and lower specific impulses, it conversely increases the burn duration although a higher specific impulse does save propellant mass. However the longer burn time jeopardizes the mission reliability. Thus the original design point remains the most suited for the given system requirements.

Table 12.10: Sensitivity analysis for design points for orbit maintenance maneuvers.

Orbit Maintenance: Total Delta V Required = 19.52 m/s			
	Original Design Point	**Design Point 1**	**Design Point 2**
Specific Impulse (s)	3200	4000	2400
Thrust (mN)	0.42	0.38	0.29
System Power (W)	40	40	25
Total Impulse (Ns)	7840	9800	5880
Single Execution Burn Time (hours)	3.04	3.41	4.41
Total Impulse Required (Ns)	390.4		
Required Propellant Mass (g)	11.45	9.16	15.27

Table 12.11 shows the results when the same analysis was performed for the collision avoidance maneuver. The design points considered for this maneuver were the same as those considered when conducting a sensitivity analysis for the orbit maintenance maneuver. The burn time is even more critical for collision avoidance. A higher specific impulse decreases the propellant required by 20 % but also increases the burn time by the same amount. This increases the risk and puts the system reliability in jeopardy. Thus the net gain from the alternate design point are not sufficient to outweigh the advantages of the current design point.

Table 12.11: Sensitivity analysis for design points for collision avoidance maneuvers.

Collision Avoidance: Total Delta V Required = 7.31 m/s			
	Original Design Point	**Design Point 1**	**Design Point 2**
Specific Impulse (s)	3200	4000	2400
Thrust (mN)	0.42	0.38	0.29
System Power (W)	40	40	25
Total Impulse (Ns)	7840	9800	5880
Single Execution Burn Time (hours)	10.74	12.03	15.56
Total Impulse Required (Ns)	146.2		
Required Propellant Mass (g)	4.29	3.43	5.72

The chosen design point for the EOL deorbitting maneuver was at the IFM Nano Thruster highest specific impulse setting, and the highest power setting. Table 12.12 evaluates two alternate design points: Design Point 1 has a marginally lower thrust setting allowing for a reduced operating power but required the same amount of propellant mass as the original design and an even longer burntime. Although the operating power is lower for this design point, as it is an EOL maneuver there is no specific gain in having more systems functioning at this point. Design Point 2, is inherently worse that the original design point; even though it has a reduced burntime for execution, it needs almost twice the amount of propellant due to the lower specific impulse setting which would increase the total propellant budget, or jeopardize other maneuvers if they are required to be executed more frequently than anticipated. Therefore the original design point remains the best option for the deorbitting maneuver.

Table 12.12: Sensitivity analysis for design points for de-orbitting maneuver.

De-orbitting: Total Delta V Required = 150 m/s			
	Original Design Point	**Design Point 1**	**Design Point 2**
Specific Impulse (s)	6000	6000	2400
Thrust (mN)	0.29	0.25	0.42
System Power (W)	40	33	40
Total Impulse (Ns)	147000	147000	7840
Single Execution Burn Time (days)	125.05	145.06	86.34
Total Impulse Required (Ns)	3133.2		
Required Propellant Mass (g)	49.02	49.02	91.92

12.7. Verification & Validation

Proceeding with the original design points, table 12.13 makes evident that this propulsion system design complies with all subsystem requirements.

Table 12.13: Sensitivity analysis for design points for orbit maintenance maneuvers.

REQ	Compliance	Section
REQ-SYS-PROP-01		12.3.4
REQ-SYS-PROP-01-01		12.3.4
REQ-SYS-PROP-01-02		12.3.4
REQ-SYS-PROP-01-03		12.3.4
REQ-SYS-PROP-02		12.5
REQ-SYS-PROP-02-01		12.5
REQ-SYS-PROP-03		12.3
REQ-SYS-PROP-03-01		12.4.1
REQ-SYS-PROP-04		12.3.3
REQ-SYS-PROP-04-01		12.4.1
REQ-SYS-PROP-04-02		12.4.1
REQ-SYS-PROP-05		12.4.1
REQ-SYS-PROP-05-01		12.4.3

12.7.1. On-Ground Testing

The IFM Nano Thruster is a certified ion thruster that has gone through extensive on-ground testing as well as IODs in 2017 [72]. This significantly depletes the additional research and development as well as subsystem testing that the propulsion systems needs to go through before it is ready for flight.

The afore mentioned extensive on ground verification testing includes specialized evaluation of the thrusters' propellant liquefaction, neutralizer operation and most importantly the thrusting operation. The thrusting operation was tested by simulating firing periods for 15 and 30 minute periods, allowing for the thruster capability to handle burns for this duration. As is evident from Section Section 12.6 the burntimes required for the maneuvers in this mission are orders of magnitude larger than this. Therefore additional thruster firing testing will be required to be performed during the on-ground verification to assess the capability of the IFM Nano Thrusters burning for extended period of time, 4 hours for orbit maintenance and 10 hours for collision avoidance maneuvers. This would require thermal testing in vacuum chambers.

12.8. Recommendations

Propellant efficient de-orbitting maneuvers can be explored that take advantage of atmospheric drag and reduce the ΔV required up to 50 % [73]. This maneuver has typically been designed for much larger spacecraft and thus would require a significant amount of addition research in order to be applicable to this mission. Its implications for spacecraft mass and efficiency make it worth pursuing.

Furthermore, at the current stage, design points chosen have been done so assuming each spacecraft will carry one thruster. However, if not placed aligned with the center of gravity of the spacecraft this will introduce additional torque loads. Thus moving forward, the implication on the design point for having two thrusters instead of one need to be considered. An option is to proceed to have two thrusters of the same design that was elaborated on in this chapter, at the same maneuver design points, which would by extension increases the net thrust provided on one spacecraft and reduce the burntime for maneuvers which would be a large advantage in terms of reliability especially for collision avoidance maneuvers. However this would also require the addition of a second battery in the EPS system so required further study.

Last but not least, the ΔV budget used needs some in-depth research on the number of avoidance maneuvers. This is because a unusually and straightforward preliminary estimation was used to determine the number of avoidance. The analysis was based on the avoidance manoeuvres performed by the ISS from 1999 to 2018. This is not a realistic approach as the debris in LEO depends on the altitude and in the last five years there is much more debris than twenty years ago.

13
Attitude Determination and Control System

In this chapter, the attitude determination and control system (ADCS) will be looked into. A functional analysis is carried out, followed by a requirement analysis. Then, there will be an explanation of the ADCS design, accompanied by a description of the sensitivity analysis and verification & validation procedures used. Lastly, the RAMS characteristics and future recommendations are given.

13.1. Functional Analysis

The ADCS plays a significant role in the accomplishment of the mission objectives. The spacecraft needs to make sure to move rapidly towards the object detected to center the Focus payload and then precisely track it, as well as to determining its orbit position and performing all movements correctly autonomously. All these factors need to be taken into account for the functional analysis. The ADCS functions are the following:

- **FUNC-ADCS-01** Provide pointing capabilities in all directions. *Flowdown Section 7.6.2.*
  - **FUNC-ADCS-01-01** Provide accuracy such that payload can perform tracking successfully. *Flowdown from 4.3.2.10.*
  - **FUNC-ADCS-01-02** Provide swift manoeuvre in order to point the bright pixel with the Focus payload. *Flowdown from 4.3.2.3.*
- **FUNC-ADCS-02** Provide the current attitude. *Flowdown from 4.2.5.*
  - **FUNC-ADCS-02-01** Provide orbit determination. *Flowdown from 4.5.4.*
- **FUNC-ADCS-03** Provide commands realized to the main OBC.
- **FUNC-ADCS-04** Autonomously execute commands.
- **FUNC-ADCS-05** Manoeuvres being tested before the ADCS system is being integrated into the satellite.
- **FUNC-ADCS-06** Perform operations and calculations locally on the CubeSat.

13.2. Requirement Analysis

From the functional analysis performed in Section 13.1, a requirement analysis is accomplished. The requirements are the following:

- **REQ-SYS-ADCS-01** The ADCS shall be able to determine its own attitude.
  - **REQ-SYS-ADCS-01-01** The ADCS shall handle pointing knowledge to an accuracy of at least 10″ within 1-sigma to capture the object data. *Flowdown from FUNC-ADCS-01.*
- **REQ-SYS-ADCS-02** The ADCS shall perform orbit determination and pointing calculations. *Flowdown from FUNC-ADCS-06.*
- **REQ-SYS-ADCS-03** The ADCS shall be capable of manual control if an anomaly is detected. *Flowdown from FUNC-ADCS-04.*
- **REQ-SYS-ADCS-04** The ADCS and satellite properties shall be characterized before launch. *Flowdown from FUNC-ADCS-05.*
- **REQ-SYS-ADCS-05**The ADCS shall accommodate functioning of all modes and necessary orientations. *Flowdown from FUNC-ADCS-06.*
- **REQ-SYS-ADCS-06** The ADCS shall be connected to the main OBC to receive the commands. *Flowdown from FUNC-ADCS-03.*
- **REQ-SYS-ADCS-07** The ADCS shall be capable to slew until an angular velocity of $16.53\,^{\circ}\,s^{-1}$ per each axis. *Flowdown from FUNC-ADCS-01-02.*
- **REQ-SYS-ADCS-08** The ADCS shall be able to determine its own orbit.
  - **REQ-SYS-ADCS-08-01** The ADCS shall be able determine its position with an accuracy

of 5 m in radial and normal directions and 50 m in along-track direction. *Flowdown from FUNC-ADCS-02-01.*

13.3. ADCS Design

The following section is concerned with the ADCS design. Firstly, a research is performed into the sensors and actuators needed for the system to fulfill the requirements. After this, the investigation of an integrated ADCS unit on the market is performed. Once the most suitable integrated ADCS unit with certain external components is found, a tool to determine the time to move the spacecraft for each axis and the maximum angular velocity is made to understand if the image is blurry.

13.3.1. Architecture

In Figure 13.1, the ADCS architecture needed for each 12U CubeSat is shown in detail. After some research, the most suitable integrated unit is the iADCS400 from Hyperion Technologies[1]. This product contains most of the sensors and actuators that the system needs to perform all the operations correctly and safely. Most of the components used are COTS and from the same company in order to integrate them in a sustainable approach.

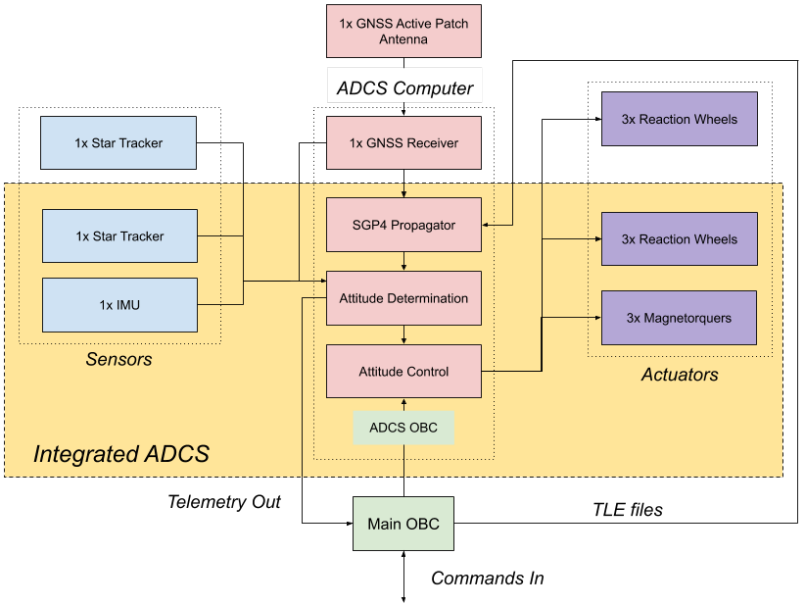

Figure 13.1: ADCS Block Diagram.

Attitude Control Six reaction wheels and three magnetorquers are required to have full-three axis control with the required torque level and momentum storage capabilities in the spacecraft. The reaction wheels are the main components for attitude control as they should provide an accurate pointing capability [74]. In order to accelerate and slew rapidly, the reaction wheels should supply high momentum storage and maximum torque. Then, magnetorquers are used when the reaction wheels are saturated and utilised to remove excess momentum [75]. Inside the integrated ADCS, there are three reaction wheels and three magnetorquers. In order to be able to move rapidly to point the bright pixel with the FOCUS payload, the ADCS needs to increase its performance. Each reaction wheel provide a maximum torque of 12 mN s and a momentum storage of 50 mN m s and its performance is not good enough for the M-STAR mission. As the mission needed more torque and momentum storage, the number of reaction wheels has been doubled for each axis by using the same type of reaction wheels. The Hyperion's RW400-series of reaction wheels provide for each axis a maximum torque of 24 mN m and a momentum storage of 100 mN m s. [2]

Attitude Determination A number of ADCS sensors are needed to have enough precision to determine the spacecraft's attitude [74]. In this case, the ADCS component that has improved a lot in

[1]Retrieved from `https://hyperiontechnologies.nl/wp-content/uploads/2015/07/HT_iADCS400_v2.1-flyer.pdf`

[2]Retrieved from `https://hyperiontechnologies.nl/wp-content/uploads/2015/07/HT_RW400_v2.1-flyer.pdf`

the last years is the star tracker. Nowadays, the start tracker is the most common sensor for high-accuracy missions only at low spacecraft rotation rates. The Hyperion's ST200 star tracker is included in the integrated ADCS unit and it offers an attitude determination accuracy of 30″ within 3-sigma[3]. However, when the spacecraft is rotating extremely quick ($12.95\,^{\circ}\,s^{-1}$), the ST200 does not work effectively due to its reduced lens size and the only way to still achieve promising accuracy is to use a combination of gyros (measuring inertial or relative attitude) and a larger star tracker (measuring absolute attitude) [75]. Therefore, an additional star tracker will be needed to still have accurate determination while slewing. The supplementary star tracker, positioned at the top of the spacecraft, will be the Hyperion's ST400 star tracker with determination accuracy of 10″ within 3-sigma[4]. For the gyros, the integrated ADCS has the possibility to include an IMU which is a combination of accelerometers, gyroscopes and magnetometer sensors.

Orbit Determination The CubeSat needs to embark a GNSS receiver and SGP4 Propagator. The GNSS receiver is a component used to accurately determine position and velocity. Hyperion Technologies provides a GNSS receiver for CubeSat which can be connected externally using the TLL UART interface. The Hyperion's GNSS200 series receiver[5] offers multi-constellation outputs and it will be connected with a GNSS active patch antenna from ISIS[6]. This GNSS receiver is suitable for the M-STAR-mission as it is a low mass and power receiver for small satellites and its position accuracy is about 8 m. Considering that Hyperion's receiver offers multi-constellation and the antenna works for the GPS-L1 and GALILEO-E1 band frequencies, the spacecraft could get its position from two different navigation constellations. However, the STAR-mission should rely as little as possible on external systems, therefore the M-STAR-mission is designed to be able to determine the spacecraft's position from the European constellation Galileo. If by any chance, the GNSS receiver or the navigation constellation stops working, the iADCS 400 has the option to have an internal computer used for Attitude Determination and Control as well as for the Simplified General Perturbations (SGP4) propagator. The SGP4 propagator utilizes the Two-Line Element (TLE) files which specify all the orbital parameters of the spacecraft and should be given from ground stations. In order to achieve accurate position with just the propagator, the TLE files have to be updated every couple of hours by ground station as the data changes with time. For this reason, the SGP4 propagator gives precise position for a maximum of 5 days and its orbit uncertainty is better than 5 m in radial and out-of-plane directions and 50 m in along-track direction [38]. The SGP4 propagator is convenient when the GNSS receiver does not receive any signal due to a damage in the navigation constellation. For instance, in 2019 the GALILEO constellation stopped working for seven days from 11 July till 18 July.

13.3.2. Attitude Calculations

In order to determine some valuables results for attitude, the moments of inertia of the CubeSat shall be computed beforehand. Giving the mass and the dimensions of the spacecraft and solar arrays, the moments of inertia can be estimated by assuming that the mass is uniformly distributed along the spacecraft. The tool determines how much time the spacecraft takes to center the FOCUS payload into the bright pixel for each axis. In addition, the program calculates the maximum angular velocity between the three axis to understand if when the spacecraft rotates the image becomes blurry. To do so, the inputs needed are the moments of inertia of the spacecraft, the rotation angle for each axis, the maximum torque that the reaction wheels provide and the momentum storage. With all these parameters, the total time and maximum angular velocity can be estimated. Before for each axis, the software has to understand if the the spacecraft reaches the maximum velocity of the reaction wheels be computing Equation (13.1) and Equation (13.3). Therefore, there are two possible cases in which

[3]Retrieved from https://hyperiontechnologies.nl/wp-content/uploads/2015/07/HT_ST200_v2.1-flyer.pdf

[4]Retrieved from https://hyperiontechnologies.nl/wp-content/uploads/2019/11/HT_ST400.pdf

[5]Retrieved from https://hyperiontechnologies.nl/wp-content/uploads/2015/07/HT_GNSS200_v2.1-flyer.pdf

[6]Retrieved from https://www.isispace.nl/wp-content/uploads/2020/04/ISIS.GAPA_.DS_.00001_v1.4-Datasheet.pdf

the reactions wheels will work:

- **Case A, Reactions wheels accelerate and slew without reaching the maximum angular velocity:** If the angular velocity determined with Equation (13.1) is lower than the Equation (13.3) means that the time can be calculated by using the Equation (13.2).
- **Case B, Reactions wheels accelerate and slew with reaching the maximum angular velocity:** If the angular velocity determined with Equation (13.1) is larger, means that the spacecraft accelerates, it rotates with constant velocity and then it slews down. In this case, the time shall be calculated by using the Equation (13.4).

$$\dot{\theta} = \frac{d\theta}{dt} = \frac{T}{2I}t = \frac{T}{2I}\sqrt{\frac{4I\theta}{T}} \tag{13.1}$$

$$t = \sqrt{\frac{4I \cdot \theta}{T}} \tag{13.2}$$

$$\dot{\theta} = \frac{d\theta}{dt} = \frac{I}{p} \tag{13.3}$$

$$t = \frac{p}{T} + \frac{I\theta}{p} \tag{13.4}$$

Where $\dot{\theta}$ is the angular velocity for one axis, T is the maximum torque of the reaction wheels for one axis, I is the moments of inertia for one axis, t is the time it takes to rotate in one direction, θ is the rotation angle for one axis, and p is the momentum storage of the reaction wheels.

An example of the program would be the following. The worst case scenario for the circular imaging technique would be rotating 180° in yaw direction and 23° in roll direction. Assuming that the spacecraft weight is about 20.5 kg and the spacecraft size is 12U, the moments of inertia of the spacecraft without the contribution of the solar arrays can be calculated. Then, the moment of inertia of the spacecraft needs to include the solar array contribution, so the solar array weight (1.077 kg) and solar array area (0.322 m^2) are required. Having the moments of inertia, the angles of rotation, the maximum torque and the momentum capacity given from the ADCS characteristics, the time and maximum angular velocity can be computed. The time it takes to rotate 23° in one axis and 180° in another axis is about 24.36 s and the maximum angular velocity is 12.95 $^\circ s^{-1}$. This velocity is considerably higher than the maximum velocity the spacecraft could need to slew at when tracking a missile at burnout height and velocity [12] (4.17 $^\circ s^{-1}$) in the worst-case scenario.

13.4. Sensitivity Analysis

A sensitivity analysis for the ADCS is desired, as there can be some uncertainties in the assumptions made. This is done in order to understand if the outputs from the ADCS program are valuable results and to check if the requirements is still met. The major assumption made is that the mass of the spacecraft is uniformly. In this way, the moments of inertia are symmetric, therefore the product moments of inertia are equal to zero. Therefore, the mass of the spacecraft without solar arrays has been taken from the Section 16.2.1 and is 19.423 kg with a contingency for each component. If the contingency of each component is zero, the mass for the spacecraft without the two arrays contribution will be 16.973 kg.

In addition to the uniform mass, the solar array mass and area are also inputs applied, which are respectively 1.077 kg and 0.322 m^2. The last two values depend on the power generated and used for all the subsystems and the contingency is 20%. Thus, the maximum deviation is when there is no contingency, so the solar array mass and area become respectively 0.847 kg and 0.251 m^2. The other possibility of maximum deviation is when the contingency is doubled, so the solar array mass and area are specifically 1.371 kg and 0.406 m^2. The results of the sensitivity analysis can be seen in Table 13.1.

Table 13.1: ADCS Sensitivity Analysis.

Input	Output	Change	Conclusion
S/C mass w/o SA = 16.973 kg	Time = 23.44 s & max($\dot{\theta}$)=13.64 rad s^{-1}	-3.77% & 5.32%	An investigation is not needed as the maximum angular velocity is larger and the **REQ-SYS-ADCS-07** still satisfied.
SA mass = 0.847 kg & SA area = 0.251 m^2	Time = 19.84 s & max($\dot{\theta}$)=17.83 ° s^{-1}	-18.55% & 37.68%	An investigation must be taken as the **REQ-SYS-ADCS-07** is not satisfied due to a larger maximum angular velocity. This can be done by taking a more look into the components for attitude control and in the design of the solar panels.
SA mass = 1.371 kg & SA area = 0.406 m^2	Time = 32.44 s & max($\dot{\theta}$)=8.63 ° s^{-1}	33.17% & -33.35%	An investigation must be taken to reduce the time it takes to rotate. This is because the requirement off the 90 s latency might not be satisfied. More research in the design of solar panels is needed.

13.5. Verification & Validation

In this section, the verification & validation procedures of the ADCS will be carried out. Firstly, the calculations are verified, and then the subsystem verification and the compliance matrix are presented.

13.5.1. Attitude Calculation

In order to verify the tool introduced in Section 13.3.2, a number of tests have been performed. Firstly, the script of determining the moments of inertia should be checked. With the help of CATIA, the moments of inertia around the centroid can be computed. If the result between them is similar the tool is verified. Secondly, the time and the maximum angular velocity are checked by plotting the velocity against time. By using the plots, the behaviour of the graphs determine whether is Case A or B. Case A is when the plot's behaviour is a triangle, instead for Case B is when the plot's behaviour is a rectangular trapezoid. Case B has a plateau because the reaction wheel reached the top speed. Last but not least, the last check will be doubling the thickness of the solar array. Varying the thickness of the solar array while keeping mass constant should not bring any difference as the moments of inertia will scarcely change.

13.5.2. Subsystem Verification

The iADCS 400 and the reaction wheels are the only two products that have never flown before. Inside the integrated iADCS 400, all the components have flown before separately except for the reaction wheels. Even though the Hyperion's reaction wheels do not have a flight heritage their TRL is of 7. Thus, the only test that need to be performed would be integration test between the components of the subsystem. For more information on integration test, see Table 17.3.

13.5.3. Compliance Matrix

For the ADCS compliance matrix, each requirement is met. Below, the Table 13.2 shows the compliance matrix for the ADCS sub-system requirements with the reference to the distinct sections.

Table 13.2: ADCS Requirement Compliance Matrix.

REQ	Compliance	(Sub)-Section
REQ-SYS-ADCS-01		Section 13.3.1
REQ-SYS-ADCS-02		Section 13.3.1
REQ-SYS-ADCS-03		Section 13.6
REQ-SYS-ADCS-04		Section 13.6
REQ-SYS-ADCS-05		Section 13.3.2
REQ-SYS-ADCS-06		Section 13.3.1
REQ-SYS-ADCS-07		Section 13.3.2
REQ-SYS-ADCS-08		Section 13.3.1

13.6. RAMS Characteristics

Reliability Most of the components of the ADCS sub-system have gone through ground testing and have flown since 2017. The star tracker, the GNSS antenna and receiver already have flight heritage and their TRL is 9. However, the reaction wheels and the integrated ADCS have not flown yet and their TRL is 7. In order to mitigate this risk, an approach is to take all the ADCS components with flight heritage or to have just an integrated ADCS with all the components needed.

Availability The ADCS subsystem is connected to the main On-Board Computer in which its connected to the other subsystems. Therefore, the ADCS subsystem can receive commands from all subsystem and in particular payload commands need to be executed quickly since it is possible that commands are that the spacecraft needs to change its attitude swiftly in order to center and track the Focus payload towards the bright pixel.

Maintainability The ADCS sub-system can be maintained after launch, if a software anomaly is detected. The system can go into manual control from the ground station whenever a software bug is found. The health of the system is monitored in the ADCS On-Board Computer and anomalies detected are sent to ground stations immediately. However, if the problem is mechanical, then the maintenance can not be performed and leads to failure in the spacecraft. To mitigate a possible mechanical anomaly, the ADCS should be more reliable by using just an integrated ADCS without external additional components, by performing more testing or by adding redundant components.

Safety For space missions, safety is one of the most important measures. In this case, in order to not have collisions, the attitude determination and control needs to work correctly. A failure in the reaction wheels or in the star tracker leads to vehicle loss, as no type of manoeuvre cannot be performed. As well, the components related to orbit determination should be operate correctly to not loose the spacecraft positioning.

13.7. Recommendations

Deeper research into quantifying the maximum time needed to slew the spacecraft is suggested. In order to have a better time budget and understand if the **REQ-SYS-COM-04-01** is still satisfied, the maximum time needed to slew shall be a requirement. It is also recommended to estimate the saturation of reaction wheels at the start of the maneuvers to provide a more accurate slew time and further adjust the reaction wheel and magnetorquers sizing and count.

In addition, a more in-depth research will be needed on the position of the star tracker ST400. The most suitable position was found to be the rear of the spacecraft, but the propulsion units are as well located at the rear of the spacecraft. This means that there is a risk whenever the propulsion system is used because the accuracy of the star tracker will be lowered and the star tracker might encounter a brighter light. The **REQ-SYS-ADCS-01-01** can be satisfied with the star tracker ST400 and not with the star tracker ST200, therefore the position of the ST400 is fundamental to fulfill the requirement.

Moreover, two star trackers were taken for redundancy. This is because a more detailed investigation is needed to understand if having one star tracker and an IMU provides accurate enough pointing while slewing. For this purpose, it is important to know more specifications from the star tracker by further contacting the manufacturer.

Last but not least, the ADCS subsystem contains six identical reaction wheels. A more comprehensive investigation in ADCS reliability and in reaction wheels positioning is recommended. Increasing number of reaction wheels can increase redundancy but also failure rate of components and interference within the reaction wheels. Mission failure has to be determined properly in terms of ADCS performance to determine whether a smaller number of larger reaction wheels is desirable against a larger number of smaller wheels. Commonly, the reaction wheels have a tetrahedron composition for redundancy, therefore a research on positioning needs to be done.

14
Structure

In this chapter the structure subsystem is further analysed. Firstly the functional analysis is presented, followed by a a requirement analysis. Then, the design is looked into, and lastly, the RAMS characteristics and future recommendations are presented.

14.1. Functional Analysis

- **FUNC-STR-01** Carry all static and dynamic loading. *To prevent failure, loading on all spacecraft subsystems should not exceed their operational loading.*
- **FUNC-STR-02** Keep all components within their operational vibration load. *During the complete mission all subsystems should be operated within the operational vibration load in order to prevent failure of the system.*
- **FUNC-STR-03** Allow for the installation of all components with their required openings or cutouts in the structure. *This function includes the openings for those components requiring interfaces with the space environment.*

14.2. Requirement Analysis

- **REQ-SYS-STR-01** The spacecraft structure shall withstand all mechanical static and dynamic loads experienced during the spacecraft's lifetime. *Flown down from FUNC-STR-01.*
  - **REQ-SYS-STR-01-01**The structural system shall withstand all mechanical static and dynamic lunch loads.
- **REQ-SYS-STR-02** The structural system shall keep all components within the operational vibration load. *Flown down from FUNC-STR-02.*
- **REQ-SYS-STR-03** The structural system shall allow for the required openings or cutouts. *Flown down from FUNC-STR-03.*
  - **REQ-SYS-STR-03-01** The structural system shall have an opening of at least 100x100mm in the nadir face to allow for functioning of the Focus payload optic system.
  - **REQ-SYS-STR-03-02** The structural system shall have an opening of at least 65mm diameter in the nadir face to allow for functioning of the Coverage payload optic system.
  - **REQ-SYS-STR-03-03**The structural system have an opening of at least 35mm diameter in the side face to allow functioning of the iADCS410 unit.
  - **REQ-SYS-STR-03-04** The structural system have an opening of at least 70mm diameter in the zenith face to allow functioning of the HTBST-ST400 star-tracker.
  - **REQ-SYS-STR-03-05** The structural system have two openings of at least 100mmx100mm in the zenith face to allow functioning of the IMF Nano Thrusters.

14.3. Structure Design

In this section a discussion on the use of COTS and custom structures will be presented in order to come up with the design of the structure.

Spacecraft structures must be validated through vacuum thermal tests, acoustic tests, static and dynamic load scenarios, radiation tests (depending on the materials used) and, in some cases, by means of in-orbit demonstrations. The time and cost associated with performing these procedures and structure design in house is too large for an IOD mission of a missile detection constellation. Thus, for this IOD it is preferred to employ a COTS structure. When deploying a constellation made of roughly 300 spacecraft, however, the development and testing costs become a smaller fraction of the total mission costs, so a custom platform could be developed. This could allow the spacecraft to

drift away from its 12U structure, and optimize its packaging factor. Nevertheless, due to the relatively low cost of the structure with respect to the rest of the spacecraft components and its mass fraction, the benefits for a custom structure can not outweigh the time delay caused for an IODs.

Before determining the 12U COTS structure, the various options were analysed to ensured the structure meets the requirements. COTS from ISIS, AAC clyde space, NPC Space Mind and Nano avionics were considered. Out of these, only Nano avionics and NPC Space Mind satisfy all requirements. Other structures fail to provide adequate cutouts on the nadir side. NPC Space Mind structure[1] was chosen over Nano avionics due to its modular frame, end frame options and transparent pricing.

14.4. Subsystem Verification

Despite the lack of flight heritage, all testing described in Section 14.3 is performed by the manufacturer. In the case of npc space mind, Tests are performed according to ECSS-E-ST-10-03 and JX-ESPC-101133-B standards. It can not be proven whether **REQ-SYS-STR-01** and **REQ-SYS-STR-02** are satisfied despite the mass of the system being smaller than other common 12U architectures

14.4.1. Compliance Matrix

Table 14.1 shows the compliance matrix for the Structures sub-system primary requirements with the reference to the distinct sections.

Table 14.1: Structures Requirement Compliance Matrix.

REQ	Compliance	(Sub)-Section
REQ-SYS-STR-01		Section 14.4
REQ-SYS-STR-02		Section 14.4
REQ-SYS-STR-03		Section 14.3

14.5. RAMS Characteristics

In this section, a RAMS analysis is performed for the COTS 12U structure from NPC Space Mind.

Reliability COTS structures have no moving parts and are sized for launch loads thus, once in space, contribute to the failure rate in a negligible manner.

Availability The structure effect on the availability of the constellation is negligible as they do not require any turned-off time. As for their availability from a manufacturer, the use of aluminium makes these COTS structures easily procurable.

Maintainability The structure subsystem does not generate housekeeping data in CubeSats. The sensors included in other components, such as temperature sensors, could potentially be used to analyse whether the structure is maintained in its operational range.

Safety Structural failure during launch can lead to spacecraft loss and potential launch vehicle loss. This is mitigated due to the fact that COTS structures are mechanically tested on the ground.

14.6. Recommendations

As mentioned in Section 14.3, a custom structure may not modify the cost by a large amount on a full constellation roll-out with respect to a COTS structure. A CubeSat structure in which the secondary structure acts as primary structure at the same time could provide significant weight and volume saving. In a similar manner, a CubeSat structure optimized for large scale manufacturing could provide significant cost savings. It is thus a recommendation to quantify the impact of a custom structure on cost, mass and volume if enough resources are allocated to its design.

[1]Retrieved from `https://www.npcspacemind.com/solutions/nanosatellite-hardware/cubesat-structure/sm12-12u/`

15
Constellation

In this chapter, the constellation will be looked into more in-depth. As previous chapters, a functional analysis is implemented, followed by its requirement analysis. Then, the design of the constellation is carried out, and the sensitivity analysis and the verification procedures are being described. Similarly, the RAMS characteristics are introduced and finally recommendations for future work are presented.

15.1. Functional Analysis

The constellation subsystems plays a prominent role in the accomplishment of the M-STAR-mission. The main task of the satellite constellation is to make sure that the M-STAR satellites are covering all of the Earth surface. However, there are several other functions that the constellation needs to take care and accomplish to succeed the M-STAR mission. The following list arises from such functional analysis.

- **FUNC-ORB-01** *Provide global coverage.*
  - **FUNC-ORB-01-01** Provide efficient orbit inclination.
    - ◊ **FUNC-ORB-01-01-01**Provide an orbit inclination suitable for launch provider.
- **FUNC-ORB-02** Provide revisit time for scanning. *In order to fulfill the **REQ-SYS-COM-04-01** and to be able to send the detection signal to ground, the M-STAR constellation should revisit less than* 90 s.
- **FUNC-ORB-03** Provide scalability capabilities.
- **FUNC-ORB-04** Provide efficient orbit altitude.
- **FUNC-ORB-07** Provide optimised collision probability of CubeSats.
- **FUNC-ORB-08** Provide a feasible inter-satellite communication architecture. *In order to meet the **REQ-SYS-COM-04-01** about the* 90 s*, the M-STAR constellation should be able to have an inter-satellite communication architecture to be able to communicate within in-plane satellites.*

15.2. Requirement Analysis

From the functional analysis presented in the Section 15.1, the requirements shown below follow.

- **REQ-ORB-01** The orbit shall be LEO (400 −2000 km). *Flow down from FUNC-ORB-04.*
  - **REQ-ORB-01-01** The constellation have an orbital altitude less than 600 km. *Flow down from FUNC-ORB-04.*
- **REQ-ORB-02** The CubeSat shall deorbit accordingly to the Debris Mitigation Act. *Flow down from FUNC-ORB-07.*
- **REQ-ORB-03** The constellation shall use polar orbits. *Flow down from FUNC-ORB-01-01.*
- **REQ-ORB-04** The constellation shall be able to provide global coverage. *Flow down from FUNC-ORB-01.*
  - **REQ-ORB-04-01** The constellation shall be able to contain at least double coverage. *Flow down from FUNC-ORB-01.*
- **REQ-ORB-05** The constellation shall be able to support alerting the ground station within 90 s of a ICBM launch. *Flow down from FUNC-ORB-08.*
- **REQ-ORB-06** The distance between satellites in the same orbital plane should be a maximum of 1300 km. *Flow down from FUNC-ORB-10.*
- **REQ-ORB-07** The constellation shall be able to provide a scanning revisit time of 1 s. *Flow down from FUNC-ORB-02.*

15.3. Constellation Design

As explained in the Midterm Report the method of streets of coverage is being used [5]. After detailed evaluation of the possible methods to optimise the constellation it was determined that the best one was by increasing the covered area by the satellite. This decision lead to the creation of Section 7.4.1 and the subsequent sections which analysed different possible imaging techniques and their applications in the project. It was decided that the circular imaging method will be used, according to the results from trade-off in Section 7.4. For more references into what are the properties of the circular imaging please refer to Section 7.5.3. With this imaging method there is an increase in the area covered by the satellites.

Once the imaging method was decided the constellation could be created. The method to calculate the constellation will essentially be the same as that explained in the Midterm Report [5]. There will be some changes in terms of how to place the satellites in order to get double continuous coverage. The process was the following:

- For the number of satellites per orbital plane one divides the circumference of the Earth by the ”thickness” of the doughnut, see Figure 7.5, which is 1187 km.
- For the number of orbital planes one divides half of the circumference of the Earth by two times 1284 km.

The value of 1284 km comes form the fact that the satellites are not placed at exactly the end of the radius of the covered area on Earth, see Figure 15.2. Thus the value used is not the radius of coverage on Earth, which is 1348 km, but 1284 km. This is due to the fact that if such placement is implemented there would be no complete constant Earth coverage. It is also important to note that this configuration also fits with the requirements from communications as the distance between satellites in the same orbital plane is less than 1300 km, as it is 1284 km.

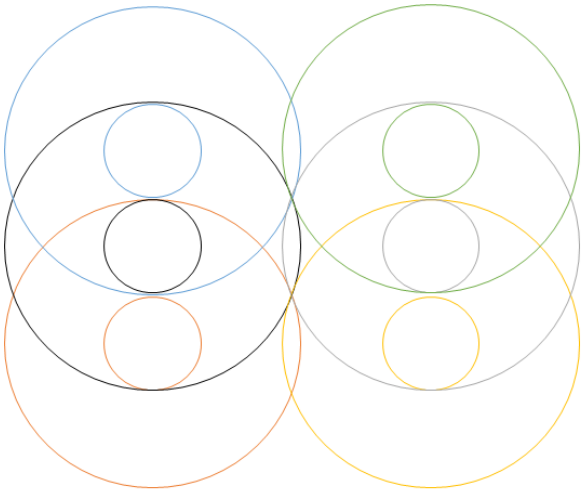

Figure 15.1: Placement of satellites.

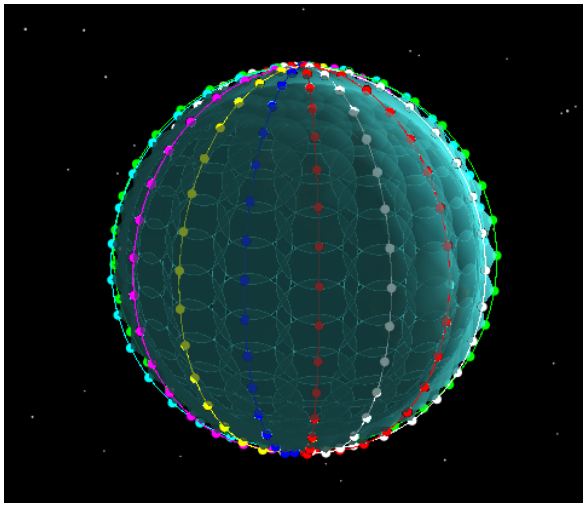

Figure 15.2: Constellation design.

As it can be seen in Figure 15.1 there is overlapping both in plane and between planes. In the figure the small circles represent the center of the imaging technique that is not covered. In order to reduce the revisit time and have double coverage the next satellite in the same plane is placed such that the outer diameter of the second satellite matches the inner diameter of the first satellite. With this method there is no revisit time apart from the time taken for the imaging method to do one full revolution, 1 second. For the inter plane overlapping this is such that all places are covered. If one was to place the orbital planes at the end of radius then some areas would not be covered due to the geometry of circles.

Overall, the constellation would consist of 9 orbital planes at an altitude of 600 km with an inclina-

tion of 90°, evenly spaced in half of the equator, and with 34 satellites per orbital plane. A visual representation on how the constellation would look can be seen in Figure 15.2.

15.4. Compliance Matrix

In this subsection the compliance matrix is shown. The green colour means that the requirement is fulfilled.

Table 15.1: Constellation Requirement Compliance Matrix.

REQ	Compliance	(Sub)Section
REQ-SYS-ORB-01		Section 15.3
REQ-SYS-ORB-02		Section 16.6
REQ-SYS-ORB-03		Section 15.3
REQ-SYS-ORB-04		Section 15.3
REQ-SYS-ORB-05		Section 16.2.3
REQ-SYS-ORB-06		Section 15.3
REQ-SYS-ORB-07		Section 15.3

15.5. RAMS Characteristics

A RAMS analysis will now be done for the constellation chapter.

Reliability Reliability is not an applicable characteristic of a constellation, thus it is not considered.

Availability The constellation design is key in the availability requirement. This is due to the fact that the position of orbits and orbital planes define if the availability requirement will be fulfilled. To this end the constellation was designed for double coverage in case one satellite fails there will still be coverage of that part of Earth but with a small revisit time.

Maintainability In order to maintain the desired orbit, satellites will need to correct the orbit every once in a while. This is due to the fact that there are disturbances which modify the orbits over time. Therefore, the altitude and position of satellites will be needed in order to make sure they are still in the correct orbit. This will be done together with the propulsion subsystem.

Safety In terms of safety the role of the constellation is making sure the payload can detect an ICBM. If the constellation was not designed properly some places would not have constant coverage which could lead to some ICBM's to go undetected. Therefore, the constellation design is a safety-critical function.

15.6. Recommendations

First of all, research into the debris behaviour in LEO orbit is recommended. As it is known, in LEO there is a significant amount of debris [76]. It would be important to see how this affects the structure of the satellite in order to protect it or even a change of orbital altitude.

Moreover, it was assumed that the constellation could be placed in any orbit at any altitude. In order to confirm this assumption, two topics could be further researched. Firstly, it would be important to learn more about the constellations to see if the constellation could interfere with existing systems. Secondly, it is suggested to research the means by which each spacecraft would be delivered into its correct orbital position.

Finally, it will be important to analyse how the satellites will be seen from Earth. By placing 300 satellites in a LEO orbit some issues might arise as they might affect observations of the sky.

16
Final System

In this chapter, the information of all the subsystems provided in the previous chapters is integrated into the final system. Firstly, the configuration and layout of the spacecraft is reported in Section 16.1. Next to that, the technical resources are budgeted for in Section 16.2 and the cost is budgeted for in Section 16.3. Finally, the risk is analysed on a system level in Section 16.5 and the chapter is concluded by the sustainability plan in Section 16.6.

16.1. Configuration and Layout

In this section the integration of the spacecraft is presented. Renders of each subsystem are shown and the packaging is described.

16.1.1. Payload

The components that compose the payload system are the scanning mirror, Coverage optics lenses which are shown in blue behind the primary mirror of the telescope, Focus optics mirror or telescope system, the payload switch mechanism, filter switch mechanism with its corresponding electronics in the blue pcb, an infrared imager with the camera electronics and FPA in yellow and the cryocooler. The smaller mirrors that bounce light inside the spacecraft into the camera have not been included in the model

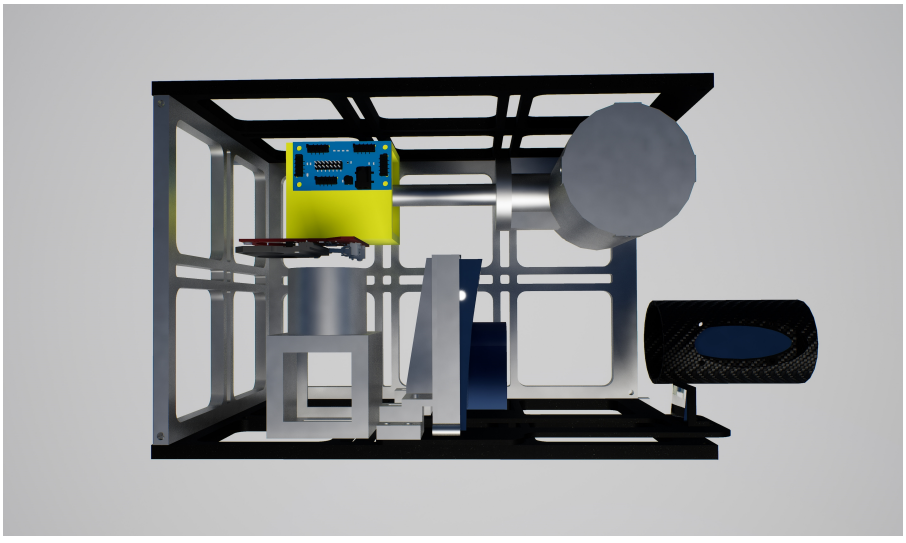

Figure 16.1: Payload subsystem render.

The optical path of the system is described next. In case imaging with the Coverage optics is being performed, light comes into the scanning mirror, inside the cylinder sticking out of the nadir face and reflects into the Coverage optics lenses shown. By means of a small mirror the light is bounced into the payload switch mechanism, that is the the cube with a cylindrical motor on top. The optical path continues on to the back of the payload switch mechanism where a mirror bounces the light vertically upwards into the filter and finally by using another mirror into the camera.

The process of imaging with the Focus payload is largely similar. The only differences occur before the light reaches the payload switch mechanism. The light comes into the spacecraft through the large opening in the nadir face. Bounces in the primary mirror and secondary mirror of the Ritchey–

Chrétien telescope, goes through the cutout in the primary mirror and reaches the payload switch mechanism. After this, it follows the path described above.

16.1.2. ADCS

The ADCS system consists on an integrated ADCS system for CubeSats, the iADCS400, with some extra components. The iADCS400 includes one star tracker, reaction wheels and magnetotorquers in all axis and the required logic. The extra components added are three RW400 reaction wheels, another higher precision star tracker shown with its baffle on the back of the spacecraft and a GPS patch antenna also on the back of the spacecraft. The reaction wheels are placed between the cooler and the side Parnell, the integrated ADCS system between the camera and side panel and the star tracker on the back of the spacecraft as far inside as the optical path allows. The GPS antenna is supplied by ISIS, while the rest of the components are supplied by Hyperion.

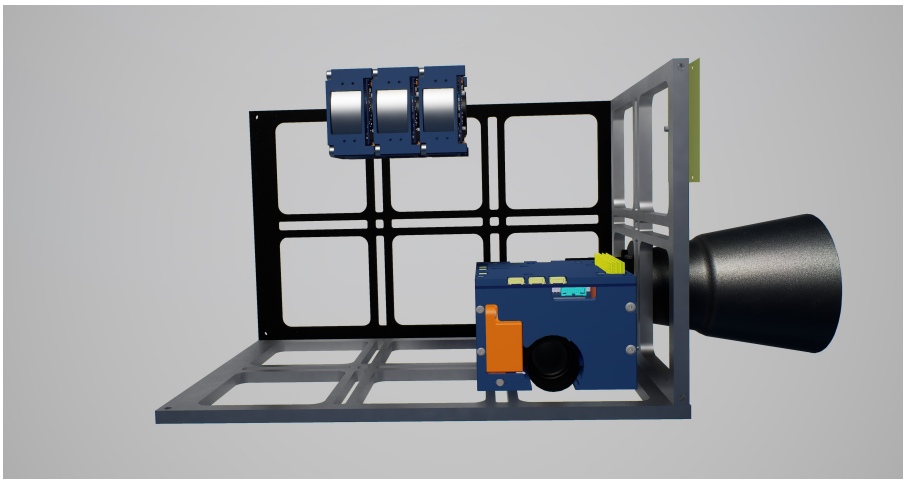

Figure 16.2: Attitude determination and control subsystem render. Note there is an error in the positioning of the reaction wheels in the render. The three extra reaction wheels should point different directions.

16.1.3. EPS

The EPS systems consists of the solar arrays and their gimbals, four battery packs and and a power conditioning and distribution module. The batteries are placed on the side and top of the spacecraft, between the side panel and the optical path of the Coverage payload. The power conditioning and distribution is placed between the payload switch mechanism and the other spacecraft side panel. Both the batteries and the power conditioning and distribution module are provided by Gomspace.

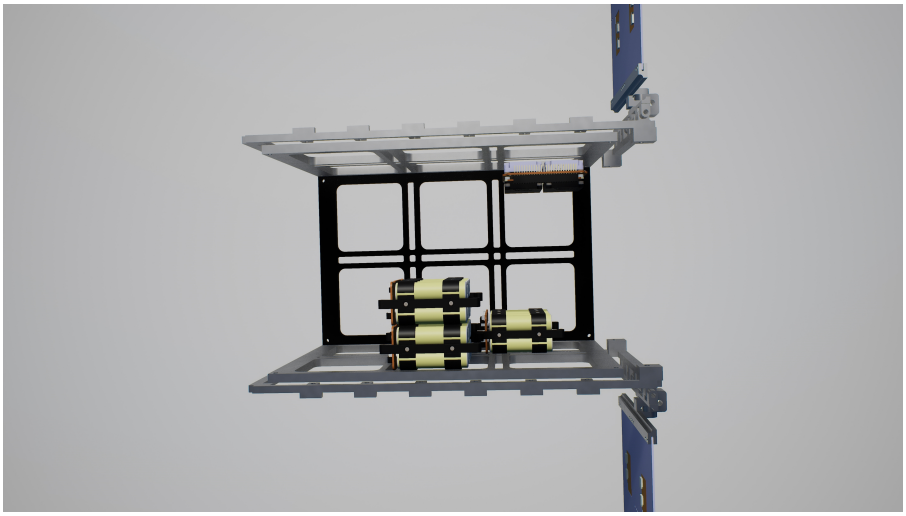

Figure 16.3: Electrical power subsystem render

16.1.4. Others

In this section the placement of other components in introduced. This includes the OBC, shown in blue, the copper thermal straps (CuTS) allowing for heat conduction to the radiators behind the the solar arrays and the two electric propulsion units from IFM nano thruster.

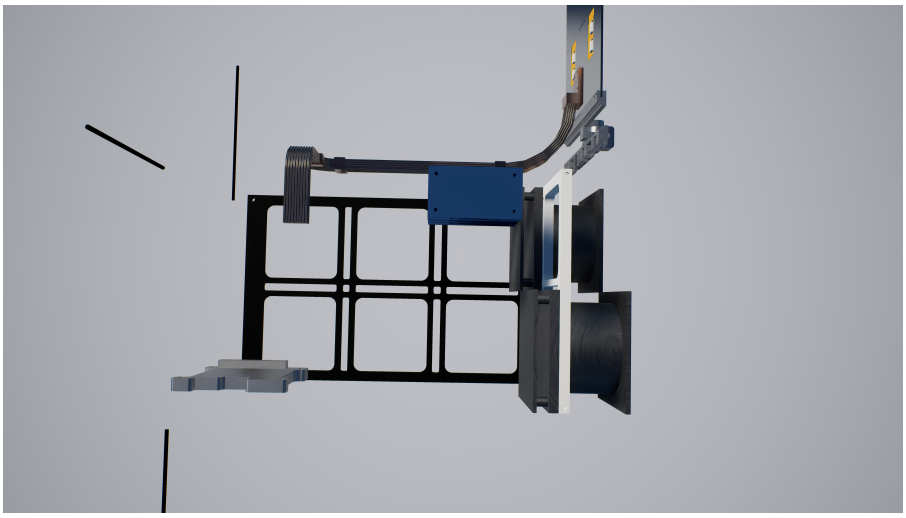

Figure 16.4: Other components render

16.1.5. Volume

As evidenced in the renders, multiple components are located on the outside of the spacecraft, such as the propulsion units, the star tracker baffle and the scanning mirror. Deployment system dimensions were taken from [1]. In order to fit the spacecraft in a 12u launcher it needs to be shortened by 140mm, this means the star tracker baffle would need to be removed or made deployable, the thrusters moved further into the spacecraft body and the rotating mirror be shortened by 10mm. This requires too many changes to be a viable option for the IOD but may prove worthwhile for a full constellation deployment. Alternatives are using clamp bands which can prove cheaper as companies like SpaceX allows for 200kg ride share payloads for 1M$ [2], however this would require moving away from cots structures thus its not recommended for an IOD mission and using a 16u deployment system which only requires shortening the spacecraft by 20mm. From the cad models, the rotating assembly can be shortened/ moved back by 10mm. The star tracker can be moved to a location that allows integration further inside the spacecraft or the baffle can be shortened. The effects of shortening the baffle on ADCS performance are unknown, however due to the multiple ways the, a specialist team in the detail design should have no problem saving 10mm of space. Deploying with a 16u system is thus deemed feasible with minimal impact on the mission.

16.2. Resource Allocation

In this section, al the spacecraft subsystems are integrated to create technical resources system budgets. For this mission, the relevant resources are the mass in Section 16.2.1, the power in Section 16.2.2 and the time in Section 16.2.3.

The mass budget for M-STAR is shown in Table 16.1. The contingency plan introduced in Section 6.2.1 is used, and the subsystem masses also include this margin. Most of the components in the payload subsystem will require further R&D and thus present the largest uncertainty in this budget. The total spacecraft mass is below the 24 kg limit specified in **REQ-SYS-06-02**.

Table 16.1: Detailed mass budget for M-STAR.

Subsystem	Subsystem Mass [kg]	Component	Units	Unit Mass [kg]	Margin	Total Mass [kg]
PAY	8.86	Main mirrors	1	0.70	*20%*	0.88
		Secondary mirrors	1	0.30	*20%*	0.38
		Lenses	1	0.50	*20%*	0.63
		Cooler	1	2.80	*20%*	3.50
		IR camera	1	0.90	*20%*	1.13
		Imaging system	1	1.00	*20%*	1.25
		Optics switch	1	0.50	*20%*	0.63
		Filters (with switch)	1	0.46	*5%*	0.48
ADCS	3.27	iADCS400	1	1.70	*5%*	1.79
		ST400	1	0.28	*5%*	0.29
		Extra RW400	3	0.38	*5%*	1.18
TTC	0.33	UHF antenna	1	0.03	*2%*	0.03
		UHF transceiver	1	0.15	*10%*	0.17
		S-Band antenna	1	0.05	5%	0.05
		S-Band transceiver	1	0.08	5%	0.08
OBC	0.10	Q7S	3	0.03	*2%*	0.10
EPS	3.96	BPX	4	0.50	*2%*	2.04
		P60 Dock	1	0.08	*2%*	0.08
		P60 ACU	2	0.05	*2%*	0.11
		P60 PDU	2	0.06	*2%*	0.12
		Solar array	2	0.52	*5%*	1.10
		Gimbals	2	0.24	*5%*	0.51
PROP	1.63	IFM NanoThruster (wet)	2	0.80	*2%*	1.63
STR	1.84	Primary 12U structure	1	1.43	*5%*	1.51
		Secondary 12U structure	1	0.32	*5%*	0.34
THER	0.08	CuTS	1	0.07	*10%*	0.08
TOTAL SPACECRAFT MASS						**20.27**

16.2.1. Mass Budget

16.2.2. Power Budget

The power budget for M-STAR is shown in Table 16.2. The contingency plan introduced in Section 6.2.1 is used. "*Nom.*" refers to the nominal power usage, and is thus required continuously during the operation of the component. Using the values of the power budget, the power modes introduced in Chapter 10 are quantified in Section 10.3.1.

16.2.3. Time Budget

The time budget is relevant for this mission due to **REQ-SYS-01-02**. Thus, this budget is shown in Table 16.3 up until the L3 alert reaches a ground station, with the added information of the time needed for the first 3D target position to be downlinked (this last action, however, is outside the scope of the latency requirement mentioned above). It must be noted that the time budget has been constructed for the worst case scenario. The missile time to climb to 14 km (where the atmosphere does not absorb its signal, see Section 7.3.1) is that for a Minuteman III missile flying its most depressed trajectory, per the simulations of Dr. Savelsberg. In addition, also the time needed to determine that the anomaly is moving is for the worst case scenario, where the missile trajectory resembles closest a stationary point. Finally, slew time to target is again the worst-case scenario (Section 13.3.2), where one of the spacecraft must yaw an angle of 180° and pitch for 23° due to the circular imaging technique (see Section 7.4.3).

[1]Retrieved from `https://www.exolaunch.com/user_guides/EXOpod_User_Guide.pdf`
[2]Retrieved from `https://rideshare.spacex.com/search`

Table 16.2: Detailed power budget for M-STAR.

Subsystem	Component	Mode	Power [W]	Margin	Design Power [W]
PAY	IR camera	*Nom.*	8.00	*20%*	10.00
	Mirror motor	*Nom.*	0.84	*20%*	1.05
	Cooler	*Nom.*	25.00	*20%*	31.25
ADCS	iADCS400	*Nom.*	2.00	*5%*	2.11
		Peak	6.00	*5%*	6.32
	ST400	*Nom.*	0.70	*5%*	0.74
TTC	UHF Transceiver	*Nom.*	0.48	*10%*	0.53
		Peak	7.00	*10%*	7.78
	S-band	*Peak*	9.00	*5%*	9.47
OBC	2xQ7S	*Nom.*	2.00	*2%*	2.04
EPS	NanoPower P60	*Nom.*	0.60	*2%*	0.61
PROP	IFM NanoThruster	*Peak*	40.00	*2%*	40.82

Table 16.3: Detailed time budget for M-STAR (includes a 10% margin).

Action	Time needed [s]
Launch of missile - ***T+0s***	
Missile climbs above 13km altitude	53.3
SC1 H2O imaging	1.1
SC1 processes H2O image	0.04
L1: H2O anomaly - ***T+54.5s***	
SC1 switches to CO2 filter	0.44
SC1 CO2 imaging	1.1
SC1 processes CO2 image	0.04
L2: H2O+CO2 anomaly - ***T+56.1s***	
SC1 determines that anomaly is not stationary	5.5
L3: confirmation that object is moving - ***T+60.5***	
SC1 sends SC2 preliminary target location	0.11
SC1, SC2 slew to target	27.07
SC1, SC2 switch to FOC payload	0.22
Data relay to GS	4.4
L3 alert reaches GS - ***T+64.9s***	
First 3D target location reaches GS - ***T+92.3s***	

16.2.4. DeltaV Budget

The ΔV required to accomplish the mission has been calculated using the same procedure that was introduced in the Baseline Report [4]. Nonetheless, the values for the orbital height and other specific parameters such as the characteristics of the propulsion system (see Chapter 12) have been updated and are shown in Table 16.4. This analysis focuses on three main maneuvers: orbital station-keeping, collision avoidance and a de-orbit burn. It should be noted that an orbital insertion is not taken into account because, after deliberation with the costumer, it is assumed that the launch provider carries the spacecraft to its final orbit. From this, the values in Table 16.5 follow.

Table 16.4: Parameters used for ΔV budget of M-STAR.

Parameter	Symbol	Value
Orbital altitude	h	600 km
Drag coefficient	C_D	2.2
Mass of the S/C	m	20.19 kg
Cross-sectional area	A	0.06 m^2
Specific impulse	Isp	2250 s
Minimum miss distance	d_{min}	1.5 km
Number of avoidance maneuvers	-	9

Table 16.5: ΔV and propellant mass budget for M-STAR.

ΔV for altitude maintenace	23.21 m s^{-1}
ΔV for de-orbit	156.66 m s^{-1}
ΔV for collision avoidance	7.31 m s^{-1}
Total ΔV	187.17 m s^{-1}

Nominal propellant	0.171 kg
Propellant margin (25% of nominal)	0.043 kg
Residual propellant (2% of total)	0.004 kg
Total propellant mass	0.220 kg

16.3. Cost Breakdown

As the final system architecture is known, a detailed cost analysis is constructed based on the multiple subsystem components. The cost of the technical demonstration mission is built up of several components. First, the recurring cost per manufacturing of one satellite. These are comprised of the actual part costs, as described in each subsystems chapter. Secondly, development costs are included for each component in order to accommodate for the proper research and development needed to make all components into one working system. These costs are only accounted for once in the entire technical demonstration mission, where the recurring costs are counted per satellite built. Lastly, there are operational and maintenance costs. As the budget requirement set by the RNLAF does not include operational and maintenance cost, these are not included in the budget. A breakdown of the costs of the mission is given in Figure 16.5.

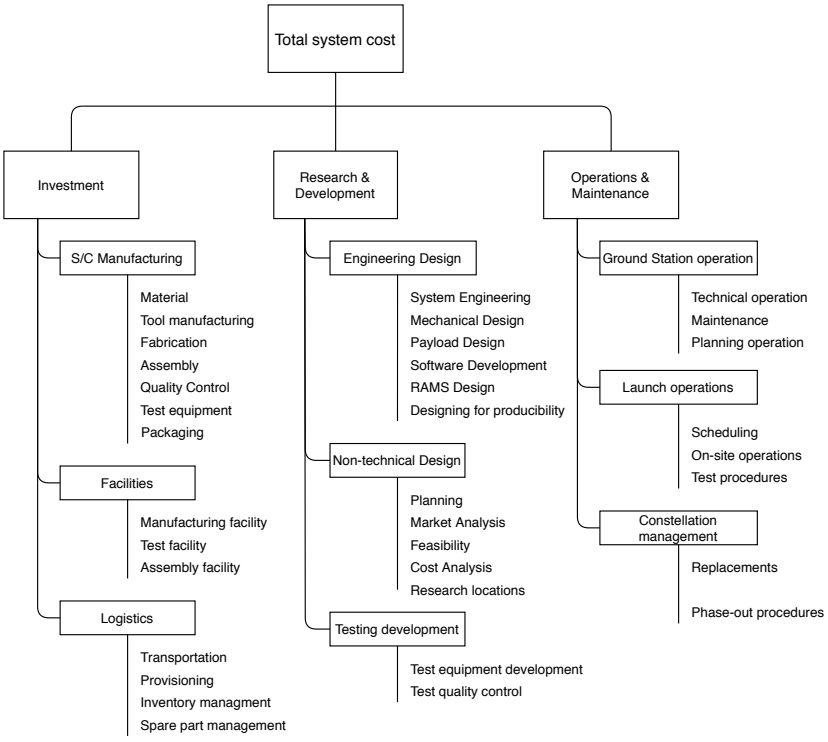

Figure 16.5: Cost Breakdown Structure.

Table 16.6 below gives an overview of the recurring and R&D costs for a single satellite, as well as the Theoretical First Unit (TFU) price. Please note that these values need to be taken with at least 20 % contingency, as it is impossible to fully estimate development costs for example for the optical system, as this is a system to be fully developed.

Table 16.6: Cost breakdown of a single satellite.

S/C component	R&D cost	Recurring cost
12U Bus structure	€ -	€ 11,950.00
Coverage Camera	€ 1,000,000.00	€ 250,000.00
Focus Camera	€ 1,000,000.00	€ 250,000.00
Cooler	€ 1,000,000.00	€ 50,000.00
Filter	€ 50,000.00	€ 600.00
Thermal system	€ 4,556.09	€ 11,390.22
Battery	€ 12,000.00	€ 30,000.00
ACU + PDU	€ 13,600.00	€ 34,000.00
Solar Panels	€ 800,000.00	€ 50,000.00
GNSS Receiver	€ 3,712.00	€ 9,280.00
L-band patch antenna	€ 700.00	€ 1,750.00
ADCS standard comp.	€ 13,314.40	€ 33,286.00
Large reaction wheels	€ 6,443.60	€ 16,109.00
Star trackers	€ 9,612.00	€ 24,030.00
Large torquers	€ 2,242.80	€ 5,607.00
Gyroscope	€ 11.48	€ 11.48
Ground station	€ 86,500.00	€ -
UHF Duplex tranceiver	€ 4,200.00	€ 10,500.00
UHF Antenna	€ -	€ 3,500.00
OBC	€ 22,140.00	€ 18,450.00
Flight software	€ 217,500.00	€ -
Ground software	€ 11,000.00	€ -
Propulsion	€ 10,000.00	€ 38,400.00
IA&T	€ -	€ 117,992.05
Program level	€ 194,389.79	€ 97,194.89
Total TFU price		**€ 1,064,050.65**

Now with the recurring and non recurring costs known, an estimation of the budget for the technical demonstration mission consisting of 7 satellites can be made. Table 16.7 below shows that the total cost for the demonstration mission is estimated at to equal approximately €11.3 M. This is well below the budget of €30 M set as a requirement by the RNLAF.

Table 16.7: Final budget costs for 7 satellites.

Total TFU price	€ 1,064,050.65
Total RDT&E	€ 4,461,922.16
Total production	€ 6,814,021.45
Average unit price	€ 973,431.64
Budget needed	€ 11,275,943.60

As can be seen in the Table 16.7, the average unit cost of a satellite is a bit lower then the TFU price. This is because a learning curve is applied to the production of multiple satellites. [77] gives a relation for the price drop due to a learning curve when manufacturing multiple units, shown in Equation (16.1) and Equation (16.2), where S is taken as 95%, as described in [77].

$$\text{Production Cost} = TFU \cdot N^{B} \tag{16.1}$$

$$B = 1 - \frac{ln((100\%)/S)}{ln2} \tag{16.2}$$

16.4. System Sensitivity Analysis

Following the final configuration and resource allocation, a system-wide sensitivity analysis must be performed. This sensitivity analysis is limited to the parameters that affect the most critical and driving system requirements of the demonstration mission, namely:

- **REQ-SYS-01-02**:The system shall inform the ground station of the ICBM detection within 90 seconds after launch of the missile.
- **REQ-SYS-01-05**: The system shall have 99% availability for communication for detection relays.
- **REQ-SYS-01-06**: The system shall have a 99% reliability for communication for detection relays.

In order to perform a sensitivity analysis on the entire system and ensure that these main system requirements are met, the budget allocations are manipulated in order to identify the most critical elements.

Throughout the subsystem sensitivity analyses, the effect of the errors associated to the inputs that came from other subsystems were analysed. Hence, smaller system sensitivity analyses were performed by looking at the errors between the interfaces of different subsystems. Thus, this analysis is concerned mainly with critical components that may potentially affect the ability of the system to meet the above stated system requirements. As mass is not a limiting design constraint for this mission, it will not be explicitly evaluated in this analysis.

Time Budget

Currently, the time budget outlines the time necessary to perform the series of tasks during missile detection, tracking and relay. The 90 second time latency requirement is of importance to the level 3 alert. The two main assumptions made are:

- The missile is visible above a 14km altitude.
- The CDH is able to process data at the same frequency as the Focus payload (30Hz).

The first assumption was made based on noise in the environment and the absorption of relevant wavelengths by the atmosphere. Between altitudes of 4km and 14km, the noise is variable. However, the assumption was made that below 14km, the missile would not be distinctly visible in the image. This is a conservative estimation. In the sensitivity analysis performed in Chapter 8 for the velocity check time threshold tool, it was found that for an anomaly located on the surface of the earth, the time threshold was calculated to be 7 seconds. For which the latency requirement is still met.

In order to find the maximum altitude at which the system must be able to detect an ICBM, the maximum time for which the anomaly can be visible in the image is found and run through the preliminary missile trajectory model in order to check the approximate altitude at which this occurs. From the time budget, given the 10% contingency, the missile should be visible in the image 71 seconds after launch in order to still meet the 90 second latency requirement. At this time, one may expect the missile to have an altitude below 80km.

The second assumption is most relevant to the image processing pertaining to the CO_2 and H_2O filtered images, but also the velocity check algorithm, as an additional calculation needs to be carried out for each image. This assumption was made as estimating computing time is outside of the scope of this design phase. However, as future studies should show, it could potentially be a largely limiting design factor.

Thus, as estimating an accurate image throughput time is not feasible, the lowest allowable processing frequency that would ensure the requirement is still met can be found. From the time budget, given the 10% contingency, an image throughput frequency of around 0.7 Hz can be achieved. This

indicates that the image throughput frequency may lie between 30Hz and 0.7Hz to meet the latency requirement. However, a higher frequency is desired in order to allow for a sufficient resolution of the Focus payload, and to allow for closer measurements at burnout. This is crucial for the trajectory prediction of the missile. The calculation of the lowest necessary frequency at which the payload, and thus also the data processing, should operate at is outside the scope of this design phase, however, the system has been designed to allow for a large range of frequencies.

16.4.1. Power Budget

Currently, the power budget is driven by the power requirements of the cooler, which is an estimated value. With the current design, if the cooler requires more power than what was estimated, a new battery pack as well as larger solar panels would be necessary to generate and store sufficient power.

This must be checked, as the cooler ensures that the instrument noise is reduced in the payload. As was specified in Chapter 7, the noise in the instrument increases exponentially with increasing temperature. Thus, for the current system configuration, if more power is required by the cooler than what has been budgeted, two outcomes are possible. Either the 99% reliability requirement may not be met, as the system is not able to detect a missile due to instrument noise; or the 99% availability requirement may not be met, as more power is supplied to the cooler as compared to other subsystems. Thus the CDH and communication systems may not have sufficient power.

Given that the spacecraft could be reconfigured to fit an additional battery pack, the power supplied to the cooler could be increased by 60%, from 31W to 50W. This would increase the battery mass to 2kg, the solar array mass to 1.43kg, and the solar array area to $0.424m^2$, thus all increase by 38%. However, this new mass would still meet the system mass requirement of 24kg as stated in Chapter 5. However, by increasing the mass of the system, and the size of the solar arrays, the ADCS will also be affected.

As the rate at which the spacecraft slews determines the time at which the first missile 3D location dataset reaches the ground station, it must also be checked how much this increase in mass affects the time at which this happens. For the original configuration, the first 3D location would be received by the ground 27 seconds after the level 3 Alert; 93 seconds after missile launch. Given the increase in power for the cooler, the first 3D location would be received by the ground 39 seconds after the level 3 alert (44% increase); 104 seconds after the missile launch (12% increase). As the time latency requirement is not relevant for this task, an analysis should be performed at a later design stage to identify an optimum slew rate based on missile trajectories as specified in the recommendations in Chapter 7. It should be checked that enough power can be supplied to all subsystems, and that the 99% availability and reliability requirements are met given this optimum slew rate.

16.5. Risk Management

This section will concern itself with the risk management performed for the M-STAR project. The approach to the generated risk register will be explained, and the most threatening risks will be discussed in more detail together with their corresponding mitigation acts. Finally, a summary of all risks is presented in the form of a risk map both before and after mitigation actions are considered.

16.5.1. Risk Management Approach

The risk management is conducted following the the guidelines set by the European Cooperation for Space Standardization (ECSS, ECSS-M-ST-80C). The process is broken down into three main steps:

1. Risk identification | 2. Risk assessment | 3. Risk mitigation

Risk identification was performed by individual team members. Individuals were tasked with identifying possible technical or non-technical risks that could impact the course of the mission. Due to the input from team members working in various subsystems of the spacecraft, more detailed risk sce-

narios could be identified with respect to the midterm phase. Identified risks have been documented in a so called risk register. In the risk register, each risk contains a brief description about what has been assumed to happen under ideal circumstances, what an actual risk scenario would be and the reason why a certain risk can occur. Each documented risk is scored on two aspects: its likelihood of happening (L) and the severity of the risk (S). For both aspects, a grade from 1 to 5 could be awarded for which the scales are shown on the right of Figure 16.6. The multiplication of these grades results in a risk index that could be used for ranking of the risks. Following the ranking of the risks, a brainstorm session was held to identify possible mitigation acts which were documented in the risk register as well, after which another grading could take place to asses the residuals of the risks. A total of 26 risks have been identified using the procedure described above. Out of these, the 10 highest ranking risks are shown in risk register form in Table 16.8. Risks are also shown in the accompanying risk map.

16.5.2. Mitigation Acts

The 10 risks shown in the risk register achieved the most alarming risk index scores. Without mitigation measures, these risks pose an imminent threat to a successful course of the mission. Below, the top risks together with their mitigation act and their residual score will be discussed in more detail.

24-Velocity and Position Determination Errors According to **REQ-SYS-PAY-08-04** the constellation shall be able to achieve a specified ICBM positioning accuracy in three dimensional space. Besides this, accurate three dimensional data is needed to determine a detected ICBMs velocity and allow for trajectory estimations. Without three dimensional coordinates, complete mission failure is imminent and therefore results in an index of 25. Early on in the mission design process it became apparent that multiple satellites will be required to achieve three dimensional coordinates. Regardless, positioning errors will still be present albeit in orders of magnitude smaller resulting in a residual likelihood of 3. Additional cost and complexity will still be present nonetheless, resulting in a residual severity of 4.

25-Thermal System Damage Space is a hostile environment, extreme temperatures pose a threat to on board systems. After analysis of the expected temperatures experienced by the spacecraft, thermal control was found to be needed to be able to achieve a functioning spacecraft. By means of passive thermal control in the form of blankets or sheets the temperature ranges experienced could be kept to an acceptable level resulting in a residual score of 2 for both likelihood and severity for additional thermal control problems.

11-Reaction Wheel Saturation The reaction wheels will be used for attitude determination and payload slewing manoeuvres. Without considering the saturation of reaction wheels a high chance of saturation occurring will be present for all spacecraft resulting in the provided scores. Multiple sets of reaction wheels as well as magnetotorquers are implemented to allow for faster slewing but also provide redundancy and provide a desaturation torquer. This reduces the chance of saturation in turn reducing the number of satellites affected resulting in the mitigated risk score of 3,3.

7-Power Shortcoming A functioning EPS is vital for a spacecraft to be operated. Without a proper EPS requirements analysis, structural EPS design errors can be made leading to a high chance of power problems across the constellation. As a result a risk index of 20 was assigned. During the development of the power budget and array sizing, contingencies should be used. The use of batteries in the spacecraft will allow the spacecraft to be independent from constant sun exposure and calculations should be verified, validated and if possible EPS components should be tested. These mitigation acts were assumed to lower the chance of possible power shortages as well as decrease the effect when a power problem would occur.

1-Thermal Noise The infrared camera that will be used is sensitive to noise. To allow for more reliable missile detection and tracking a high signal to noise or clutter ratio is desired. Despite the cold temperatures of space, infrared radiation originating from the spacecraft itself in the form of heat will decrease the sensitivity of the sensor to an unusable level. If left unaccounted for, this is almost certain to affect all spacecraft resulting in the shown risk scores. This problem will be mitigated effectively by the use of an on-board pulse tube cooler, keeping the senor temperatures to an optimal 77K. As the possibility for thermal noise will not be completely eliminated and could still affect several spacecraft, the residual likelihood and severity remain 2 and 3 respectively.

3,4-R&D Time Delay and Cost Increase To achieve an optimised solution for the mission, COTS components might not be ideal. For the payload subsystem alone it was already found that some form of R&D will be needed for the camera, cooler, filters and optics. Besides the additional cost and time required for R&D, it also introduces uncertainty. Because of the nature of research itself, the process might exceed the expected time and cost schedules with no guarantee of a finished product. With multiple components undergoing R&D, the chances of delays are relatively large and budget increases of 20% are not unfeasible. This risk is difficult to predict and therefore difficult to mitigate. By planning R&D in advance and adhering to an organised Project Management and System Engineering plan it is believed however that the likelihood can be lowered to 3.

2-Mechanical Failure Part of the spacecraft components employed are mechanically operated. Due to induced loads and wear these parts introduce a reliability risk. Structural failure of major components could lead to multiple spacecraft failures within the constellation in the mission lifetime. To mitigate the chances of mechanical problems special attention has to be given to the quality and TRL of these parts. Components should be tested and their expected lifetimes should meet the mission lifetime with a significant margin. Nonetheless, mechanical risks will remain but both their likelihood and severity can be decreased somewhat.

26-EOL Degradation Component performance and specifications can not be assumed to be constant over the mission lifetime. Components such as solar arrays and batteries show a decrease in efficiency and mechanical components in reliability. By analysing the required properties of components for different phases throughout the mission, the chances of unexpected decreased performance due to degradation can be lowered. Furthermore, the use of components with the highest possible TRL will be beneficial. These acts could decrease the chance of unexpected problems occurring but do not necessarily lower the severity.

17-OBC Failure With the OBC functioning as the brain of the satellite, OBC failure can lead to subsystem failure and consequently spacecraft failure. Structural problems such as software glitches can affect the entire constellation and is therefore a threat to the entire mission. To mitigate any OBC problems many robust, redundant and reliability improving mechanisms are already included in the COTS OBC design. Additionally, a backup OBC will be present in case of main OBC failure to lower the severity of such events.

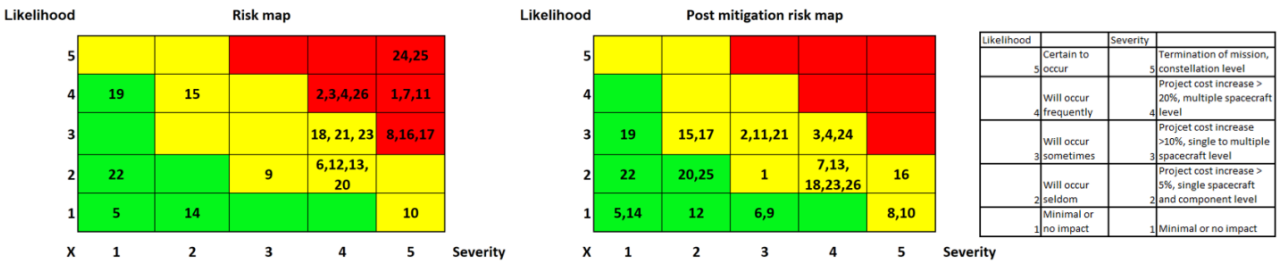

Figure 16.6: Pre- and post mitigation risk maps

Table 16.8: Risk register containing 10 highest risk index risk scenarios.

Risk number	Subsystem	Risk	Assumption, risk & why	Risk description	L	S	Score	Mitigation	Residual L	Residual S	Score
24	CDH	Velocity and position determination errors	**Assumption:** A single satellite will be able to both determine an ICBMs position and velocity in 3D **Risk:** A single satellite is not sufficient for precise 3D velocity and position determination **Why:** Two or more satellites are needed for 3D triangulation	At least two satellites are required to provide accurate 3D position and velocity triangulation. Without 3D accuracy, trajectory estimations and tracking towards the end of boost phase is not possible.	5	5	25	Allow the constellation to use multiple satellites to track a single ICBM	3	4	12
25	THERMAL	Thermal system damage	**Assumption:** The S/C does not need any form of thermal control **Risk:** The S/C requires either passive or active thermal control for safe operation **Why:** Too high or low temperatures/fluctuations causing functions to not function properly	Without any shielding or other form of action againt the extreme temperatures of space many subsystems are not able to function and the S/C as a whole will not be able to fulfill its mission.	5	5	25	Analysis of thermal environments during launch and operation. Use of active or passive thermal control.	2	2	4
11	ADCS	Reaction wheel saturation	**Assumption:** The reaction wheels do not saturate over time **Risk:** Reaction wheels reach a saturation point after a ceratin time of use. **Why:** Reaction wheels are only capable of storing a limited amount of momentum before saturating.	Reaction wheels are capable of rotating to maximum rpms and store a limited amount of momentum. Without further action, saturated reaction wheels could render the ADCS non-functioning.	4	5	20	Analyse the required reaction wheel specifications needed, size the reaction wheels accordingly, allow for redundant or secondary systems to dump or take over stored momentum.	3	3	9
7	EPS	Power shortcoming	**Assumption:** The solar arrays will provide sufficient power for continuous operation **Risk:** The solar arrays do not generate sufficient power for continuous operation **Why:** Erroneous power budgeting/array sizing, mechanical/electrical failure	Mechanical and/or electrical malfunctions leading to insufficient power reaching components. Additionally, undersized arrays due to miscalculations or unforseen power demands causing power shortcomings.	4	5	20	Verification & validation of power budget calculations. Applying contingencies in power budget and allow for energy storage to allow for continuous power during eclipse.	2	4	8
1	Payload	Thermal noise	**Assumption:** The infrared camera is able to operate without active cooling **Risk:** Excessive thermal noise **Why:** Increased instrument termperature	Insufficient instrument cooling leads to an excessive amount of thermal noise introduced to the infrared camera, resulting in an insufficient SCR for ICBM detection.	4	5	20	Active instrument cooling implemented within spacecraft	2	3	6
3	Non-technical	R&D time delay	**Assumption:** R&D will be performed within the scheduled time span **Risk:** Required R&D will not be finished within scheduled time span **Why:** Unforseen design difficulties, complex and slow manufacturing processes	Due to the specific and complex nature of space missions, several components require additional R&D to meet requirements. R&D is difficult to schedule and unforseen implications lead to deadlines not being met.	4	4	16	Detailed planning and creation of Gantt chart in early stage of the R&D process. Include contingencies in time management budgets to lower the possibility of missed deadlines.	3	4	12
4	Non-technical	R&D cost increase	**Assumption:** R&D costs will adhere to its predefined budget **Risk:** R&D costs increase beyond predefined budget **Why:** Unforseen design difficulties, development of "not-yet" existing solutions.	Due to the specific and complex nature of space missions, several components require additional R&D to meet requirements. Besides additional time introducing cost, new and untested solutions introduce cost.	4	4	16	Include contingencies in R&D budgeting. Detailed planning to avoid time delays increasing cost. Avoid solutions untested in principle.	3	4	12
2	GEN	Mechanical failure	**Assumption:** The mechanical payload components will not fail during operation lifetime **Risk:** One or more mechanical components fail during operation lifetime **Why:** Decreased reliability due to wear and miscalculated loads	Mechanical components are subject to increased wear and loads resulting in an increased possibility of failure of e.g. mirror/solar array rotating mechanisms	4	4	16	Use of high TRL components for mechanical parts especially. Where possible add redundancy for mechanical components that introduce a single point to failure	3	3	9
26	GEN	EOL degradation	**Assumption:** degradation during mission lifetime does not have to be accounted for **Risk:** Degradation has to be accounted for to ensure a functioning S/C thoughout lifetime **Why:** Components show wear/degradation resulting in decreased performance and an increase in probability of failure	Component performance does not nessecarely stay constant thoughout the S/C lifetime. Components wear out and show decreased performance and reliability. If not accounted for, S/C have a significantly increased chance of disfunctioning before retirement, requiring the launch of additional satellites or a complete mission failure.	4	4	16	Consider degradation of S/C components in the design of the mission. Use high TRL, high reliability componetns for parts prone to wear and failure. Use of components with a sufficient lifetime for a 7 year mission.	2	4	8
17	CDH	OBC failure	**Assumption:** OBC is redundant and reliable throughout mission lifetime **Risk:** Unexpected hardware/software malfunction **Why:** Unforeseen circumstances (faulty part, electromagnetic interference, single event upsets etc)	The OBC hardware forms an integral part of the mission. Unexpected hardware malfunction or software glitches could lead to satellite subsystem failure and subsequent mission failure. Failures in the hardware could occur due to fluctuations in the obc, interfaces, subsystems and systems	3	5	15	Many robust, redundant, reliability improving mechanisms are already included in COTS obc designs. Next to this, a backup OBC is present in sleep mode, ready to wake up at all times when the main OBC would fail.	3	2	6

16.6. Sustainability

Any space mission has to considered for the economic, societal and environmental consequences of its actions. The mission shall bring long-term benefit to humanity. This cannot be ensured without

examining all aspects of the mission. In this chapter, a comprehensive list of measures is listed in order to create a mission that would meet mission requirements while not posing a danger to future generations.

16.6.1. Debris Mitigation

For Earth Orbiting constellation, debris mitigation is one of the most important sustainability considerations. A cascading effect of collisions creating more debris which increase further collision risk known as Kessler Syndrome is continuing to be a bigger problem every year. Constellation such as the one described in this report further contribute to increased risk and it is of utmost importance to take necessary measures to limit the risk of in-orbit collisions.

A list of requirements has been developed to create a mission that would not contribute to long-term space pollution. Those include both the disposal and collision avoidance.

- **SUS-D-R1:** The EOL procedures for the spacecraft shall be in agreement with the IADC Space Debris Mitigation Guidelines [78].
- **SUS-D-R2:** The spacecraft specification shall follow the UN Space Debris Mitigation Guidelines [79].
- **SUS-D-R3:** The spacecraft shall not release any debris during its complete lifetime.
- **SUS-D-R4:** The spacecraft shall be capable of performing debris evasion manoeuvres.
- **SUS-D-R5:** The spacecraft at EOL shall be deorbited.

The design has been adjusted to match those requirements. One of the main implications of the debris mitigation in the satellite was the propulsion system. The repeatable capability of evasive manoeuvres couldn't be provided in another form, therefore thrusters were used. The same propulsion system will be used to perform the deorbit procedure.

The communication system is capable of a rapid relay of commands from the ground station to any spacecraft of the constellation. This allows for both long-term collision avoidance planning, but also for last-minute corrections of orbital trajectory in case debris is discovered with small lead time.

From different deorbit mechanisms, the semi-controlled deorbit was chosen to be the most suitable for the mission. It is commonly used by different LEO constellations such as Iridium [80]. The satellite would perform reentry burn that would reduce its orbit periapsis sufficiently that the atmospheric drag would lead to an expedient deorbit.

Design for demise approach has to be used when designing the spacecraft. As it is not possible to accurately determine the position of the landing of debris on Earth, it is preferred to design the satellite that would completely burn during atmospheric reentry. The optic system is of particular importance as some optic materials have a very high thermal resistance.

Before reentry, passivation is conducted. That includes fully depleting the propulsion tank and other energy reservoirs such as batteries. The spare propellant is used to further reduce the deorbit time if used in a retrograde burn.

16.6.2. Operations

To reduce the impacts of prolonged use of the constellation, the system is largely autonomous. This includes the housekeeping of the satellites, detection and contingency management. While it is not possible or desirable to create a system that would be independent of human involvement, routine tasks shall be conducted without the need for excessive supervision.

Moreover, such an autonomous system should have the capability to function for a long time without replacement. For this to be possible, it improves itself over time. This is achieved by increasing the capability of detection and communication algorithms by deep learning based on measured data. Separate rapid downlink S-band antenna enables transmission of big amount of data for this purpose.

Having redundant components in the spacecraft, especially ones that are necessary for deorbit proce-

dures are another way to increase the lifespan of the satellite. This reduces the number of launches and ensures that the satellite can be deorbited safely. Communication and propulsion system are examples of critical components for sustainability that are redundant.

The use of the system is military and national security depends on the performance of the system. False positives create a danger of unnecessary reaction from involved parties. Risk of such events should be minimized. Multiple confirmation methods should be used when detection occurs. In most operational regions the system has at least double-fold coverage. Additional information from neighbouring satellites combined with different, independent systems are used to increase the reliability of the system, as described in Section 16.5.

Another aspect that needs to be taken into account is the transportation. Options of transport that create less pollution are preferred. This might require planning in advance and using transport by water and in bulk.

16.6.3. Manufacturing

Manufacturing of large constellation involves much bigger production cycles than producing one-off satellite. The environmental impact of such large quantities of spacecraft put sustainable manufacturing at a much more important place. The philosophy of lean manufacturing shall be applied when it comes to large-scale production of spacecraft [81]. Manufacturing processes shall not only reduce the waste overall but also limit the use of rare elements.

COTS components are an option that has the potential of reducing the environmental impact of the mission. However, added mass or reduced performance could lead to an unfavourable score of COTS parts when compared to custom made option. Therefore it is necessary to trade-off the benefits of COTS versus products tailored for the mission.

Contractors of the mission shall be examined according to their approach to sustainable development, such as the investments in environmentally friendly technologies and reduced production of greenhouse gasses. If the products they offer have comparable performance, a more sustainable option shall be chosen.

16.6.4. Launch

CubeSats are often deployed as a secondary payload of the mission. This reduces their environmental footprint as well as cost. It is a preferred strategy for the mission, however, it might not be achievable for the set-up of the whole constellation. It is likely that mission-specific launches need to be performed. It is desirable to reduce the number of launches needed to complete the constellation. Therefore the maximum number of spacecraft should be deployed at the same time.

Custom orbit insertion with a reduced number of launches can be achieved with the use of the onboard propulsion systems. The launcher could deploy satellites at parking orbit, and the final position would be established afterwards.

16.6.5. Sustainability assessment

Spacecraft uses COTS components for much of the design, which are produced in larger quantities. Therefore, the production can often be optimized and made more sustainable, when compared to one-off components. Additionally, the small size of the spacecraft reduces the environmental footprint of production.

A large number of satellites pose a threat of space-debris. This risk was mitigated by redundant communication and propulsion systems which enable deorbit of spacecraft and evasive manoeuvres. As a whole, the system serves as a deterrent from the use of ICBM, which increases worldwide safety. Use of ICBM would have disastrous consequences for the world, therefore prevention is crucial, also from a sustainability perspective.

17
Development Overview

In this chapter, an overview is provided of all M-STAR Mission Phases, according to ECSS standards [82]. An explanation will be presented about the work done until now, and a plan is proposed for future development. The future development is concerned with satellite manufacturing, assembling, integration and testing. The IODs are subsequently proposed aimed to enable verification of the technical demonstration mission designed, followed by a mission validation plan. After this, in Phase E, operational logistics are elaborated upon. Conclusively, finalizing with an assessment of Phase F a mission retirement plan is presented.

17.1. Phases 0 to B

This section provides an overview of the work done in the phases 0 to B completed by team Project Group S12 with regards to the M-STAR Mission.

17.1.1. Phase 0: Mission Definition

This phase focused on the generation of the mission and project objective. Project planning is the primary focus of this phase; Gantt charts were generated, work flow and work break down structures [3]. This is a fundamental phase that sets the pace for the design phases that proceed. Team roles and internal communication practises are established. Conclusions from this phase were seen in Chapter 2.

17.1.2. Phase A: Mission Reliability

During Phase A the feasibility of the mission is assessed on a preliminary scale. The implied cost, necessary operations and production timeline is evaluated. The intended market is also evaluated alongside sustainability and risk analyses [4]. In addition to this, the initial technical design for the driving subsystems commences, again with the goal of assessing feasibility of the entire mission. Furthermore, extensive literature studies are conducted to identify all possible routes that could be taken to develop the solution. This includes creating design option trees. The conclusions from this phase are revisited, refined and further developed in the following phases. The results of this detailed revising can be seen in Section 16.6, Section 16.5 and Section 16.3.

17.1.3. Phase B: Preliminary Definition

During Phase B, design possibilities are narrowed down, rejecting the design routes that are blatantly unfeasible and incompatible with the system requirements. Remaining subsystem design options are put through extensive trade-offs evaluating the compatibility of subsystem options on a system level. This allows for the most optimised full system configuration to be chosen to move into the detailed definition phase, phase C. This process was done with regards to the driving subsystems: communication, command and data handling, payload and constellation [5]. This provides a preliminary definition of the mission as it evaluates the constrains posed from the driving subsystems.

17.2. Phase C: Detailed Definition

Phase C delves into the final designs for subsystems and draws preliminary plans for manufacturing, assembly and integration. Furthermore, on ground verification plans are identified and developed.

17.2.1. System Compliance Matrix

Table 17.1 provides an overview of the system requirements of the mission, and whether or not they have been met. Green indicates compliance, and yellow indicates partial or unknown compliance. The right column shows in which parts of the report one can find explanations pertaining to the associated system requirement. It was decided that for the subrequirements of **REQ-SYS-01**, compliance would also be shown, as these are considered to be mostly driving requirements.

As was discussed in the compliance matrix of the Command and Data handling subsystem in Table 8.9, as well as the error calculations carried out in Section 7.5.1, more extensive analysis needs to be done in order to define a 3 dimensional error for the stereo imaging approach described, justifying the unknown compliance of **REQ-SYS-01-04**. For **REQ-SYS-01-05** and **REQ-SYS-01-06**, it is hard to say at this design phase whether or not these requirements have been met. Each subsystem has been designed to use high TRL components, and extra R&D has been specified. Moreover, RAMS characteristics of each subsystem discuss meeting these requirements, and the system has been designed to have communication at all times, except for during thrust maneuvers. However, a more detailed mathematical model must be made to verify these requirements. As for **REQ-SYS-18**, it is not possible at this point to say that this requirement has been met. All the components of the system are COTS, and have undergone testing/orbit demonstrations etc. However, the loads have not been specifically calculated as of now, thus it can not be stated that this requirement has been explicitly met. Lastly, **REQ-SYS-06** has been partially complied. The final configuration of the spacecraft fits within existing launch systems, and the components used are COTS meaning that they have standard dimensions. However, due to sub-optimal packaging as a result of using a standardised 12U structure, parts of some components protrude from the spacecraft's frame.

Table 17.1: System Compliance Matrix.

REQ	Compliance	Chapter/(Sub)-Section/Figure
REQ-SYS-01-01		Chapter 15, Section 7.5.1
REQ-SYS-01-02		Section 16.2.3
REQ-SYS-01-03		Section 4.1, Table 8.1, Chapter 13
REQ-SYS-01-04		Section 7.5.1
REQ-SYS-01-05		Section 17.2.2
REQ-SYS-01-06		Section 17.2.2
REQ-SYS-01-07		Section 7.5.1, Table 8.1
REQ-SYS-02		Section 9.3.6
REQ-SYS-03		Section 17.5
REQ-SYS-04		Section 10.3, Chapter 12
REQ-SYS-05		Section 16.3
REQ-SYS-06		Section 16.1
REQ-SYS-07		Figure 17.2

REQ	Compliance	Chapter/(Sub)-Section/Figure
REQ-SYS-08		Section 15.3
REQ-SYS-10		Section 8.4, Section 9.3
REQ-SYS-11		Section 8.4.2
REQ-SYS-12		Table 8.3
REQ-SYS-13		Section 17.2.4
REQ-SYS-14		Chapter 12
REQ-SYS-15		Figure 13.1
REQ-SYS-16		Chapter 12
REQ-SYS-17		Chapter 12
REQ-SYS-18		Chapter 14
REQ-SYS-19		Chapter 9
REQ-SYS-20		Chapter 10

17.2.2. System-Wide RAMS Analysis

Reliability

On a system level, the reliability of the mission can be studied from two points of view. On the one hand, by taking a closer look at how the different spacecraft interact in order to successfully perform the mission, and thus regarding the reliability of ICBM detection. On the other hand, by analysing the hardware design and its possible failure modes. Unfortunately, a system-wide quantitative analysis of the reliability of the system has not been performed due to the needed R&D work on the payload sub-system and is left as a recommendation for future work.

When looking at the ICBM detection, firstly, by designing the constellation such that double coverage is present for the entire globe, single points of failure for ICBMs detection are eliminated. Moreover, by filtering all signals outside of the absorption bands the probability of a false positive decreases drastically. Secondly, the CDH system is designed in such a way that each spacecraft is autonomous up to the tracking of the ICMBS. Consequently, the malfunction of one spacecraft does not influence the ability of another to raise a level 3 alert, as was explained in Chapter 4. Thirdly, by spreading the gathered data through a network of satellites the risk of a spacecraft missing a pass and not being

able to communicate to the ground station is mitigated, as the next satellite possesses the same information and can take on the task itself.

As for the hardware, critical components such as the OBC and the EPS are designed with redundancy in mind to avoid single points of failure. Despite this fact, it is unrealistic to have redundancy in every spacecraft component. Thus, the M-STAR spacecraft has been assembled using components with high TRL which minimize the possibility of failure. For some components where this is not possible, further investigation is needed. This is specially true for the rotating parts that allow for circular imaging.

Availability

The availability of the system during nominal operations is only challenged by the orbital station keeping or collision avoidance maneuvers that the spacecraft might need to perform. During this time, the payload instrument ceases operations and is thus not able to continue imaging for ICBM detection. The system, however, is designed such that no requirements are compromised during this events: double coverage allows for continuous global coverage also under these circumstances and the communication subsystem remains operational to maintain constellation interlinking.

If off-nominal situations arise, the constellation is designed to continue performing its mission due to its low dependence on other external systems. For example, data relay does not depend on any third-party constellation. Moreover, the position determination does not depend on one single GPS constellation and can still perform its function (even though with less accuracy) with a propagator if GPS signals are turned off.

Finally, availability of the hardware components on the ground is simplified by the extended use of COTS components that can be mass produced. The extrapolation of this to the payload components, however, will have to be studied in more detailed in the following phase of the design.

Maintainability

For the system, there is not much active maintenance that can be performed during operation. As was mentioned throughout the sub-system RAMS, one can identify the sub-system health parameters that can be analysed in order to determine system health on ground. A table summarising the necessary housekeeping data for each subsystem was summarised in Table 8.5.

Furthermore, for the entire mission, orbit and constellation maintenance are also considered. The designed mission relies heavily on the functioning of the constellation in order to successfully meet the requirements. Thus, orbit maintenance is an important factor to ensure that global coverage is always achievable, and such that communication between satellites can be done without problems. This is more specifically covered in Chapter 12.

As for constellation maintenance, it is imperative that if housekeeping data indicates a failure or severe degradation of a system, that the satellite can be replaced. The constellation has been designed to account for redundancy, so if a single satellite in the constellation fails, communication can still occur. However, if two neighbouring satellites fail, the global coverage and communication links are lost; meaning that the reliability, availability and global coverage requirements could no longer be met. Thus, the mission has been designed to allow for the accommodation of new satellites. In order to reduce constellation maintenance costs, a high reliability is required.

Safety

In order to reduce the risk of spacecraft loss under operational conditions outside of the design conditions, a safe mode has been developed for the M-STAR mission. This mode is triggered when the on-board sensors detect an anomaly or when the spacecraft loses communication to the ground for 48 h hours (each spacecraft should have 5-7 ground station fly-bys per day). In case of entering such a mode, the payload (including the IR camera, the rotating mirror and the cooler) and the propulsion system are shut down. The ADCS is the system of utmost importance when entering this mode, as

regaining control of the spacecraft's attitude allows for better thermal control as well as pointing of the solar arrays. Until then, the energy stored in the EPS batteries is used. Next to that, the antennas remain operational to any receiving signal from the ground, but their transmitting functionality is lost. This means that interlinking communications can not go through a spacecraft in safe mode. Finally, the OBC is restarted to regain control of the satellite.

In the functional flow shown in Figure 4.1, the spacecraft enters safe mode in 3 different cases. In function 2.2, the deployment from the launcher has failed and M-STAR enters safe mode before being re-purposed for a different objective or its mission being ended. In function 2.6, the attitude readings show off-nominal behaviour after deployment from the launcher (for example the spacecraft is tumbling), and the satellite goes into safe mode to stop this motion. In function 3.5, the M-STAR spacecraft goes in saving if the initiation of the remaining subsystems causes unpredicted operational conditions. Finally, more frequently the spacecraft could enter this mode when its housekeeping data shows off-nominal readings, or when it does not receive ground communication for 48 h, see function 4.2.12. When this event happens, the spacecraft is unable to continue imaging and thus becomes unavailable, which would mean that the 99% availability system requirement could not be met.

As well as this, the market analysis specified a potential threat of the satellite being targeted by a missile (T.3) due to increased political tensions as a result of the defensive act of placing an early warning system in space (T.2). Thus, the reliability of the system plays a large role in ensuring the safety of the system. If a false detection were to occur, political tensions may arise and the probability of being targeted may increase.

Furthermore, as was discussed in the safety characteristics of the subsystem RAMS analyses; each individual subsystem defines manners in which it contributes to the safety of the overall system. The notable one being a propulsion safety characteristic; namely, collision avoidance and end of life procedures. As was discussed in the propulsion chapter, Chapter 12, it has been ensured that a system that can account for these maneuvers was designed.

17.2.3. Manufacturing, Assembly and Integration Plan

In this section an explanation of further steps to take after the end of the detailed design phase is presented. This involves the manufacturing, assembly and integration plan (MAIP). It is important to note that only the MAIP for the first 7 satellites entailing the Technical Demonstration Mission is going to be explained. For the whole constellation a new MAIP should be generated.

Manufacturing

The manufacturing of satellites is usually subdivided in multiple contractors. This applies for the project as there are multiple parts that need to be manufactured. The manufacturing section is divided into two sections, one for parts that are COTS and one for parts that need to be manufactured specifically for this. For the COTS products each company does their own verification, validation and testing of their products, therefore there would be no need for the team to do them ourselves. The COTS components are from the following companies:

- ADCS: Hyperion, located in The Netherlands
- Communications: Nanoavionics, located in USA and Endurosat, located in Bulgaria
- Structures: NPC SPACEMIND, located in Italy
- Propulsion:Enpulsion, located in Austria
- EPS: GOMspace, located in Denmark
- Solar arrays: MMA Design, located in USA

For the hardware that has to be built specifically for this mission, the payload, tests need to be performed. It was decided that type testing would be performed. This is due to the fact that as the same hardware will be used in all satellites if one of the pieces is approved all subsequent pieces which follow the same production procedure are subjected to less intensive tests [77]. For the manufactured

components most of the tests performed will be delta qual as only specific parts of the manufactured components are different from the previously qualified ones. It is important to note that all components will have qualification tests as explained in Section 17.2.4.

Assembly

The final goal of the assembly is to produce flight hardware with sufficient functionality such that it can be tested and measured [77]. This part will focus on lower level assembly of hardware. The higher level, spacecraft level, will be explained in the next section of Integration. For the assembly of the S/C there are two main methods. One in which first all components are manufactured and then assembly starts and the other one where manufacturing begins and as soon as a component is ready it is sent to be assembled. Both of these methods have their advantages and disadvantages. For the first method, the assembly cannot start until the last component is produced which could be significantly longer than the rest of the components. For the second method, the main advantage is that assembly can start as soon as components are manufactured. However, in case there is a problem with the delivery of components the whole assembly could be delayed.

For this project assembly of a Prototype Model (PM) and Flight Model (FM) are required in order to perform tests. Therefore, it was decided that for both the PM and the FM the satellite will use the method of assembly once all components are manufactured. This is done since in case anything goes wrong, it is possible to change it without having to change all the other parts that are already being produced for the other satellites. The other 6 satellites that are needed for the technical demonstration mission will use the assembly as delivery happens method. It is important to note that the time taken from production and delivery to final assembly of the spacecraft is assumed to be about 6-9 months. For the first spacecraft this might be longer. This is due to the fact that more tests will have to be performed and in the case a manufactured component does not comply with standards, or a major change needs to occur due to a design flaw, the time to finish manufacturing and assembly will increase.

It is also important to describe where the assemblies will take place. The assembly could be done in Italy. This is due to the fact that assembly usually takes place where the bus of the payload is from. For this mission as the proposed structure is from NPC SPACEMIND then assembly should be done in their facilities. Such assembly place also has another advantage. As most of the tests are being done in Germany, having an assembly in Italy simplifies the shipping process for the assembly to the testing facilities. As for the shipping, in order to ship the spacecraft from Italy to Germany the best way would be using ground transport. It is important that the shipping container is ready as well, as all the documentation necessary such as licenses and notifications of hazardous materials are required too.

Integration and Test

The final step of the MAIP is Integration and Test (I&T) of the spacecraft. This is when the pieces of the hardware and software are put together and tested as a whole system to make sure they are integrated properly and the spacecraft can withstand launch and operate as intended. The main components of I&T are Hardware Configured Items (HWCIs) and Software Configured Items (SWCIs) and all relevant tests and testing facilities [77]. The tests that are going performed can be seen in Figure 17.1. Firstly, the I&T for the bus occurs. This is done before the addition of the payload. Once all the tests are performed the payload is integrated and tested. Following the payload I&T all the deployables are tested. Finally, the spacecraft is prepared to be shipped. As seen in Figure 17.1 it is normal to tests subsystems one by one once they are totally integrated in the spacecraft.

It is important to note that I&T is the main reason for delays. This is due to the fact that some of the facilities have to be booked well in advance, a special crew is needed to carry out the tests and the results from the tests need to be reviewed. Once the I&T is done, the shipping of the satellite to the launch site will take place. Assuming the launch is the same as for the BRIK-II then the launch will be

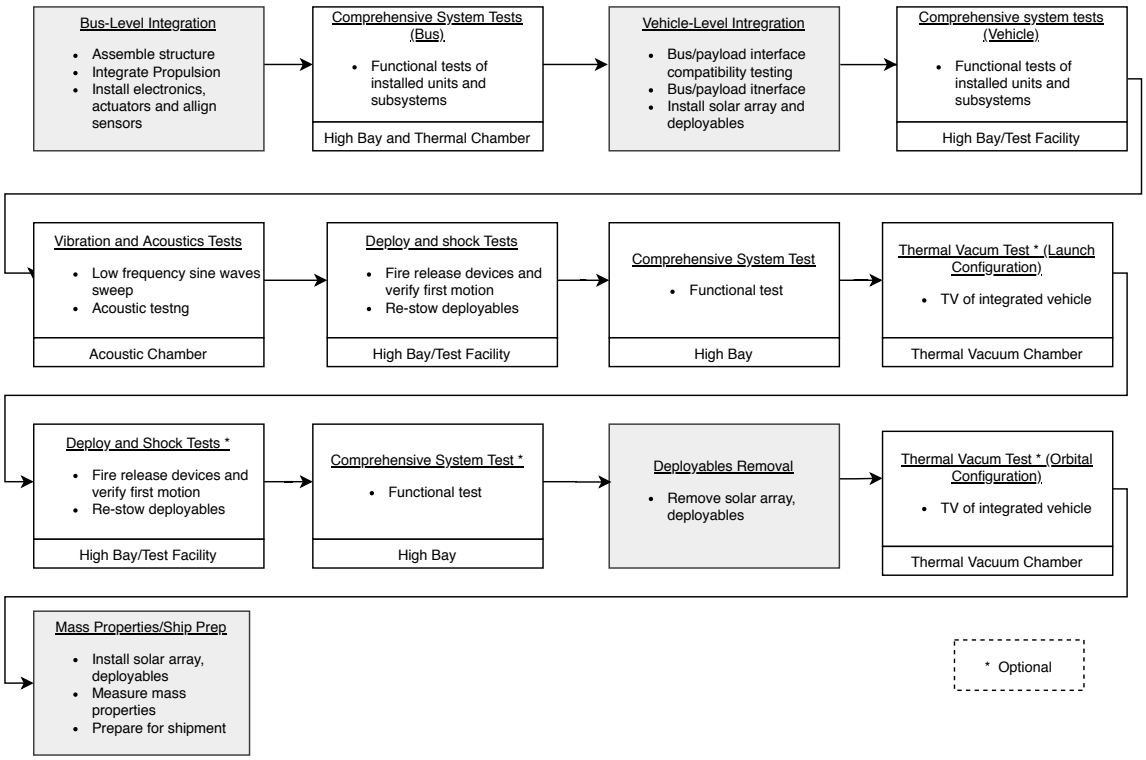

Figure 17.1: Integration and testing flow [77].

in California, US. For this the final product will have to be shipped. As the cargo for the mission would be from a military mission the protocols for the shipment of the satellite are not of public knowledge. The customer should follow the same procedure as for the BRIK-II mission.

17.2.4. Ground Testing and System Verification

The system on-ground verification and testing necessary can be categorized into two main types: environmental tests and interface/integration tests. Environmental tests focus on assessing the compatibility of the system with space and launch procedures. This involves simulating possible mechanical loads, vibrations, temperatures and testing deployment strategies. The table below summarizes the required tests along with the standard to which each test is conducted if available by the facility. Environmental tests are to take place at the IABG facility in Ottobrunn, Germany [1]. As is evident, for several tests, it is possible to preset the testing standard to that of local military standards. Furthermore, every test listed has been ISO 9001 certified, proving compliance with **SYS-REQ-13**.

Interface and integration testing focuses on the efficiency and performance on co-dependent communication modules between subsystems; this pertains to analyzing the time required to relay information between systems, different satellites as well as the actual functioning of these relays. This is especially relevant to this mission as inter-satellite communication, followed by relay to ground stations, plays an integral role. The table below briefly describes and explains these tests that need to take place; they will be performed with the help of Rohde & Schwarz, Munich, Germany[2].

In addition to these tests, an internal system interface test is necessary. This would involve the generation of several pseudo infra-red images, containing an ICBM, without an ICBM and containing rockets or decoy missiles. These pseudo images would be fed to the system interface in order to verify it's capability of detection, tracking and classification, (**REQ-SYS-01** and all its children requirements).

[1]Retrieved from `https://www.iabg.de/en/services/test-services-and-analysis/acoustics/`
[2]Retrieved from `https://www.rohde-schwarz.com/nl/contact_63733.html`

Table 17.2: Overview of environmental on-ground verification tests.

	Test	Description	Testing Standard/ Certification
	Acoustics	Acoustic loads are simulated that develop during the initial phases of launch that lead to strenuous mechanical loads on the spacecraft especially on panels of large surface area. Acoustic testing includes the simulation of these loads as well as acoustic stability analysis.	MIL-STD 810
	EMC	The electromagnetic compatibility is tested; this involves assessing emissions and testing the systems immunity interference. In addition to this high intensity radiated fields are simulated to examine the satellite's performance. These tests are conducted through the use of absorber chambers as well as an unshieled laboratory.	MIL-STD-461 MIL-STD-1275 MIL-STD-704
Thermal Testing	**Thermal Vacuum Tests**	High vacuum conditions are simulated for the complete system as well as the cooler subsystem and other thermally constrained systems by exposing them to a range of temperatures.	ECSS-Q-20-ST-07C
	Thermal Balanced Tests	Similar to thermal vacuum tests but the focus is on thermal model calculations and its verification.	
	Thermal Vacuum Cycling Tests	The spacecraft or subsystem is cyclically exposed to preset maximum and minimum temperatures, with preset cycle durations and temperature gradients.	
	Bakeout Tests	Gassing products and silicone present in parts of the spacecraft can be removed by creating an environment of very high temperatures in a vacuum for preset periods of time.	
	Low Temperature Testing	Instruments on-board, especially the payload in this mission, require fairly intensive and active cooling. In this test cooled optical instruments are put to the test; a chamber containing a helium cooling system which allows for the generation of absolute zero environments.	
Vibration and Shock Testing	**Vibration and Shock**	Pulse or transient shocks are generated within a defined range. Vibrations that follow a sine pattern, random or combination of these are simulated often in combination with simulated environmental temperature ranges.	CSS MIL-STD-810
	Constant Acceleration	Involved centrifuge testing with constant acceleration settings up to 100g.	-
	Solar Panel Deployment	Deployment of the solar panels plays a critical role in the functioning of the satellites, thus the satellite deployment mechanism needs to be tested.	-
Large Scale	**Space Simulation**	Simulation includes: low background temperatures, high vacuum and solar exposure simulation using xenon lamps. Furthermore a rotation movement s simulator allows for the movement of the spacecraft within this simulation with respect to the direction of the artificial sunlight.	-
	Flight Test	Zero gravity flight test for system performance	ECSS

Table 17.3: Overview of Integration and Interface Tests.

Test	Description
Group Delay Measurements	Serves to assess the quality and efficiency of the transmission paths involved in inter-satellite and ground station communication schemes. Phase distortions are identified and addressed.
Linearity and Gain Transfer Measurements	Serves to assess components such as satellite transponders, amplifiers and frequency converters. Outputs of this test include evaluating gain compression, AM/AM, AM/PM and distortion.
Signal Quality Measurements	Serves to assess modulation accuracy and BER (Bit Rate Error). Furthermore, it would aid in verifying the quality of satellite links during the integration and IODs.
Spurious Measurements	This focuses on identifying whether spurious emission measures interfere or appear on detection instruments on-board.
Digital Interface Testing	This aims to test the data relay and communication between the subsystems onboard for all possible operating conditions.

17.3. Phase D: Qualification/Verification and Production

Once the Critical Design Review is passed Phase D starts [3]. For this phase it is proposed to build a Prototype Model (PM) and Flight Model (FM). Subsequently, the PM will undergo the final set of Qualification Tests, aimed to stress the hardware resulting in potential structural failures. The capability of the design to cope with conditions experienced during launch and in orbit is assessed at 50% more severity [83]. When the PM is tested to an acceptable extent, the FM will undergo Acceptance Test meant to check what the hardware can survive under the requirement of full functionality [82].

17.3.1. In Orbit Demonstrations

After the Flight Acceptance Review and Operational Readiness Review are performed successfully the FM is ready for flight [82]. For this phase, the difference between the Technical Demonstration Mission and the Operational Mission needs to be clearly identified. It is found that only a fully operational mission can meet all requirements as proposed by the customer, while it is within the scope of the DSE to design a Technical Demonstration Mission. For M-STAR it is decided to make use of In Orbit Demonstrations (IODs). Traditionally, IODs are used to take newly invented and developed technologies and verify their in-space performance [4]. After careful consideration with the customer, it was defined that IODs can also be used to demonstrate concepts. For example, when your mission employs payload for a task that it was originally not designed for. It is apparent that this definition matches seamlessly with the proposed satellite design for M-STAR, and hence 3 subsequent IODs to enable complete mission verification are proposed.

IOD1

IOD 1 entails one satellite and is performed to verify all functions deduced from Chapter 4, Figure 4.1, that can be performed by an individual satellite. The IOD is concerned with verifying payload performance, including Filter Switch, Optics and the Mirror and all data processing performed by the DPU. Besides this, the OBC performance is verified to a limited extend. This IOD pertains functionalities 4.3.1.1 until 4.3.1.10, function 4.3.2.3, 4.3.2.6 and 4.3.2.7, concluding with obtaining a Focus image of the pixel containing an intensity anomaly and store that data according to function 4.3.2.8.

In Table 17.4 the data set is listed required to be down linked to the GS enabling complete IOD1 verification. Next to this, it is indicated what data is needed to verify a specific mechanism. Hence, when a part of the set is missing or corrupted, it is evident which mechanism cannot be verified yet.

Table 17.4: Data Set for Verification of IOD 1, verified mechanism indicated.

Data	Verified Process
H2O raw image	IR Imager Performance, Filter Performance
H20 processed image, threshold and pixel range indicated, bright pixel location and intensity	Threshold algorithm
CO2 raw image	Filter Switch
CO2 processed image, threshold and H20 pixel range indicated, bright pixel location and intensity	Combined Data Processing
Velocity Evaluation Image Set: Set of Bright Pixel Vectors + Timestamps + Alert	Velocity Procedure Algorithm
Last Coverage image, Focus image	Optics Mechanism

IOD2

IOD 2 is performed with two satellites and the main focus is verification of the interlinking communication system and triangulation process. As IOD2 will be performed only when IOD2 has been completed successfully, it can be assumed that all functionalities mentioned for IOD1 have been verified at this stage. The functionalities required for a successful execution of the M-STAR mission that will be verified during IOD2 are the following: 4.3.2.1, 4.3.2.2, 4.3.2.8 until 4.3.2.13, 4.3.3.1 to 4.3.2.6, 4.3.3.4, 4.3.3.5, 4.3.2.8, 4.3.2.10, 4.3.3.8, 4.3.2.11, and 4.3.2.13. That is, all functions involving tracking by two satellites can be verified limited to inter-plane interlinking.

[3] Retrieved from `https://www.esa.int/Science_Exploration/Space_Science/Building_and_testing_spacecraft`

[4] Retrieved from `https://www.esa.int/Enabling_Support/Space_Engineering_Technology/CDF/To_IOD_or_not_to_IOD_that_is_the_question`

The dataset required for IOD2 verification can be found in Table 17.5. It can be seen that the focus of the IOD is on triangulation and interlinking, indicating what data is expected if those mechanism function properly.

Table 17.5: Data Set for Verification of IOD 2, verified mechanism indicated.

Data	Verified Process
2x Focus Image (+ Timestamps, S/C Position)	Interlinking Communication
Triangulation Data for 600 seconds + Timestamps,	Triangulation Procedure Algorithm

IOD3

For IOD3 it is less obvious what functionalities within the satellite still need verification and what data would be required to enable this. First of all, it is expected that an assessment can be made with regards to the redundancy of the constellation. In addition, when more than 2 satellites start to cooperate, resulting induced latency estimations can be performed. It is proposed to arrange the satellites in 3 orbits, in a 2-2-2 arrangement, enabling verification of all processes stated in these paragraphs. The final functionalities left from Chapter 4, Figure 4.1, that require verification are the following: 4.3.2.4, 4.3.3.6, 4.3.3.7, 4.3.4.1 and 4.3.2.4.

No specific data can be defined for verification of IOD3, as all internal processes with regards to satellite performance are already verified in IOD1 and IOD2. The most important data for this IOD is the spacecraft identifier, enabling verifying all types of out-of-plane satellite interlinking. The types of communication including out-of-plane communication as identified enable evaluating the redundancy of the nanosatellite constellation; what happens when a satellite fails. Next to this, the communication system will be tested extensively. For example, when continuous receiving and transmitting of information is required. What the transceiving latency would be when data is transmitted over multiple nanosatellites can be assessed, and the impact on data quality received by third satellite and its effect on the results of subsequent processing such as the Velocity Check Procedure as outlined before. The list as it has been defined up until now is the following, where the specific tests and data that need to be obtained for on-ground verification have not been determined yet:

- Redundancy of Constellation
  - Out-Of-Plane Interlinking
  - Inter-plane Satellite-Skip Interlinking
  - Out-Of-plane Skip Plane interlinking
- Latency
  - Continuous Transceiving
  - Data latency 3rd Satellite

As IOD3 will be performed with 6 satellites, it meets the requirement for amount of satellites as stated by the Royal Netherlands Airforce in [1], and thus a successful execution of IOD3 implies a success of the Technical Demonstration Mission that was required to be designed by Project Group S12 during the Design Synthesis Exercise.

17.3.2. Mission Validation

While the third IOD is in-orbit and has been verified, mission validation can take place. As validation is concerned with building the right system, has a system been build that can detect ICBMs, the resources for validation are limited as ICBM launches are not publicly known and occur unexpectedly. For the M-STAR mission validation, two types of tests have been distinguished, respectively CDH validation and Data validation. They have already been established during the Midterm Phase but will now be elaborated upon in more detail [5].

- **CDH Validation**: The CDH validation is based on the following process. While planned ICBM launches are not publicly known, it is expected that the existence of rocket launches and their

location mostly are known or can be known rapidly. The characteristics of a missile that our system is built to detect are also common to a rocket, hence it is expected that a rocket launch will induce the detection process as elaborated upon in Chapter 4, Figure 4.1. Therefore, when the coordinates of the detection of a moving object are communicated to the GS, they can be cross-referenced to the coordinates of the known rocket launch / launch location and as such the process can be validated.

- **Data Validation**: The communication of detection of a moving object to ground is accompanied by a data set made up of amongst others a chronological order of spacecraft identifiers, timestamps, spacecraft attitude, moving-object coordinates and trajectory indicators. Throughout our collaboration with the RNLAF, the existence of "Missile Trajectory Prediction Programs" has been made clear. Next to this, it was offered that data downlinked by M-STAR can be implemented in the program to generate trajectories. These generated missile trajectories can subsequently be compared to trajectories deduced from the existing database, and as such enables data validation. Alongside validation based on trajectory prediction, the transmitted data can be analysed based on amongst others quality, noise and possible lacking of inputs.

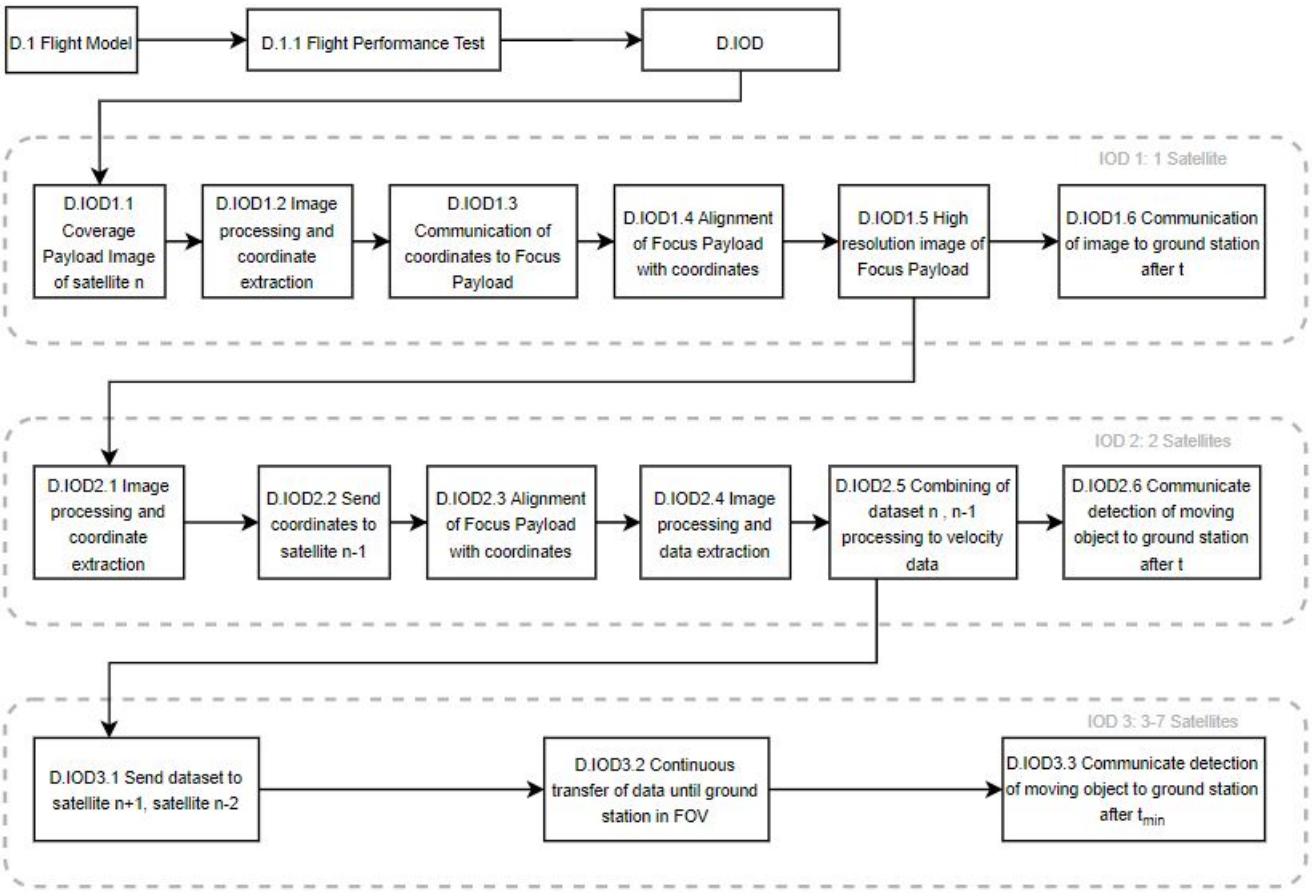

Figure 17.2: IOD Operation Sequence [5]

17.4. Phase E: Operations and Utilization

Phase E is focused on the operations and logistics involved in the M-STAR mission. Here the technicalities of the mission's progression are worked out and expected results are evaluated. Furthermore, ground segment activities such as launch procedures are delved into.

17.4.1. Operational Logistics

This section focuses on creating a road-map of the exact sequence of events involved in the technical demonstration mission. Furthermore, it elaborates on the logistics involved in launch.

System Operation Sequence
The mission is split into two parts: the technical demonstration mission and the full-scale operational mission. The sequence of operations for the full-scale mission can be seen in as a schematic in Figure 4.2. For the technical demonstration mission not all functions seen in this schematic are possible as it uses merely 7 satellites. The specific verification processes made possible through the IODs are elaborated on in the previous section and the according sequence of operations can be seen in Figure 17.2. The logical order between the IODs was explained in detail in the previous chapter.

17.4.2. Launch Procedures

Considering that the RNLAF has worked with Virgin Orbit in the past for planned launch of the BRIK-II satellite, it is a possibility to consider this to be the launch location for this technical demonstration mission too. Virgin Orbit is considered optimal because it is a mobile launch system, and their equipment can be transported globally; this allows for the possibility of conducting the launch from within the Netherlands, for example from Curacao. For the IODs elaborated upon in Section section 17.3.1, it is possible to stage individual launches for each satellite placed into orbit. This allows for the assumption for the IODs that launch will place the satellites directly into the intended orbits. The positions of the satellites to be sent during each IOD can be seen in the figure below:

Two orbital planes are involved in the three IODs planned. These will be neighboring orbital planes. IOD1 will launch one satellite into one of the orbital planes, and IOD2 places another satellite on the same plane. As explained prior, this is done to allow for the verification of intersatellite communication. Following this, IOD3 systematically places the four satellites until the neighboring planes have an equal distribution of satellites. This addresses verification of intersetllite communication. The 7th satellite should ideally be placed in an orbital plane that puts the satellites at a critical distance from eachother with regards to intersatellite communication. Further R&D is required to determine the placement of this satellite; it has been done to a preliminary extent in chapter 9.

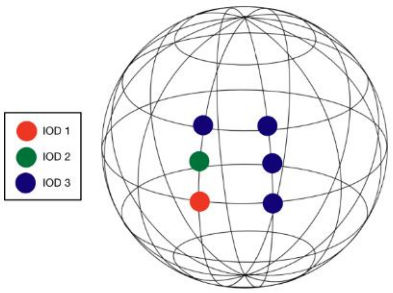

Figure 17.3: Satellite placement within the IODs

17.5. Accomplishing the Technical Demonstration Mission

With the execution of the third IOD as elaborated upon in section 17.3.1, there are 7 satellites in orbit. With 7 satellites all driving requirements of the mission are proven, thus indicating a successful technical demonstration.

Within the IODs, there are two satellites, of the total 7, which are launched into neighboring orbital planes, and evaluated at the equator, as can be seen in Figure 17.3. These orbital planes are chosen because it is at the equator that there is a critical case for global coverage; this is because, given that all orbital planes are polar, the largest distance between two neighboring planes occurs at the equator. Hence the placement of the satellites is done in order to prove the feasibility of the requirement dictating continuous global coverage, **REQ-SYS-01-01**; if two neighboring satellites, in neighboring orbital planes at the equator provide the field of view estimated, then it is possible to say that this requirement is met. This is because this field of view per satellite was estimated in a calculation that determined the number of satellites required per orbital plane (9) to achieve double coverage. Therefore, it is possible to extrapolate that if 9 satellites were present in the orbital planes continuous global coverage is feasible and will be achieved with 306 satellites. If the IOD proves otherwise, it raises the need to revisit the constellation design.

In addition to this, the technical demonstration mission addressed the requirement dictating a 90 s time latency by performing the full scale operational mission on a low level, **REQ-SYS-01-02-04**.

With the 6 satellites present across the neighboring orbital planes, the placement of them is such that the passing of at least one over a ground station is ensured (there is an average of 36 passes over ground station in a period of 24 h). Furthermore, cooperating within NATO countries should allow for the anticipation of a rocket launch; this would then be an opportunity to test the time latency of the entire system of 6 nanosatellites on a minimized scale. Study of the results of this demonstration would allow for the extrapolation and estimation of the feasibility of this relay on a global scale, utilizing 306 satellites.

Moreover, the steps described in this chapter lead to the timeline reported in Figure 17.4 for the M-STAR technical demonstration mission. Through this chart, it is shown that all the IODs will be launched by 2024, thus meeting REQ-SYS-03. The time estimates were discussed in Section 17.2.3 and the format derives from ESA standards [84].

Consequently, it is clear that through the correct execution of the three in-orbit demonstrations, this technical demonstration mission will fully evaluate and demonstrate the feasibility of this mission.

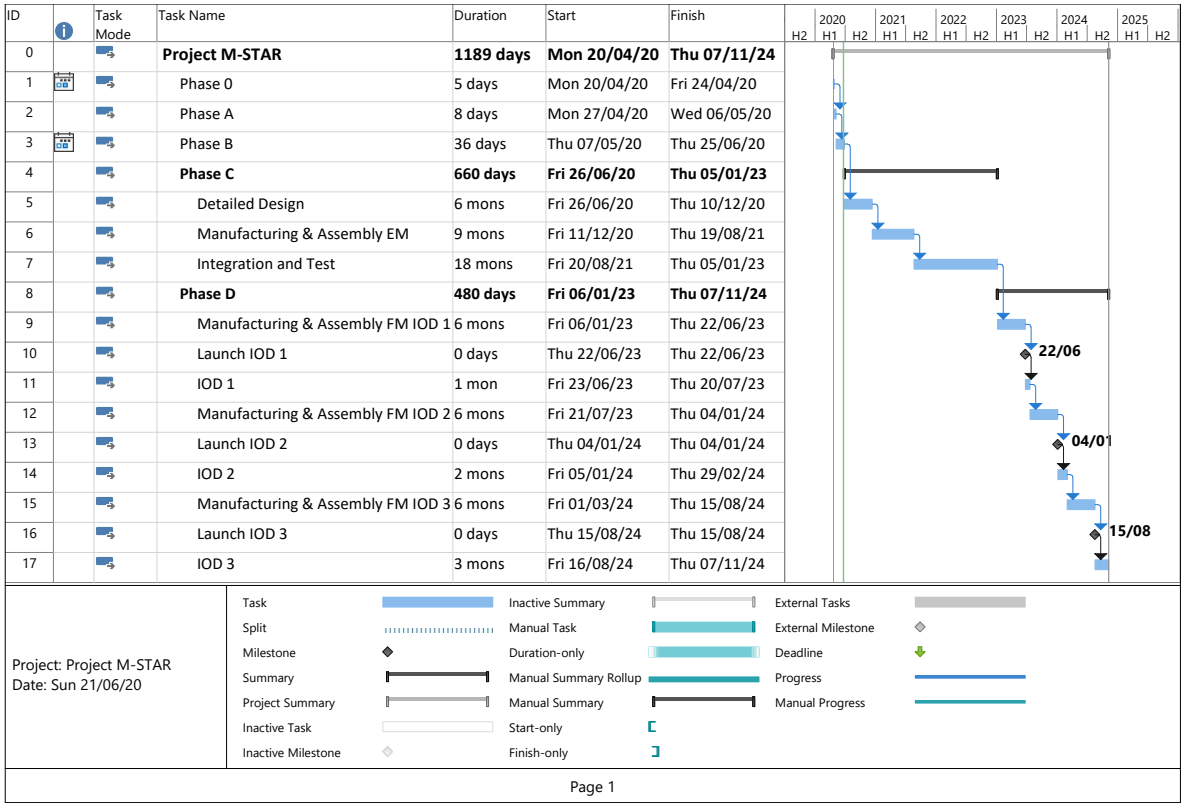

Figure 17.4: Gantt chart for the M-STAR project.

17.6. Phase F: Retiring the Mission

This sections focuses on the end of life procedures of the technical demonstration mission. In addition to this, the implications of a successful technical demonstration are evaluated as well as the steps involved in making the transition to a full-scale operational mission.

17.6.1. Retiring Technical Demonstration Mission

This retirement strategy for the technical demonstration mission largely depends on the outcomes of the three IODs. The satellites must remain in orbit for a minimum of 7 years so as to verify the intended lifetime of the system, **REQ-SYS-04**. However during this time, the success of the IODs would

determine whether or not transition designs for the full-scale operational mission will commence. If the second IOD is completed successfully, transitional design in the form of adjusting processes from Phase D to a larger scale would start.

However, in the case that the IODs are falling short in certain functional tests underway, the satellites still remain in orbit for a minimum of 7 years as this allows for the ground station teams to collect and assess data, enabling the identification of the design flaws in the system. In this case the next step would be to revisit the mission design from Phase B, assessing the overall feasibility and reconsidering design choices made in subsystems, and possibly even on a higher system level; a fundamental change in the design. In this scenario, at the end of the 7 year lifetime of the technical demonstration mission, the satellites sequentially deorbit using maneuvers resulting from the proposed R&D in Section 12.8. Documentation of the entire technical demonstration mission is used in the feasibility analysis and optimization of the mission

17.6.2. Transition to Full-Scale Operational Mission

The primary changes in the mission design that take place during the transition from a technical demonstration mission to a full-scale operational mission is in Phase C. Phase C addresses the manufacturing, production, integration and assembly of components involved in the system. As is evident from Section 17.2.3, for the technical demonstration mission, satellites were assembled cooperating with producers of COTs elements and were manufactured in batches of 6 at most. When dealing with the manufacture, integration and assembly of 306 units considerations about the cost advantage in manufacturing the COTs components internally need to be analyzed, as well as the reduction in unit cost due to the increase in number of units. Furthermore, a new shipment and transportation plan will need to be considered as the batches being transported will increase.

In addition to this, more extensive research is required regarding the logistics of launching 306 satellites. Given one launch site, additional maneuvers need to designed and incorporated in the design in order to maneuver batches of satellites into the correct individual positions after the launch (to avoid single location clusters of satellites); this poses additional load on the performance on the propulsion system. However, the current propulsion system is a conservative design, approximately 80 m/s over the required mission ΔV, and so might still be a valid choice. However, this design choice needs to be revisited. R&D conducted regarding de-orbitting maneuvers, see Section 12.8, may aid in staying within the original ΔV budget despite the necessity for additional maneuvers. All other subsystems were designed to be compatible to the full-scale operational mission.

18
Conclusions and Recommendations

The feasibility of the application of a nanosatellite constellation for an ICBM early warning system has been evaluated and confirmed by means of the preliminary study executed by Project Group S12 for the Design Synthesis Exercise Project. The following chapter aims to illustrate system level conclusions and recommendations for future studies.

18.1. Conclusions

From a technical standpoint, the characteristics of the system result in a technologically feasible mission. It has been shown in Chapter 15 that such a nanosatellite constellation could be made up of as few as 306 spacecraft, while still achieving double continuous global coverage from a LEO orbit. This is made possible thanks to the use of IR filters that focus on certain absorption bands (which reduces background noise and increases pixel size) and the implementation of a circular imaging technique by means of rotating mirrors. When compared against other LEO constellations, this number is slightly higher than that of Iridium (around 150) but much lower than Starlink (around 1500), thus proving the feasibility of the constellation design. In addition, the use of polar orbits ensures that all ICBMs can be detected, even those launching from remote Earth locations due to the use of mobile launch platforms such as submarines.

From an economical standpoint, a financially feasible demonstration mission has been designed. As was specified in the market analysis, the nanosatellite market has been growing over the last 10 years. Due to this, the development time of such satellites has decreased, and the cost of COTS components are competitive and public. Consequently, following this decrease in small satellite components cost as well as reduced launch costs, the mission has been proven to be an economically viable project. As seen in Chapter 16, the use of COTS and high TRL components can significantly reduce the unit cost of these small satellites. Unfortunately, other components such as those that make up the payload subsystem can not be directly used off-the-shelf. This is also true, although with less significant consequences, for the propulsion system and other small components such as the solar array gimbals or the moving imaging parts. The research and development needed for these systems, which was detailed in their respective chapters, increases the cost and lengthens the development time. Nonetheless, when accounting for all these nuances the cost budgeted for this mission adds up to 11.3 M€, significantly below the 30 M€ (excl. launch cost) requirement given by the RNLAF; and the expected launch date by 2024 is achieved. Even though this value excludes launch costs, as was commissioned by the costumer, and the calculation of them is left as a recommendation, the reduced number of orbital planes (9) reduces the number of orbital launches required for the deployment of a full constellation after the IODs.

In order for the M-STAR spacecraft to be ready for launch, however, it has been concluded that an extensive R&D program on the IR instrument is necessary. This development phase should start directly after the completion of this DSE and procure the true specifications for the payload. The in-depth optical engineering knowledge required, combined with the time limitation if this student project, has placed such R&D outside the scope of this DSE.

18.2. Recommendations

Firstly, a 12U satellite platform has been adopted, even though some components stand out of this form factor's structure. The reason behind this choice was so that the development time would be reduced by using a widely standardised form factor. Even though this has been shown to be the correct decision for the technical demonstration mission, it is left a recommendation to analyse the

possibility of using a self-developed satellite structure. The possible benefits of a more personalised spacecraft sizing, such as better packaging and a potential reduction in weight, could outweigh its cons when producing 300+ satellites.

Secondly, while the existence of missile trajectory prediction programs was known throughout the project, they could not been implemented in the design process so far. The following applications are proposed for future studies: Firstly, the existing trajectory database can be used as a reference to improve the accuracy of the velocity calculation program. Secondly, as triangulation in 3D coordinates was found out of the scope of the DSE, this can be examined using the trajectory data generated as a starting point. Thirdly, the possibility to generate thousands of possible trajectories could be used to optimise the hierarchical structure by which the spacecraft decide on their roles during detection and tracking. Lastly, the downlinked data can be implemented in the program to assess data quality and completeness as elaborated upon in Chapter 17.

Thridly, during the design of this mission it has been assumed, in agreement with the costumer, that the system would focus on the detection of one single ICBM. Consequently, the system has been shown to meet the requirements set by the RNLAF when one target is in a spacecraft's field of view. It is thus left as a recommendation for future work to analyse the implications of ICMBs being launched next to decoy targets. A possible solution would to have a more complex command sequence for the neighbouring satellites in order to ensure that each target has two spacecraft locked on it to allow for stereo imaging. A different scenario would be to eliminate the circular imaging technique and invest on the development of higher resolution IR cameras that allow for large fields of view while still maintaining the required GSD to meet the ICBM position accuracy requirement.

To conclude, subsystems recommendations are summarized in Table 18.1. For an exhaustive explanation of subsystem design recommendations please refer to their respective sections.

Table 18.1: Subsystem recommendations summary.

Subsystem	Section	Recommendations
PAY	Section 7.9	Analysing instrument noise in-depth; analysing the effect of direct sunlight; defining specific camera parameters; calculating 3D position error; accurately modeling the ICBM exhaust.
CDH	Section 8.8	Implementing a probabilistic model; determining the processing frequency/memory/storage required; researching into hardware data interfaces; analysing the OBC lifetime.
TTC	Section 9.7	Researching into additional relay constellations; researching into optical communication link; researching into Solomon error correction coding.
EPS	Section 10.7	Researching into gimbals; characterising specific battery cell behaviour.
THER	Section 11.7	Sizing of the flexible copper straps; implementing conductive heat transfer into the model.
PROP	Section 12.8	Researching into propellant efficient de-orbiting maneuvers; analysing the effect of a two-thruster configuration.
ADCS	Section 13.7	Defining a maximum slew time requirement; analysing star tracker accuracy while slewing.
STR	Section 14.6	Quantifying the impact of a custom structure on cost, mass and volume.

Bibliography

[1] Watts, T., *Project Guide DSE: Concept Mission Nanosat Constellation for Ballistic Missile Defence Early Warning*, Delft University of Technology, April 2020, [Unpublished Guide].

[2] Xiphos Systems Cooperation, "Q7S Specifications," URL: http://xiphos.com/products/q7-processor/, 2020, [Accessed on 10-06-2020].

[3] DSE Group 12, "Concept Mission Nanosat Constellation for Ballistic Missile Defence Early Warning Project Plan," Tech. rep., TU Delft, April 2020.

[4] DSE Group 12, "Concept Mission Nanosat Constellation for Ballistic Missile Defence Early Warning Baseline Report," Tech. rep., TU Delft, May 2020.

[5] DSE Group 12, "Concept Mission Nanosat Constellation for Ballistic Missile Defence Early Warning Midterm Report," Tech. rep., TU Delft, May 2020.

[6] Chepkemoi, J., "Countries by Number of Military Satellites," *World Atlas*, March 2018.

[7] Market Research Future, "Military Satellite Market Research Report - Global Forecast till 2025," Sep 2019.

[8] Kulu, E., "Nanosats Database," URL: https://www.nanosats.eu, 2020, [Accessed on 04-05-2020].

[9] Kim, Y., Axellband, E., Doll, A., Eisman, M., Hura, M., Keating, E. G., Libicki, M. C., Martin, B., McMahon, M. E., Sollinger, J. M., and et al., *Review of Selected DoD Space Programs*, Vol. 7, RAND Corporation, 2015, p. 7–11.

[10] Missile Threat, "Space-based Infrared System (SBIRS)," URL: https://missilethreat.csis.org/defsys/sbirs/, June 2018, [Accessed on 04-05-2020].

[11] Spaceflight 101, "Tundra Satellite Overview," URL: http://spaceflight101.com/spacecraft/tundra/, 2020, [Accessed on 04-05-2020].

[12] Savelsberg, R., "Ballistic Missiles: an Introduction," May 2020, [Unpublished Presentation Slides].

[13] Liou, J., "USA Space Debris Environment, Operations, and Research Updates," NASA, February 2017.

[14] Brodecki, M., "BRIK-II Main System Budgets," Tech. rep., Netherlands Ministry of Defense, NLR, TU Delft, and ISIS, November 2018.

[15] Hamamatsu Photonics K.K., "Characteristics and use of Infrared Detectors," *Hamamatsu City*, 2011.

[16] Humboldt State University, "Atmospheric Absorption & Transmission," URL: http://gsp.humboldt.edu/OLM/Courses/GSP_216_Online/lesson2-1/atmosphere.html, 2019, [Accessed on 28-05-2020].

[17] US Congress, "SDI: Technology, Survivability, and Software," 1988.

[18] Qinglin, N., Zhihong, H., and Shikui, D., "IR radiation characteristics of rocket exhaust plumes under varying motor operating conditions," *Chinese Journal of Aeronautics*, Vol. 30, No. 3, 2017.

[19] Montenbruck, O. and Gill, E., *Satellite Orbits Models, Methods and Applications*, Springer, 2000.

[20] Schweitzer, C., Stein, K., and Wendelstein, N., "Evaluation of appropriate sensor specifications for space based ballistic missile detection," *Proceedings of SPIE - The International Society for Optical Engineering*, Vol. 8541, 10 2012.

[21] ThorLabs, "Camera Noise and Temperature," URL:https://www.thorlabs.com/newgrouppage9.cfm?objectgroup_id=10773/, [Accessed on 9-06-2020].

[22] de Jong, M., "Sub-Poissonian shot noise," *Physics World*, 1996.

[23] Capper, P. and Elliott, C., *Infrared Detectors and Emitters: Materials and Devices*, Springer, 2001.

[24] Remacle, P., *Study of a cooling system for a CubeSat infrared detector*, Master's thesis, University of Liège, 2018.

[25] Emery, W. J. and Camps, A., *Introduction to satellite remote sensing : atmosphere, ocean, land and cryosphere applications*, Elsevier, 2017.

[26] Cai, H., "Three-Dimensional Numerical Analysis of LOX/Kerosene Engine Exhaust Plume Flow Field Characteristics," Tech. rep., November 2017.

[27] Nagaraja, D. M. P., "The Earth's Radiation Budget," *Tour of the Electromagnetic Spectrum*, 2010.

[28] LaMorte, W. W., "Central Limit Theorem," URL: http://sphweb.bumc.bu.edu/otlt/MPH-Modules/BS/BS704_Probability/BS704_Probability12.html#:~:text=Central%20Limit%20Theorem,will%20be%20approximately%20normally%20distributed., 2016, [Accessed on 04-05-2020].

[29] Movitherm, "What is NETD in a Thermal camera," URL: https://movitherm.com/knowledgebase/netd-thermal-camera/, 2018, [Accessed on 08-05-2020].

[30] Gopal, V., "Noise equivalent temperature difference performance of an IR detector in a hybrid focal plane array," Tech. rep., October 1995.

[31] IRCameras, "QUAZIR™ MWIR InSb Camera Cores," URL:http://52ebad10ee97eea25d5e-

d7d40819259e7d3022d9ad53e3694148.r84.cf3.rackcdn.com/UK_ICA_QuazIR-MWIR-InSb-Camera-Cores_DS.pdf/, [Accessed on 05-06-2020].
[32] Mullié, J., Arts, R., Tanchon, J., and Trollier, T., "LPT6510 Pulse-tube Cooler for 60-150K applications," URL:https://www.thales-cryogenics.com/wp-content/uploads/2018/11/2018-04-04-ESA-SCW-Presentation-LPT6510-Pulse-tube-Cooler-Concepts-for-60-150K-applications.pdf, 2018.
[33] Schweitzer, C., Gulde, M., Horch, C., et al., "Nanosat-Based detection and tracking of launch vehicles," *Target and Background Signatures IV*, Vol. 10794, 2018.
[34] Marsi, S. et al., "PicoAgri. Realization of a low-cost, remote sensing environment for monitoring agricultural fields through small satellites and drones," *2017 40th International Convention on Information and Communication Technology, Electronics and Microelectronics (MIPRO)*, IEEE, 2017, pp. 1073–1078.
[35] Odenwald, S., *Remote Sensing Math*, NASA, 2011, [Retrieved from http://www.nasa.gov/audience/foreducators/topnav/materials/listbytype/Remote_Sensing_Math.html].
[36] Jin, H., Lim, J., Kim, Y., and Kim, S., "Optical Design of a Reflecting Telescope for CubeSat," Tech. rep., School of Space Research, Kyung Hee University, Korea Satellite Technology Research Center, Korea Yunam Optics, October 2013.
[37] ESA Earth Observation Portal, "CIRiS Compact Infrared Radiometer in Space," URL: https://directory.eoportal.org/web/eoportal/satellite-missions/c-missions/ciris, [Accessed on 20-06-2020].
[38] Aida, S. and Kirschner, M., "Accuracy assessment of SGP4 orbit information conversion into osculating elements," *Sixth European Conference on Space Debris. ESA/ESOC, Darmstadt, Germany*, 2013, pp. 22–25.
[39] Leonardo DRS, Electro-Optical Infrared Systems, "MCT's Advantages as an Infrared Imaging Material," Tech. rep., 2010.
[40] Carey, J., "Understanding Bit Depth," *Conserve O Gram*, 2008.
[41] Goh, T. Y., Nisha Basah, S., Yazid, H., et al., "Performance analysis of image thresholding: Otsu Technique," *Measurement*, Vol. 114, 2018.
[42] Fetter, S., "A ballistic missile primer," URL: http://faculty.publicpolicy.umd.edu/sites/default/files/fetter/files/1990-MissilePrimer.pdf, 1990.
[43] Huq, R., Islam, M., and Siddique, S., "AI-OBC: Conceptual Design of a Deep Neural Network based Next Generation Onboard Computing Architecture for Satellite Systems," *1st China Microsatellite Symposium*, 2018.
[44] Thomas, N., Spohn, T., Lara, L., Christensen, U., Seiferlin, K., Michaelis, H., Castro, J., Kallenbach, R., Affolter, M., Beck, T., et al., "The BepiColombo Laser Altimeter: Novel instrument elements," *EPSC*, 2013, pp. EPSC2013–339.
[45] Horch, C., Schnelle, N., Gulde, M., Watson, E., Schimmerohn, M., and Schäfer, F., "An MWIR payload with FPGA-based data processing for a 12U nanosatellite," *Small Satellites for Earth Observation. 11 International Symposium of the International Academy of Astronautics 2017*, 2017, pp. 339–342.
[46] Burlton, B., Battochio, B., et al., "Carleton CuSAT Design Project, Command & Data Handling," Tech. rep., Department of Mechanical & Aerospace Engineering, Carleton University, December 2017.
[47] "What is an SoC FPGA?" URL: https://www.intel.com/content/dam/www/programmable/us/en/pdfs/literature/ab/ab1_soc_fpga.pdf, 2014, [Accessed on 09-06-2020].
[48] Parkes, S., "High-speed, low-power, excellent EMC: LVDS for on-board data handling," *Proceedings of the 6th International Workshop on Digital Signal Processing Techniques for Space Applications, ESTEC, Sept*, Citeseer, 1998.
[49] Kumar, V., Pandey, V., Kumar, K. A., Sandya, S., et al., "Redundancy Management of On-board Computer in Nanosatellites," 2019, pp. 565–570.
[50] Altera Cooperation, *Cortex-A9 Microprocessor Unit Subsystem*, August 2014.
[51] Hu, Y. and Li, V., "Logical topology-based routing in LEO constellations," *ICC 2001. IEEE International Conference on Communications. Conference Record (Cat. No. 01CH37240)*, Vol. 10, IEEE, 2001, pp. 3172–3176.
[52] He, J., Yong, J., Dongming, B., and Li, G., "Routing strategy research based on ISL states and topology snapshot in LEO satellite constellation," *2008 11th IEEE International Conference on Communication Technology*, IEEE, 2008, pp. 13–16.
[53] Qu, Z., Zhang, G., Cao, H., and Xie, J., "LEO satellite constellation for Internet of Things," *IEEE Access*, Vol. 5, 2017, pp. 18391–18401.
[54] Speretta, S., *Slides Link Budget Desing from Space Systems Engineering*, Faculty of Aerospace Engineering, TU Delft, June 2020.
[55] Popescu, O., "Power Budgets for CubeSat Radios to Support Ground Communications and Inter-Satellite

Links," *IEEE*, Vol. 5, 2017, pp. 12618–12625.
[56] van Valkenburg, M. E., *Reference data for engineers: radio, electronics, computers and communications*, Elsevier, 2001.
[57] Anderson, J. B., *Digital transmission engineering*, Vol. 12, John Wiley & Sons, 2006.
[58] Space Inventor, "TTC-P3 Dual Hot-Redundant VHF/UHF Satellite TTC radio data sheet," 2019.
[59] Space Quest, "TRX-U Satellite UHF Transceiver data sheet," 2020.
[60] Fennel, J. W. and Heinz, M. T., "Encryption using destination addresses in a TDMA satellite communications network," November 1983, US Patent 4,418,425.
[61] Nanoavionics, "UHF Antenna System Data Sheet," 2018.
[62] Endurosat, "Endurosat UHF Tranceiver," URL: https://www.endurosat.com/cubesat-store/cubesat-communication-modules/uhf-transceiver-ii/, [Accessed on 20-06-2020].
[63] Cervone, A., *Slides ADSEE AE2111-II*, Faculty of Aerospace Engineering, TU Delft, September 2019.
[64] Zandbergen, B., *AE1222-II: Aerospace Design & Systems Engineering Elements I - Part: Spacecraft (bus) design and sizing*, Delft University of Technology, February 2020, [Unpublished Guide].
[65] Center for Near Earth Object Studies, "Glossary - Astronomical Unit," URL: https://cneos.jpl.nasa.gov/glossary/au.html, [Accessed on 17-06-2020].
[66] NASA Earth Observatory, "Measuring Earth's Albedo," URL: https://earthobservatory.nasa.gov/images/84499/measuring-earths-albedo#:~:text=Using%20satellite%20measurements%20accumulated%20since,%2C%20and%20December%2031%2C%202011., [Accessed on 17-06-2020].
[67] Hemmer, J. H., "Solar Absorptance and Thermal Emittance of Some Common Spacecraft Thermal-Control Coatings," Tech. rep., NASA, April 1984.
[68] Technology Application. Inc., "Thermal Straps - Cabled Copper Thermal Straps (CuTS®)," URL: https://www.techapps.com/copper-thermal-strap-assemblies, [Accessed on 19-06-2020].
[69] Dejoie, Joyce and Truelove, Elizabeth, "StarChild Question of the Month for January 2003," URL: https://starchild.gsfc.nasa.gov/docs/StarChild/questions/question53.html#:~:text=On%20January%204%2C%202003%2C%20our,this%20year%20on%20July%204.), 2003, [Accessed on 21-06-2020].
[70] European Space Agency, "Thermal Data Handling Facilities," URL: https://www.esa.int/Enabling_Support/Space_Engineering_Technology/Test_centre/Thermal_Data_Handling_Facilities, [Accessed on 21-06-2020].
[71] Sanchez Ortiz, N., Bello-Mora, M., and Klinkrad, H., "Collision Avoidance Manoeuvres during Spacecraft Mission Lifetime: Risk Reduction and Required DV," Vol. 35, 2004, pp. 2491.
[72] Krejci, D., Reissner, A., Seifert, B., et al., "Demonstration of the ifm nano feep thruster in low earth orbit," *Proceedings of the 4S Symposium, Sorrento, Italy*, Vol. 28, 2018.
[73] Bruijn, F., Bewick, C., Lübke-Ossenbeck, B., and Janovsky, R., "Propellant-efficient Method for Controlled Deorbit of LEO Satellites," October 2013.
[74] Agasid, E., Burton, R., Carlino, R., et al., "Small spacecraft technology state of the art," *NASA, Ames Research Center, Mission Design Division Rept. NASA/TP-2015-216648/REV1, Moffett Field, CA*, 2015.
[75] Starin, S. R. and Eterno, J., "Attitude determination and control systems," 2011.
[76] Liou, J. C., Johnson, N. L., and Hill, N. M., "Controlling the growth of future LEO debris populations with active debris removal," *Acta Astronautica*, Vol. 66, No. 5-6, 2010, pp. 648–653.
[77] Larson, W. J. and Wertz, J. R., *Space Mission Analysis and Design*, Springer, 2006.
[78] Inter Agency Space Debris Coordination Committee, "IADC Space Debris Mitigation Guidelines," URL: https://www.unoosa.org/documents/pdf/spacelaw/sd/IADC-2002-01-IADC-Space_Debris-Guidelines-Revision1.pdf, 2007, [Accessed on 01-05-2020].
[79] United Nations Office for Outer Space Affairs, "Space Debris Mitigation Guidelines of the Committee on the Peaceful Uses of Outer Space," URL: https://www.unoosa.org/pdf/publications/st_space_49E.pdf, 2010, [Accessed on 03-05-2020].
[80] Ailor, W. and Patera, R., "Spacecraft re-entry strategies: meeting debris mitigation and ground safety requirements," *Proceedings of the Institution of Mechanical Engineers, Part G: Journal of Aerospace Engineering*, Vol. 221, No. 6, 2007, pp. 947–953.
[81] Shah, R. and Ward, P. T., "Lean manufacturing: context, practice bundles, and performance," *Journal of operations management*, Vol. 21, No. 2, 2003, pp. 129–149.
[82] Cripps, V., "Phases of an ESA hardware project explained," https://www.space.irfu.se/seminars/20180523-Cripps-HW_Project.pdf, 2018, [Accessed 15-05-2020].
[83] Takashi, I. et al., *Satellite Communications, System and its Design Technology*, Ohmsha, LtD., 2000.
[84] Cripps, V., "Phases of an ESA Harware Project Explained," URL:https://www.space.irfu.se/seminars/20180523-Cripps-HW_Project.pdf, [Accessed on 21-06-2020].